PSDF

Power Systems Development Facility

Topical Report
Gasification Test Run TC12

May 16, 2003 -
July 14, 2003

DOE Cooperative Agreement Number
DE-FC21-90MC25140

SOUTHERN COMPANY

Energy to Serve Your World®

POWER SYSTEMS DEVELOPMENT FACILITY
TOPICAL REPORT

GASIFICATION TEST RUN TC12

MAY 16, 2003 – JULY 14, 2003

DOE Cooperative Agreement Number
DE-FC21-90MC25140

POWER SYSTEMS DEVELOPMENT FACILITY

DISCLAIMER

ABSTRACT

This report discusses Test Campaign TC12 of the Kellogg Brown & Root, Inc. (KBR) Transport Gasifier train with a Siemens Westinghouse Power Corporation (SW) particle filter system at the Power Systems Development Facility (PSDF) located in Wilsonville, Alabama. The Transport Gasifier is an advanced circulating fluidized-bed reactor designed to operate as either a combustor or a gasifier using a particulate control device (PCD). While operating as a gasifier, either air or oxygen can be used as the oxidant.

Test run TC12 began on May 16, 2003, with the startup of main air compressor and the lighting of the gasifier startup burner. The Transport Gasifier operated until May 24, 2003, when a scheduled outage occurred to allow maintenance crews to install the fuel cell test unit and modify the gas cleanup system. On June 18, 2003, the test run resumed when operations relit the startup burner, and testing continued until the scheduled end of the run on July 14, 2003. TC12 had a total of 733 hours using Powder River Basin (PRB) subbituminous coal. Over the course of the entire test run, gasifier temperatures varied between 1,675 and 1,850°F at pressures from 130 to 210 psig.

ACKNOWLEDGMENT

CONTENTS

TABLES

FIGURES

1.0   EXECUTIVE SUMMARY

1.1 SUMMARY

This report discusses Test Campaign TC12 of the Kellogg Brown & Root, Inc. (KBR) Transport Gasifier train with a Siemens Westinghouse Power Corporation (SW) particle filter system at the Power Systems Development Facility (PSDF) located in Wilsonville, Alabama. The Transport Gasifier is an advanced circulating fluidized-bed reactor designed to operate as either a combustor or a gasifier using a particulate control device (PCD). While operating as a gasifier, either air or oxygen can be used as the oxidant. Test run TC12 began on May 16, 2003, with the startup of the main air compressor and the lighting of the gasifier start-up burner. The Transport Gasifier operated until May 24, 2003, when a scheduled outage occurred to allow maintenance crews to install the fuel cell test unit and modify the gas clean-up system. On June 18, 2003, the test run resumed when operations relit the start-up burner, and testing continued until the scheduled end of the run on July 14, 2003. TC12 had a total of 733 hours using Powder River Basin (PRB) subbituminous coal. Over the course of the entire test run, gasifier temperatures varied between 1,675 and 1,850°F at pressures from 130 to 210 psig.

1.2 PSDF ACCOMPLISHMENTS

The Transport Gasifier has achieved over 4,985 hours of operation on coal feed; about 6,470 hours of solids circulation as a pressurized combustor; 5,665 hours of solid circulation; and 4,359 hours of coal feed as a gasifier. The major accomplishments in TC12 are summarized below. For combustion-related accomplishments, see the technical progress report for the TC05 Test Campaign. For gasification-related accomplishments in GCT1 through TC11, see the technical progress reports for the TC06, TC07, TC08, TC09, TC10, and TC11 Test Campaign technical progress reports.

1.2.1 Transport Gasifier Train

The major accomplishments and observations in TC12 included the following: see Table 1.2-1 for a summary of the operating data.

Process:
- The Transport Gasifier operated for 733 hours in TC12 using Powder River Basin coal, accumulating 116 hours in air-blown mode and 603 hours in oxygen-blown mode (remaining hours in transition). A short scheduled outage occurred in the middle of the test run to install the new fuel cell test skid and other gas clean-up equipment.

- The test run experienced some of the most stable oxygen-blown operation to date. However, a deposit formed in the lower mixing zone (LMZ) during an air-to-oxygen transition when temperatures climbed too high. Despite the fact that the deposit covered much of the LMZ, the run continued for another 364 hours without any major problems.

- Gasifier temperatures mostly varied from 1,675 to 1,850°F. The mass flux in the riser ranged from 100 to 400 lb/ft²•s, assuming a slip factor of 2.

- Due to a low solids inventory, the standpipe operated in a more stable manner in TC12 than it did in previous test runs. With less material in the gasifier, the standpipe level never became high enough to interfere with the loop seal. The new nuclear density gauges in the standpipe proved useful in monitoring the standpipe solids level. Although material tended to slightly pack when the gasifier inventory increased, adjusting the standpipe aeration alleviated the problem, which allowed the gasifier to continue operating smoothly. Standpipe operations were more stable when the riser velocity was above 35 ft/s.

- The steady-state operating periods included a period of minimum coal-feed rate as well as a period of low coal-feed rate supplemented by coke breeze. These periods may be useful in determining the turndown rate for the gasifier, which is valuable knowledge for conditions that may occur when idling the gasifier or servicing auxiliary equipment.

- The carbon conversions are listed in Table 1.2-1 and were slightly higher than the carbon conversion normally seen when using PRB coal.

- The sulfur content in the syngas is listed in Table 1.2-1. According to the gas analyzers, the sulfur removal due to the limestone fed into the gasifier was minimal, regardless of the limestone feed rate.

- The ammonia content in the syngas is listed in Table 1.2-1. To remove ammonia from the syngas, a commercially available nickel-based cracking catalyst was added to the gasifier from the sorbent feeder. The catalyst's effect on ammonia content was modest, likely due to a short catalyst residence time and nonuniform feed rate.

- Automation work on the Transport Gasifier continued in TC12. The new multiparameter control scheme for controlling gasifier temperatures in oxgyen-blown mode was tested, but it still needs some improvement. The single-element temperature control loop for air-blown mode worked well. The new standpipe level control loop accurately maintained the standpipe level at acceptable values by automatically starting the standpipe screw cooler and conveying system whenever the level reached the maximum height.

- The solids obtained from the standpipe sampling system have a mass mean particle diameter of 150 to 350 microns SMD and an organic carbon content typically below 0.6 percent except during periods of coke breeze feed.

- As in past runs, a large number of gasifier pressure taps became plugged during the run, resulting in the loss of some of the gasifier pressure differential pressure data. Although the plugged taps were not as numerous as in TC10, studies are continuing to examine the cause of the plugging pressure taps and to develop further recommendations for avoiding plugged taps.

- The test run ended as scheduled on the night of July 14, 2003. As expected, the post-run inspections showed the large restriction in the LMZ. The gasifier and primary gas cooler appeared to be in relatively good condition, but a couple of the hexagonal refractory hex-mesh pieces had fallen from the cyclone roof into the loop seal.

Equipment:
- A prototype solid oxide fuel cell (SOFC), developed by Delphi Corporation, was operated on syngas for the period of June 21 to June 27. The SOFC stack subsystem (two 15-cell stack modules in electrical series) was heated up to operating temperature of 1,400°F and was operated on coal-based syngas. As expected, the SOFC stack produced 420 W at 21 V. This experiment was repeated with a second SOFC stack and produced 450 W at 20.5 V. The two stacks together were operated for a period of over 75 hours. This test was the first step towards developing a highly efficient clean-coal-based energy conversion technology. The lessons learned from the test will be used for further development and are critical in moving this technology forward towards commercialization.

- For this fuel cell test, a syngas clean-up system was added to remove contaminants such as sulfur, chlorine, and tar. The system included both hot and cold gas clean-up modules as well as a crystal/oil removal tank. The hot gas cleanup included three vessels (high temperature zinc oxide for bulk removal of the sulfur compounds,

Trona for removing chlorides, and lower temperature zinc oxide for sulfur polishing) and the cold cleanup included four vessels (water, sodium hypochlorite, zinc acetate, and water). Not only was the schedule for installing this clean-up system aggressive, but significant process development was required. The clean-up system performed well removing sulfur to levels below 60 ppb and chlorine compounds to levels below 1 ppm and sections were bypassed at the end of the fuel cell test to evaluate the effects of small amounts of sulfur contamination.

- Both coal feeders performed well in TC12. The new fluidized-bed feeder fed coal in tandem with the original rotofeeder ran for a period of time totaling 230 hours. At the end of the test run, the new feeder ran steadily as the primary feeder for several continuous periods that lasted as long as 50 uninterrupted hours. The new feeder easily achieved a maximum feed rate of around 3,800 pph and responded well to changes in the conveying line differential pressure while maintaining steady temperature profiles in the gasifier.

- The coal milling system reliably produced pulverized coal with moisture levels below 23 percent. The low coal moisture eliminated the excessive conveying line plugging that plagued the previous two test runs, allowing for steady operating conditions in the gasifier and coal-feed systems.

- A new steam drum control loop proved effective in maintaining the steam drum level and pressure, even in the event of coal feeder trips and restarts.

- Most of the gas analyzers were online for the majority of the test run, presenting good gas composition data. The dry gas compositions added up to between 98 and 102 percent on a consistent basis.

- During TC12, the atmospheric fluidized-bed combustor system operated only on fuel oil and provided 650°F superheated steam to the rest of the gasifier loop. Consequently, operations were smooth with the bed temperatures for most of the run between 1,250 and 1,550°F. The G-ash was disposed into a landfill.

1.2.2 PCD

The highlights of PCD operation for TC12 are listed below.

- PCD operations were stable throughout TC12. No filter element failures and no bridging occurred. During most of the run, the baseline pressure drop was about 50 to 65 inches of water. During steady-state operations, the inlet temperature was about 700 to 775°F, and the face velocity usually ranged from 3.0 to 4.0 ft/min.

- The PCD back-pulse pressure was 220 psid on the top plenum and 400 psid on the bottom plenum. These pressures were lower than the 400 to 600 psid settings used in previous test runs.

- The back-pulse frequency was varied from 5 to 20 minutes in an effort to further optimize back-pulse parameters. Pressure differential measurements at the PCD

inlet were taken at different back-pulse conditions to quantify the back-pulse effects on the system.

- Failsafe testing with g-ash injection occurred during the run. The testing included long-term injection into the PSDF failsafe and into the Pall fuse.

- Testing of metal filter elements continued. The filter layout for TC12 included all Iron Aluminide (FEAL) filter elements.

- PCD outlet loading samples indicated excellent sealing of the filter vessel. All the measurements showed outlet concentrations below the sampling system lower limit of detection of 0.1 ppmw (except for the samples taken during injection tests for failsafe evaluation and outlet monitor calibration).

- The fines removal system operated fairly well during normal operations. However, during the run, the dispense vessel spheri valve seal ruptured and had to be replaced. While the system was out of commission, the bypass system successfully removed solids from the PCD cone.

- New resistance probes serving as level indicators, installed in the lock vessel of the spent fines system, showed repeatable response to solid level changes and may be used in future runs to control the system cycle frequency.

- Solids obtained from the spent fines feeder possessed a mean particle diameter of under 20 microns and an LOI varying from under 15 to over 30 percent.

Table 1.2-1

Operating Data Summary

	Units	Air Blown	Oxygen Blown
Hours	hr	116	603
Pressure	psig	210	130-155
Riser Velocity	ft/s	45-50	30-65
Raw Syngas Heating Value	Btu/scf	55-58	59-100
Projected Syngas Heating Value for Commercial Operation	Btu/scf	98-109	126-255
Carbon Conversion Based on Corresponding Flow of Coal, PCD Solids, and Synthesis Gas	%	96-98	92-98
Sulfur Content in Syngas Leaving the Gasifier - Total Reduced Sulfur (TRS)	ppm	163-249	152-568
Gasifier Ammonia Emissions	ppm	1,000-1,500	2,000-2,500

2.0 INTRODUCTION

This report provides an account of the TC12 test campaign with the Kellogg Brown & Root, Inc. (KBR) Transport Gasifier and the Siemens Westinghouse Power Corporation (Siemens Westinghouse) filter vessel at the Power Systems Development Facility (PSDF) located in Wilsonville, Alabama, 40 miles southeast of Birmingham. The PSDF is sponsored by the U.S. Department of Energy (DOE) and is an engineering-scale demonstration of advanced coal-fired power systems. In addition to DOE, Southern Company Services, Inc., (SCS), Electric Power Research Institute (EPRI), and Peabody Energy are cofunders. Other cofunding participants supplying services or equipment currently include KBR, the Lignite Energy Council, and Siemens Westinghouse. SCS is responsible for constructing, commissioning, and operating the PSDF.

2.1 THE POWER SYSTEMS DEVELOPMENT FACILITY

SCS entered into an agreement with DOE/National Energy Technology Laboratory (NETL) for the design, construction, and operation of a hot gas clean-up test facility for pressurized gasification and combustion. The purpose of the PSDF is to provide a flexible test facility that can be used to develop advanced power system components and assess the integration and control issues of these advanced power systems. The facility also supports programs to eliminate environmental concerns associated with using fossil fuels for producing electricity, chemicals, and transportation fuels. The facility was designed as a resource for rigorous, long-term testing and performance assessment of hot stream clean-up devices and other components in an integrated environment.

The PSDF now consists of the following modules for systems and component testing:

- A full stream Transport Reactor module.
- A full stream hot gas clean-up module (particulate filter system).
- A full stream compressor/turbine module.
- A slip stream gas clean-up module, including hot and cold gas units.

The Transport Reactor module includes KBR Transport Reactor technology for pressurized combustion and gasification to provide either an oxidizing or reducing gas for parametric testing of hot particulate control devices. The Transport Gasifier can be operated in either air- or oxygen-blown modes. Oxygen-blown operations are primarily focused on testing and developing various Vision 21 programs to benefit gasification technologies in general. The hot gas clean-up filter system tested to date at the PSDF is the particulate control device (PCD) supplied by Siemens Westinghouse. The gas turbine is an Allison Model 501-KM gas turbine, which drives a synchronous generator through a speed reducing gearbox. The Model 501-KM engine was designed as a modification of the Allison Model 501-KB5 engine to provide operational flexibility. Design considerations include a large, close-coupled external combustor to burn a wide variety of fuels and a fuel delivery system that is much larger than the standard system. A small portion of the synthesis gas (taken from downstream of the PCD) can also flow to a gas clean-up system to provide a synthesis gas suitable for use in testing additional downstream equipment, e.g., use in a fuel cell.

2.2 TRANSPORT GASIFIER SYSTEM DESCRIPTION

The Transport Gasifier is an advanced circulating fluidized-bed reactor operating in air- or oxygen-blown mode, using a hot gas clean-up filter technology (particulate control devices [PCDs]) at a component size readily scaleable to commercial systems. The Transport Gasifier train is shown schematically in Figure 2.2-1. A tag list of all major equipment in the process train and associated balance-of-plant is provided in Tables 2.2-1 and -2.

The Transport Gasifier consists of a mixing zone, a riser, a disengager, a cyclone, a standpipe, a loop seal, and a J-leg. Steam and air or oxygen are mixed together and introduced in the lower mixing zone (LMZ) while the fuel, sorbent, and additional air and steam (if needed) are added in the upper mixing zone (UMZ). The steam and air or oxygen along with the fuel, sorbent and solids from the standpipe are mixed together in the UMZ. The mixing zone, located below the riser, has a slightly larger diameter than the riser. The gas and solids move up the riser together, make two turns and enter the disengager. The disengager removes larger particles by gravity separation. The gas and remaining solids then move to the cyclone, which removes most of the particles not collected by the disengager. The gas then exits the Transport Gasifier and goes to the primary gas cooler and the PCD for final particulate cleanup. The solids collected by the disengager and cyclone are recycled back to the gasifier mixing zone through the standpipe and a J-leg. The nominal Transport Gasifier operating temperature is 1,800°F. The gasifier system is designed to have a maximum operation pressure of 294 psig with a thermal capacity of about 41 MBtu/hr. Due to a lower oxygen supply pressure the maximum operation pressure is about 160 psig in oxygen-blown mode.

For start-up purposes, a burner (BR0201) is provided at the gasifier mixing zone. Liquefied propane gas (LPG) is used as start-up fuel. The fuel and sorbent are separately fed into the Transport Gasifier through lockhoppers. Coal is ground to a nominal average particle diameter between 250 and 400 microns. Sorbent is ground to a nominal average particle diameter of 10 to 30 microns. Limestone or dolomitic sorbents are fed into the gasifier for sulfur capture. The gas leaves the Transport Gasifier cyclone and goes to the primary gas cooler which cools the gas prior to entering the Siemens Westinghouse PCD barrier filter. The PCD uses ceramic or metal elements to filter out dust from the gasifier. The filters remove almost all the dust from the gas stream to prevent erosion of a downstream gas turbine in a commercial plant and to reduce the plant particulate emissions. The operating temperature of the PCD is controlled both by the gasifier temperature and by an upstream gas cooler. For test purposes, 0 to 100 percent of the gas from the Transport Gasifier can flow through the gas cooler. The PCD gas temperature can range from 700 to 1,600°F. The filter elements are back-pulsed by high-pressure nitrogen in a desired time interval or at a given maximum pressure difference across the elements. There is a secondary gas cooler after the filter vessel to cool the gas before discharging to the stack or atmospheric syngas combustor (thermal oxidizer). In a commercial process, the gas from the PCD would be sent to the gas turbine of a combined cycle unit. At the PSDF, a small portion of the synthesis gas can also flow to a specialized gas clean-up system downstream of the PCD. The gas clean-up system removes sulfur, nitrogen, and chlorine compounds, providing a synthesis gas suitable for use in a fuel cell. The main flow of fuel gas continues down one of the following two alternative paths.

In one case, the fuel gas flows to the secondary gas cooler and is sampled for on-line analysis. After exiting the secondary gas cooler, the gas is then let down to about 2 psig through a pressure control valve. The fuel gas is then sent to the atmospheric syngas burner to burn the gas and oxidize all reduced sulfur compounds (H_2S, COS, and CS_2) and reduced nitrogen compounds (NH_3 and HCN). The atmospheric syngas burner uses propane as a supplemental fuel. The gas from the atmospheric syngas burner goes to the baghouse and then to the stack. In the alternative path, the fuel gas flows for combustion in the piloted syngas burner to supply the gas turbine/generator, and then the flue gas goes to the stack.

The Transport Gasifier produces both fine ash collected by the PCD and coarse ash extracted from the Transport Gasifier standpipe. The two solid streams are cooled using screw coolers, reduced in pressure in lock hoppers and then combined together. Any fuel sulfur captured by sorbent should be in the form of calcium sulfide (CaS). Testing of the gasification ash (g-ash) has shown that it does not contain hazardous levels of CaS and that the waste solids are suitable for commercial use or disposal. Therefore, the ash is currently sent directly to the ash silo for disposal though the capability to feed the ash to the AFBC is retained.

Table 2.2-1

Major Equipment in the Transport Reactor Train

TAG NAME	DESCRIPTION
BR0201	Reactor Start-Up Burner
BR0401	Syngas Combustor (Thermal Oxidizer)
BR0602	AFBC (Sulfator) Start-Up/PCD Preheat Burner
CO0201	Main Air Compressor
CO0401	Recycle Gas Booster Compressor
CO0601	AFBC (Sulfator) Air Compressor
CY0201	Primary Cyclone in the Reactor Loop
CY0207	Disengager in the Reactor Loop
CY0601	AFBC (Sulfator) Cyclone
DR0402	Steam Drum
DY0201	Feeder System Air Dryer
FD0206	Spent Solids Screw Cooler
FD0200	Fluidized Bed Coal Feeder System
FD0210	Coal Feeder System
FD0220	Sorbent Feeder System
FD0502	Fines Screw Cooler
FD0510	Spent Solids Transporter System
FD0520	Fines Transporter System
FD0530	Spent Solids Feeder System
FD0602	AFBC (Sulfator) Solids Screw Cooler
FD0610	AFBC (Sulfator) Sorbent Feeder System
FL0301	PCD — Siemens Westinghouse
FL0302	PCD — Combustion Power
FL0401	Compressor Intake Filter
HX0202	Primary Gas Cooler
HX0203	Combustor Heat Exchanger
HX0204	Transport Air Cooler
HX0402	Secondary Gas Cooler
HX0405	Compressor Feed Cooler
HX0601	AFBC (Sulfator) Heat Recovery Exchanger
ME0540	Heat Transfer Fluid System
RX0201	Transport Reactor
SI0602	Spent Solids Silo
SU0601	Atmospheric Fluidized-Bed Combustor (AFBC)

Table 2.2-2 (Page 1 of 3)

Major Equipment in the Balance-of-Plant

TAG NAME	DESCRIPTION
BO2920	Auxiliary Boiler
BO2921	Auxiliary Boiler – Superheater
CL2100	Cooling Tower
CO2201A-D	Service Air Compressor A-D
CO2202	Air-Cooled Service Air Compressor
CO2203	High-Pressure Air Compressor
CO2601A-C	Reciprocating N_2 Compressor A-C
CR0104	Coal and Sorbent Crusher
CV0100	Crushed Feed Conveyor
CV0101	Crushed Material Conveyor
DP2301	Baghouse Bypass Damper
DP2303	Inlet Damper on Dilution Air Blower
DP2304	Outlet Damper on Dilution Air Blower
DY2201A-D	Service Air Dryer A-D
DY2202	Air-Cooled Service Air Compressor Air Dryer
DY2203	High-Pressure Air Compressor Air Dryer
FD0104	MWK Coal Transport System
FD0111	MWK Coal Mill Feeder
FD0113	Sorbent Mill Feeder
FD0140	Coke Breeze and Bed Material Transport System
FD0154	MWK Limestone Transport System
FD0810	Ash Unloading System
FD0820	Baghouse Ash Transport System
FL0700	Baghouse
FN0700	Dilution Air Blower
HO0100	Reclaim Hopper
HO0105	Crushed Material Surge Hopper
HO0252	Coal Surge Hopper
HO0253	Sorbent Surge Hopper
HT2101	MWK Equipment Cooling Water Head Tank
HT2103	SCS Equipment Cooling Water Head Tank
HT0399	60-Ton Bridge Crane
HX2002	MWK Steam Condenser
HX2003	MWK Feed Water Heater

Table 2.2-2 (Page 2 of 3)

Major Equipment in the Balance-of-Plant

TAG NAME	DESCRIPTION
HX2004	MWK Subcooler
HX2103A	SCS Cooling Water Heat Exchanger
HX2103C	MWK Cooling Water Heat Exchanger
LF0300	Propane Vaporizer
MC3001-3017	MCCs for Various Equipment
ME0700	MWK Stack
ME0701	Flare
ME0814	Dry Ash Unloader for MWK Train
ML0111	Coal Mill for MWK Train
ML0113	Sorbent Mill for Both Trains
PG0011	Oxygen Plant
PG2600	Nitrogen Plant
PU2000A-B	MWK Feed Water Pump A-B
PU2100A-B	Raw Water Pump A-B
PU2101A-B	Service Water Pump A-B
PU2102A-B	Cooling Tower Make-Up Pump A-B
PU2103A-D	Circulating Water Pump A-D
PU2107	SCS Cooling Water Make-Up Pump
PU2109A-B	SCS Cooling Water Pump A-B
PU2111A-B	MWK Cooling Water Pump A-B
PU2300	Propane Pump
PU2301	Diesel Rolling Stock Pump
PU2302	Diesel Generator Transfer Pump
PU2303	Diesel Tank Sump Pump
PU2400	Fire Protection Jockey Pump
PU2401	Diesel Fire Water Pump #1
PU2402	Diesel Fire Water Pump #2
PU2504A-B	Waste Water Sump Pump A-B
PU2507	Coal and Limestone Storage Sump Pump
PU2700A-B	Demineralizer Forwarding Pump A-B

Table 2.2-2 (Page 3 of 3)

Major Equipment in the Balance-of-Plant

TAG NAME	DESCRIPTION
PU2920A-B	Auxiliary Boiler Feed Water Pump A-B
SB3001	125-V DC Station Battery
SB3002	UPS
SC0700	Baghouse Screw Conveyor
SG3000-3005	4160-V, 480-V Switchgear Buses
SI0101	MWK Crushed Coal Storage Silo
SI0103	Crushed Sorbent Storage Silo
SI0111	MWK Pulverized Coal Storage Silo
SI0113	MWK Limestone Silo
SI0114	FW Limestone Silo
SI0810	Ash Silo
ST2601	N_2 Storage Tube Bank
TK2000	MWK Condensate Storage Tank
TK2001	FW Condensate Tank
TK2100	Raw Water Storage Tank
TK2300A-D	Propane Storage Tank A-D
TK2301	Diesel Storage Tank
TK2401	Fire Water Tank
XF3000A	230/4.16-kV Main Power Transformer
XF3001B-5B	4160/480-V Station Service Transformer No. 1-5
XF3001G	480/120-V Miscellaneous Transformer
XF3010G	120/208 Distribution Transformer
XF3012G	UPS Isolation Transformer
VS2203	High-Pressure Air Receiver
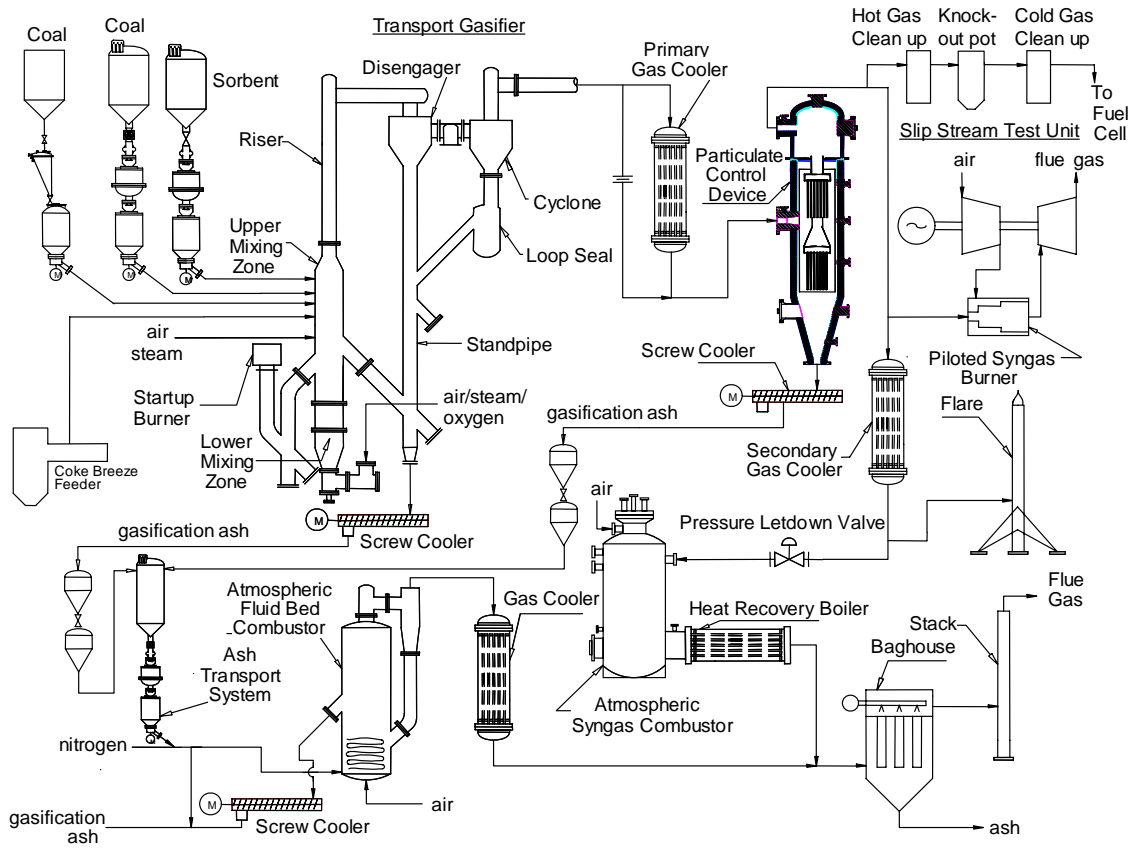
Figure 2.2-1 Flow Diagram of the Transport Gasifier Train

2.3 SIEMENS WESTINGHOUSE PARTICULATE CONTROL DEVICE

The PCD that has been used in all of the testing to date was designed by Siemens Westinghouse. The dirty gas enters the PCD below the tube sheet and flows through the filter elements, depositing the particulate on the filter element surface. The clean gas passes from the plenum/filter element assembly through the plenum pipe to the outlet pipe. As the particulate collects on the outside surface of the filter elements, the pressure drop across the filter system gradually increases. The filter cake is periodically dislodged by injecting a high-pressure gas pulse to the clean side of the filter elements. The cake then falls to the discharge hopper.

Until the first gasification run in late 1999, the Transport Reactor had been operated only in the combustion mode. Initially, high-pressure air was used as the pulse gas for the PCD, however, the pulse gas was changed to nitrogen early in 1997. The pulse gas was routed individually to the two-plenum/filter element assemblies via injection tubes mounted on the top head of the PCD vessel. The pulse duration was typically 0.1 to 0.5 seconds.

A sketch of the Siemens Westinghouse PCD is shown in Figure 2.3-1.

Clean
Gas Out

Dirty Gas
In

Shroud

- Maximum of 91 filter element Candles on two plenums
- Top and bottom plenums are back-pulsed separately
- Tangential inlet
- Cylindrical shroud

Top View

Shroud
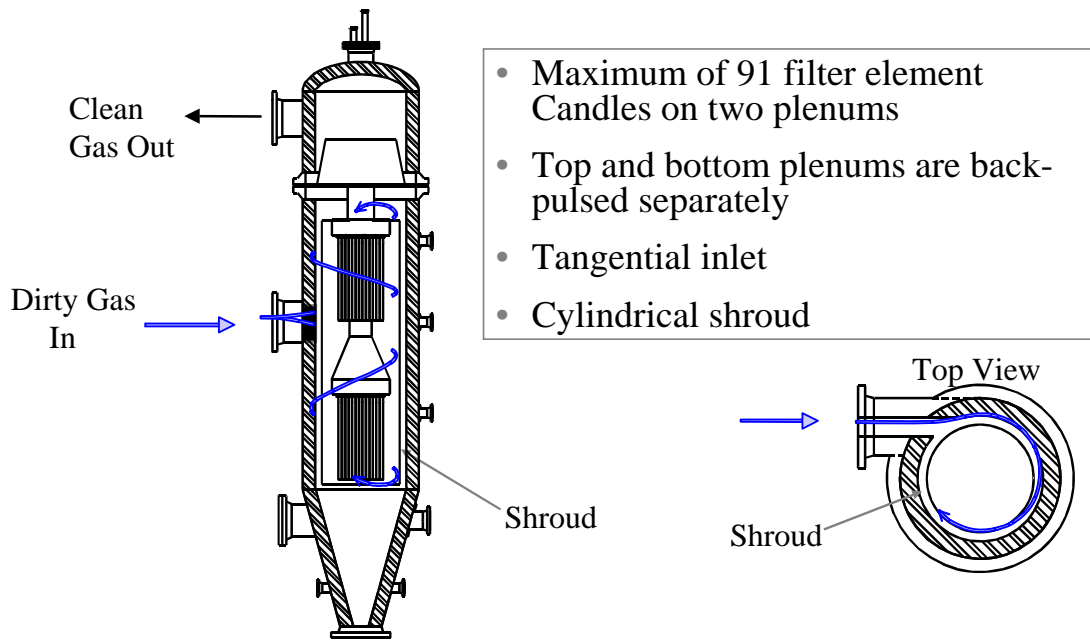
Figure 2.3-1 Siemens Westinghouse PCD (FL0301)

2.4 OPERATION HISTORY

Conversion of the Transport Reactor train to gasification mode of operation was performed from May to September 1999. The first gasification test run, GCT1, was planned as a 250-hour test run to commission the Transport Gasifier and to characterize the limits of operational parameter variations. GCT1 was started on September 9, 1999, with the first part completed on September 15, 1999 (GCT1A). The second part of GCT1 was started on December 7, 1999, and completed on December 15, 1999 (GCT1B-D). This test run provided the data necessary for preliminary analysis of gasifier operations and for identification of necessary modifications to improve equipment and process performance. Five different feed combinations of coal and sorbent were tested to gain a better understanding of the gasifier solids collection system efficiency.

GCT2, planned as a 250-hour characterization test run, was started on April 10, 2000, and completed on April 27, 2000. Additional data was taken to analyze the effect of different operating conditions on gasifier performance and operability. A blend of several Powder River Basin (PRB) coals was used with Longview limestone from Alabama. In the outage following GCT2, the Transport Gasifier underwent a major modification to improve the operation and performance of the gasifier solids collection system. The most fundamental change was the addition of the loop seal underneath the primary cyclone.

GCT3 was planned as a 250-hour characterization with the primary objective to commission the loop seal. A hot solids circulation test (GCT3A) was started on December 1, 2000, and completed December 15, 2000. After a 1-month outage to address maintenance issues with the main air compressor, GCT3 was continued. The second part of GCT3 (GCT3B) was started on January 20, 2001, and completed on February 1, 2001. During GCT3B a blend of several PRB coals was used with Bucyrus limestone from Ohio. The loop seal performed well needing little attention and promoting much higher solids circulation rates and higher coal-feed rates, which resulted in lower relative solids loading to the PCD and higher char retention in the gasifier.

GCT4, planned as a 250-hour characterization test run, was started on March 7, 2001, and completed on March 30, 2001. A blend of several PRB coals with Bucyrus limestone from Ohio was used. More experience was gained with the loop seal operations and additional data was collected to better understand gasifier performance.

TC06, planned as a 1000-hour test campaign, was started on July 4, 2001, and completed on September 24, 2001. A blend of several PRB coals with Bucyrus limestone from Ohio was used. Both gasifier and PCD operations were stable during the test run with a stable baseline pressure drop. Due to its length and stability, the TC06 test run provided valuable data necessary to analyze long-term gasifier operations and to identify necessary modifications to improve equipment and process performance.

TC07, planned as a 500-hour test campaign, was started on December 11, 2001, and completed on April 5, 2002. A blend of several PRB coals and a bituminous coal from the Calumet mine in Alabama were tested with Bucyrus limestone from Ohio. Due to

operational difficulties with the gasifier (stemming from instrumentation problems) the unit was taken offline several times. PCD operations were relatively stable considering the numerous gasifier upsets.

TC08, planned as a 250-hour test campaign to commission the gasifier in oxygen blown mode of operation, was started on June 9, 2002, and completed on June 29, 2002. A blend of several PRB coals was tested in air blown, enriched air and oxygen blown modes of operation. The transition from different modes of operation was smooth and it was demonstrated that the full transition could be made within 15 minutes. Both gasifier and PCD operations were stable during the test run with a stable baseline pressure drop.

TC09 was planned as a 250-hour test campaign to characterize the gasifier and PCD operations in air- and oxygen-blown mode of operations using a bituminous coal. TC09 was started on September 3, 2002, and completed on September 26, 2002. A bituminous coal from the Sufco mine in Utah was successfully tested in air- and oxygen-blown modes of operation. Both gasifier and PCD operations were stable during the test run.

TC10 was planned as a 500-hour test campaign to conduct long-term tests to evaluate the gasifier and PCD operations in oxygen-blown mode of operations using a blend of several PRB coals. TC10 was started on November 16, 2002, and completed on December 18, 2002. Despite problems with the coal mills, coal feeder, pressure tap nozzles, and the standpipe, the gasifier did experience short periods of stability during oxygen-blown operation. During these periods, the syngas quality was high. During TC10, over 609 tons of Powder River Basin subbituminous coal was gasified.

TC11 was planned as a 250-hour test campaign to conduct short-term tests to evaluate the gasifier and PCD operations in air- and oxygen-blown mode of operations using lignite from North Dakota. TC11 was started on April 7, 2003, and completed on April 18, 2003. During TC11, as a result of the high moisture content in the fuel, the lignite proved difficult to feed due to difficulties in the mill operation. However, the gasifier operated better using lignite than with any other feedstock used to date. The lignite allowed high circulation rates and riser densities. Consequently, the temperature distribution in both the mixing zone and the riser was more uniform than in any previous test run, varying less than 10°F throughout the gasifier.

TC12 was planned as a 250-hour test campaign to conduct short-term tests to evaluate the gasifier and PCD operations in air- and oxygen-blown mode of operations using a blend of several PRB coals. TC12 was started on May 16, 2003, and completed on July 14, 2003. A primary focus for TC12 was commissioning a new gas clean-up system and operating a fuel cell on syngas derived from the Transport Gasifier. The fuel cell system and gas clean-up system both performed well during the testing.

Figure 2.4-1 provides a summary of operating test hours achieved with the Transport Reactor at the PSDF.
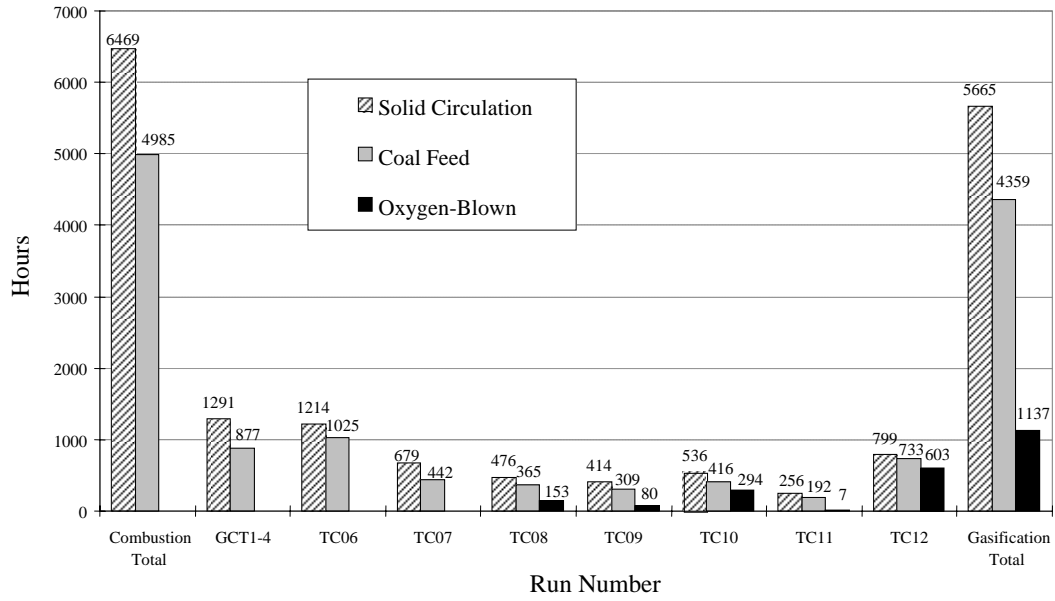
Figure 2.4-1 Operating Hours Summary for the Transport Reactor Train

3.0 TRANSPORT GASIFIER

3.1 TC12 RUN SUMMARY

Test run TC12 began on May 16, 2003, with the startup of main air compressor and the lighting of the gasifier start-up burner. The Transport Gasifier operated until May 24, 2003, when a scheduled outage occurred to allow maintenance crews to install the fuel cell test unit and modify the gas clean-up system. On June 18, 2003, the test run resumed when operations relit the start-up burner, and testing continued until the scheduled end of the run on July 14, 2003. Over the course of the entire test run, gasifier temperatures varied between 1,675 and 1,850°F at pressures from 130 to 210 psig.

The primary objectives of test run TC12 were:

- Operational Stability – Characterize gasifier loop and PCD operations in both air- and oxygen-blown modes with short-term tests by varying the coal-feed rate, the oxygen-to-coal ratio, the riser velocity, the solids-circulation rate, the system pressure, and oxygen distribution.

- Fuel Cell Operations – Operate a 1-kW fuel cell on syngas derived from the Transport Gasifier.

- Gas Cleanup – Clean the pollutants from a slipstream of syngas, lowering the total reduced sulfur content to less than 100 ppb, at both low and high temperatures to support the fuel cell testing.

Secondary objectives included the following:

- Gasifier Operations – Evaluate the effects of process operations on heat release, heat transfer, and accelerated fuel particle heat-up rates. Study the effect of changes in gasifier conditions on temperature profiles and product gas composition.

- Effects of Gasifier Conditions on Synthesis Gas Composition – Continue to evaluate the effects of different gasifier parameters such as steam-to-coal ratio, air distribution, and gasifier temperature on CO/CO_2 ratio, carbon conversion, synthesis gas lower heating value (LHV), product gas composition, sulfur and ammonia emissions, cold and hot gas efficiencies.

- Test the New Coal-Feed System – Test the new fluidized-bed coal-feed system, and streamline the integration of the gasifier logic with the feeder logic.

- Automation – Demonstrate and improve the automatic control of the gasifier including refining the single parameter temperature control in air-blown mode, implementing multiparameter temperature control in oxygen-blown mode, handling steam drum upsets, and improving key gasifier control loops.

- Evaluate Instrumentation Required for Automation – Continue to improve thermowell life and pressure differential measurement reliability in the Transport Gasifier. This includes testing various materials of construction, design details, fabrication, and variations in

pressure tap purge including temperature and flow rate. Continue commissioning and evaluating nuclear density instruments for solids flow rates and solids inventory measurements.

- Study the Effects of Moisture on the Coal-Feed System – Study the effect of pulverized PRB moisture content on feed system operations. Improve the coal grinding process to reduce the moisture content in the coal.

- Evaluate Sulfur Emissions – Evaluate the sulfur emissions using PRB coal without limestone addition. Determine if the coal ash contains sufficient calcium for sulfur capture.

- Evaluate Ceramic Ferrules – Continue to evaluate the performance of the ceramic ferrules in the syngas cooler.

- Maintain Consistent Syngas Quality to Fuel Cell – During the fuel cell testing, operate the gasifier over a narrow range of conditions to provide a consistent supply of high quality syngas.

- Ammonia Reduction – Test a new nickel-based catalyst in the gasifier for use in removing ammonia from the syngas.

The activities that occurred during the outage preceding test run TC12 and the short outage in the middle of TC12 included 21 equipment revisions. The installation and modifications listed below affected the process the most.

- A new fuel cell test skid provided cleaned syngas from the Transport Gasifier to a solid oxide fuel cell.

- A new standpipe level controller monitored the level according to LI339 and started and stopped the coarse solids screw cooler as needed to maintain the standpipe level within a certain range.

All gasifier start-up processes, including the PCD preheat, and gasifier preheat using the start-up burner, went smoothly. When the gasifier temperature reached 1,100°F, at 16:51 on May 17, coke breeze feed began. At 18:24, once the gasifier temperature reached 1,650°F, coal feed began. The gasifier operated for 3 days at a coal-feed rate between 3,400 and 4,200 pph at 210 psig in air-blown mode. Occasionally limestone was fed as a sorbent. Other than a short gasifier trip that occurred due to a problem in the distributed control system (DCS) at 00:52 on May 20, the gasifier ran in a stable manner.

The gasifier ran extremely well in oxygen-blown operation at 150 psig for almost 4 days, which started at 20:45 on May 20. At this time, testing on the hot gas clean-up system and on the new fluidized-bed coal feeder took place. Both systems showed great promise, although the gas clean-up system experienced a few problems with crystals plugging its lines, it was able to significantly reduce the amount of sulfur in the slipstream of syngas. The fluidized-bed feeder ran for several hours without interruption, a large improvement over its performance in previous test runs.

At 09:40 on May 24, the gasifier was shut down for a scheduled outage to add a crystal knock-out pot to the slipstream gas clean-up system and to install the fuel cell test unit. The work went as scheduled, and the test run resumed on June 18, followed by coal feed at 02:00 on June 20. After the subsequent transition to oxygen-blown operations, the gasifier ran at a pressure of about 150 psig and at a mixing zone temperature of around 1,825°F for the next several days.

Early in the morning of June 22, the coal conveying line plugged, but operators were able to unplug the line, and coal feed resumed within 10 minutes of the gasifier trip. After the trip, gasifier operations were stable, allowing the fuel cell testing to proceed without difficulty. During this time, packing or bubble formation would occasionally take place in the gasifier standpipe, but the adjustment of standpipe aeration flows, solids inventory, and riser velocities corrected the problem each time before a major gasifier upset could occur. The standpipe abnormalities did not affect the fuel cell testing.

The solid oxide fuel cell ran intermittently during the period of June 21 to June 27, testing two stacks for a total period of 75 hours. With the new knock-out pot in place, the slipstream gas clean-up system operated well, preventing sulfur, chlorine, and crystals from entering the fuel cell, and the new knock-out pot prevented crystals from plugging the clean-up system. Later in the test run, some of the gas clean-up system was bypassed to test the effects of small amounts of sulfur to the fuel cell. No major problems occurred in the fuel cell due to sulfur contamination at that time.

At 15:05 on June 28, a day after the fuel cell tests were complete, a motor inverter fault in the coal feeder caused a gasifier trip. Although the motor restarted easily, a large amount of carbon accumulated in the lower mixing zone (LMZ). During the subsequent transition to oxygen-blown operations, the temperatures in the LMZ increased to the point where a large deposit formed. However, the deposit did not completely restrict the flow path through the LMZ and the test run continued. Once conditions stabilized, the gasifier ran at lower temperatures and with a higher steam flow rate to minimize the growth of the deposit.

On June 30, testing resumed on the fluidized-bed coal feeder. While running in tandem with the coal rotofeeder, the fluidized-bed feeder performed well during the most of the remainder of the test run, accumulating over 200 hours of operation (as many as 50 continuous hours).

On July 2 the MWK coal milling system began to experience problems with coal moisture, primarily plugging in the mill screw cooler. At that time, the gasifier ran at a reduced coal-feed rate while feeding supplemental coke breeze. Coal moisture also created difficulties for the coal rotofeeder. At 14:26 on July 3, while feeding the high moisture coal, the gear shaft sheared. The gasifier operated on coke breeze for over 20 hours while maintenance repaired the gearbox.

Coal feed resumed the afternoon of July 4. The as-received coal moisture was much lower over the next few days, and coal feeder performance improved dramatically. As a result, the gasifier ran steadily in the oxygen-blown mode for the next few days at a mixing zone temperature of between 1,750 and 1,800°F and at a pressure of 135 psig.

Ammonia removal testing occurred during the final portion of the test run and comprised injecting a nickel-based catalyst into the gasifier. The nickel-based catalyst had only a modest effect in

ammonia removal, most likely due to its short residence time in the system and inconsistent feed rate.

The remainder of the test run was stable. At 23:25 on July 14 a semidirty gasifier shut down occurred, leaving a filter cake on the upper PCD plenum, while allowing the lower plenum to back-pulse clean. During the test run, the gasifier accumulated 733 hours of coal feed, 603 of which were in oxygen-blown mode, bringing the total gasification time to 4,359 hours.

The post-run inspections revealed that the gasifier refractory continued to show only minor wear. A few pieces of the hexagonal refractory hex-mesh pieces had fallen from the cyclone roof into the loop seal, but otherwise, the cyclone, disengager, and primary gas cooler were in good condition. The deposit in the lower mixing zone was large, at about 5 feet in height and covering the entire LMZ with the exception of a few paths in which the air and oxygen could flow. Other than the LMZ, the gasifier was clear of any significant deposits. (See Table 3.1-1.)

The test run contained the following steady-state test periods:

Name	Comments
TC12-1	First steady-state period.
TC12-2	Increased temperature, circulation.
TC12-3	Increased temperature.
TC12-4	Decreased coal-feed rate, circulation.
TC12-5	Decreased temperature.
TC12-6	Decreased steam flow rate.
TC12-7	Started the fluid-bed coal feeder.
TC12-8	Stopped the fluidized-bed feeder. Decreased coal.
TC12-9	Transition to oxygen-blown mode.
TC12-10	Increased mixing zone temperature.
TC12-11	Decreased pressure.
TC12-12	Decreased pressure further.
TC12-13	Decreased temperature.
TC12-14	Increased steam flow rate.
TC12-15	Increased temperature, lowered steam.
TC12-16	Started the fluid-bed coal feeder.
TC12-17	Increased the coal-feed rate.
TC12-18	First steady-state after outage (EA).
TC12-19	Completed oxygen-blown transition.
TC12-20	Raised temperature. Lowered pressure.
TC12-21	Lowered pressure.
TC12-22	Increased coal-feed rate.
TC12-23	Increased mixing zone temperature.
TC12-24	Reduced temperature and pressure.
TC12-25	Increased temperature, steam.
TC12-26	Increased temperature, reduced steam.
TC12-27	Reduced inventory.
TC12-28	Increased steam flow rate.

Name	Comments
TC12-29	Reduced coal-feed rate.
TC12-30	Increased temperature.
TC12-31	Increased circulation rate.
TC12-32	Increased temperature.
TC12-33	Increased steam, lowered temperature.
TC12-34	Started the fluidized-bed coal feeder.
TC12-35	Increased temperature.
TC12-36	Increased temperature, lowered steam.
TC12-37	Coke breeze and coal minimum fire.
TC12-38	Return to normal operation.
TC12-39	Lowered coal-feed rate.
TC12-40	Recovery after small unsteady period.
TC12-41	Recovery after unsteady period.
TC12-42	Increased temperature.
TC12-43	Increased coal-feed rate.
TC12-44	Reduced steam. Started the fluidized-bed coal feeder.
TC12-45	Reduced pressure. Raised steam.
TC12-46	Increased pressure.
TC12-47	Reduced temperature.
TC12-48	Increased coal-feed rate.
TC12-49	Continuation of previous.
TC12-50	Reduced coal-feed rate.
TC12-51	Increased coal-feed rate, temperature.
TC12-52	Increased pressure.
TC12-53	Reduced pressure, steam flow rate.

Table 3.1-1

TC12 Operating Conditions for Transport Gasifier

Start-Up Bed Material	Sand ($\sim$ 120 μm)
Fuel Type	Powder River Basin
Fuel Particle Size (mmd)	250 μm
Average Fuel-Feed Rate (pph)	1,300 to 5,200
Sorbent Type	Ohio Bucyrus Limestone
Sorbent Particle Size (mmd)	25 μm MMD
Sorbent Feed Rate	0 - 800 pph
Gasifier Temperature (°F)	1,675 to 1,775
Gasifier Pressure (psig)	130 to 210
Riser Gas Velocity (fps)	30 to 65
Riser Mass Flux, lb/s·ft^2	350 - 450 (average slip ratio = 2)
Standpipe Level, in. H$_2$O (LI339)	75 - 200
Primary Gas Cooler Bypass	0%
PCD Temperature, °F	660 – 810
Total Gas Flow Rate, pph	12,500 - 24,100
Oxygen/coal Mass Ratio, lb/lb	0.66 - 0.84
Steam-to-Coal Ratio	0.15 to 1.31

3.2 GASIFIER TEMPERATURE PROFILES

To better understand gasifier operations and evaluate the effect of different parameters on the temperature in different areas of the gasifier, the temperature profile in the gasifier is studied. Section 3.2 discusses these results. A schematic of the gasifier with relative thermocouple locations is given in Figure 3.2-1. The gasifier was operated in air- and oxygen-blown modes during TC12 with a mixture of Powder River Basin (PRB) coals. In this section the temperature profile for air- and oxygen-blown operations are discussed and the effect of carbon content in the circulating solids on the temperature profile is evaluated.

The temperature profile for a steady-state period in air-blown mode is shown in Figure 3.2-2 (TC12-3). The temperature in the lower mixing zone (LMZ), increases quickly (T1-T3) as the heat released from char combustion heats the air, steam, and solids in the LMZ, but then decreases as the carbon in the LMZ is consumed (T4-T5). The temperature (T6) decreases further when cooler solids from the J-leg (T22) enter the upper mixing zone (UMZ). Additional air is injected into the UMZ and the temperature (T7-T9) increases due to char combustion throughout the UMZ. Coal is added before the UMZ transitions into the riser as shown in Figure 3.2-1. Heating the coal and conveying gas, as well as coal devolatilization and endothermic gasification reactions combined with heat losses decrease the temperature (T10-T14) as the gas and solids flow up through the riser. The solids removed by the disengager and cyclone cool as they flow down the standpipe (T15-T21). The solids are heated (T22) as they reenter the UMZ (T6) by the hot gases and solids in the LMZ.

The temperature profile for a steady-state period in oxygen blown mode is shown in Figure 3.2-3 (TC12-10). The LMZ temperature (T1-T5) increases quickly as the heat released from char combustion heats the oxygen, steam, and solids in the LMZ. The temperature (T6-T9) increases further as char combustion continues in the UMZ. Coal and conveying gas heat-up, coal devolatilization, and endothermic gasification reactions combined with heat losses decrease the temperature (T10-T14) as the gas and solids flow up through the riser. The solids removed by the disengager and cyclone cool as they flow down the standpipe (T15-T22). As in air blown mode, the solids are heated (T22) when they reenter the UMZ (T6) by the hot gases and solids in the LMZ.

Several operating parameters influence the temperature profile: coal-feed rate, amount of carbon in circulating solids, solids circulation rate, and oxygen and steam-flow rates and distribution. The temperature profiles for two steady-state periods during oxygen-blown mode with lower and higher carbon content in the circulating solids (TC12-14 and -22) are shown in Figure 3.2-4. With lower carbon content in the circulating solids, the temperature in the LMZ decreases (T4-T5) after the initial temperature increase (T1-T3) since all of the carbon is quickly consumed. With higher carbon content the temperature continues to increase throughout the LMZ resulting in a higher LMZ operating temperature (T4-T5).
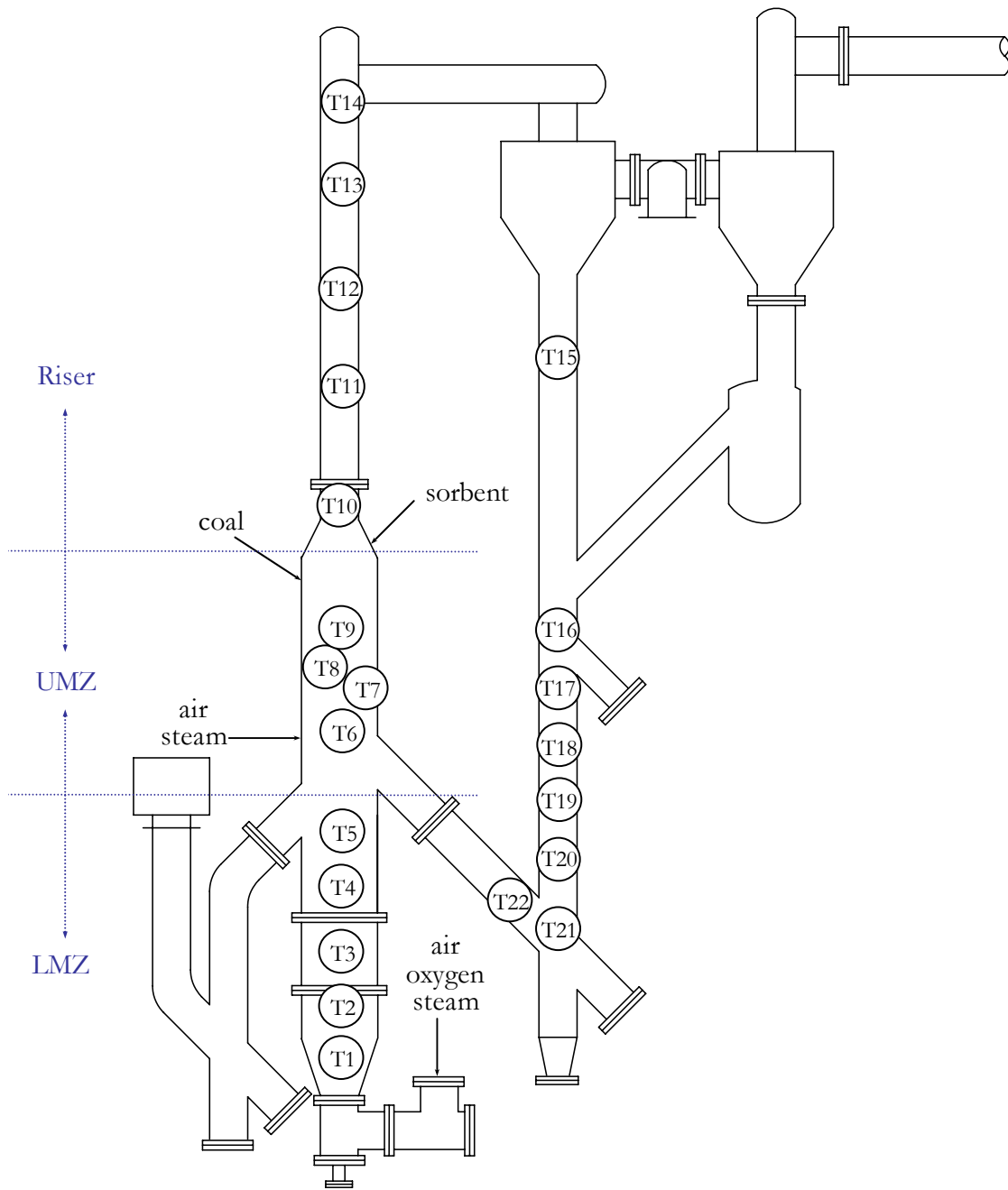
Figure 3.2-1   Transport Gasifier Schematic
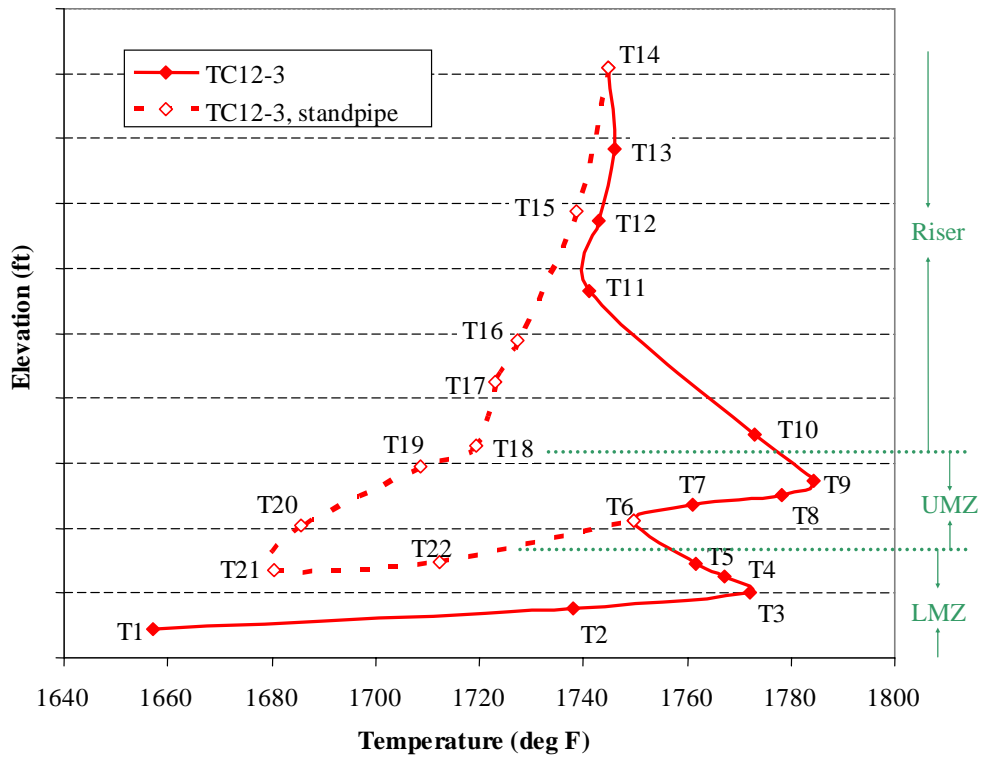
Figure 3.2-2   Temperature Profile in Air-Blown Mode in TC12 (TC12-3)
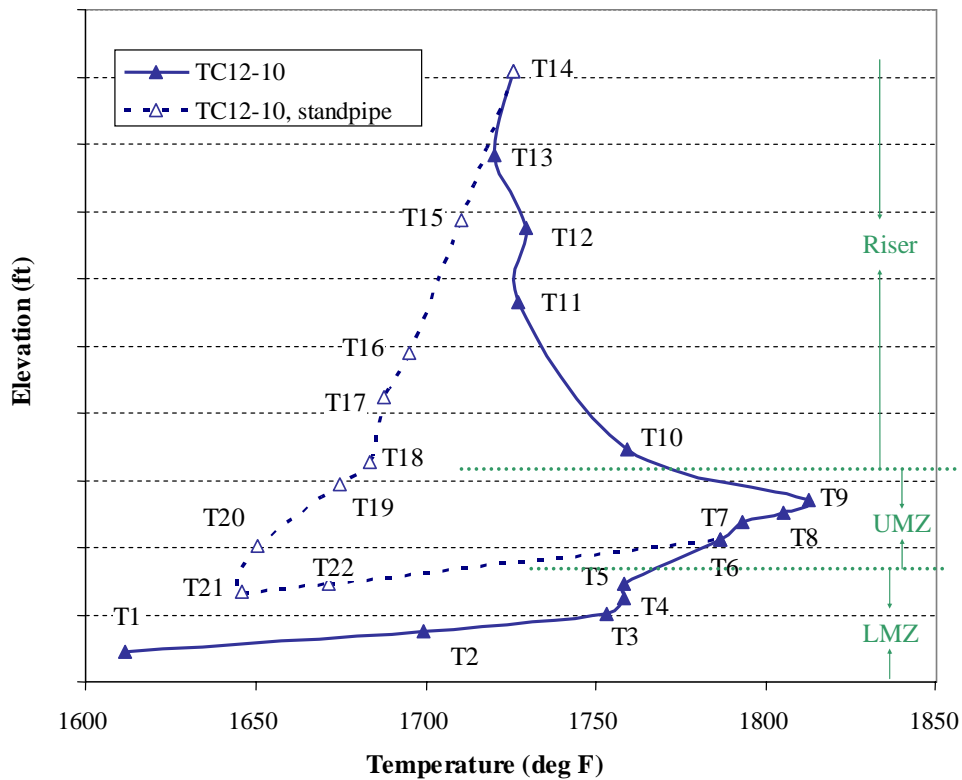
Figure 3.2-3   Temperature Profile in Oxygen-Blown Mode in TC12 (TC12-10)
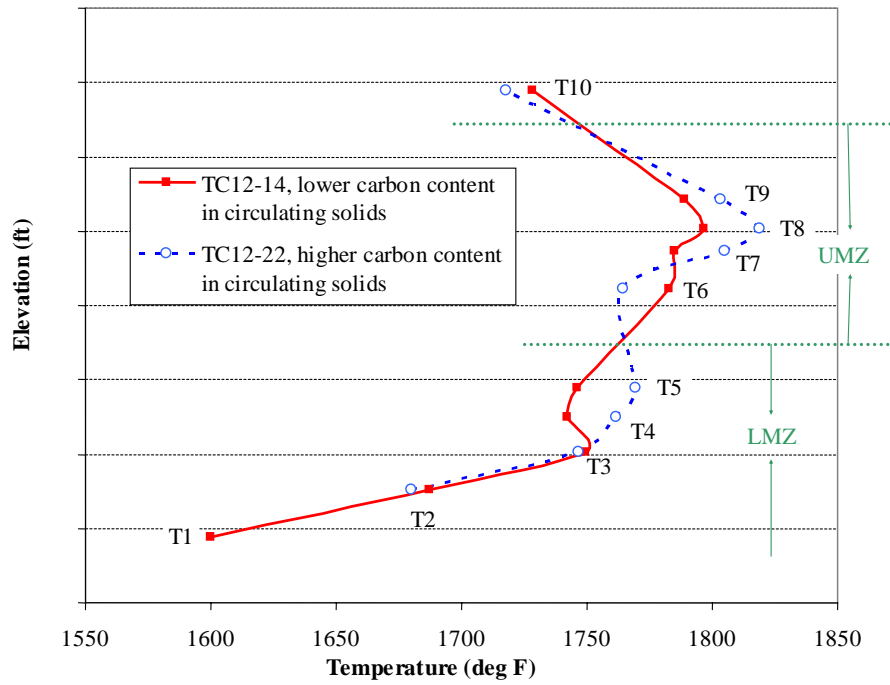
Figure 3.2-4　　Temperature Profile in TC12 for Lower and Higher Carbon Conversion (TC12-14 and -22)

3.3   GAS ANALYSIS

3.3.1 Summary and Conclusions

- The raw synthesis gas lower heating values (LHVs) were between 55 and 58 Btu/scf for air-blown operation and between 59 and 100 Btu/scf for oxygen-blown operation. During one period of coal and coke breeze cofeeding, the LHV dropped to 19 Btu/scf.

- The LHV for both modes of operation was a strong function of the relative amount of oxygen fed to the Transport Gasifier.

- The nitrogen-corrected, adiabatic synthesis gas LHV ranged from 98 to 109 Btu/scf for air-blown operation, and between 126 and 255 Btu/scf for normal oxygen-blown operation. The coke breeze/coal cofeed period produced syngas with a nitrogen-corrected LHV of 126 Btu/scf.

- Total reduced sulfur (TRS, mostly H_2S) emissions were between 163 and 249 ppm for air-blown operations and between 152 and 568 ppm for oxygen-blown operations.

- Synthesis gas analyzer data for CO was good, with four out of six analyzers in agreement for all of TC12, and another analyzer in agreement for the majority of the test run.

- Synthesis gas analyzer data for H_2 was good with both gas chromatographic analyzers in agreement for most of TC12.

- Synthesis gas analyzer data for CH_4 was good in that two of the CH_4 analyzers were in agreement for most of TC12.

- Synthesis gas analyzer data for C_2^+ was unreliable in that AI419 read zero for the second half of the run, while AI464 was erratic for the entire test run.

- Synthesis gas analyzer data for CO_2 was good in that three out of four analyzers were in agreement for most of TC12.

- Synthesis gas analyzer data for N_2 was excellent in that both GC analyzers (AI464 & AI419) were in agreement for almost all of TC12.

- The synthesis gas H_2O measured by AI475H agreed with the in situ H_2O measurements for all in situ moisture contents below 25 percent.

- The sum of the dry gas analyzer concentrations was between 98 and 102 percent.

- One of the syngas H_2S analyzers reasonably agreed with the sulfur emissions indicated based on the syngas combustor SO_2 analyzer.

- The total reduced sulfur (TRS) was approximately the same as the minimum equilibrium H_2S concentration.

- The two NH_3 gas analyzers did not agree with each other during TC12.

- The NH_3 emissions were between 1,000 and 1,500 ppm for air-blown mode and were between 2,000 and 3,000 ppm for oxygen-blown mode.

- The NH_3 emissions best agreed with equilibrium calculations at 60°F above the PCD inlet temperature.

- The naphthalene analyzer was out of service for air-blown operation and ranged between 0 and 500 ppm for oxygen-blown operation.

- The CO/CO_2 ratio was around 1.0 in air-blown mode and between 0.2 and 1.0 for oxygen-blown mode.

- The water-gas shift constants using the in situ H_2O measurements were between 0.53 and 0.92, despite large variations in H_2O, H_2, CO, and CO_2 concentrations.
- The water-gas shift constants using the H_2O analyzer were between 0.47 and 0.87, despite large variations in H_2O, H_2, CO, and CO_2 concentrations.
- The synthesis gas molecular weight was between 26.8 and 27.0 pounds/mole for air-blown mode and between 23.3 and 25.5 pounds/mole for oxygen-blown mode.
- The synthesis gas combustor oxygen balance was excellent.
- The synthesis gas combustor hydrogen balance was excellent.
- The synthesis gas combustor carbon balance was acceptable.

3.3.2 Introduction

The major goal for TC12 was to supply syngas from the Transport Gasifier in oxygen-blown mode to the gas cleanup system and fuel cell. The coal used in the Transport Gasifier during TC12 was from the Powder River Basin. Steady coal feed began on May 17, 2003, using air as an oxidant. After about 70 hours of air-blown operation, the oxygen-blown tests began. On May 24, 2003, 159 hours after the beginning of the test run, a scheduled outage occurred, when Delphi installed a fuel cell test skid, and the PSDF maintenance personnel made a few adjustments to the gas cleanup train. Coal feed resumed on June 20, 2003, and the gasifier ran fairly continuously for about 300 hours until the gearbox on the FD0210 coal feeder failed, tripping the unit on July 3, 2003. After the coal feeder was repaired, the test run achieved another 250 hours from July 4 to July 14, 2003.

There were 53 steady periods of operation between May 17 and July 14. The steady periods of operation are given on Table 3.3-1. Operating periods TC12-28 and TC12-36 were very long steady-state periods that were broken down into smaller periods for more detailed analysis, giving a total of 56 periods for analysis. The first eight operating periods (TC12-1 through TC12-8) were air-blown, while the remainder (TC12-9 through TC12-53) occurred during oxygen-blown operation. Even during oxygen-blown operation, about 1,000 to 2,000 pph of air flowed through the upper mixing nozzles to prevent them from plugging and to ensure sufficient riser velocity. Test run TC12-37 differed from the other test periods in that a small amount of coke breeze was fed to the reactor along with the coal.

Sorbent was injected into the Transport Gasifier during portions of TC12. The operating periods that featured sorbent injection were TC12-4 through TC12-13, TC12-47, and TC12-52.

Table 3.3-2 lists some of the TC12 operating conditions, including mixing zone temperatures, pressure control valve pressures, PCD inlet temperatures, air rate, oxygen rate, syngas rate, steam rate, and nitrogen rate. The system pressure was 210 psig for the air-blown periods. During the oxygen-blown periods the system pressure ranged from 130 to 155 psig.

3.3.3 Raw Gas Analyzer Data

During TC12, the Transport Gasifier and synthesis gas combustor outlet gas analyzers continuously monitored the syngas, and the Plant Information System (PI) recorded the data.

Twenty-one in situ grab samples of synthesis gas moisture content were measured during PCD outlet loading sampling.

The gas analyzer system analyzed synthesis gas for the following gases during TC12 using the associated analyzers:

Gas   Analyzer Tag Name

CO   AI419C, AI425, AI434B, AI453G, AI464C, AI475C
CO_2 AI419D, AI434C, AI464D, AI475D
CH_4 AI419E, AI464E, AI475E
C_2^+ AI419F, AI464F
H_2 AI419G, AI464G
H_2O AI419H, AI475H, AI479H, AI480H
N_2 AI419B, AI464B
H_2S AI419J, AI480J
NH_3 AI475Q, AI480Q
HCl   AI479R
HCN   AI479S
COS   AI479T
CS_2 AI480W
$C_{10}H_8$ AI480X

The locations of the synthesis gas analyzers are shown on Figure 3.3-1. The AI464 and AI419 analyzers use a gas chromatograph and typically have about a 6-minute delay. Three of the other CO analyzers (AI425, AI434B, AI453B) and CO_2 analyzer (AI434C) are infrared-based and give more real-time measurements. All analyzers except for the AI475, AI479, and AI480 banks of analyzers require that the gas sample be conditioned to remove water vapor. Therefore, those analyzers report gas compositions on a dry basis.

The gas analyzers obtain synthesis gas samples from three different locations:

- Between the PCD (FL0301) and the secondary gas cooler (HX0202).
- Between the secondary gas cooler (HX0202) and the pressure letdown valve (PCV-287).
- Between the pressure letdown valve (PCV287) and the atmospheric syngas combustor (BR0401).

Having six CO analyzers allows for a measure of self-consistency when all or several of the six analyzers read the same value. A choice of which analyzer to use is necessary if the analyzers do not agree. The TC12 hourly averages for the six CO analyzers are given in Figure 3.3-2. The CO analyzer AI475C data was corrected to a dry composition using the H_2O analyzer AI475H data to compare with the other CO analyzers that measure on a dry basis. For the majority of the test run, the AI419C, AI425, AI453G, and AI464C CO analyzers were in good agreement. The values from the AI475C analyzer were close to those of the other analyzers at the beginning of the test run, but ran almost 5 percent higher over the last several hundred hours. The AI434B analyzer was out of service for a portion of TC12, as shown by the zero values in the

figure. From hour 246 to hour 333, the AI434B values were around 5 percent lower than the values from the other gas analyzers. For the remainder of the test run, however, AI434B agreed closely with the four agreeing analyzers.

The analyzer selection for each operating period is given in Table 3.3-3. AI419 was used for almost half of the operating periods. The good agreement between the CO analyzers gives confidence to the accuracy of the CO data. The low CO measurements occurred either in periods when the gas analyzers were being calibrated or were measurements made during a coal feeder trip. The CO data used in calculations were interpolated during times when the gas analyzers were being calibrated. The unit outage at hour 159 and the enhanced air- and oxygen-blown periods of operation are noted on Figure 3.3-2.

TC12 hourly averages data for the H_2 analyzers are shown on Figure 3.3-3. With the exception of a few periods at the beginning of the test run, analyzer AI464G gave reasonable results for the entire run, and AI464G and AI419G agreed with each other for several long periods of time. AI419G briefly went out of service for a few moments during the middle of the test run, forming the downward spike at hour 437. For the most part, the analyzers performed well, and either analyzer was used for the operating periods as shown in Table 3.3-3.

The TC12 hourly average gas analyzer data for CH_4 are given in Figure 3.3-4. From hour 340 until the end of the test run, analyzers AI464E and AI419E agreed well with each other. Prior to hour 340, the AI464E data followed the same trend as the AI419E data, but the AI464E data were very noisy and difficult to interpret. The AI475E dry-corrected data typically ran about 12 percent higher than the other two analyzers. Since it was more stable throughout the test run, analyzer AI419E was the selected analyzer for all of the operating periods, as shown in Table 3.3-3.

The TC12 hourly average gas analyzer data for C_2^+ are given in Figure 3.3-5. Analyzer AI419F ranged from 0.33 to 0.49 percent for the first 340 hours of TC12. It then read around 0.05 percent for the remainder of the test run. Analyzer AI464F either read zero or read erratically for all of TC12. Since the analyzers gave unreliable data with only small values, the C_2^+ content was assumed to be negligible for all of the TC12 data analysis.

The TC12 hourly carbon dioxide analyzer data are given on Figure 3.3-6. Analyzers AI419D and AI434C agreed with each other for most of TC12. Analyzer AI464D was erratic at the beginning of TC12, but agreed well with AI419D and AI434C, the last 400 hours of the test run. The AI475D data (dry) was consistently higher than AI419D and AI434C and clearly out of calibration. AI419D was the selected analyzer for all of the operating periods, as shown in Table 3.3-3.

The nitrogen analyzer data is given in Figure 3.3-7. With the exception of a few periods when the AI464B analyzer was out of service, the AI464B and AI419B data agreed for all of TC12. Analyzer AI464B was the selected analyzer for the first 17 test periods, while analyzer AI419B was used for the remaining operating periods (see Table 3.3-3).

Since both GC analyzers AI419 and AI464 analyze for nearly the entire spectrum of expected gas components, a useful consistency check of each analyzer is to plot the sum of the gases

measured by each bank of analyzers and evaluate how close the sums of compositions are to 100 percent. The sums of both GC analyzer banks are given on Figure 3.3-8. Analyzer AI419 was fairly consistent during TC12, usually between 98 and 101 percent. The analyzer AI464 sums were erratic for the first 340 hours of TC12 varying between 76 and 104 percent. During the latter portion of the test run, the AI464 analyzers stabilized, and their sums ranged between 97 and 103 percent, once dropping down to 90 percent. The inconsistent behavior of the AI464 sums gives one reason why the AI419 values were used for most analyses, rather than the AI464 values.

The H_2O analyzer AI419H is part of the AI419 GC. Since AI419 operates dry, and the synthesis gas H_2O is removed prior to analysis, AI419H always read 0.0 percent, and will not be discussed further.

The raw H_2S analyzer AI419J data is shown on Figure 3.3-9. The AI419J H_2S data seem reasonable in that the values were lower (100 to 300 ppm) during air-blown mode than during oxygen-blown mode (300 to 900 ppm), and all values seemed to be in the expected range for PRB coal. The AI480J data was not plotted since all of the reported concentrations were less than zero and clearly in error. The AI419J data will be compared with synthesis gas combustor SO_2 analyzer data in Section 3.3.8.

The raw ammonia analyzer AI475Q and AI480Q data are shown on Figure 3.3-10. Although the analyzers indicated the expected higher ammonia concentrations in oxygen-blown mode, the values did not agree with each other. AI480Q, in particular, was problematic in that the data consisted mostly of spikes, except during the air-blown portion of the test run when it read nearly zero.

According to AI475Q (the more stable of the two ammonia analyzers), the ammonia concentrations in air-blown mode were mostly between 1,000 and 1,500 ppm. These values were higher than those seen in Falkirk lignite testing, but typical for PRB air-blown testing. During the initial oxygen-enhanced testing, AI475Q ranged from 1,700 ppm to 3,050 ppm, with the majority of the values closer to 2,100 ppm. The TC12 oxygen-blown ammonia data were consistent with the oxygen-blown PRB ammonia emissions seen in previous test runs and higher than those seen during the oxygen-blown portions of the Falkirk lignite test run.

The raw hydrogen cyanide analyzer AI479S data is shown on Figure 3.3-11. For the first 360 hours of TC12, the analyzer was reading incorrectly. At hour 360, the analyzer value jumped to 120 ppm and fluctuated between 120 and zero for the remainder of the test run. Based on the HCN extractive samples for TC09 and TC10, the oxygen-blown HCN content is between 25 and 75 ppm. Unfortunately, no extractive samples were available for the TC12 test run.

Figure 3.3-12 shows all available COS and $C_{10}H_8$ data for TC12. Analyzer AI479T reported COS data for all of TC12. The data varied from 300 to 360 ppm and did not respond to changes in H_2S concentrations when in different modes of operation. The values are also higher than the expected COS concentrations of about 60 to 120 ppm in air-blown mode and 140 to 180 ppm in oxygen-blown mode (10 percent of the H_2S concentrations). In fact, the analyzer seems to indicate that the air-blown COS concentrations were higher than the oxygen-blown concentrations. The poor response to mode changes and higher than expected values lead to

the conclusion that the COS data from AI479T are not reliable and, therefore, not suitable for further analysis.

The raw naphthalene analyzer AI480X data is shown on Figure 3.3-12. The naphthalene analyzer was purchased to help measure the amount of hydrocarbons produced by the Transport Gasifier that were not being measured by the C_2^+ component of the GC analyzers. The amount of naphthalene also might indicate periods of tar formation. The data remained close to zero during air-blown operation. After the transition to oxygen-blown mode, the analyzer began indicating values from 0 to 500 ppm. The reliability of this measurement is not known at this time.

Analyzer AI479R reported HCl data for all of TC12, but was only active for the first 40 hours of the test run. The AI479R data varied from 0 to 50 ppm until hour 43 when the analyzer read less than zero for the remainder of TC12. The higher values are not in the expected range of syngas HCl. The maximum HCl syngas concentration can be determined from the PRB chloride concentration, the coal-feed rate, and the syngas flow rate. The maximum HCl syngas composition, assuming no HCl removal by the Transport Gasifier and PCD solids, is 14 ppm for air-blown mode and 18 ppm for oxygen-blown mode. The higher-than-possible HCl concentrations lead to the conclusion that the HCl data from AI479R are not reliable and therefore should not be used for analysis.

Analyzer AI480W reported CS_2 data for all of TC12. The data remained close to zero during air-blown operation. After the transition to oxygen-blown mode, the analyzer began indicating values from 0 to 100 ppm. The analyzer data were erratic and did not respond to changes in H_2S concentrations due to changes from air to enhanced air to oxygen-blown operation. The values were within the expected range of CS_2 (1 percent of the H_2S concentrations). The instability of the data, however, leads to the conclusion that the CS_2 data from AI480W are not reliable and therefore should not be used for analysis.

3.3.4 Gas Analysis Results

The dry, raw synthesis gas analyzer data was adjusted to produce the best estimate of the actual gas composition in three steps:

1. Choice of CO, H_2, CH_4, N_2, and CO_2 analyzer data to use (see Table 3.3-3).
2. Normalization of dry gas compositions (force to 100 percent total).
3. Conversion of dry compositions to wet compositions.

For the rest of this section, the data analysis will be based only on the TC12 operating periods (Table 3.3-1). The operating period averages of the sums of the dry gas analyses selected are shown on Figure 3.3-13. All of the operating periods have the sums of dry gas compositions between 98 and 102 percent. The average of all the operating sums of the dry gas composition is 99.9 percent, indicating virtually no bias.

During TC12 testing, there were two operating H_2O analyzers, AI475H and AI480H. The H_2O concentration was also measured at the PCD exit during PCD outlet particulate measurements. In previous gasification runs, the water-gas shift reaction was used to interpolate H_2O

measurements between in situ H_2O measurements and to check the consistency of the H_2O analyzer data, if available. The water-gas shift equilibrium constant should be a function of a Transport Gasifier mixing zone or riser temperature.

The water-gas shift reaction and equilibrium constant:

$$CO + H_2O \leftrightarrow H_2 + CO_2 \tag{1}$$

$$Kp = \frac{(H_2)(CO_2)}{(H_2O)(CO)} \tag{2}$$

Plotted on Figure 3.3-14 are the AI475H, AI480H, in situ H_2O concentrations, and the H_2O concentrations calculated from the water-gas shift equilibrium constant. The water-gas shift H_2O concentrations are based on the mixing zone temperature TI367 and the measured H_2, CO, and CO_2 concentrations. Except for one operating period, analyzer AI480H was higher than AI475 by 5 to 15 percent H_2O, and did not agree with the in situ H_2O measurements. Analyzer AI480H was clearly giving erroneous results and will not be used for further analyses.

Analyzer AI475 was close to the in situ data for all of the in situ H_2O analyses below 25 percent moisture (the design maximum moisture concentration of the analyzer). A comparison of analyzer AI475H, the moisture content predicted by the water-gas shift reaction, and the in situ moisture concentrations are shown on Figure 3.3-15. Except for a few initial periods, the WGS or AI475H H_2O measurements agree with each other for moisture contents below 25 percent, suggesting that both accurately predict the moisture concentration. The AI475H H_2O concentrations will be used for further data analysis when the analyzer indicates a moisture content of below 25 percent. If the moisture analyzer indicates that the moisture content is at or above 25 percent, the data analysis will use the WGS values to predict the moisture content.

Table 3.3-4 lists the H_2O concentrations used for the operating periods. The H_2O concentration was around 8 to 10 percent for the first eight operating periods (the air-blown periods). The moisture content jumped to between 20 and 25 percent for the next few periods as the system began oxygen-blown operation. The moisture content then ranged widely—from 15 to 37 percent as testing in oxygen-blown operation continued until the end of the test run.

Based on the moisture content discussed above, the best estimates of the wet-gas compositions for the TC12 operating periods are given on Table 3.3-4 and shown on Figure 3.3-16. Table 3.3-4 also shows the synthesis gas molecular weights for each operating period.

During the air-blown (first eight) operating periods, the wet CO concentration varied only slightly, from 8.6 to 9.7 percent. Once the system entered oxygen-blown mode, the CO content then increased to around 12 percent, and ran between 9 and 12 percent for the next several test periods. The higher steam flow rates caused the CO content to decrease to between 4.9 and 9 percent due to the water-gas shift reaction. The value was at a minimum at hour 471 (during TC12-37), when an extremely low coal-feed rate accompanied by coke breeze feed lowered the CO content to 1.8 percent. (Problems with the coal feeder gearbox limited the coal-feed rate). After the repairs to the coal feeder gearbox were completed, the higher coal-feed rate returned

the CO content to levels around 9 percent, and the CO content achieved 13.1 percent at the end of the test run.

The H_2 concentration remained steadily between 5.1 and 5.5 percent from the beginning of TC12 to hour 59, when the transition to oxygen-blown operations occurred. At this point, the hydrogen content jumped to 11 percent and began to fluctuate between 9.6 and 12.8 percent until the period of extremely low coal-feed rate at hour 471 (TC12-37), where the value decreased to 3.7 percent. After the coal-feed rate returned to normal, the hydrogen content achieved values of between 10.6 and 13.6 percent for the remainder of the test run. Note that the high steam flow rates during the middle of the test run kept the hydrogen content high (via the water-gas shift reaction), while the carbon monoxide content declined.

The CO_2 concentrations were almost uniformly 8.8 percent during the initial air-blown portion of TC12. After hour 59, the CO_2 concentration increased to about 14.1 percent and remained between 11 and 14.5 percent for the remainder of the test run, with the exception of the period of low coal-feed rate coupled by coke breeze at hour 471.

The CH_4 concentration was between 1.2 and 1.4 percent for the air-blown operating periods. During the oxygen-blown operating periods, the CH_4 concentration increased to between 1.9 and 3.0 percent. The methane content was around 0.3 percent during the period of coal and coke breeze cofeed.

The C_2^+ analyzers were unreliable during TC12. The data analyses assume them to be zero.

The syngas molecular weight and nitrogen concentration are plotted on Figure 3.3-17. The air-blown molecular weights are all around 26.9 lb/lb mole. The oxygen-blown operating periods had molecular weights between 23 and 26 lb/lb mole, with two large groups of data around 24 and 25, respectively. The molecular weights decrease in oxygen-enhanced operations because the nitrogen is replaced by lower molecular compounds such as H_2 and H_2O.

The CO/CO_2 ratios were calculated from the gas data for each operating period, and are listed on Table 3.3-4. The TC12 CO/CO_2 ratio varied from 0.2 to 1.1.

The raw (LHV) for each gas composition was calculated based on the gas analyzer data. Table 3.3-4 gives the values for the LHV, while Figure 3.3-18 plots the data.

The following formula yields the raw LHV:

$$\text{LHV(Btu/SCF)} = \left\{ \begin{array}{l} 275 \times (H_2\%) + 322 \times (CO\%) + \\ 913 \times (CH_4\%) + 1641 \times (C_2^+\%) \end{array} \right\} / 100 \qquad (3)$$

The raw LHV fluctuated between 52 and 58 Btu/scf during the initial air-blown testing in TC12. After the transition to oxygen-blown mode, the LHV increased to 96 Btu/scf. Over the next few oxygen-blown tests, the LHV ranged from as low as 59 to as high as 99 Btu/scf. During the period of coke breeze/coal cofeed, the LHV dropped to 19 Btu/scf, due to the low coal-feed

rate and the lack of volatiles in the coke breeze. When conditions returned to normal, the LHV jumped back to 68 Btu/scf and reached as high as 100 Btu/scf by the end of the test run.

Past test runs have indicated that LHV is most affected by coal rate and steam rate. The LHV increases as the coal rate increases (see Figure 4.5-5 of TC06 Final Report). The coal rate affects the LHV due to the way that the Transport Gasifier operates, that is, the aeration and instrument nitrogen remain constant as the coal rate increases. As the coal rate increases, the syngas flow rate also increases, but the nitrogen flow rate remains constant. The nitrogen concentration in the syngas becomes smaller (less nitrogen dilution), and the syngas LHV increases. When oxygen replaces air during enhanced air- and oxygen-blown operation, the nitrogen content of the syngas also decreases, resulting in an increase in LHV. An increase in steam reduces the lower heating values by the diluting the syngas with water. A way to combine the effects of changes in steam, mode of operation, and coal rates is to determine the overall percent of oxygen of all the gas that is fed to the Transport Gasifier. The overall percent of oxygen (overall percent O_2) compensates for the different amounts of nitrogen and steam added to the gasifier. The overall percent O_2 is calculated by the following formula:

$$\text{Overall } \%O_2 = \frac{.21 * \text{air} + \text{oxygen}}{\text{air} + \text{oxygen} + (\text{pure nitrogen}) + \text{steam}} \qquad (4)$$

The air, oxygen, nitrogen, and steam flows are in moles/hr. At the PSDF, a large amount of pure nitrogen is fed to the gasifier for instrument purges, coal and sorbent transport, and equipment purges. In PSDF air-blown operation, about 50 percent of the nitrogen in the syngas comes from air and 50 percent comes from the pure nitrogen added to the system. The TC12 overall percent O_2 are listed on Table 3.3-4 and range from 12.5 to 13.1 percent in air-blown mode and from 14.6 to 19.8 percent in oxygen-blown mode. The period of coal/coke breeze cofeeding (TC12-37) was not a typical oxygen-blown period, since the air flow rate was high compared to the oxygen flow rate. The relatively low oxygen flow rate along with very high steam and nitrogen flow rates lowered the overall percentage of oxygen for period TC12-37 to only 9.9 percent, lower than the air-blown periods.

The TC12 raw LHV data are plotted against overall percent O_2 on Figure 3.3-19. The TC12 data ranges from 19 Btu/scf at 9.9 percent O_2 to 100 Btu/scf at 19.8 percent O_2 and follow a clear trend of increasing Btu/scf with percent O_2. With the exception of the TC12-37 coke breeze cofeed period (at 9.9-percent oxygen), all of the TC12 air- and oxygen-blown data fit closely to the same straight line shown on Figure 3.3-19. TC12-37 most likely behaved differently from the other operating periods in that the coke breeze had less volatile matter than coal and was, thus, less conducive to making quality syngas. Therefore, the LHV for TC12-37 fell lower than the straight line fit for the remainder of the oxygen-blown data.

Also plotted on Figure 3.3-19 are the straight line correlation of TC06, TC07, TC08, and TC10 PRB coal data, the TC09 Hiawatha bituminous data, and the TC11 Falkirk lignite data. All of the correlations contain air- and oxygen-blown mode data. When the three coals are compared at the same level of percent O_2, the LHV generated from PRB coal typically falls between that of the LHV generated from the Hiawatha bituminous and the Falkirk lignite. The air-blown LHV data from TC12 is consistent with previous PRB LHV data while the TC12 oxygen-blown LHV data appears to be slightly lower than previous LHV data.

3.3.5 Nitrogen and Adiabatic Corrected Synthesis Gas Lower Heating Values

The PSDF Transport Gasifier produces syngas of a lower quality than a commercially sized gasifier due to the use of nitrogen at the PSDF rather than recycle gas in a commercial gasifier for aeration and PCD back-pulse cleaning. Also, a commercially sized gasifier has a lower heat loss per pound of coal gasified when compared to the PSDF Transport Gasifier due to the high surface area/reactor volume ratio at the PSDF compared to a commercially sized gasifier. The following corrections are made to the measured, raw synthesis gas composition to estimate the commercial syngas LHV.

1. All nonair nitrogen is subtracted from the syngas. This nitrogen is used for Transport Gasifier aeration and instrument purges. In a commercial plant there will be less instrumentation than at the PSDF. Because the instruments in a commercial plant will require the same purge flow rate as the instruments at the PSDF, the total instrument purge flow will be less. This correction assumes that recycled syngas or steam will be used in a commercial plant for aeration and steam for the instrument purges to replace the nonair nitrogen. The nonair nitrogen was determined by subtracting the air nitrogen from the synthesis gas nitrogen. This correction increases all the nonnitrogen syngas compositions and decreases the nitrogen syngas composition. The syngas rate will decrease as a result of this correction. For oxygen blown mode, this correction removes all the nitrogen from the syngas, thus oxygen blown syngas will have 0-percent nitrogen. The water-gas shift equilibrium constant and the CO/CO_2 ratios will not change.

2. The nonair nitrogen (that has been eliminated by not using nitrogen for aeration or instrument purges) no longer has to be heated to the maximum gasifier temperature. This eliminated heat is counteracted by the additional energy required to heat the gas used for aeration and instrument purges. A recent commercial design will be used to estimate the amount and temperature of the aeration and instrument purge gas required. Since the total amount of instrument and aeration gas required is reduced, the coal and air rates will decrease by the amount of energy no longer required. This results in decreased coal, air, and oxygen rates to the Transport Gasifier. It is assumed that this eliminated coal (to heat up the nonair nitrogen) is combusted to CO_2 and H_2O. Eliminating this additional coal reduces the syngas CO_2 and H_2O concentrations. The lower corrected air rates for air blown mode also decrease the nitrogen in the corrected syngas. This correction decreases the synthesis gas flow rate. For this correction the water-gas shift constant and the CO/CO_2 ratio both change due to the reduction in CO_2 and H_2O.

3. The PSDF higher heat loss per pound of coal gasified due to its smaller size is also taken into account. Smaller scale pilot and demonstration units have higher surface area to volume ratios than their scaled up commercial counterparts, and hence the PSDF Transport Gasifier has a higher heat loss per pound of coal gasified than a commercial plant. Since the heat loss of a commercial plant is difficult to estimate, the corrected heat loss is assumed to be zero (adiabatic). The correction uses the same method to correct for the no longer required energy to heat up the decreased amounts of aeration and instrumentation gas. The coal, air, and oxygen rates are reduced; the syngas CO_2, H_2O, and N_2 concentrations are reduced; the water-gas shift equilibrium constant and the CO/CO_2 ratio change. This correction is reasonable since the commercial plant heat

loss per pound of coal gasified is much smaller than the PSDF Transport Gasifier heat loss per pound of coal gasified.

4. The steam rates are reduced for oxygen-blown operation, since in oxygen-blown operation steam is added to control the gasifier temperature. As the oxygen rate is decreased in a commercial plant, the steam rate will also be decreased. It was assumed that the steam-to-oxygen ratio will be the same for the PSDF and the commercial Transport Gasifier, and hence the corrected steam rate will be lower than the original steam rate. The effect of lowering the steam rate will decrease the amount of H_2O in the syngas by the amount the steam rate was reduced. This correction reduces the steam rate and the H_2O content of the syngas and hence the LHVs and water-gas shift equilibrium constant also changes. The steam-to-oxygen ratio is a function of the detailed design of the Transport Gasifier. It is difficult to estimate what a commercial steam-to-oxygen ratio will be since typically in oxygen-blown mode steam is added to control local temperatures.

5. The water-gas shift is corrected to reflect the gasifier mixing zone temperature. Corrections #2, #3, and #4 all change the water-gas shift equilibrium constant without changing the mixing zone temperature. The commercial plant will operate at the PSDF mixing zone temperature and hence have the same water-gas shift equilibrium constant as the commercial plant. The H_2O, CO_2, CO, and H_2 concentrations are then adjusted to return to the measured PSDF water-gas shift equilibrium for that particular operating period. In respect to LHV, the LHV could go up if H_2 and CO_2 are converted to H_2O and CO since the LHV for CO is higher than H_2. The LHV could decrease if H_2O and CO are converted to H_2 and CO_2. This correction is usually small on a LHV basis, but is important if the syngas is used for fuel cell or chemical production where the H_2 concentration is a critical design parameter.

For correction #2 it is assumed that the recycle gas is 2.4 percent of the syngas from the gasifier and is available at 234°F. The recycle gas is taken from the exit of a "cold" syngas sulfur removal system which decreases the syngas temperature to 150°F, prior to sulfur removal. Decreasing the syngas temperature to 150°F will condense most of the syngas H_2O out as liquid water, which is then removed from the syngas. For the commercial design at 388 psia, the syngas water composition is 0.96 percent. In a commercial plant the cleaned syngas would be sent to a gas turbine, fuel cell, or for chemical production. For correction #2, it is assumed that the aeration steam is 1.45 percent of the syngas from the gasifier and available at 660°F. For correction #3 it is assumed that the heat loss for the PSDF Transport gasifier is 3.5 million Btu/hr. This heat loss will be discussed further in Section 3.5.

The sum of all five corrections is the adiabatic nitrogen corrected LHV. Correction #1 (Removing the nonair nitrogen) adds an average of 19 Btu/scf to the raw LHV for air-blown LHV and an average of 47 Btu/scf to the oxygen-blown LHV. Correction #2 (Correcting the Transport Gasifier energy balance for the commercial amount and type of aeration and instrument gas) adds an average of 9 Btu/scf to the raw LHV for air-blown LHV and an average of 22 Btu/scf to the oxygen-blown LHV. Correction #1 and #2 both increase the oxygen-blown LHV more than for the air-blown LHV because 100 percent of the syngas nitrogen is removed in the oxygen-blown correction, while only about 50 percent of the syngas nitrogen is removed for the air-blown correction. The sum of corrections #3 and #4 (adiabatic gasifier and correcting the steam rate) adds an average of 19 Btu/scf to the raw LHV for air-blown LHV and

an average of 43 Btu/scf to the oxygen-blown LHV. Correction #5 (water-gas shift correction) subtracts an average of 0.5 Btu/scf for air blown LHV and adds an average of 0.4 Btu/scf to the oxygen-blown LHV.

These calculations are an oversimplification of the gasification process. A more sophisticated model is required to correctly predict the effects of decreasing pure nitrogen and gasifier heat loss. Note that the corrected syngas compositions are based on a corrected coal rate, a corrected air rate, a corrected oxygen rate, a corrected steam rate, and a corrected syngas rate.

The adiabatic, nitrogen-corrected LHV for each operating period are given in Table 3.3-5 and plotted on Figure 3.3-20. The corrected LHV ranged between 98 and 109 Btu/scf for air-blown operation and between 126 and 255 for oxygen-blown operation. TC12-37, the coke breeze/coal cofeed test period, possessed a corrected LHV of around 126 Btu/scf. The average increase for the all the corrections was 47 Btu/scf for the air-blown syngas and 112 Btu/scf for the oxygen-blown syngas. The correction is higher for the oxygen-blown periods because the syngas flow rate is less in the oxygen-blown mode of operation. Therefore, removing the same amount of pure nitrogen from the syngas has a larger effect.

For comparing the raw LHV with the adiabatic N_2-corrected LHV, an equivalent to the overall percent O_2 is defined as:

$$Corrected\ Overall\ \%O_2 = \frac{0.21*(corrected\ air) + (corrected\ oxygen)}{(corrected\ air) + (corrected\ oxygen) + (corrected\ steam)} \quad (5)$$

All flow rates in the above equation are expressed as moles per hour. The corrected air rate, corrected oxygen rate, and corrected steam rate help determine the corrected LHV. The corrected overall percent O_2 for oxygen-blown mode is a direct function of the steam-to-oxygen ratio, since the corrected air flow rate is zero.

The adiabatic N_2-corrected LHV data from TC12 are plotted against the adiabatic overall percent O_2 in Figure 3.3-20. Also plotted are the raw TC12 LHV data. The TC12-corrected air-blown lower heating values are higher than the raw LHV at equivalent overall percent O_2. The TC12-corrected LHV data seem to form a straight line.

Figure 3.3-20 shows a straight line fit of the corrected LHV data from previous PRB test runs (TC06, TC07, TC08, and TC10) as well as the corrected LHV data from the Hiawatha bituminous test run (TC09) and the LHV data from the Falkirk Lignite test run (TC11). The TC12-corrected LHV data fit between the data for the Hiawatha coal and the Falkirk lignite. The TC12 data were similar to the data of the previous PRB test runs. The air-blown data from TC12 were especially consistent with the data seen in previous PRB test runs.

3.3.6 Synthesis Gas Water-Gas Shift Equilibrium

The water-gas shift (WGS) equilibrium constants (K_p) were calculated for the 21 in situ moisture measurements and are given on Table 3.3-6. Of the 21 in situ moisture measurements, 16 were taken during an operating period. The equilibrium constants varied from 0.53 to 0.92. Lower equilibrium constants tend to have less H_2 and CO_2 and higher H_2O and CO. The WGS varied

moderately over the wide range of H_2O (8.9 to 38.8 percent), dry CO (2.5 to 14.8 percent), dry H_2 (5.4 to 18.4 percent), and dry CO_2 (9.7 to 20.4 percent) during TC12. These data indicate that the water-gas shift reaction plays a major role controlling the relative H_2, H_2O, CO, and CO_2 concentrations in the Transport Gasifier synthesis gas.

The thermodynamic equilibrium temperature was calculated for each equilibrium constant using thermodynamic data and is shown on Table 3.3-6. The thermodynamic equilibrium temperature varied from 1,529 to 1,906°F. These temperatures are all within 150°F of the mixing zone temperature, which is listed in Table 3.3-6 for the in situ sampling periods. The WGS equilibrium constants calculated from the mixing zone temperatures are compared with the measured WGS equilibrium constants in Figure 3.3-21. The oxygen-blown equilibrium constants and air-blown equilibrium constants are plotted separately on Figure 3.3-21. The calculated and measured K_p values agree well with each other at measured values close to 0.7. The calculated values begin to digress from the measured values at measured K_p values above 0.75 and below 0.65. The equilibrium constants appeared to be more varied in TC12 than in previous test campaigns.

The WGS constants determined from the mixing zone temperature have less variation than the measured WGS constants. Since a 0°F approach temperature was used to curve fit the data, all points are centered around the 45-degree line on Figure 3.3-21.

The measured water-gas shift equilibrium constants (K_p) were calculated for the analysis periods and are given in Table 3.3-7. During air-blown operations, the measured equilibrium constants remained fairly constant at between 0.47 and 0.50, with one outlier at 0.64. For the 41 operating periods that used the measured moisture content, rather than the WGS-calculated moisture content, the measured equilibrium constant during the oxygen-blown operating periods trended upwards from 0.55 and 0.87. The K_p values were relatively constant and did not change dramatically despite the range of H_2O (8.9 to 25 percent maximum measured amount), CO (8.2 to 13.1 percent), H_2 (9.6 to 13.6 percent), and CO_2 (12.2 to 14.1 percent) seen during TC12. The stable K_p value indicates that the water-gas shift reaction controls the relative H_2, H_2O, CO, and CO_2 concentrations in the Transport Gasifier.

The thermodynamic equilibrium constants for each operating period based on TI367 are also shown in Table 3.3-7. For the 41 analysis periods using the AI475H analyzer data, the operating period WGS equilibrium constants calculated from the mixing zone temperatures are compared with the measured WGS equilibrium constants in Figure 3.3-22. Figure 3.3-22 does not contain information about the 15 operating periods that used the WGS equilibrium data to estimate the moisture, since the two different equilibrium constant would simply be the same. One of the air-blown K_p operating periods and several of the oxygen-blown operating periods exhibited good agreement between the measured and calculated values. The other air-blown periods each had a measured value lower than the calculated value. Many of the oxygen-blown operating periods, however, exhibited a measured K_p slightly higher than the calculated value. The overall trend of the data indicates a satisfactory fit for the entire spectrum of data. The WGS constants determined from the mixing zone temperature have less variation than the measured WGS constants, since the mixing zone temperature was fairly constant during TC12. Since the approach temperature of 0°F was used to curve fit the data, all the data points are centered around the 45-degree line on Figure 3.3-22.

The ability to predict the water-gas shift constant is important in the process design of a commercial Transport Gasifier, since the water-gas shift constant should be a function of the mixing zone temperature. The water-gas shift constant then can be used to determine the concentrations of the H_2, CO, CO_2, and H_2O, if the carbon conversion, LHV, and the CH_4 content are available.

3.3.7 Synthesis Gas Combustor Oxygen, Carbon, and Hydrogen Balance Calculations

The synthesis gas compositions and synthesis gas flow rate can be checked by oxygen balances, hydrogen balances, and carbon balances around the syngas combustor, since the syngas combustor flue gas composition is measured by the following syngas combustor flue gas analyzers (See Figure 3.3-1 for the analyzer location):

- AI8775 - O_2
- AI476H - H_2O
- AI476D - CO_2

The above analyzers all measure "wet" and do not require correcting for syngas moisture.

The synthesis gas combustor gas composition was calculated for each operating period by using the syngas composition, the syngas flow rate, FI463, and the following syngas combustor flow rate tags:

- Primary air flow, FI8773
- Secondary air flow, FI8772
- Quench air flow, FI8771
- Propane flow, FI8753

The measured oxygen content in the flue gas from AI8775 and the calculated oxygen content from a mass balance are shown in Figure 3.3-23 and Table 3.3-8. The measured and calculated oxygen concentrations agreed well for all of the operating periods—within 10 percent error for all but two operating periods (those two periods had an error of around 15 percent each). The air-blown periods exhibited a slight bias to having higher calculated oxygen concentrations than measured oxygen concentrations. A higher calculated oxygen concentration indicates that that the assumed synthesis gas composition had less combustibles (a lower LHV) than the actual syngas and that the actual syngas LHV was higher than the syngas analyzers would indicate. The comparisons for the measured and calculated oxygen concentrations are consistent with previous testing. The oxygen-blown periods possessed no apparent bias.

The CO_2 concentration, measured by AI476D, and the CO_2 concentration calculated by synthesis gas combustor mass balance are shown in Figure 3.3-24 and Table 3.3-8. In September 2003, it was discovered that the carbon dioxide analyzer, AI476D, was reading about 1 to 2 percent too low during TC12. To compensate, 1.5 percent was added to the actual AI476D reading. The calculated CO_2 concentrations agreed fairly well with the adjusted

measured CO_2 concentrations with most of the measured carbon dioxide concentrations agreeing within 10 percent of the calculated carbon dioxide concentrations.

Analyzer-measured (AI475H) and mass-balance-calculated H_2O values are shown in Figure 3.3-25 and Table 3.3-8. Note that Figure 3.3-25 distinguishes between the operating periods that used the AI475H analyzer to determine the syngas moisture content and the operating periods that used the WGS equilibrium data to estimate the moisture content. The calculated moisture content entering the syngas burner agreed well with the exit analyzer moisture values—within 15 percent for all of the operating periods and within 10 percent for all but six of the operating periods.

The results of the SGC flue gas analyzers indicate that the syngas compositions and flow rates are consistent with the syngas combustor flow rates and flue gas compositions.

An energy balance around the synthesis gas combustor can estimate the synthesis gas LHV. The syngas combustor energy balance adjusts the syngas combustor heat loss to ensure that the syngas LHV calculated from the syngas combustor energy balance agrees with the LHV calculated from the syngas analyzer data. In some of the commissioning tests (GTC test series), the gas analyzers were not operational during the entire run, and a LHV derived from the syngas combustor energy balance was used to estimate the syngas LHV during periods when no gas analyzers were available. A comparison between the measured TC12 LHVs and the LHVs determined from the syngas combustor energy balance is given on Figure 3.3-26. The values shown in the figure assume a syngas combustor heat loss of 2.5 million Btu per hour, a value consistent with the loss seen in previous test campaigns. The syngas combustor energy balance LHV and the analyzer LHV were within 10 percent of each other except for TC12-37, the test period that featured coal and coke breeze cofeeding.

3.3.8 Sulfur Emissions

For the TC12 operating periods, the wet H_2S concentration from analyzer AI419J is plotted on Figure 3.3-27 and compared with the synthesis gas combustor SO_2 analyzer AI476N/P, and the synthesis gas total reduced sulfur (TRS). The wet H_2S concentration measured by AI419J and the synthesis gas TRS are listed on Table 3.3-8. The AI419 analyzers measure the gas composition dry, so the values from AI419J were corrected to allow for the H_2O in the syngas. The synthesis gas combustor SO_2 analyzer, AI476N/P, measures the total sulfur emissions from the Transport Gasifier. Two AI476 SO_2 analyzers, N and P, are necessary to measure over a wide range of SO_2 values. Since the low range SO_2 analyzer, AI476N, has a maximum of 500 ppm SO_2, and the SO_2 content in the syngas was always much lower than 500 ppm, AI476N was the analyzer used in each of the operating periods. SO_2 forms when the syngas combustor burns sulfur compounds in the syngas. These compounds consist of H_2S, carbon oxysulfide (COS), and CS_2. The main sulfur species in coal gasification are H_2S and COS.

The H_2S content (based on AI419J analyzer data) was less than the TRS for about the first 20 hours of TC12. From hour 59 until the end of the test run, the H_2S analyzer AI419J value was around the value of the TRS or above it (with the exception of the period at hour 172, when the analyzer was out of service). The operating periods when the H_2S content was equal to the TRS would indicate no COS and CS_2 compounds present in the syngas, while operating periods when

the H_2S content was less than the TRS, would indicate that some COS and CS_2 compounds are present in the syngas. Obviously, the analyzers are not in perfect agreement with each other in that the AI419J H_2S value often exceeded the TRS value, a physical impossibility. Based on the performance of other gasifiers, the COS emissions should be about 100 ppm. The measured TRS is plotted against the wet AI419J H_2S data on Figure 3.3-28. Most of the data lie below the agreement line, indicating that either the syngas combustor SO_2 analyzer or the H_2S analyzer was not reading correctly. Since TC12 AI419J readings were not always consistent with AI476P, H_2S analyzer AI419J data will not be used for the remainder of this report.

At the beginning of TC12, the TRS emissions were about 220 ppm, and remained less than 250 ppm during air-blown operations. Once the oxygen-blown testing began, the TRS content increased to around 400 ppm. The value then ranged from 200 and 600 ppm for the remainder of the test run, with most values being above 300 ppm.

3.3.9 Ammonia Equilibrium

At the high temperature of the Transport Gasifier mixing zone, thermodynamic equilibrium predicts that minimal ammonia is present. The presence of ammonia in the syngas is therefore a result of ammonia production while the syngas cools to the location where the ammonia is sampled. The ammonia formation reaction and equilibrium constant is as follows:

$$\left(\frac{1}{2}\right)N_2 + \left(\frac{3}{2}\right)H_2 \leftrightarrow NH_3 \tag{6}$$

$$Kp = \frac{P_{NH_3}}{\left(P_{N_2}\right)^5\left(P_{H_2}\right)^{1.5}} \tag{7}$$

where P is the partial pressure of ammonia, hydrogen, or nitrogen. The equilibrium ammonia concentration was estimated using the PCD inlet temperature TI458 and an approach temperature of 60°F. The AI475Q measured ammonia concentrations and the equilibrium calculated ammonia concentrations are compared on Figure 3.3-29 and Table 3.3-7. Just over half of the 56 analysis period equilibrium calculation ammonia concentrations are within 20 percent of the measured ammonia concentrations, indicating a correlation exists, albeit a somewhat poor correlation. The wide range of measured ammonia concentrations (from 300 to over 3,000 ppm) may have contributed to the discrepancies. Using equilibrium calculations may permit the estimation of syngas ammonia concentrations for commercial reactors. In TC10 and TC11, all but two of the equilibrium NH_3 concentrations fell within 20 percent of the measured NH_3 concentrations.

Table 3.3-1 (Page 1 of 2)

Operating Periods

Operating Period	Start Time	End Time	Duration Hours	Operating Period		Notes
				Average Time	Relative Hours	
TC12-1	5/18/03 2:00	5/18/03 3:30	8:00	5/18/03 2:45	8	(1)
TC12-2	5/18/03 4:00	5/18/03 5:30	11:00	5/18/03 4:45	10	(1)
TC12-3	5/18/03 6:15	5/18/03 17:45	6:15	5/18/03 12:00	17	(1)
TC12-4	5/18/03 23:00	5/19/03 7:15	6:15	5/19/03 3:07	32	(1)
TC12-5	5/19/03 8:30	5/19/03 14:15	7:30	5/19/03 11:22	40	(1)
TC12-6	5/19/03 15:00	5/19/03 18:30	8:00	5/19/03 16:45	46	(1)
TC12-7	5/19/03 20:00	5/20/03 0:45	8:00	5/19/03 22:22	51	(1)
TC12-8	5/20/03 3:30	5/20/03 7:45	7:45	5/20/03 5:37	59	(1)
TC12-9	5/21/03 1:30	5/21/03 3:00	4:00	5/21/03 2:15	79	
TC12-10	5/21/03 7:15	5/21/03 11:30	4:00	5/21/03 9:22	86	
TC12-11	5/21/03 20:00	5/22/03 10:00	5:30	5/22/03 3:00	104	
TC12-12	5/22/03 19:30	5/23/03 2:00	6:45	5/22/03 22:45	124	
TC12-13	5/23/03 2:00	5/23/03 4:00	8:00	5/23/03 3:00	128	
TC12-14	5/23/03 9:00	5/23/03 11:15	4:45	5/23/03 10:07	135	
TC12-15	5/23/03 16:00	5/23/03 18:00	9:00	5/23/03 17:00	142	
TC12-16	5/23/03 19:45	5/23/03 23:15	8:30	5/23/03 21:30	146	
TC12-17	5/24/03 5:00	5/24/03 7:30	9:00	5/24/03 6:15	155	
TC12-18	6/20/03 11:00	6/20/03 18:00	6:45	6/20/03 14:30	172	
TC12-19	6/20/03 22:00	6/21/03 7:15	7:30	6/21/03 2:37	184	
TC12-20	6/21/03 14:30	6/21/03 18:30	4:30	6/21/03 16:30	197	
TC12-21	6/21/03 22:45	6/22/03 3:15	4:00	6/22/03 1:00	206	
TC12-22	6/22/03 11:30	6/22/03 14:30	4:30	6/22/03 13:00	218	
TC12-23	6/22/03 23:15	6/23/03 5:30	6:15	6/23/03 2:22	231	
TC12-24	6/23/03 10:00	6/23/03 23:15	13:15	6/23/03 16:37	246	
TC12-25	6/24/03 4:00	6/24/03 10:45	6:45	6/24/03 7:22	260	
TC12-26	6/24/03 11:15	6/24/03 16:00	4:45	6/24/03 13:37	267	
TC12-27	6/25/03 0:15	6/25/03 15:15	15:00	6/25/03 7:45	285	

Notes:

1. TC12-1 through TC12-8 were air-blown. All others were oxygen-blown.

2. Small amount of coke breeze fed as fuel with coal.

Table 3.3-1 (Page 2 of 2)

Operating Periods

| Operating Period | Start Time | End Time | Duration Hours | Operating Period | | Notes |
				Average Time	Relative Hours	
TC12-28a	6/25/03 15:30	6/26/03 4:15	12:45	6/25/03 21:52	299	
TC12-28b	6/26/03 4:15	6/26/03 17:15	13:00	6/26/03 10:45	312	
TC12-28c	6/26/03 17:15	6/27/03 6:00	12:45	6/26/03 23:37	325	
TC12-29	6/27/03 9:45	6/27/03 14:30	4:45	6/27/03 12:07	337	
TC12-30	6/27/03 14:45	6/27/03 18:00	3:15	6/27/03 16:22	341	
TC12-31	6/27/03 19:00	6/27/03 22:00	3:00	6/27/03 20:30	345	
TC12-32	6/27/03 22:45	6/28/03 11:00	12:15	6/28/03 4:52	354	
TC12-33	6/30/03 0:00	6/30/03 12:15	12:15	6/30/03 6:07	403	
TC12-34	6/30/03 12:45	6/30/03 20:00	7:15	6/30/03 16:22	413	
TC12-35	6/30/03 21:00	7/1/03 15:00	18:00	7/1/03 6:00	427	
TC12-36a	7/1/03 17:30	7/2/03 5:30	12:00	7/1/03 23:30	444	
TC12-36b	7/2/03 5:30	7/2/03 17:00	11:30	7/2/03 11:15	456	
TC12-37	7/2/03 19:30	7/3/03 9:00	13:30	7/3/03 2:15	471	(2)
TC12-38	7/4/03 17:45	7/4/03 21:00	3:15	7/4/03 19:22	490	
TC12-39	7/5/03 21:30	7/6/03 3:45	6:15	7/6/03 0:37	520	
TC12-40	7/6/03 6:00	7/6/03 20:15	14:15	7/6/03 13:07	532	
TC12-41	7/6/03 22:45	7/7/03 9:15	10:30	7/7/03 4:00	547	
TC12-42	7/7/03 12:45	7/7/03 23:30	10:45	7/7/03 18:07	561	
TC12-43	7/8/03 6:00	7/8/03 15:00	9:00	7/8/03 10:30	578	
TC12-44	7/9/03 0:15	7/9/03 13:00	12:45	7/9/03 6:37	598	
TC12-45	7/9/03 17:45	7/10/03 11:30	17:45	7/10/03 2:37	618	
TC12-46	7/10/03 23:15	7/11/03 8:00	8:45	7/11/03 3:37	643	
TC12-47	7/11/03 8:15	7/11/03 13:15	5:00	7/11/03 10:45	650	
TC12-48	7/11/03 21:15	7/12/03 1:30	4:15	7/11/03 23:22	662	
TC12-49	7/12/03 3:00	7/12/03 21:00	18:00	7/12/03 12:00	675	
TC12-50	7/13/03 8:45	7/13/03 15:45	7:00	7/13/03 12:15	699	
TC12-51	7/14/03 3:30	7/14/03 7:00	3:30	7/14/03 5:15	716	
TC12-52	7/14/03 10:30	7/14/03 12:45	2:15	7/14/03 11:37	723	
TC12-53	7/14/03 21:30	7/14/03 23:15	1:45	7/14/03 22:22	733	

Notes:

1. TC12-1 through TC12-8 were air-blown. All others were oxygen-blown.

2. Small amount of coke breeze fed as fuel with coal.

Table 3.3-2 (Page 1 of 2)

Operating Conditions

Operating Periods	Average Relative Hours	Mixing Zone Temperature TI367 °F	Pressure PI287 psig	PCD Inlet Temperature TI458 °F	Air Rate lb/hr	Oxygen[2] Rate lb/hr	Synthesis Gas Rate lb/hr	Steam Rate[3] lb/hr	Nitrogen Rate[1] lb/hr
TC12-1	8	1,746	210	780	12,944	0	24,141	875	6,642
TC12-2	10	1,759	210	785	12,973	0	24,124	876	6,615
TC12-3	17	1,773	210	792	13,055	0	23,968	910	6,333
TC12-4	32	1,762	210	782	12,272	0	22,525	898	6,433
TC12-5	40	1,751	210	781	12,339	0	23,092	884	6,153
TC12-6	46	1,750	210	773	12,428	0	22,998	713	6,341
TC12-7	51	1,758	210	775	13,062	0	23,931	653	6,423
TC12-8	59	1,767	210	752	11,845	0	21,490	815	5,670
TC12-9	79	1,734	150	731	751	2,495	15,324	2,547	6,355
TC12-10	86	1,759	150	759	1,806	2,359	15,762	2,366	5,952
TC12-11	104	1,737	140	721	933	2,423	15,090	1,967	6,308
TC12-12	124	1,727	130	702	993	2,548	15,494	1,914	6,247
TC12-13	128	1,711	130	700	834	2,461	15,292	2,003	6,311
TC12-14	135	1,728	130	709	1,378	2,398	15,804	2,416	5,873
TC12-15	142	1,727	130	686	789	2,516	14,014	1,910	5,935
TC12-16	146	1,714	130	715	1,544	2,387	16,419	2,380	5,927
TC12-17	155	1,674	140	746	1,205	2,824	19,314	3,294	6,090
TC12-18	172	1,734	155	683	2,468	1,589	13,885	1,278	6,342
TC12-19	184	1,744	151	677	623	2,013	12,495	1,326	6,349
TC12-20	197	1,731	142	668	1,026	2,064	12,892	1,241	6,490
TC12-21	206	1,718	136	659	662	1,967	12,248	1,249	5,992
TC12-22	218	1,718	136	665	839	2,121	12,667	1,250	6,151
TC12-23	231	1,703	136	696	796	1,957	13,197	1,249	6,259
TC12-24	246	1,707	134	707	1,344	1,917	12,903	1,321	6,079
TC12-25	260	1,686	134	701	917	1,917	12,571	1,595	5,950
TC12-26	267	1,684	134	703	1,557	2,009	13,253	1,329	6,092
TC12-27	285	1,676	134	709	1,229	2,060	14,096	1,512	6,536

Notes:

1. Nitrogen feed rate reduced by 1000 pph during oxygen-blown operation and 250 pph during air-blown operation to account for losses in feed systems and seals.

2. TC12-1 through TC12-8 were air blown; all other operating periods were oxygen blown.

3. Steam rate by hydrogen balance for TC12-6,TC12-7, TC12-8. By flow indicator for all others.

Table 3.3-2 (Page 2 of 2)

Operating Conditions

Operating Periods	Average Relative Hours	Mixing Zone Temperature TI367 ^{o}F	Pressure PI287 psig	PCD Inlet Temperature TI458 ^{o}F	Air Rate lb/hr	Oxygen[2] Rate lb/hr	Synthesis Gas Rate lb/hr	Steam Rate[3] lb/hr	Nitrogen Rate[1] lb/hr
TC12-28a	299	1,667	134	717	1,416	2,102	14,404	1,619	6,311
TC12-28b	312	1,659	134	722	1,360	2,108	14,467	1,680	6,219
TC12-28c	325	1,644	134	731	1,458	2,095	14,775	1,770	6,323
TC12-29	337	1,639	134	728	1,468	1,889	13,588	1,448	5,961
TC12-30	341	1,625	134	721	1,472	1,919	14,284	1,470	6,336
TC12-31	345	1,651	134	725	1,402	1,995	14,270	1,548	6,287
TC12-32	354	1,631	134	727	1,339	2,072	14,560	1,621	6,444
TC12-33	403	1,664	134	771	794	2,570	18,398	4,569	6,400
TC12-34	413	1,694	136	789	677	2,691	18,974	4,605	6,322
TC12-35	427	1,710	136	786	648	2,839	18,774	4,064	6,321
TC12-36a	444	1,715	136	754	667	2,645	16,993	3,090	6,264
TC12-36b	456	1,697	136	751	885	2,519	16,418	3,057	5,848
TC12-37	471	1,709	136	781	1,649	1,457	15,743	3,350	7,244
TC12-38	490	1,704	134	736	1,377	2,098	15,153	2,776	5,885
TC12-39	520	1,700	134	771	1,242	2,132	15,277	2,917	5,821
TC12-40	532	1,697	134	775	936	2,230	14,669	2,931	5,641
TC12-41	547	1,685	134	773	864	2,145	14,582	2,910	5,783
TC12-42	561	1,697	134	765	1,366	2,051	14,023	2,521	5,786
TC12-43	578	1,705	134	806	1,440	2,556	16,111	2,658	5,935
TC12-44	598	1,665	140	782	1,730	2,040	14,911	2,361	6,035
TC12-45	618	1,680	136	802	1,030	2,542	15,824	2,820	5,970
TC12-46	643	1,706	146	805	786	2,450	15,162	2,708	6,299
TC12-47	650	1,693	146	791	835	2,470	14,640	2,694	5,939
TC12-48	662	1,685	146	784	897	2,603	15,924	2,705	6,356
TC12-49	675	1,677	146	781	942	2,542	15,408	2,702	6,000
TC12-50	699	1,665	146	786	998	2,354	14,727	2,838	5,940
TC12-51	716	1,660	146	783	1,536	2,205	16,011	2,678	6,204
TC12-52	723	1,709	148	796	1,675	2,587	16,288	2,665	5,932
TC12-53	733	1,725	136	747	1,305	2,457	14,402	1,769	6,022

Notes:

1. Nitrogen feed rate reduced by 1000 pph during air-blown operation and 250 pph during oxygen-blown operation to account for losses in feed systems and seals.

2. TC12-1 through TC12-8 were air blown; all other operating periods were oxygen blown.

3. Steam rate by hydrogen balance for TC12-6,TC12-7, TC12-8. By flow indicator for all others.

Table 3.3-3 (Page 1 of 2)

Gas Analyzer Choices

Operating Periods	Average Relative Hours	Gas Compound						
		CO	H_2	CO_2	CH_4	C_2^+	N_2	H_2O[1]
TC12-1	8	464C	419G	419D	419E	0.0[2]	464B	475H
TC12-2	10	464C	419G	419D	419E	0.0	464B	475H
TC12-3	17	464C	419G	419D	419E	0.0	464B	475H
TC12-4	32	464C	464G	419D	419E	0.0	464B	475H
TC12-5	40	453G	464G	419D	419E	0.0	464B	475H
TC12-6	46	434B	464G	419D	419E	0.0	464B	475H
TC12-7	51	434B	464G	419D	419E	0.0	464B	475H
TC12-8	59	434B	464G	419D	419E	0.0	464B	475H
TC12-9	79	434B	464G	419D	419E	0.0	464B	475H
TC12-10	86	419C	464G	419D	419E	0.0	464B	475H
TC12-11	104	419C	464G	419D	419E	0.0	464B	475H
TC12-12	124	419C	464G	419D	419E	0.0	464B	475H
TC12-13	128	419C	464G	419D	419E	0.0	464B	475H
TC12-14	135	419C	464G	419D	419E	0.0	464B	475H
TC12-15	142	419C	464G	419D	419E	0.0	464B	475H
TC12-16	146	419C	464G	419D	419E	0.0	464B	475H
TC12-17	155	419C	464G	419D	419E	0.0	464B	WGS
TC12-18	172	419C	419G	419D	419E	0.0	419B	475H
TC12-19	184	419C	419G	419D	419E	0.0	419B	475H
TC12-20	197	419C	419G	419D	419E	0.0	419B	475H
TC12-21	206	419C	419G	419D	419E	0.0	419B	475H
TC12-22	218	464C	464G	419D	419E	0.0	419B	475H
TC12-23	231	464C	464G	419D	419E	0.0	419B	475H
TC12-24	246	464C	464G	419D	419E	0.0	419B	475H
TC12-25	260	464C	464G	419D	419E	0.0	419B	475H
TC12-26	267	464C	464G	419D	419E	0.0	419B	475H

Notes:

1. When analyzer out of range, H_2O calculated from water gas shift equilibrium using TI367, and H_2O, CO, and CO_2 data.

2. C_2^+ assumed to be 0.0, since the analyzers were not reading properly.

Table 3.3-3 (Page 2 of 2)

Gas Analyzer Choices

Operating Periods	Average Relative Hours	Gas Compound						
		CO	H_2	CO_2	CH_4	C_2^+	N_2	H_2O[1]
TC12-27	285	464C	464G	419D	419E	0.0^2	419B	475H
TC12-28a	299	464C	464G	419D	419E	0.0	419B	475H
TC12-28b	312	464C	464G	419D	419E	0.0	419B	475H
TC12-28c	325	464C	464G	419D	419E	0.0	419B	475H
TC12-29	337	464C	464G	419D	419E	0.0	419B	475H
TC12-30	341	464C	464G	419D	419E	0.0	419B	475H
TC12-31	345	464C	464G	419D	419E	0.0	419B	475H
TC12-32	354	464C	464G	419D	419E	0.0	419B	475H
TC12-33	403	419C	464G	419D	419E	0.0	419B	WGS
TC12-34	413	419C	464G	419D	419E	0.0	419B	475H
TC12-35	427	419C	464G	419D	419E	0.0	419B	475H
TC12-36a	444	464C	419G	419D	464E	0.0	419B	475H
TC12-36b	456	464C	419G	419D	464E	0.0	419B	475H
TC12-37	471	419C	419G	419D	419E	0.0	419B	475H
TC12-38	490	419C	464G	419D	464E	0.0	419B	475H
TC12-39	520	419C	464G	419D	419E	0.0	419B	475H
TC12-40	532	453G	464G	419D	464E	0.0	419B	475H
TC12-41	547	453G	464G	419D	464E	0.0	419B	WGS
TC12-42	561	453G	464G	419D	464E	0.0	419B	475H
TC12-43	578	453G	464G	419D	464E	0.0	419B	475H
TC12-44	598	453G	464G	419D	464E	0.0	419B	475H
TC12-45	618	453G	464G	419D	464E	0.0	419B	WGS
TC12-46	643	453G	464G	419D	464E	0.0	419B	475H
TC12-47	650	453G	464G	419D	464E	0.0	419B	WGS
TC12-48	662	419C	464G	419D	419E	0.0	419B	475H
TC12-49	675	419C	464G	419D	419E	0.0	419B	WGS
TC12-50	699	419C	464G	419D	419E	0.0	419B	WGS
TC12-51	716	419C	464G	419D	419E	0.0	419B	475H
TC12-52	723	419C	464G	419D	419E	0.0	419B	475H
TC12-53	733	419C	464G	419D	419E	0.0	419B	475H

Notes:

1. When analyzer out of range, H_2O calculated from water gas shift equilibrium using TI367, and H_2O, CO, and CO_2 data.

2. C_2^+ assumed to be 0.0, since the analyzers were not reading properly.

Table 3.3-4 (Page 1 of 2)
Gas Compositions, Molecular Weight, and Heating Value

Operating Period[2]	Average Relative Hour	H_2O[3] Mole %	CO Mole %	H_2 Mole %	CO_2 Mole %	CH_4 Mole %	C_2H_6 Mole %	N_2 Mole %	Total Mole %	Syngas LHV Btu/SCF	Syngas TRS[1] ppm	Syngas MW lb./Mole	O_2 in Feed %	Syngas CO/CO_2 Ratio
TC12-1	8	10.5	8.7	5.1	8.8	1.4	0.00	65.5	100.0	55	222	26.9	12.7	1.0
TC12-2	10	10.5	8.9	5.3	8.8	1.4	0.00	65.0	100.0	56	226	26.8	12.7	1.0
TC12-3	17	10.7	9.0	5.4	8.8	1.4	0.00	64.7	100.0	56	249	26.8	12.9	1.0
TC12-4	32	10.6	8.6	5.1	8.8	1.2	0.00	65.7	100.0	52	206	26.9	12.5	1.0
TC12-5	40	8.5	9.1	5.5	8.8	1.3	0.00	66.8	100.0	56	193	27.0	12.8	1.0
TC12-6	46	10.1	9.7	5.3	8.7	1.4	0.00	64.9	100.0	58	163	26.9	12.8	1.1
TC12-7	51	10.3	9.7	5.3	8.8	1.3	0.00	64.6	100.0	58	184	26.8	13.1	1.1
TC12-8	59	11.0	9.2	5.2	9.0	1.2	0.00	64.4	100.0	55	204	26.8	13.0	1.0
TC12-9	79	23.9	12.0	11.2	14.1	2.9	0.00	35.9	100.0	96	404	24.6	17.4	0.9
TC12-10	86	23.3	10.1	11.1	13.8	2.3	0.00	39.4	100.0	84	358	24.7	17.8	0.7
TC12-11	104	21.7	10.5	10.3	13.7	2.1	0.00	41.6	100.0	82	335	25.1	18.3	0.8
TC12-12	124	20.5	12.1	11.6	13.5	2.4	0.00	39.8	100.0	93	401	24.8	19.3	0.9
TC12-13	128	21.5	11.2	11.5	13.5	2.4	0.00	39.8	100.0	89	323	24.7	18.4	0.8
TC12-14	135	24.5	10.0	11.1	13.6	2.2	0.00	38.7	100.0	83	277	24.6	17.9	0.7
TC12-15	142	21.9	11.6	12.1	13.5	2.6	0.00	38.4	100.0	94	370	24.5	19.6	0.9
TC12-16	146	23.2	9.6	10.8	13.0	2.2	0.00	41.1	100.0	80	338	24.7	17.9	0.7
TC12-17	155	24.7	9.8	12.1	14.5	3.0	0.00	36.0	100.0	92	486	24.3	18.1	0.7
TC12-18	172	15.0	9.2	9.6	11.0	1.9	0.00	53.4	100.0	73	283	25.5	15.3	0.8
TC12-19	184	15.9	11.6	12.0	11.6	2.2	0.00	46.7	100.0	91	282	24.9	17.2	1.0
TC12-20	197	15.4	11.7	11.9	11.7	2.3	0.00	47.1	100.0	91	256	25.0	17.6	1.0
TC12-21	206	15.3	12.5	12.8	12.0	2.6	0.00	44.9	100.0	99	232	24.7	18.0	1.0
TC12-22	218	15.4	12.3	12.5	12.1	2.6	0.00	45.2	100.0	97	302	24.8	18.4	1.0
TC12-23	231	15.3	11.4	12.0	11.9	2.3	0.00	47.1	100.0	90	243	25.0	17.1	1.0
TC12-24	246	16.1	10.6	11.8	12.0	2.0	0.00	47.5	100.0	85	272	25.0	17.3	0.9
TC12-25	260	16.5	10.9	11.9	12.2	2.2	0.00	46.3	100.0	88	264	24.9	16.9	0.9
TC12-26	267	15.9	11.5	12.3	12.2	2.4	0.00	45.6	100.0	93	314	24.9	18.2	0.9
TC12-27	285	17.5	9.9	11.7	12.2	2.1	0.00	46.7	100.0	83	265	24.9	17.3	0.8

Notes:

1. Synthesis gas total reduced sulfur (TRS) estimated from Synthesis gas combustor SO_2 analyzer data.

2. TC12-1 through TC12-8 were air blown; all other operating periods were oxygen blown.

3. Moisture content from AI475H except for TC12-17, TC12-33 to TC12-41, TC12-45 to TC12-47, and TC12-49 and TC12-50 when the WGS was used.

Table 3.3-4 (Page 2 of 2)
Gas Compositions, Molecular Weight, and Heating Value

Operating Period[2]	Average Relative Hour	H_2O^3 Mole %	CO Mole %	H_2 Mole %	CO_2 Mole %	CH_4 Mole %	C_2H_6 Mole %	N_2 Mole %	Total Mole %	Syngas LHV Btu/SCF	Syngas TRS[1] ppm	Syngas MW lb./Mole	O_2 in Feed %	Syngas CO/CO_2 Ratio
TC12-28a	299	18.3	9.6	11.9	12.3	2.1	0.00	45.8	100.0	83	289	24.8	17.7	0.8
TC12-28b	312	18.8	9.3	11.8	12.4	2.1	0.00	45.6	100.0	82	332	24.8	17.7	0.8
TC12-28c	325	19.2	9.2	12.0	12.4	2.0	0.00	45.3	100.0	81	324	24.7	17.3	0.7
TC12-29	337	17.6	8.9	11.0	12.2	1.9	0.00	48.4	100.0	76	338	25.1	17.3	0.7
TC12-30	341	17.1	9.3	11.2	12.3	2.1	0.00	48.0	100.0	80	359	25.1	16.9	0.8
TC12-31	345	17.7	9.6	11.5	12.3	2.0	0.00	47.0	100.0	81	365	25.0	17.2	0.8
TC12-32	354	17.7	9.6	11.7	12.2	2.1	0.00	46.6	100.0	83	348	24.9	17.3	0.8
TC12-33	403	36.9	4.9	10.6	12.6	1.5	0.00	33.5	100.0	59	290	23.4	14.6	0.4
TC12-34	413	36.8	5.3	10.9	12.6	1.5	0.00	32.9	100.0	61	294	23.3	15.1	0.4
TC12-35	427	33.7	6.8	12.1	12.9	1.8	0.00	32.8	100.0	71	304	23.3	16.6	0.5
TC12-36a	444	29.5	7.8	12.6	12.5	2.0	0.00	35.6	100.0	78	309	23.5	17.5	0.6
TC12-36b	456	30.0	7.5	12.5	12.7	2.1	0.00	35.3	100.0	78	329	23.5	17.4	0.6
TC12-37	471	29.4	1.8	3.7	10.0	0.3	0.00	54.7	100.0	19	152	25.7	9.9	0.2
TC12-38	490	27.7	6.9	10.6	12.6	1.8	0.00	40.3	100.0	68	392	24.3	15.8	0.5
TC12-39	520	27.4	7.1	11.0	12.4	1.5	0.00	40.5	100.0	67	514	24.2	15.8	0.6
TC12-40	532	28.0	7.4	11.4	12.8	2.0	0.00	38.4	100.0	74	536	24.1	16.4	0.6
TC12-41	547	27.7	7.2	11.3	12.7	2.2	0.00	38.9	100.0	75	524	24.1	15.8	0.6
TC12-42	561	22.3	8.4	11.5	12.6	2.3	0.00	42.9	100.0	80	510	24.5	16.1	0.7
TC12-43	578	23.1	10.8	13.6	13.2	2.6	0.00	36.6	100.0	96	568	23.9	18.5	0.8
TC12-44	598	23.0	8.2	11.5	12.2	2.1	0.00	43.0	100.0	77	518	24.4	16.2	0.7
TC12-45	618	25.3	9.4	13.0	13.1	2.3	0.00	36.9	100.0	87	449	23.9	17.9	0.7
TC12-46	643	25.8	8.9	12.5	12.6	2.0	0.00	38.2	100.0	81	476	23.9	17.2	0.7
TC12-47	650	25.5	9.1	12.2	13.4	2.1	0.00	37.7	100.0	82	494	24.2	17.8	0.7
TC12-48	662	24.5	9.4	12.7	13.3	2.3	0.00	37.8	100.0	86	458	24.1	17.9	0.7
TC12-49	675	25.4	9.2	12.8	13.2	2.2	0.00	37.1	100.0	85	457	24.0	18.1	0.7
TC12-50	699	26.4	8.0	11.9	13.1	1.9	0.00	38.8	100.0	75	389	24.2	16.9	0.6
TC12-51	716	24.3	8.4	11.5	12.6	2.1	0.00	41.1	100.0	78	414	24.3	16.3	0.7
TC12-52	723	24.7	9.8	11.2	14.0	1.9	0.00	38.4	100.0	80	548	24.6	18.7	0.7
TC12-53	733	18.8	13.1	13.4	12.5	2.3	0.00	39.9	100.0	100	466	24.4	19.8	1.0

Notes:

1. Synthesis gas total reduced sulfur (TRS) estimated from Synthesis gas combustor SO_2 analyzer data.

2. TC12-1 through TC12-8 were air blown; all other operating periods were oxygen blown.

3. Moisture content from AI475H except for TC12-17, TC12-33 to TC12-41, TC12-45 to TC12-47, and TC12-49 and TC12-50 when the WGS was used.

Table 3.3-5 (Page 1 of 2)
Corrected Gas Compositions, Molecular Weight, and Heating Value

Operating Period	Average Relative Hour	H_2O Mole %	CO Mole %	H_2 Mole %	CO_2 Mole %	CH_4 Mole %	C_2H_6 Mole %	N_2 Mole %	Total Mole %	Syngas LHV Btu/SCF	Syngas MW lb./Mole	O_2 in Feed %	Syngas CO/CO_2 Ratio
TC12-1	8	16.0	15.1	10.6	11.2	2.6	0.0	44.4	100.0	102	25.1	17.1	1.3
TC12-2	10	15.9	15.4	11.0	11.1	2.6	0.0	44.1	100.0	103	25.0	17.1	1.4
TC12-3	17	16.1	15.2	11.0	11.0	2.5	0.0	44.3	100.0	102	25.0	17.1	1.4
TC12-4	32	16.1	15.0	10.8	11.1	2.2	0.0	44.8	100.0	98	25.1	16.9	1.3
TC12-5	40	12.8	16.6	11.9	11.3	2.5	0.0	44.8	100.0	109	25.1	16.8	1.5
TC12-6	46	15.0	16.6	10.9	10.9	2.5	0.0	44.0	100.0	107	25.1	17.5	1.5
TC12-7	51	15.2	16.3	10.6	10.9	2.4	0.0	44.6	100.0	104	25.2	17.9	1.5
TC12-8	59	16.4	15.5	10.7	11.0	2.2	0.0	44.1	100.0	100	25.1	17.1	1.4
TC12-9	79	27.9	25.9	21.7	18.4	6.0	0.0	0.0	100.0	198	21.8	33.4	1.4
TC12-10	86	31.6	21.5	22.8	19.3	4.8	0.0	0.0	100.0	176	21.4	33.8	1.1
TC12-11	104	28.2	24.9	22.8	19.2	4.9	0.0	0.0	100.0	188	21.7	38.0	1.3
TC12-12	124	26.0	26.5	24.3	18.0	5.2	0.0	0.0	100.0	200	21.3	39.8	1.5
TC12-13	128	26.8	25.4	24.5	18.1	5.2	0.0	0.0	100.0	196	21.2	37.9	1.4
TC12-14	135	32.0	21.7	23.0	18.6	4.7	0.0	0.0	100.0	176	21.2	33.6	1.2
TC12-15	142	26.8	25.3	25.1	17.3	5.5	0.0	0.0	100.0	201	20.9	39.7	1.5
TC12-16	146	31.1	22.1	23.8	18.2	4.8	0.0	0.0	100.0	181	21.0	33.7	1.2
TC12-17	155	30.5	20.6	23.2	19.8	6.0	0.0	0.0	100.0	185	21.4	30.6	1.0
TC12-18	172	21.7	27.8	28.8	15.9	5.7	0.0	0.0	100.0	221	20.2	37.2	1.7
TC12-19	184	16.3	33.4	31.0	13.2	6.1	0.0	0.0	100.0	249	19.7	41.5	2.5
TC12-20	197	17.7	31.6	30.5	14.1	6.1	0.0	0.0	100.0	241	19.8	43.8	2.2
TC12-21	206	15.1	34.0	31.2	13.2	6.6	0.0	0.0	100.0	255	19.7	42.2	2.6
TC12-22	218	16.9	32.1	30.3	14.2	6.4	0.0	0.0	100.0	245	19.9	44.4	2.3
TC12-23	231	16.4	32.5	30.8	14.1	6.1	0.0	0.0	100.0	245	19.9	41.7	2.3
TC12-24	246	19.3	29.4	30.7	15.2	5.5	0.0	0.0	100.0	229	19.9	40.8	1.9
TC12-25	260	16.3	32.8	30.2	14.4	6.2	0.0	0.0	100.0	245	20.1	36.8	2.3
TC12-26	267	19.8	28.7	29.7	15.8	6.0	0.0	0.0	100.0	229	20.1	42.1	1.8
TC12-27	285	21.8	26.8	29.6	16.3	5.5	0.0	0.0	100.0	218	20.1	39.4	1.6

Notes:

1. Correction is to assume that only air nitrogen is in the synthesis gas and that the reactor is adiabatic.

2. TC12-1 through TC12-8 were air blown; all other operating periods were oxygen blown.

3. Coal and coke breeze co-fed during TC12-37.

Table 3.3-5 (Page 2 of 2)
Corrected Gas Compositions, Molecular Weight, and Heating Value

Operating Period	Average Relative Hour	H_2O Mole %	CO Mole %	H_2 Mole %	CO_2 Mole %	CH_4 Mole %	C_2H_6 Mole %	N_2 Mole %	Total Mole %	Syngas LHV Btu/SCF	Syngas MW lb./Mole	O_2 in Feed %	Syngas CO/CO_2 Ratio
TC12-28a	299	23.6	25.1	29.4	16.7	5.3	0.0	0.0	100.0	210	20.0	38.6	1.5
TC12-28b	312	24.2	24.4	29.3	16.8	5.3	0.0	0.0	100.0	207	20.0	37.9	1.5
TC12-28c	325	24.9	23.8	29.3	17.1	5.0	0.0	0.0	100.0	203	20.0	36.7	1.4
TC12-29	337	23.1	25.3	29.3	17.1	5.2	0.0	0.0	100.0	210	20.2	38.5	1.5
TC12-30	341	22.4	25.8	29.0	17.3	5.5	0.0	0.0	100.0	213	20.3	38.4	1.5
TC12-31	345	22.9	25.9	29.0	17.0	5.1	0.0	0.0	100.0	210	20.3	38.3	1.5
TC12-32	354	22.6	25.9	29.2	16.7	5.5	0.0	0.0	100.0	214	20.2	38.2	1.5
TC12-33	403	46.0	11.3	21.8	17.7	3.2	0.0	0.0	100.0	126	20.2	22.8	0.6
TC12-34	413	45.7	11.8	21.8	17.4	3.2	0.0	0.0	100.0	127	20.2	23.4	0.7
TC12-35	427	41.6	14.2	23.5	17.3	3.5	0.0	0.0	100.0	142	20.1	26.7	0.8
TC12-36a	444	36.7	16.9	25.7	16.4	4.2	0.0	0.0	100.0	164	19.8	30.4	1.0
TC12-36b	456	37.5	16.1	25.3	16.7	4.4	0.0	0.0	100.0	162	19.8	29.7	1.0
TC12-37	471	39.4	16.2	19.5	22.6	2.2	0.0	0.0	100.0	126	22.3	17.6	0.7
TC12-38	490	36.3	17.2	24.3	17.8	4.3	0.0	0.0	100.0	162	20.4	27.9	1.0
TC12-39	520	34.8	18.4	25.8	17.3	3.7	0.0	0.0	100.0	163	20.1	27.3	1.1
TC12-40	532	34.0	18.5	25.4	17.4	4.8	0.0	0.0	100.0	173	20.2	28.2	1.1
TC12-41	547	32.9	18.8	25.7	17.2	5.3	0.0	0.0	100.0	180	20.1	27.5	1.1
TC12-42	561	26.6	23.0	27.4	17.1	5.9	0.0	0.0	100.0	203	20.3	29.4	1.3
TC12-43	578	28.6	22.2	26.7	17.1	5.3	0.0	0.0	100.0	193	20.3	33.1	1.3
TC12-44	598	30.6	20.2	27.2	17.0	5.0	0.0	0.0	100.0	185	20.0	30.5	1.2
TC12-45	618	31.0	20.5	26.6	17.1	4.8	0.0	0.0	100.0	183	20.1	31.7	1.2
TC12-46	643	31.3	20.7	27.1	16.6	4.4	0.0	0.0	100.0	181	20.0	31.6	1.3
TC12-47	650	30.8	21.0	25.8	17.7	4.6	0.0	0.0	100.0	181	20.5	32.1	1.2
TC12-48	662	29.9	21.2	26.4	17.6	4.9	0.0	0.0	100.0	185	20.4	33.0	1.2
TC12-49	675	31.1	20.4	26.3	17.4	4.8	0.0	0.0	100.0	181	20.3	32.6	1.2
TC12-50	699	32.2	19.5	26.2	17.7	4.3	0.0	0.0	100.0	174	20.3	30.0	1.1
TC12-51	716	31.3	20.4	25.9	17.5	4.8	0.0	0.0	100.0	181	20.4	29.6	1.2
TC12-52	723	32.9	20.8	23.0	19.3	4.0	0.0	0.0	100.0	167	21.3	33.4	1.1
TC12-53	733	23.1	28.2	28.2	15.7	4.8	0.0	0.0	100.0	212	20.3	40.9	1.8

Notes:

1. Correction is to assume that only air nitrogen is in the synthesis gas and that the reactor is adiabatic.

2. TC12-1 through TC12-8 were air blown; all other operating periods were oxygen blown.

3. Coal and coke breeze co-fed during TC12-37.

Table 3.3-6
Water-Gas Shift Equilibrium Constant

In-situ Start	In-situ End	Average Run Time Hours	Operating Periods	Dry CO %	Dry H2 %	Dry CO2 %	In-situ H_2O %	Kp	WGS Eqm. Temp. F	Mixing Zone Temp. F	Mixing Zone Kp^2
5/18/2003 8:45	5/18/2003 9:00	14	TC12-3	10.0	5.9	9.7	9.8	0.53	1,906	1,771	0.63
5/19/2003 9:35	5/19/2003 9:55	39	TC12-5	10.0	6.7	9.7	8.9	0.67	1,728	1,753	0.65
5/20/2003 8:45	5/20/2003 9:00	62	(1)	9.1	6.1	10.2	10.4	0.59	1,821	1,751	0.65
5/21/2003 9:15	5/21/2003 9:30	86	TC12-10	12.8	14.3	18.0	24.0	0.64	1,759	1,753	0.65
5/22/2003 11:00	5/22/2003 14:20	114	(1)	13.5	12.8	16.9	19.2	0.68	1,718	1,730	0.67
5/23/2003 9:15	5/23/2003 9:30	134	TC12-14	13.5	15.0	18.0	24.6	0.61	1,792	1,736	0.66
6/20/2003 12:25	6/20/2003 12:40	170	TC12-18	10.9	11.1	12.9	14.2	0.79	1,617	1,732	0.67
6/23/2003 12:44	6/23/2003 13:00	242	TFC12-24	14.8	15.0	14.6	15.4	0.82	1,600	1,706	0.69
6/24/2003 9:10	6/24/2003 9:25	262	TC12-25	12.7	13.7	14.6	15.3	0.88	1,558	1,694	0.71
6/26/2003 9:45	6/26/2003 10:00	311	TC12-28b	12.0	14.9	15.3	17.0	0.92	1,529	1,653	0.75
6/27/2003 10:45	6/27/2003 11:00	336	TC12-29	10.8	13.1	14.7	16.6	0.89	1,548	1,648	0.76
6/30/2003 10:45	6/30/2003 11:00	408	TC12-33	7.9	17.7	20.4	38.8	0.72	1,680	1,662	0.74
7/1/2003 10:50	7/1/2003 11:05	432	TC12-35	10.8	17.9	19.8	33.8	0.64	1,756	1,700	0.70
7/2/2003 9:10	7/2/2003 9:25	454	TC12-36b	11.0	18.4	18.6	28.4	0.79	1,622	1,707	0.69
7/3/2003 13:15	7/3/2003 13:30	482	(1)	2.5	5.4	15.2	34.3	0.63	1,776	1,689	0.71
7/7/2003 12:30	7/7/2003 12:45	556	(1)	10.8	15.6	18.0	25.7	0.75	1,655	1,676	0.72
7/8/2003 12:37	7/8/2003 12:52	580	TC12-43	14.7	18.6	17.7	23.1	0.74	1,662	1,696	0.70
7/9/2003 9:45	7/9/2003 10:00	601	TC12-44	11.2	15.7	16.8	21.9	0.84	1,582	1,664	0.74
7/10/2003 13:00	7/10/2003 13:10	628	(1)	12.2	18.4	18.3	32.7	0.57	1,845	1,706	0.69
7/11/2003 10:55	7/11/2003 11:10	650	TC12-47	12.4	16.8	18.3	26.2	0.70	1,702	1,681	0.72
7/14/2003 10:15	7/14/2003 10:30	721	TC12-52	12.5	15.0	18.9	24.1	0.71	1,685	1,678	0.72

Notes:

1. Data not taken during operating period.

2. Equilibrium constant calculated at mixing zone/riser junction temperature (TI367).

3. All data taken prior to May 21 taken during air operation. Other were taken during oxygen operation.

Table 3.3-7 (Page 1 of 2)
Transport Gasifier Equilibrium Calculations

Operating Period[1]	Average Relative Hour	Measured Syngas K_p[2]	Mixing Zone Equilibrium K_p[3]	AI475Q Ammonia ppm	PCD Equilibrium Ammonia[4] ppm
TC12-1	8	0.49	0.65	1,429	1,212
TC12-2	10	0.50	0.64	1,383	1,253
TC12-3	17	0.49	0.63	1,310	1,222
TC12-4	32	0.50	0.64	1,115	1,198
TC12-5	40	0.64	0.65	1,063	1,369
TC12-6	46	0.47	0.65	1,480	1,322
TC12-7	51	0.47	0.64	1,472	1,304
TC12-8	59	0.47	0.63	1,300	1,496
TC12-9	79	0.55	0.66	2,605	2,578
TC12-10	86	0.65	0.64	2,308	2,221
TC12-11	104	0.62	0.66	2,017	2,465
TC12-12	124	0.64	0.67	2,378	3,075
TC12-13	128	0.65	0.69	2,353	3,066
TC12-14	135	0.61	0.67	2,269	2,673
TC12-15	142	0.64	0.67	2,424	3,544
TC12-16	146	0.63	0.68	2,133	2,561
TC12-17	155	0.73	0.73	3,057	2,482
TC12-18	172	0.76	0.66	1,732	3,538
TC12-19	184	0.75	0.65	2,067	4,712
TC12-20	197	0.77	0.67	2,076	4,728
TC12-21	206	0.80	0.68	2,348	5,324
TC12-22	218	0.79	0.68	2,310	4,889
TC12-23	231	0.81	0.69	2,133	3,799
TC12-24	246	0.83	0.69	2,017	3,392
TC12-25	260	0.81	0.71	2,161	3,530
TC12-26	267	0.82	0.72	2,307	3,661
TC12-27	285	0.82	0.72	2,083	3,272

Notes:

1. Periods TC12-1 through TC12-8 were air blown. The remaining periods were oxygen blown.

2. Syngas K_p determined by hydrogen, water, carbon dioxide, and carbon monoxide measurements.

3. Mixing zone K_p determined by equilibrium calculations using the mixing zone temperature (TI367).

4. Equilibrium ammonia concentrations determined by equilibrium calculations and the partial pressures of H_2 and N_2.

Table 3.3-7 (Page 2 of 2)
Transport Gasifier Equilibrium Calculations

Operating Period[1]	Average Relative Hour	Measured Syngas K_p[2]	Mixing Zone Equilibrium K_p[3]	AI475Q Ammonia ppm	PCD Equilibrium Ammonia[4] ppm
TC12-28a	299	0.83	0.73	2,113	3,156
TC12-28b	312	0.83	0.74	2,130	3,029
TC12-28c	325	0.85	0.76	2,076	2,907
TC12-29	337	0.86	0.77	1,964	2,701
TC12-30	341	0.87	0.78	2,068	2,880
TC12-31	345	0.83	0.75	2,003	2,882
TC12-32	354	0.83	0.78	2,198	2,891
TC12-33	403	0.74	0.74	2,075	1,604
TC12-34	413	0.70	0.70	2,079	1,496
TC12-35	427	0.69	0.69	2,255	1,789
TC12-36a	444	0.68	0.68	2,256	2,415
TC12-36b	456	0.70	0.70	2,350	2,405
TC12-37	471	0.69	0.69	384	401
TC12-38	490	0.69	0.69	1,955	2,183
TC12-39	520	0.70	0.70	1,873	1,869
TC12-40	532	0.70	0.70	2,120	1,858
TC12-41	547	0.71	0.71	2,265	1,883
TC12-42	561	0.77	0.70	2,217	2,124
TC12-43	578	0.72	0.69	2,653	1,967
TC12-44	598	0.75	0.74	2,051	2,010
TC12-45	618	0.72	0.72	2,253	1,928
TC12-46	643	0.69	0.69	1,946	1,931
TC12-47	650	0.71	0.71	2,022	2,007
TC12-48	662	0.73	0.71	2,279	2,240
TC12-49	675	0.72	0.72	2,250	2,277
TC12-50	699	0.74	0.74	1,829	2,010
TC12-51	716	0.71	0.74	2,124	2,018
TC12-52	723	0.65	0.69	1,971	1,761
TC12-53	733	0.68	0.67	2,216	2,941

Notes:

1. Periods TC12-1 through TC12-8 were air blown. The remaining periods were oxygen blown.

2. Syngas K_p determined by hydrogen, water, carbon dioxide, and carbon monoxide measurements.

3. Mixing zone K_p determined by equilibrium calculations using the mixing zone temperature (TI367).

4. Equilibrium ammonia concentrations determined by equilibrium calculations and the partial pressures of H_2 and N_2.

Table 3.3-8
Synthesis Gas Combustor Calculations

Operating Period	Average Relative Hour	Syngas Combustor Exit						Gas Analyzer LHV Btu/SCF	Energy Balance LHV[1] Btu/SCF	Wet AI419J H_2S ppm	Combustor SO_2 AI476N/P ppm	Syngas Total Reduced Sulfur[2] ppm
		AIT8775 O_2 M %	Calculated O_2 M %	AI476D CO_2[4] M %	Calculated CO_2 M %	AI476H H_2O M %	Calculated H2O M %					
TC12-1	8	5.0	5.5	9.4	9.8	11.0	10.8	55	57	92	110	222
TC12-2	10	5.0	5.5	9.4	9.9	11.1	10.8	56	58	150	113	226
TC12-3	17	4.9	5.5	9.4	9.9	11.5	10.9	56	60	208	126	249
TC12-4	32	5.0	5.6	9.3	9.7	11.5	10.7	52	56	251	102	206
TC12-5	40	5.0	5.3	9.3	10.1	11.4	10.0	56	55	249	96	193
TC12-6	46	5.0	5.6	9.5	10.1	11.4	10.4	58	61	215	81	163
TC12-7	51	3.5	3.8	10.2	11.3	12.1	11.5	58	58	219	103	184
TC12-8	59	3.2	3.7	10.2	11.3	12.2	12.0	55	57	253	116	204
TC12-9	79	4.9	4.9	10.6	12.6	19.4	19.1	96	91	426	172	404
TC12-10	86	4.8	5.3	10.8	11.8	19.7	18.8	84	87	394	157	358
TC12-11	104	4.2	4.5	11.3	12.7	19.4	18.6	82	83	392	157	335
TC12-12	124	5.1	5.4	10.9	12.1	17.0	17.3	93	92	398	170	401
TC12-13	128	4.9	5.2	10.8	12.1	18.6	18.1	89	90	379	141	323
TC12-14	135	4.5	4.7	10.9	12.1	20.7	20.0	83	84	343	127	277
TC12-15	142	5.4	5.7	10.8	11.6	17.3	17.7	94	95	380	152	370
TC12-16	146	4.8	5.0	10.5	11.6	19.0	19.1	80	82	359	155	338
TC12-17	155	4.5	5.1	11.0	11.9	21.6	19.9	92	93	475	209	486
TC12-18	172	5.2	5.4	10.2	10.4	12.9	14.6	73	75	6	130	283
TC12-19	184	5.4	5.1	10.4	11.4	14.5	15.7	91	89	169	123	282
TC12-20	197	8.1	8.1	9.0	9.1	12.0	12.8	91	92	269	87	256
TC12-21	206	8.1	8.0	8.6	9.4	12.4	13.1	99	96	355	79	232
TC12-22	218	6.5	6.1	10.1	10.8	13.7	14.7	97	93	369	118	302
TC12-23	231	6.0	5.7	9.8	11.0	14.5	15.0	90	88	375	101	243
TC12-24	246	6.0	5.8	10.1	10.7	14.4	15.2	85	85	365	115	272
TC12-25	260	6.1	5.9	9.8	10.8	15.2	15.3	88	88	384	109	264
TC12-26	267	6.1	6.1	10.2	10.8	14.8	15.0	93	92	397	125	314
TC12-27	285	6.0	5.8	9.8	10.6	15.6	15.9	83	82	369	113	265
TC12-28a	299	6.0	5.8	9.8	10.6	16.0	16.3	83	82	402	123	289
TC12-28b	312	6.0	6.0	9.9	10.4	16.2	16.5	82	82	421	142	332
TC12-28c	325	6.0	5.9	9.6	10.4	16.2	16.7	81	80	433	139	324
TC12-29	337	6.0	6.2	9.5	10.1	14.8	15.5	76	77	433	140	338
TC12-30	341	6.0	6.1	9.5	10.3	14.6	15.4	80	80	446	150	359
TC12-31	345	6.0	6.2	9.6	10.3	15.0	15.6	81	81	437	153	365
TC12-32	354	6.0	6.1	9.7	10.4	15.0	15.8	83	83	423	147	348
TC12-33	403	5.1	5.4	9.2	9.7	24.9	26.5	59	63	355	144	290
TC12-34	413	6.0	6.2	9.0	9.3	22.6	24.9	61	64	354	135	294
TC12-35	427	6.0	6.2	9.4	9.7	20.8	23.4	71	73	356	135	304
TC12-36a	444	6.1	6.2	9.7	9.7	18.6	21.2	78	80	363	132	309
TC12-36b	456	5.8	6.2	10.0	9.7	19.3	21.5	78	81	359	140	329
TC12-37	471	4.5	5.5	8.0	8.0	21.4	19.8	19	27	247	69	152
TC12-38	490	4.5	4.8	9.9	10.8	22.0	22.1	68	70	473	192	392
TC12-39	520	4.0	4.2	10.2	11.1	23.1	22.9	67	69	605	266	514
TC12-40	532	4.6	4.6	10.3	11.0	22.5	22.5	74	76	604	258	536
TC12-41	547	4.6	4.5	10.1	10.9	22.2	22.4	75	77	617	251	524
TC12-42	561	5.1	5.1	10.4	10.8	18.8	18.9	80	81	592	229	510
TC12-43	578	5.8	5.7	10.5	11.1	18.6	18.7	96	93	603	231	568
TC12-44	598	4.2	4.1	10.2	11.3	19.7	20.5	77	76	568	254	518
TC12-45	618	4.6	4.5	10.7	11.6	21.1	21.3	87	84	504	207	449
TC12-46	643	4.5	4.4	10.4	11.4	20.9	21.6	81	78	550	227	476
TC12-47	650	4.5	4.5	10.9	11.8	21.0	21.2	82	81	530	232	494
TC12-48	662	5.3	5.4	10.3	11.1	19.8	19.7	86	86	541	199	458
TC12-49	675	5.8	5.9	10.2	10.6	19.4	19.5	85	86	493	192	457
TC12-50	699	6.0	6.2	9.6	10.2	20.4	19.7	75	77	491	168	389
TC12-51	716	6.0	5.9	9.5	10.3	18.9	19.0	78	77	509	180	414
TC12-52	723	5.4	5.7	10.7	11.6	19.2	19.1	80	81	580	242	548
TC12-53	733	5.9	5.8	10.8	11.4	17.0	16.4	100	96	568	187	466

Notes:

1. Energy LHV calcualted assuming the sythesis gas combustor heat loss was 2.5 x 10^6 Btu/hr.

2. Synthesis gas total reduced sulfur (TRS) estimated from synthesis gas combustor SO_2 analyzer data

3. TC12-1 through TC12-8 were air blown; all other operating periods were oxygen blown.

4. CO_2 Analyzer data adjusted by +1.5% to account for analyzer miscalibration.

N_2 - AI464B

CO - AI464C, AI453G, AI434B

CO_2 - AI464D, AI434C

CH_4 - AI464E

C_2^+ - AI464F

H_2 - AI464G

Siemens-Westinghouse PCD

From Transport Gasifier
Primary Gas Cooler

Secondary Gas Cooler

N_2 - AI419B

CO - AI419C, AI425

CO_2 - AI419D

CH_4 - AI419E

C_2^+ - AI419F

H_2 - AI419G

H_2O - AI419H

H_2S - AI419J

O_2 - AI8775

CO_2 - AI476D

H_2O - AI476H

SO_2 - L - AI476N

SO_2 - H - AI476P

PCD Fines

STM
BFW

Syngas Combustor

air

Pressure Letdown

STM
BFW

Gas Cooler

To Baghouse

CO - AI475C

CO_2 - AI475D

CH_4 - AI475E

H_2O - AI475H

NH_3 - AI475Q

H_2O - AI479H

HCl - AI479R

HCN - AI479S

COS - AI479T

H_2O - AI480H

H_2S - AI480J

NH_3 - AI480Q

CS_2 - AI480W

$C_{10}H_8$ - AI480X

Figure 3.3-1 Gas Sampling Locations
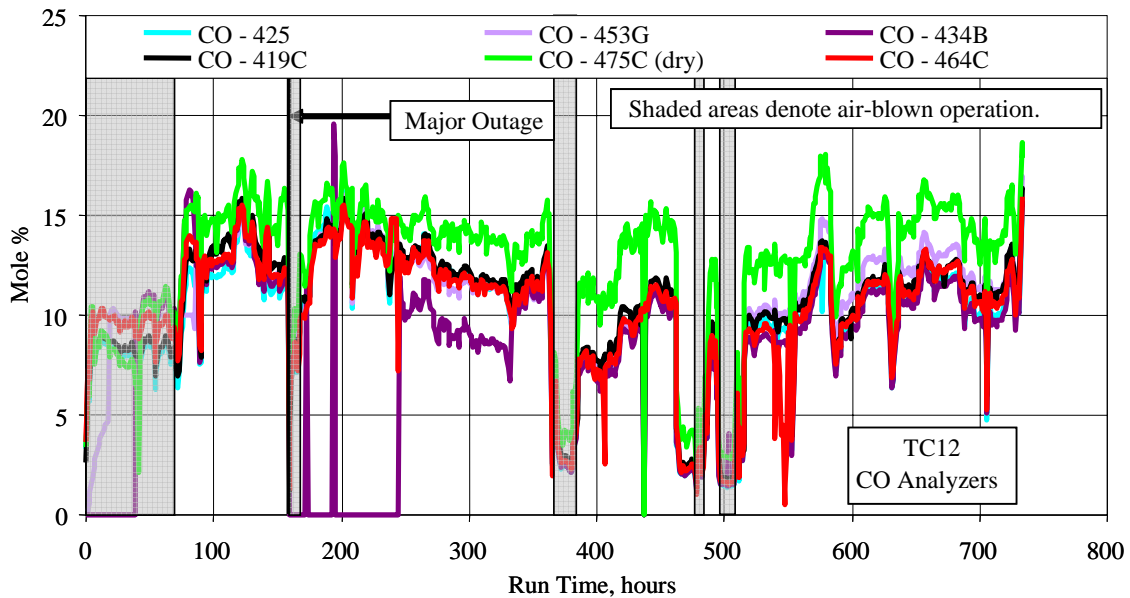
Figure 3.3-2 Carbon Monoxide Analyzer Data
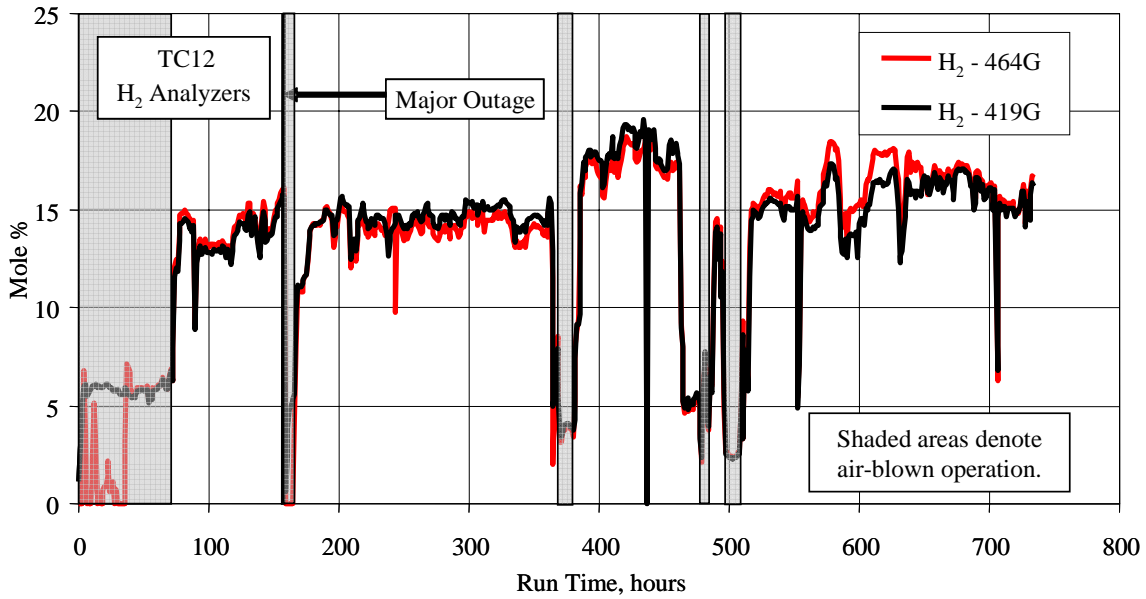
Figure 3.3-3 Hydrogen Analyzer Data
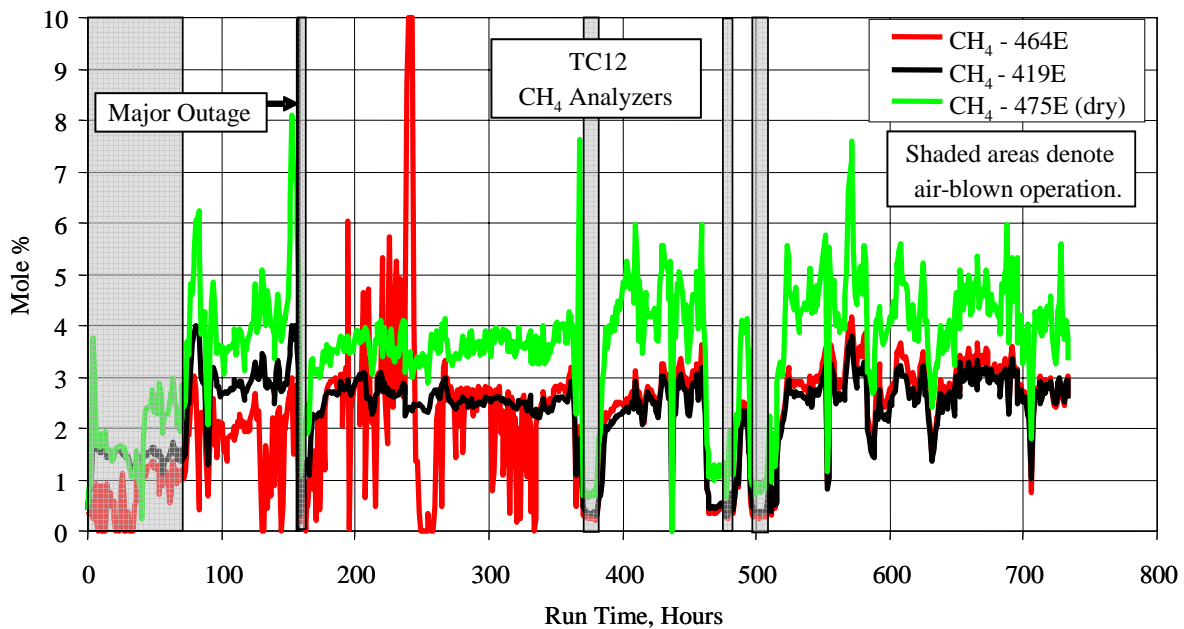
Figure 3.3-4 Methane Analyzer Data
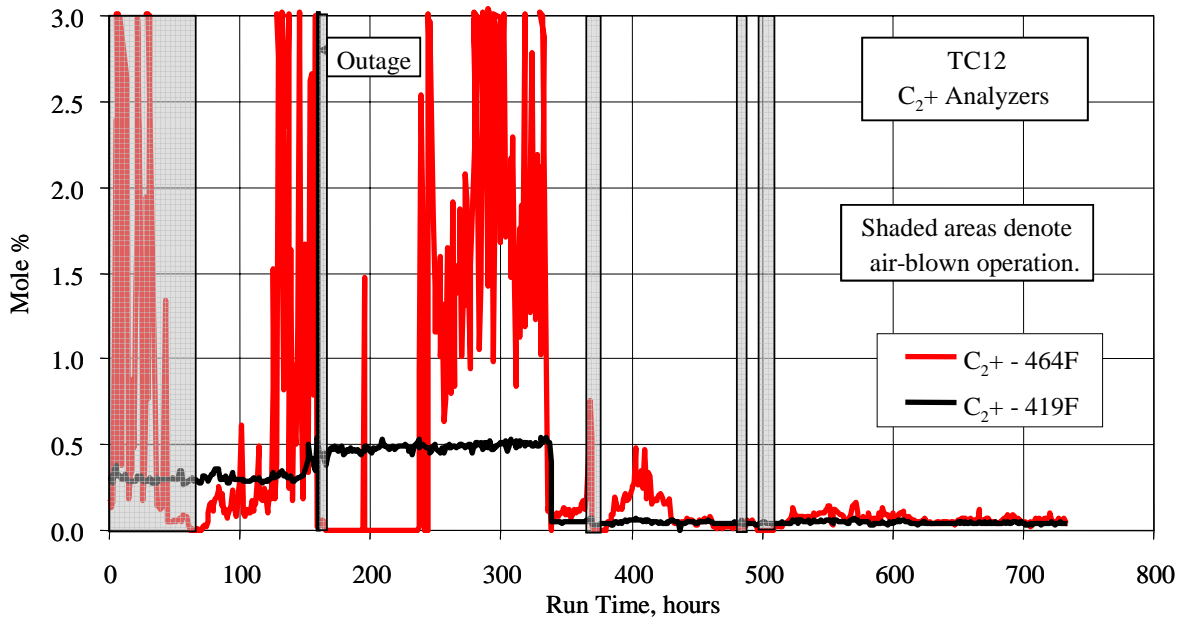
Figure 3.3-5 C₂⁺ Analyzer Data
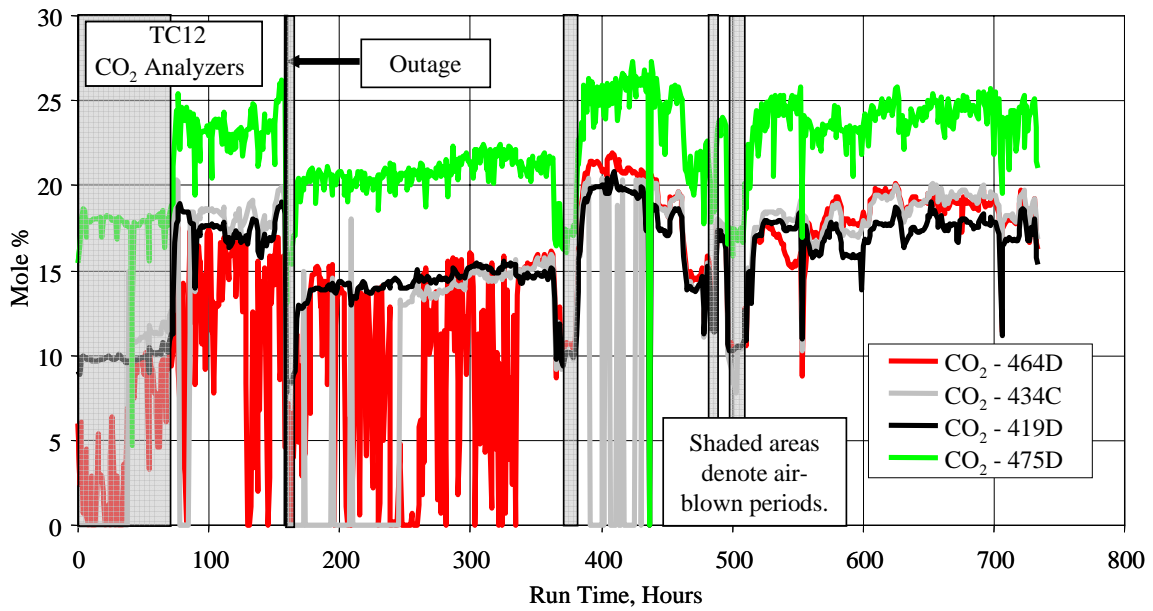
Figure 3.3-6 Carbon Dioxide Analyzer Data
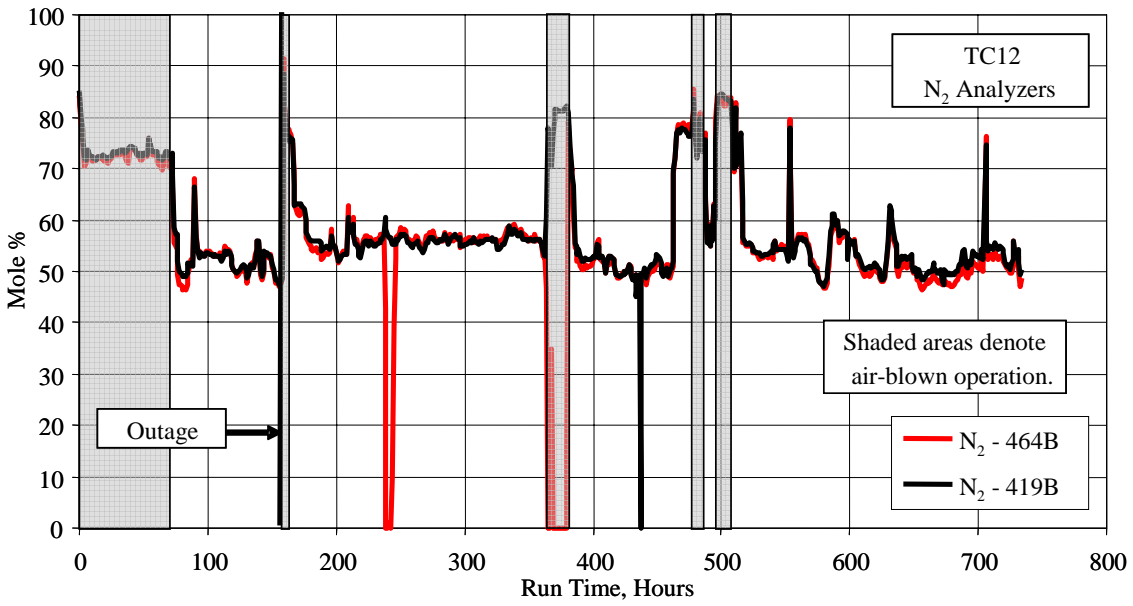
Figure 3.3-7 Nitrogen Analyzer Data
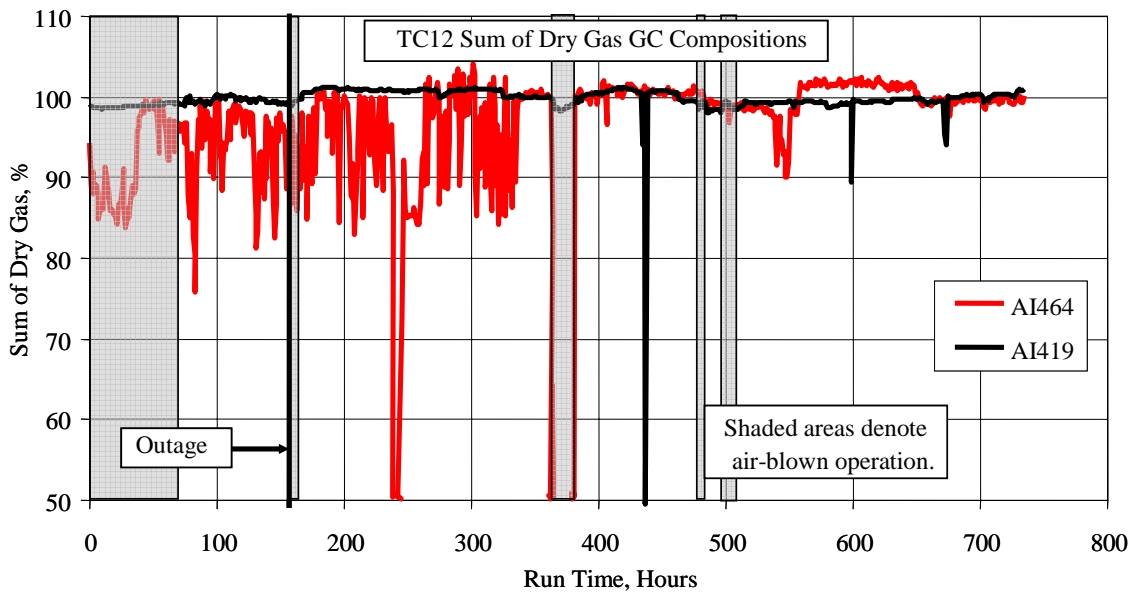
Figure 3.3-8 Sums of GC Gas Compositions (Dry)
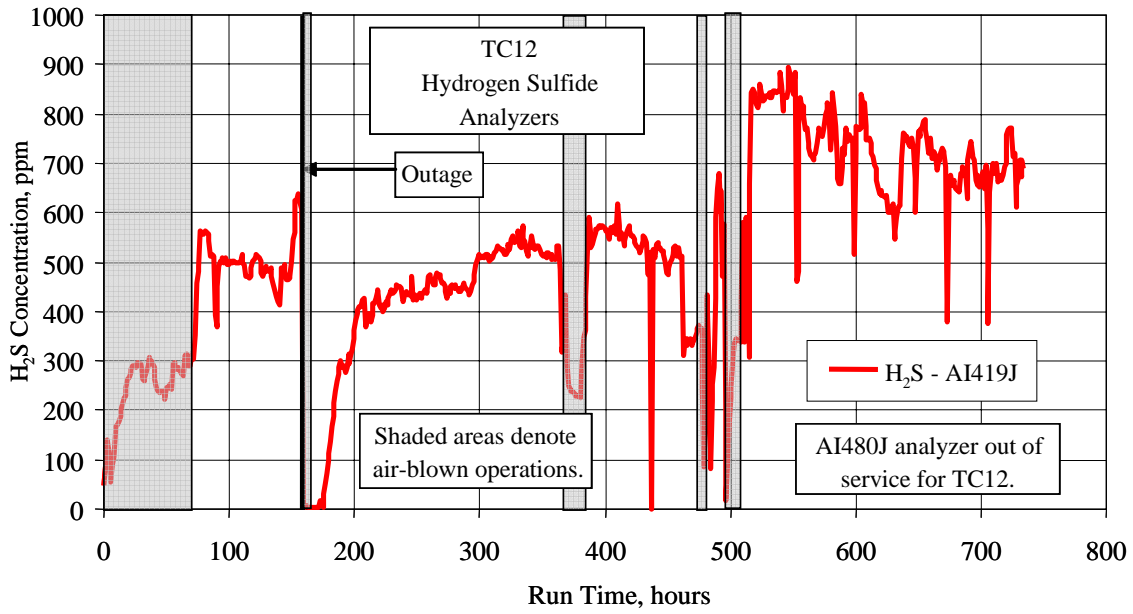
Figure 3.3-9 Hydrogen Sulfide Analyzer Data
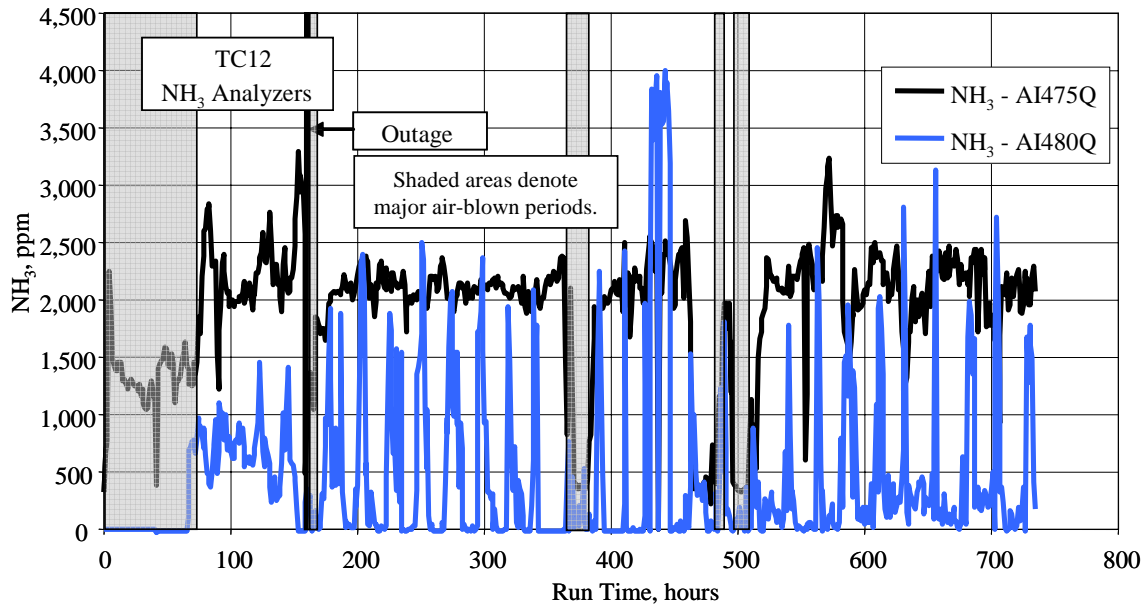
Figure 3.3-10 Ammonia Data
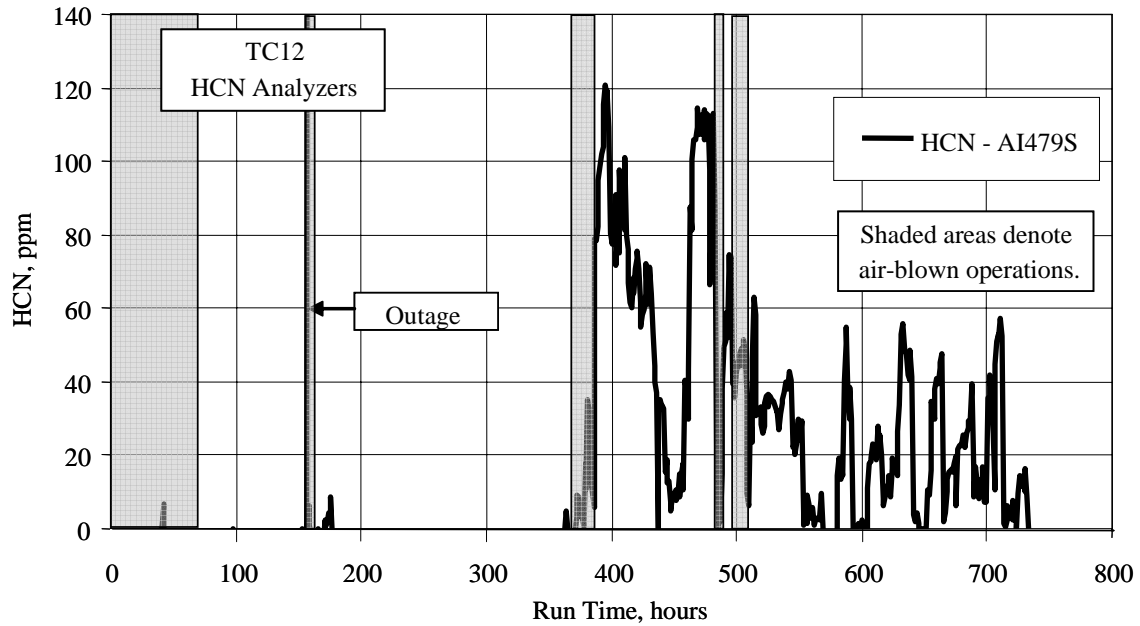
Figure 3.3-11 Hydrogen Cyanide Data
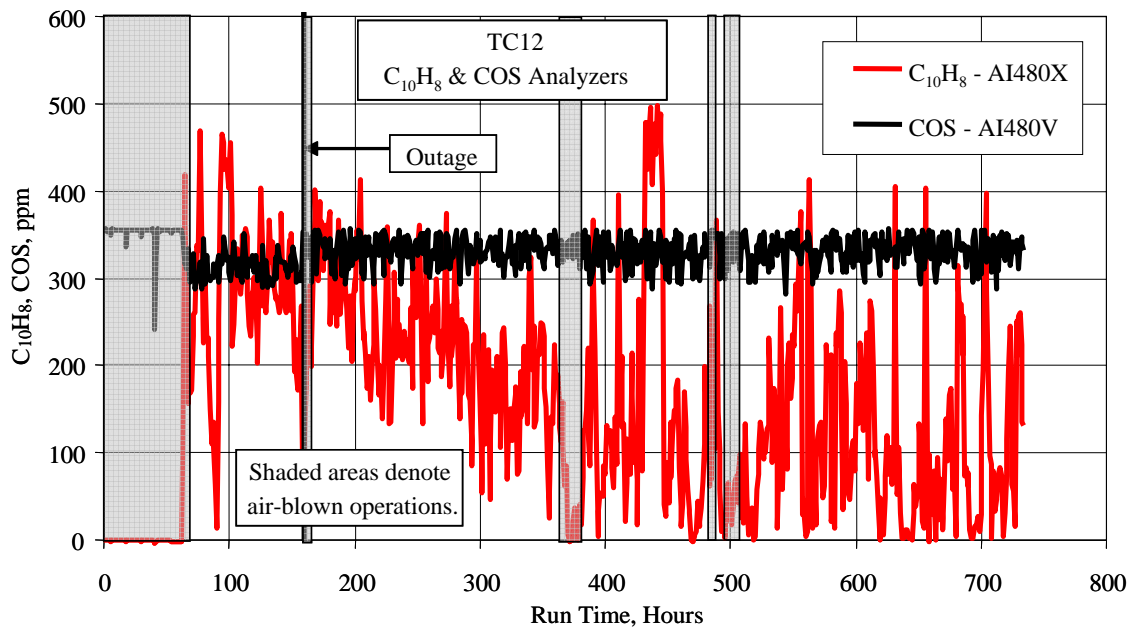
Figure 3.3-12 Naphthalene and Carbonyl Sulfide Data
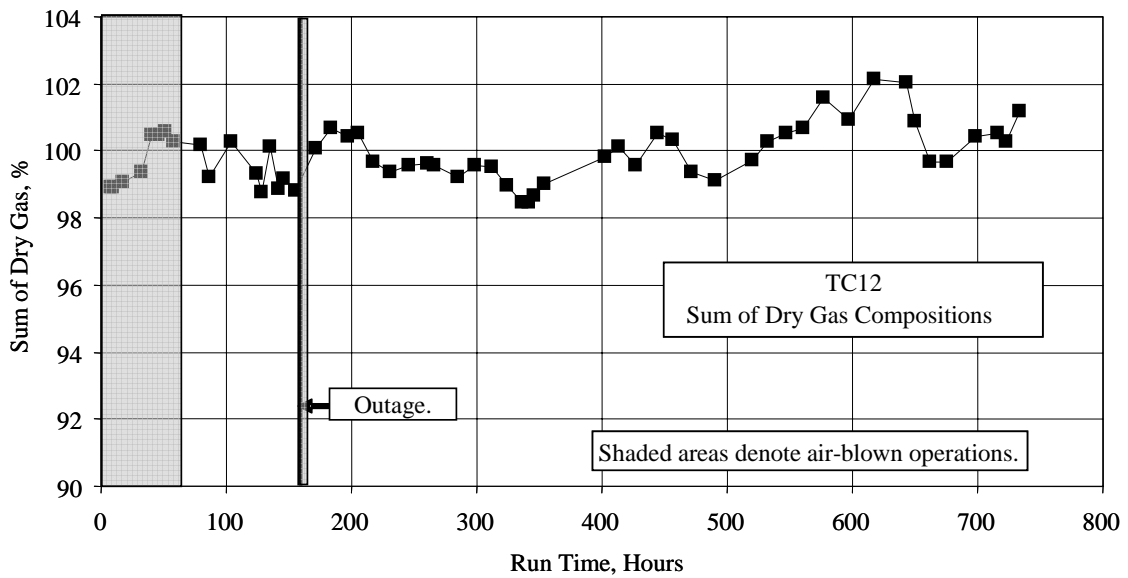
Figure 3.3-13 Sums of Dry Gas Compositions
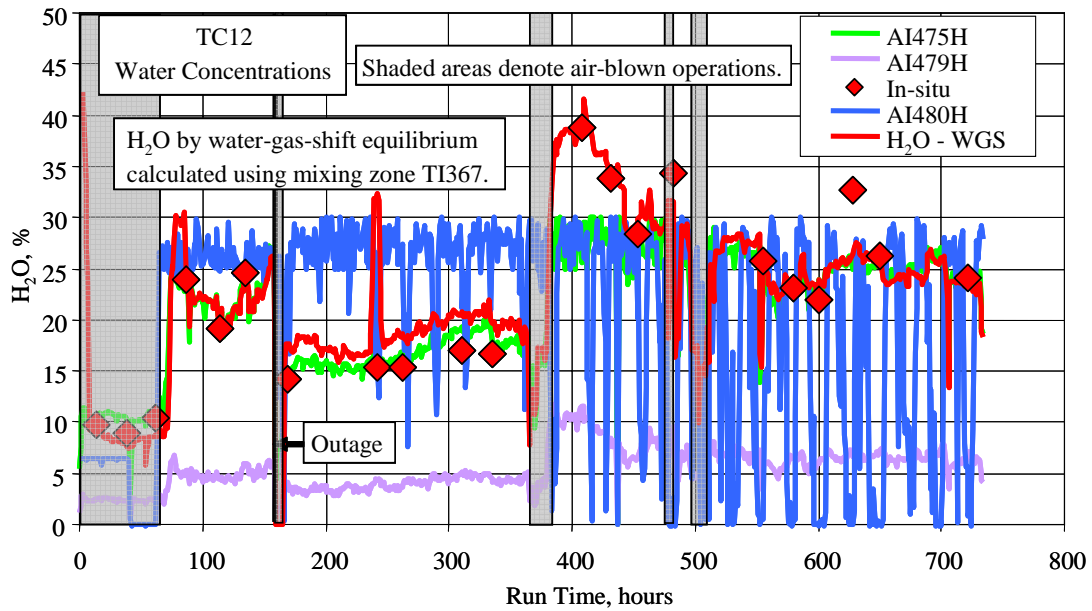
Figure 3.3-14 Continuous H2O Data
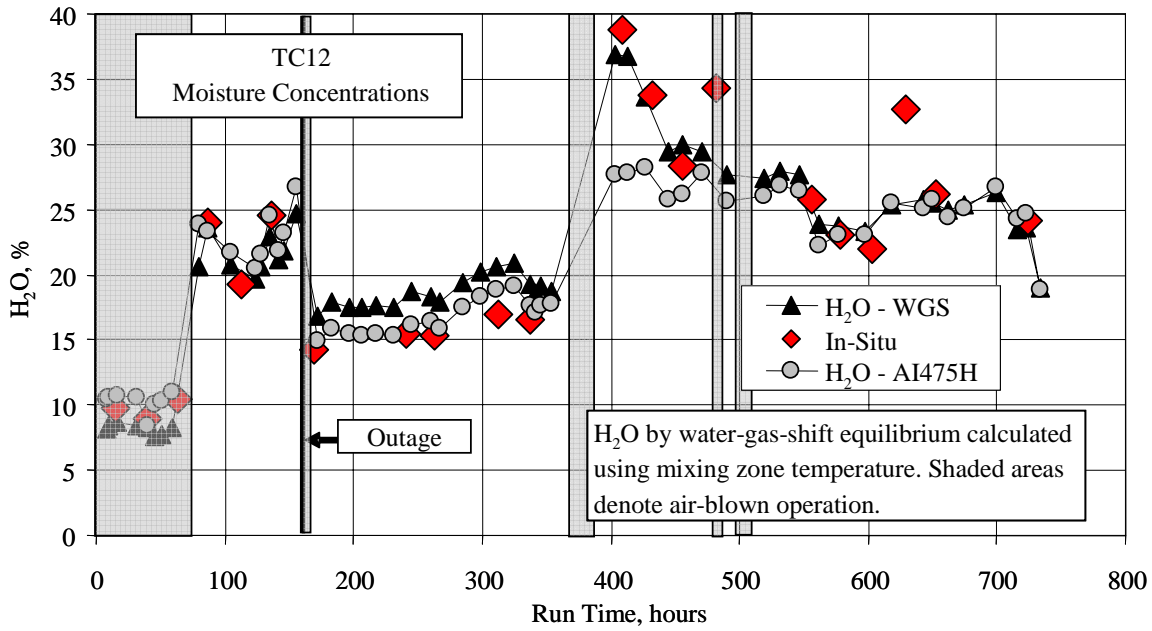
Figure 3.3-15 Comparison of Operating Period H₂O Data
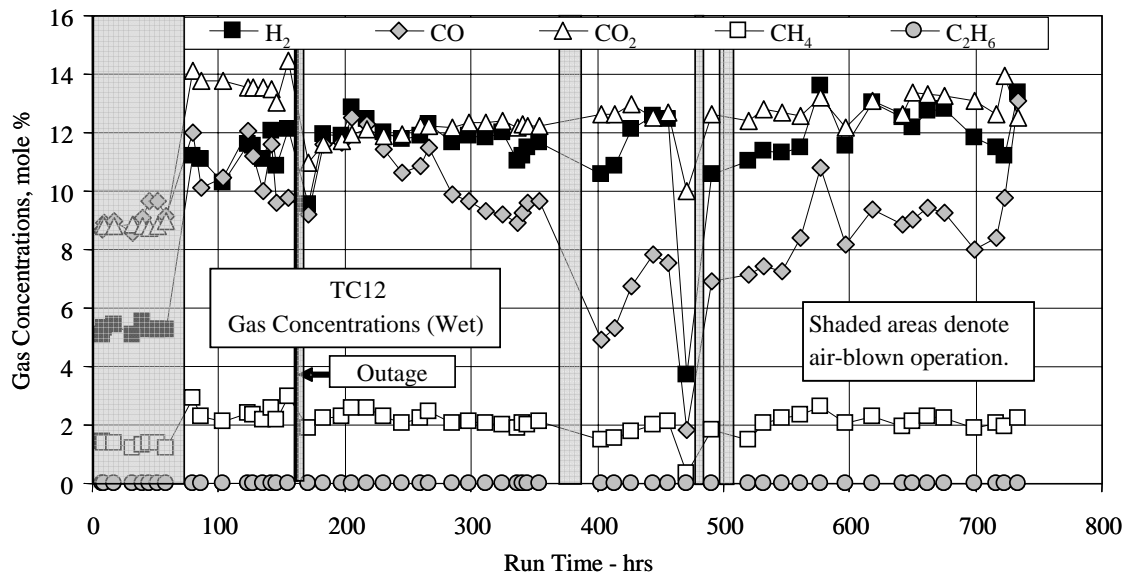
Figure 3.3-16 Wet Synthesis Gas Compositions
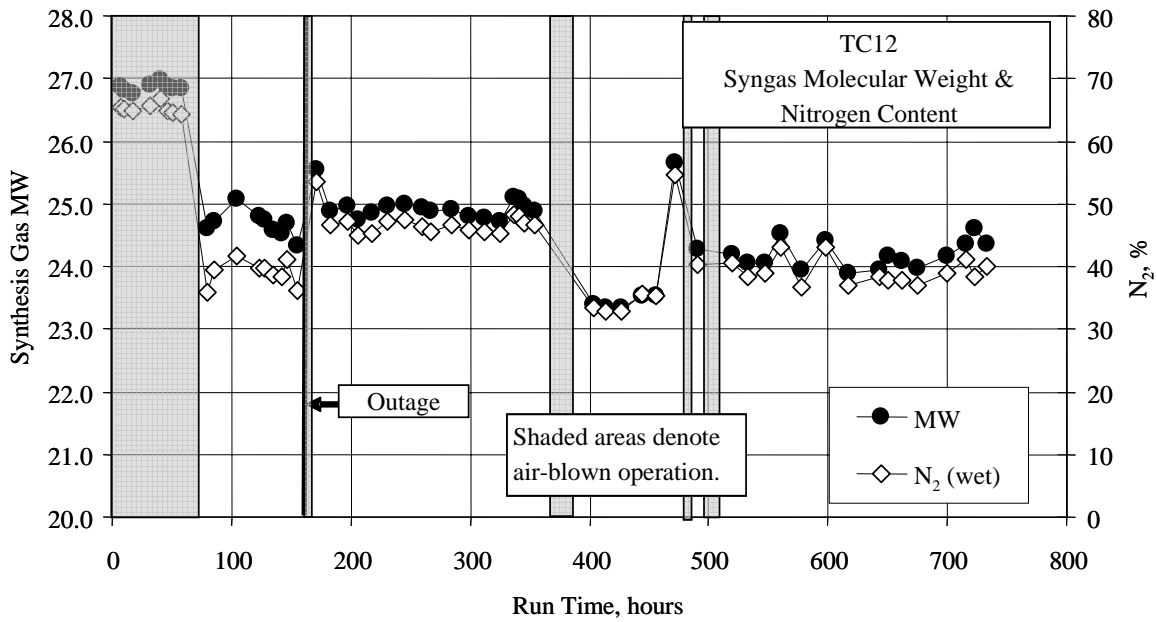
Figure 3.3-17 Syngas Molecular Weight and Nitrogen Concentration
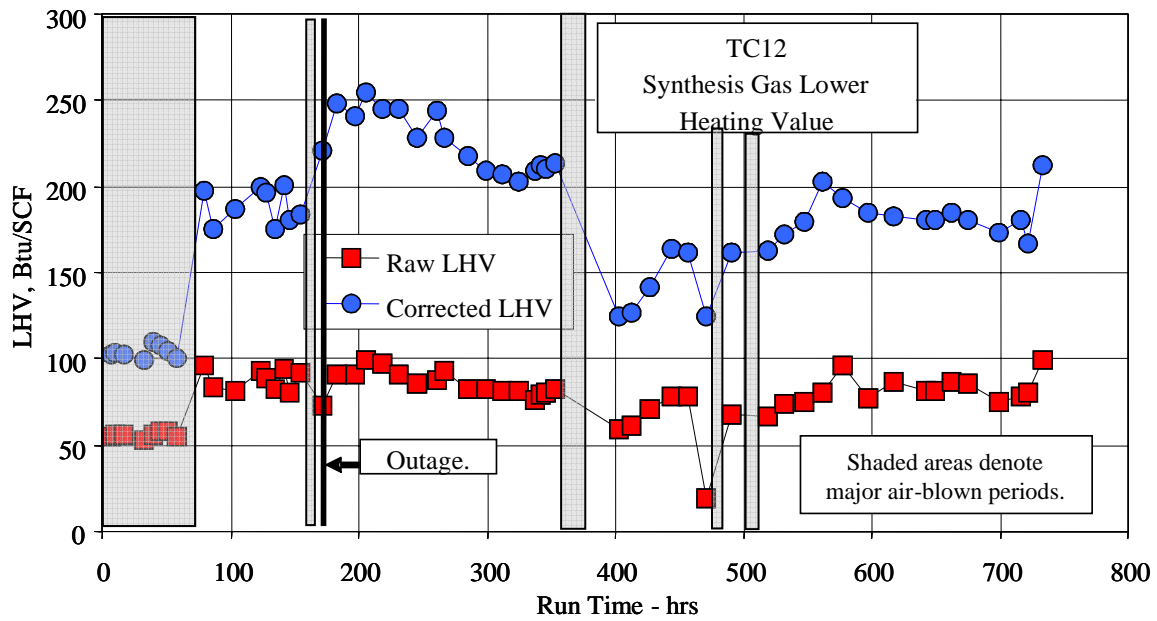
Figure 3.3-18 Synthesis Gas Lower Heating Values
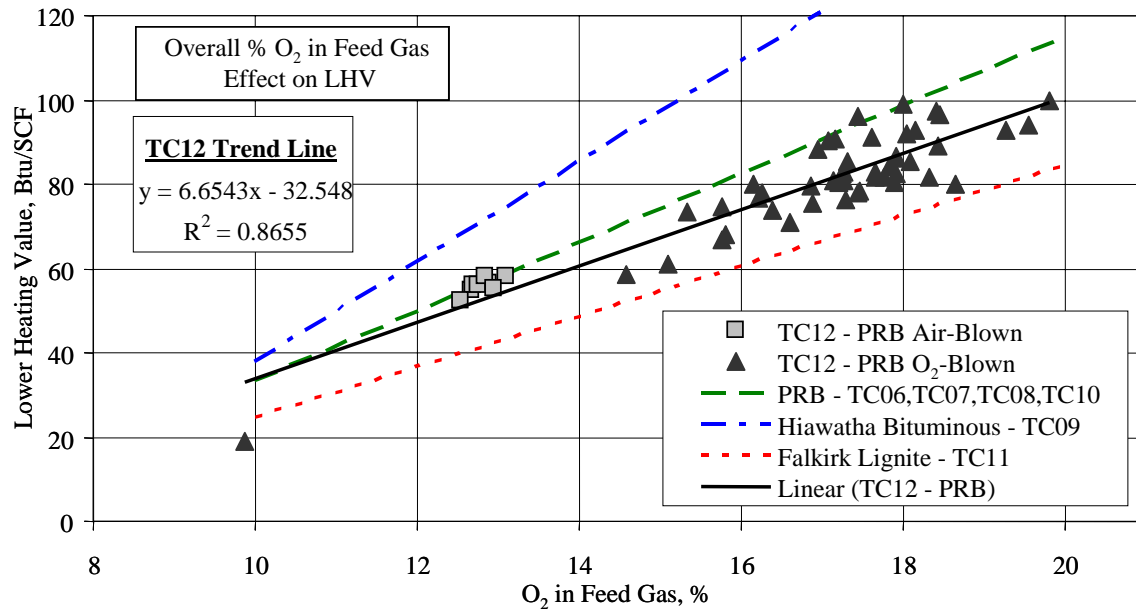
Figure 3.3-19 Raw Lower Heating Value and Overall Percent O_2
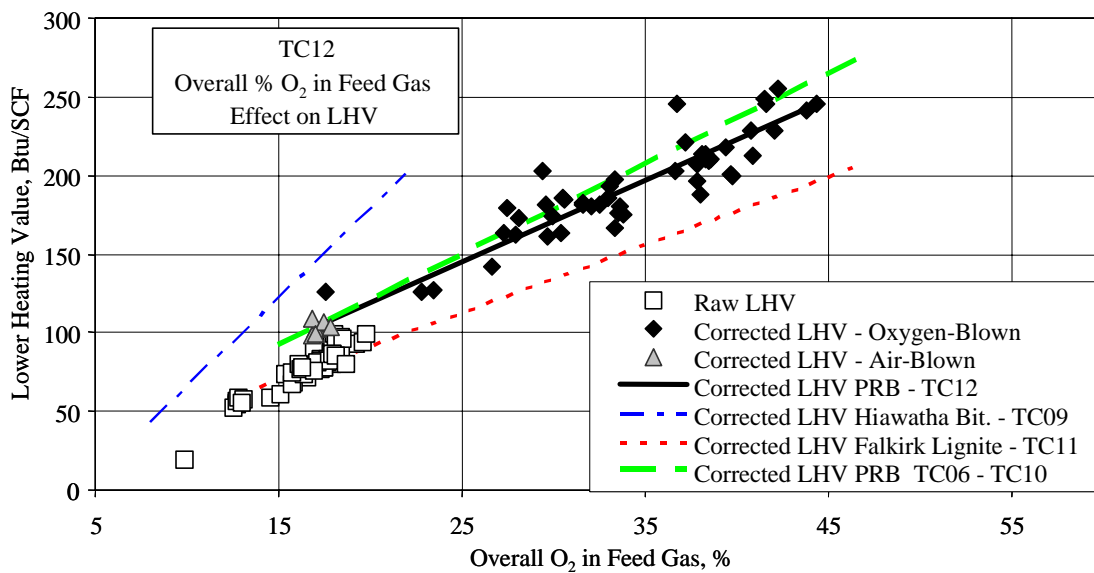
Figure 3.3-20 Corrected LHV and Overall Percent O_2
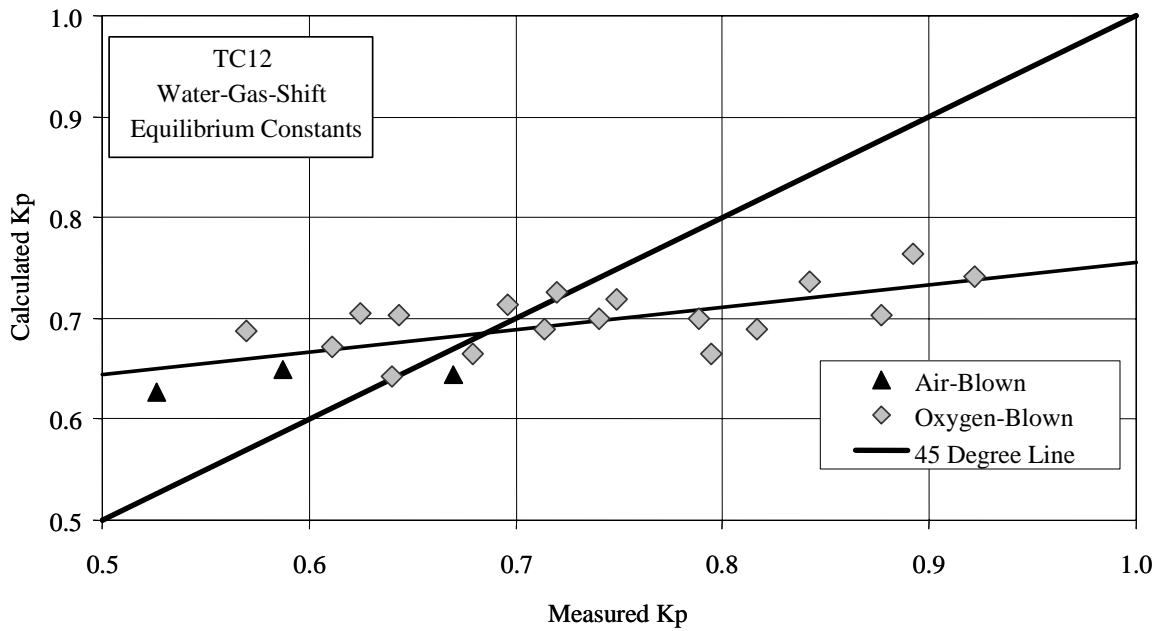
Figure 3.3-21 Water-Gas Shift Constants (In situ H_2O)
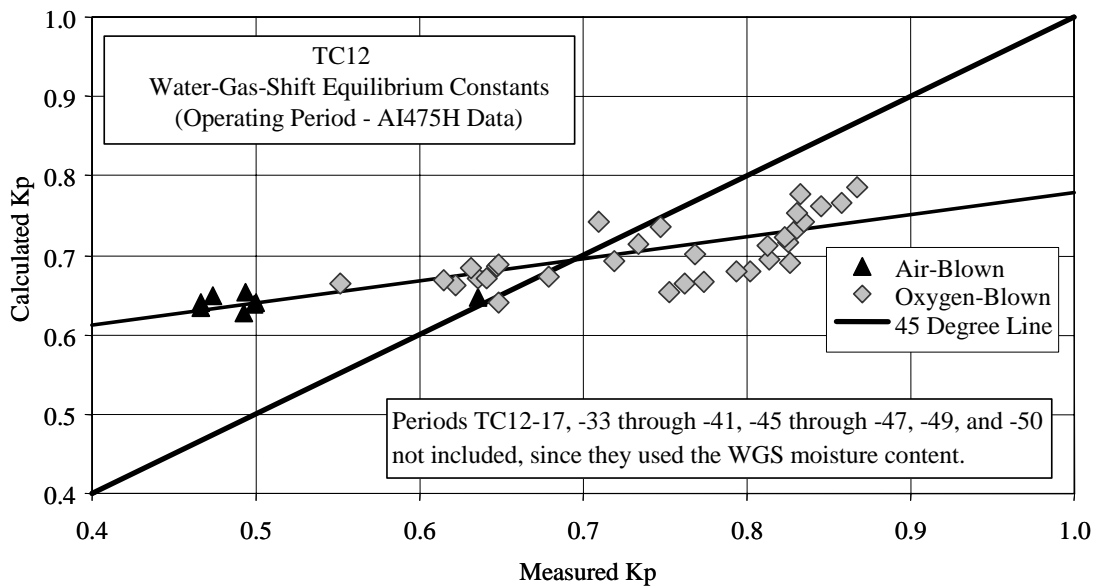
Figure 3.3-22 Water-Gas Shift Constant (AI475H H_2O)
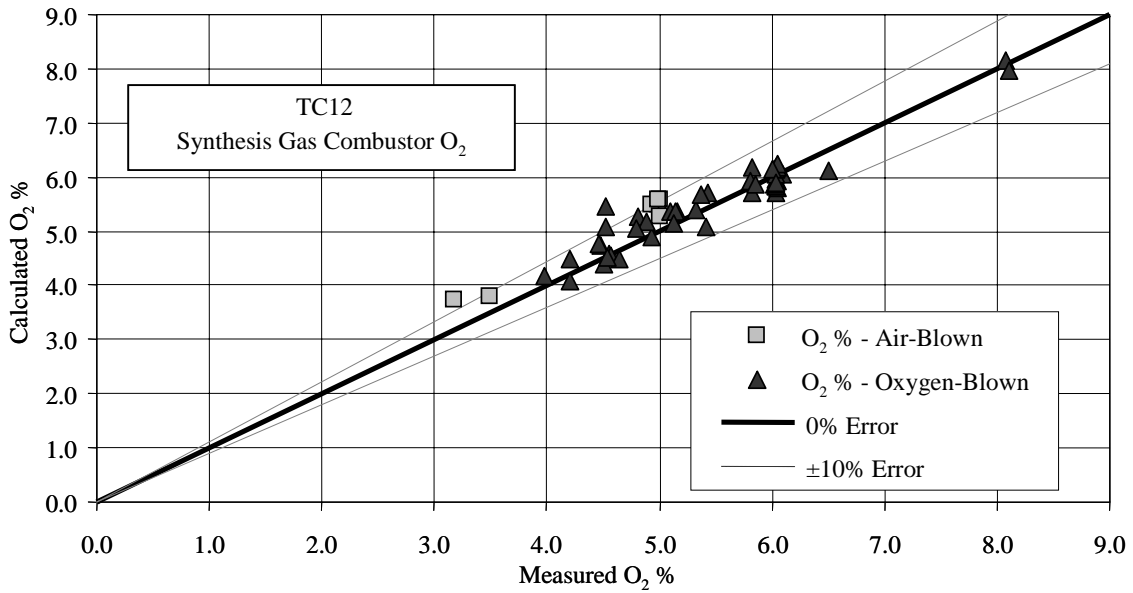
Figure 3.3-23 Synthesis Gas Combustor Outlet Oxygen
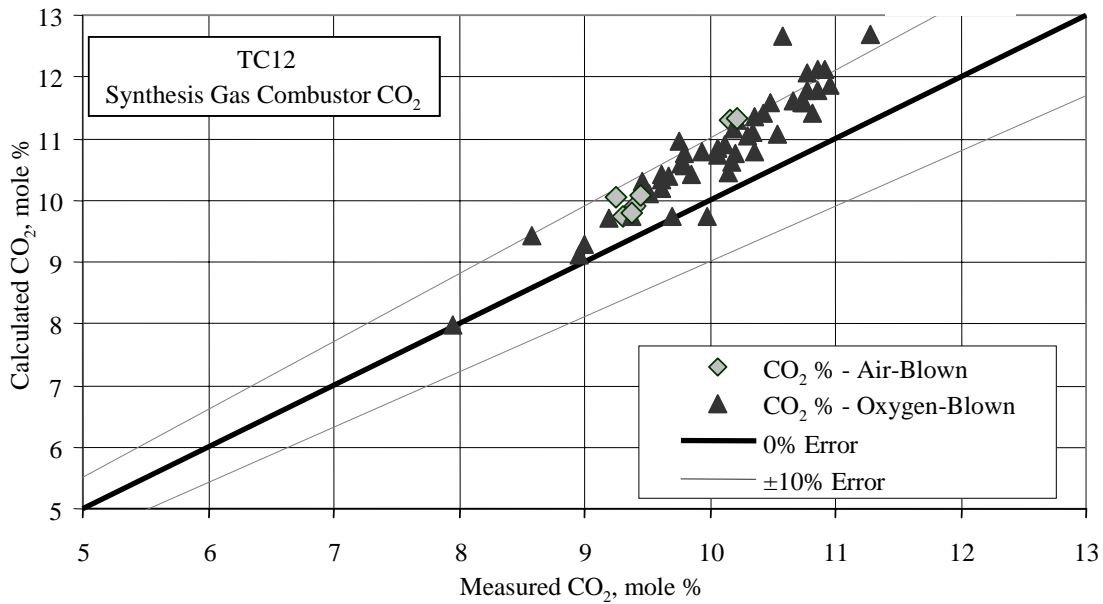
Figure 3.3-24 Synthesis Gas Combustor Outlet Carbon Dioxide
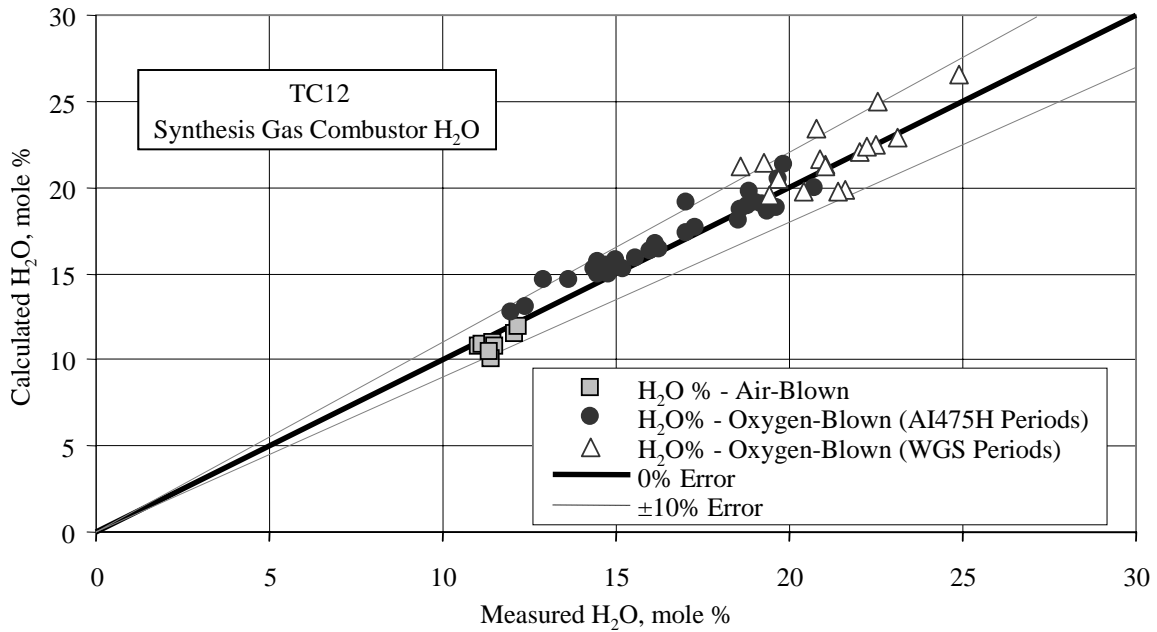
Figure 3.3-25 Synthesis Gas Combustor Outlet Moisture
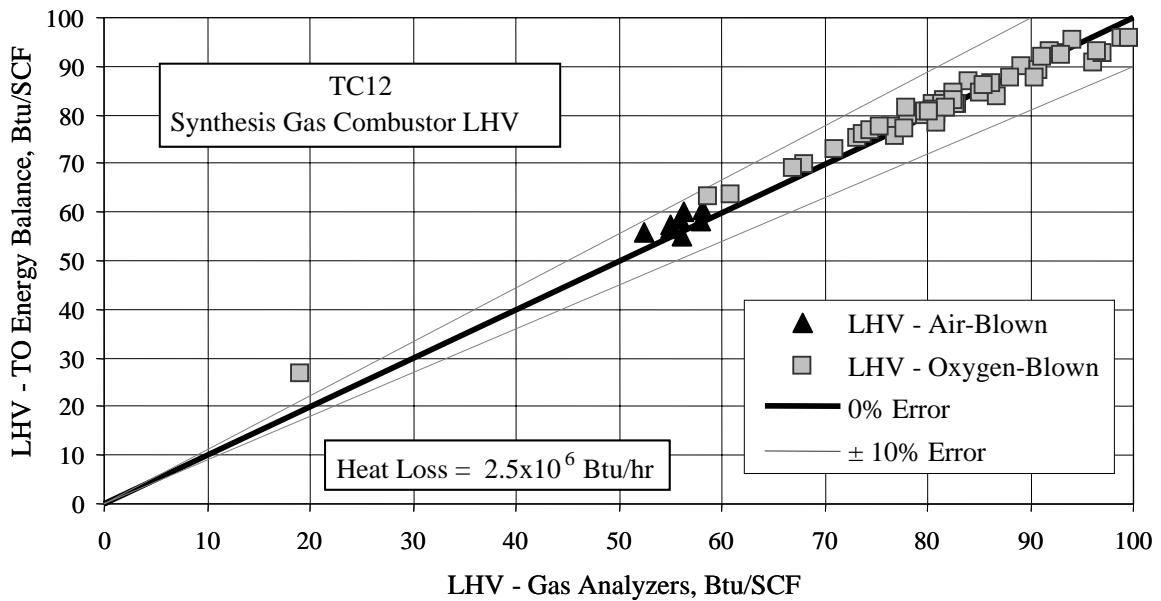
Figure 3.3-26 Synthesis Gas LHV
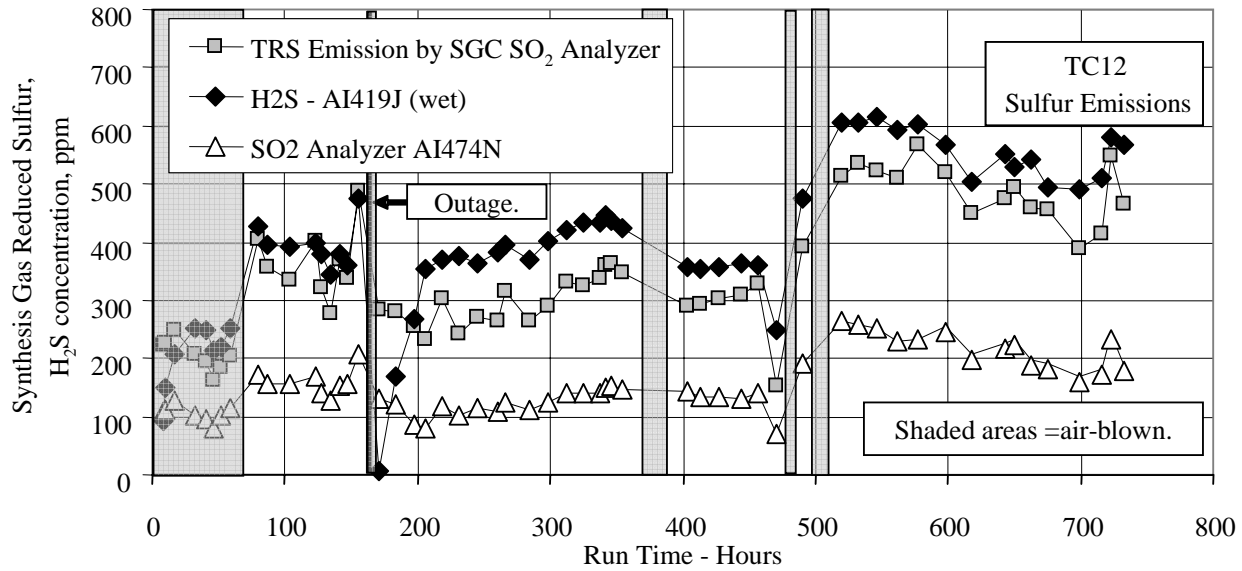
Figure 3.3-27 Sulfur Emissions
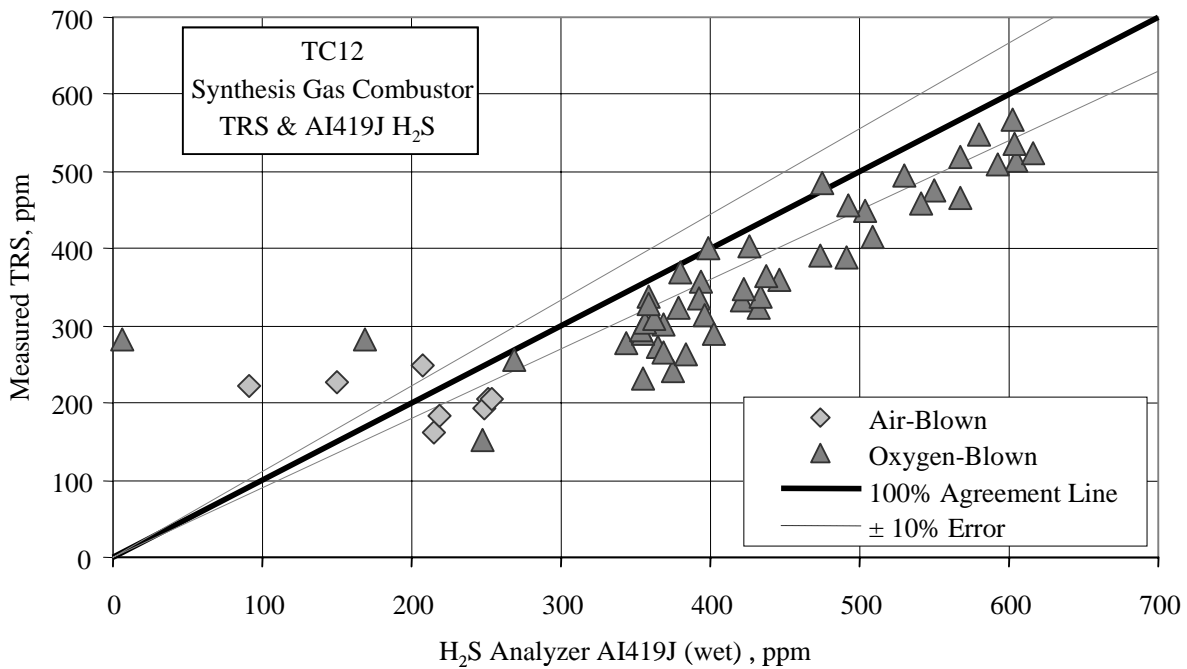
Figure 3.3-28 H2S Analyzer AI419J and Total Reduced Sulfur
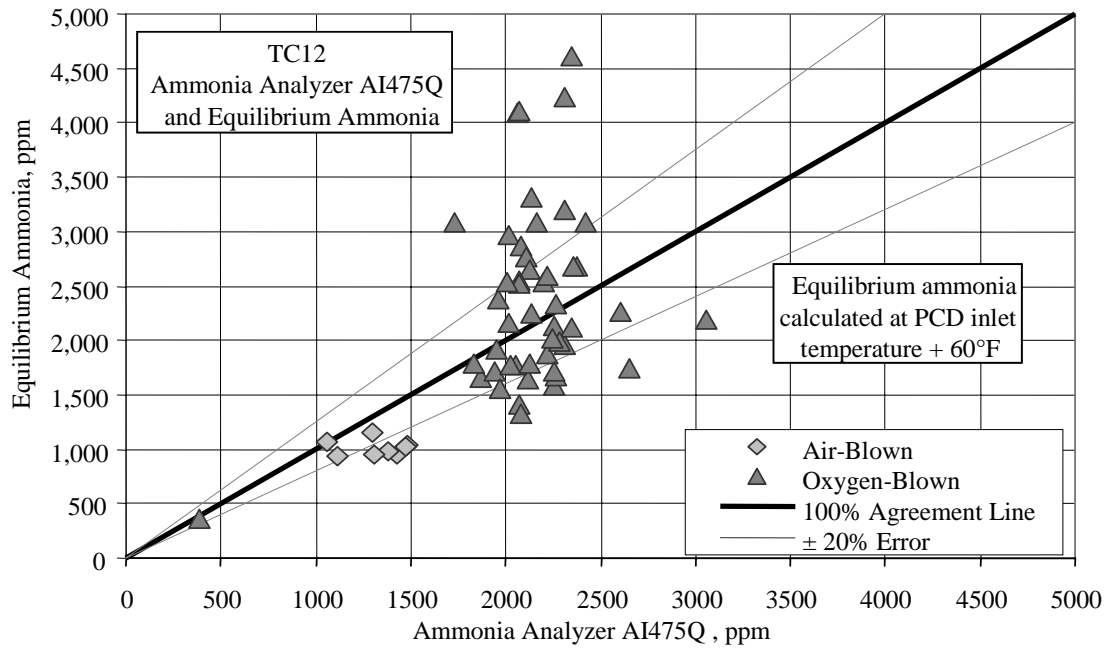
Figure 3.3-29 NH₃ Analyzer AI475Q and Equilibrium NH₃

3.4 SOLIDS ANALYSES

3.4.1 Summary and Conclusions

- PRB coal sulfur content, ash content, and LHV were not constant during TC12 testing. Other coal properties were mostly constant during TC12.
- Standpipe carbon was as high as 1.7-weight percent for periods with coal feed, but most standpipe samples contained less than 0.5-percent carbon. Coke breeze feed increased the standpipe carbon content slightly.
- The standpipe solids did not reach steady compositions with respect to SiO_2, CaO, Al_2O_3, and MgO compositions.
- Standpipe solids contained negligible amounts of CaS.
- Standpipe solids contained negligible $CaCO_3$; therefore the standpipe calcium was totally calcined.
- Loop seal carbon was as high as 46.6-weight percent, but only a limited amount of loop seal data were available because the sample system was plugged for most of the test run.
- Loop seal solids had a CaS content of up to 1.0 percent.
- Limited data suggest that the loop seal solids contained between 1.5- to 4.7-percent $CaCO_3$, meaning the loop seal calcium was about 83-percent calcined.
- PCD inlet in situ samples carbon, $CaCO_3$, CaO, CaS, and SiO_2 concentrations were, for the most part, consistent with FD0520 samples concentrations.
- The PCD fines sulfur and standpipe solids sulfur content indicate some Transport Gasifier sulfur capture.
- Regardless of operating mode, the PCD fines calcium was normally between 80- to 90-percent calcined.
- The loop seal silica and carbon compositions that were available were similar to those of the PCD solids.
- The standpipe silica and calcium compositions approached those of the PCD fines as TC12 progressed.
- The coal particle size ranged from 200 to 400 μ Sauter Mean Diameter (SMD) for the first 475 hours but then dropped to 175 μ SMD. The mass mean coal particle size was erratic at first—ranging from 680 to 960 μ at the beginning of the test run—before stabilizing at between 390 to 560 for the middle portion of the test run and between 260 and 360 μ at the end of the test run.
- The percent of fines in the coal feed increased towards the end of TC12.
- The standpipe solids particle size approached a steady-state value of approximately 300 μ SMD as the run progressed.
- The standpipe solids bulk density decreased from 90 to 80 lb/ft^3 during the run.
- Standpipe solids particle sizes were larger than in previous PRB air-blown and Hiawatha bituminous air-blown testing.
- Only one particle size datum (142 μ) was available for the loop seal solids.
- The PCD solids particle size ranged from 6 to 18 μ SMD.
- All in situ PCD fines particle sizes agreed well with the FD0520 samples particle sizes.
- The PCD solids bulk density was mostly between 20 to 30 lb/ft^3.

- The in situ PCD fines bulk densities were consistent with the FD0520 bulk densities.

3.4.2 Introduction

During TC12, solid samples were collected from the fuel-feed systems (FD0210 and FD0200), the sorbent-feed system (FD0220), the Transport Gasifier standpipe, the Transport Gasifier cyclone dipleg, and the PCD fine solids transport system (FD0520). In situ solids samples were also collected from the PCD inlet. Figure 3.4-1 illustrates these locations. The lab analyzed the solids samples for chemical composition and particle size. During TC12, sorbent and sand were added through FD0220. The FD0252 feeder fed coke breeze during startup and during periods of unstable coal feeder operation, but no samples were available from this system.

3.4.3 Feeds Analysis

Table 3.4-1 gives the average coal composition for the samples analyzed from FD0210 during TC12. Sample AB12881, taken at hour 87, was not included in the averages, since it had an unusually low carbon content. The FD0200 feeder also fed coal to the gasifier, but only a few samples were taken from that system. Since they came from the same source, the characteristics of the coal from the FD0200 feed system were very similar to those taken from the FD0210 feed system. Therefore, throughout this report the coal from both feeders is assumed to be the same. Figure 3.4-2 shows the carbon and moisture contents of the coal sampled from the FD0210 and the FD0200 coal feeders. The properties of the coal from both feeders were very similar. The average PRB coal carbon was 54.8-weight percent and the moisture content averaged 22 weight-percent. Both the carbon content of the coal and the moisture level varied only slightly. Generally, the coal possessed characteristics very similar to that of the PRB coal used in previous test runs. Note that there was a slight decrease in moisture after hour 155 (after the first shutdown) and a slight increase at hour 517.

Figure 3.4-3 shows the fuel sulfur and ash as sampled from FD0210 during TC12. The average values are given on Table 3.4-1. The average PRB coal sulfur content was 0.26-wt percent, and the average ash content was 5.27-wt percent. The sulfur and ash analyses were similar to PRB analyses from previous test runs. The maximum measured TC12 coal sulfur was an outlier at 0.53-wt percent, and the maximum coal ash was 9.11-wt percent. The coal sulfur content decreased from 0.3- to 0.2-wt percent for the first 139 hours of the test run, then remained constant until hour 510 when it increased to 0.36-wt percent. The coal sulfur content leveled off at 0.3-wt percent by the end of the run.

The higher heating value (HHV) and lower heating value (LHV) of the coal are given on Figure 3.4-4 along with the TC12 average values (also shown in Table 3.4-1). The LHVs are found by adjusting the HHVs to account for the coal hydrogen. The average HHV was 9,253 Btu/lb, and the average LHV was 8,924 Btu/lb. The heating values were low at the beginning of the test run, but stabilized 100 hours after startup, when the ash and sulfur concentrations began to stabilize.

The average values for the TC12 coal moisture, carbon, hydrogen, nitrogen, oxygen, sulfur, ash, volatiles, fixed carbon, HHV, LHV, CaO, SiO_2, Al_2O_3, MgO, and Fe_2O_3 are given in Table 3.4-1.

Also given in Table 3.4-1 are the molar ratios for coal calcium to sulfur (Ca/S). PRB coal has sufficient alkalinity in the ash to remove all of the coal sulfur.

FD0220 was used during TC12 to feed Ohio Bucyrus limestone into the Transport Reactor. The average composition of the two samples taken during TC12 is given in Table 3.4-2 (the three sand samples are excluded from the averages). The $CaCO_3$ average concentration was 76.5 percent, and the $MgCO_3$ average concentration was 16.5 percent.

3.4.4 Gasifier Solids Analysis

The chemical compositions of the solid compounds produced by the Transport Gasifier were determined using the solids chemical analysis and the following assumptions:

1. All carbon dioxide measured came from $CaCO_3$, hence moles CO_2 measured = moles $CaCO_3$.
2. All sulfide sulfur measured came from CaS.
3. All calcium not taken by CaS and $CaCO_3$ came from CaO.
4. All magnesium came from MgO.
5. Total carbon is measured, which is the sum of organic and inorganic (CO_2) carbon. The organic carbon is the total carbon minus the inorganic carbon (CO_2).
6. All iron reported as Fe_2O_3 is assumed to be present in the gasifier and PCD solids as FeO.
7. Inerts are the sum of the P_2O_5, K_2O, Na_2O, and TiO_2 concentrations.

It is assumed that all iron in both the standpipe and the PCD solids is in the form of FeO and not in the form of Fe_3O_4 or Fe_2O_3. Thermodynamically, the mild reducing conditions in the Transport Gasifier should reduce all Fe_2O_3 to FeO. The assumption of iron as FeO gives solids compositions totals that add up to around 100 percent.

It will also be assumed that no FeS is formed in the Transport Gasifier and that all the sulfur in the standpipe and PCD fines solids is present as CaS. It is thermodynamically possible that some FeS is formed. Most of the captured sulfur should be in the form of CaS due to the larger amount of calcium than iron in the system.

Table 3.4-3 gives the results from the standpipe analyses. The standpipe solids recirculate through the mixing zone, riser, and standpipe and their composition changes slowly with time as the start-up bed material is replaced with ash. The standpipe solids removal system (FD0510) was operated intermittently during TC12 to control the standpipe level. The flow rates for FD0510 and FD0520 solids during the stable operating periods are found in Section 3.5.

During startup, the standpipe mainly contained sand as mostly SiO_2. The standpipe did not contain pure sand at zero "run time" hours, since carbon was already present due to the use of coke breeze and the sporadic use of coal to heat the reactor before steady coal feed began.

As the run progressed, CaO, Al_2O_3, Fe_2O_3, and other inerts began to replace the start-up sand as shown in Figure 3.4-5, a plot of standpipe SiO_2, CaO, and Al_2O_3 contents versus run time. The SiO_2 content slowly decreased and both the Al_2O_3 and the CaO increased—the CaO content

dramatically due to a high sorbent feed rate. Sand was added at hour 159, after a brief scheduled outage. The fresh sand increased the SiO_2 content to around 90-weight percent and decreased the Al_2O_3 and the CaO contents. The same event occurred during subsequent sand additions around hours 255, 359, and 489. Due to the sand additions, and the use of coke breeze towards the end of the test run, the gasifier standpipe solids did not reach constant conditions by the end of TC12.

The standpipe organic carbon content is plotted in Figure 3.4-6. The average standpipe organic carbon content during coal operation was 0.28 percent and varied between 0.06- and 1.7-percent carbon. With the exception of the 1.7-percent carbon content at hour 47, the level of carbon was consistent with previous PRB standpipe samples that were taken during steady operations. The reason for the high carbon content at hour 47 is not readily apparent. Coke breeze feed to the gasifier occurred around the time of sampling at hours 471 and 489, causing the carbon content to be slightly higher for the samples taken at those hours than for the other samples.

As shown in Table 3.4-3, the sulfur level in the standpipe solids was very low, with all values essentially zero for all of the samples taken during coal feed. The low sulfur level indicates that all of the sulfur removed from the synthesis gas left the system via the PCD solids and neither accumulated in the gasifier nor left with the gasifier solids.

The standpipe $CaCO_3$ concentration was close to zero for most of TC12 (see Table 3.4-3), indicating that there was little inorganic carbon in the gasifier solids. The standpipe calcium was almost always 100-percent calcined to CaO. The standpipe solids calcium came from both the fuel and the sorbent added.

The standpipe MgO, Fe_2O_3, and other inerts contents are not plotted on Figure 3.4-5, but they followed the same trends as the CaO and Al_2O_3, that is, they accumulated in the gasifier as the feed solids replaced the start-up sand. The standpipe analyses consistency was good with a low bias as the total sum of the compounds in Table 3.4-3 averaged 99.4 percent with a standard deviation of only 0.3 percent. No FD0510 solid samples were analyzed during TC12, because the standpipe samples should give a more accurate view of the circulating solids composition.

Table 3.4-4 gives the results from the loop seal analyses. Unfortunately, the sampling system plugged early in the test run and only two samples were available for analysis. The loop seal solids are solids that recirculate through the mixing zone, riser, disengager, and loop seal. The composition of these solids changes slowly with time as the start-up bed material is replaced with ash from the coal. The standpipe solids consist of solids collected by both the disengager and the cyclone.

Since the first loop seal solids sample was taken only 15 hours after stable coal feed began, the first sample was basically sand and had a composition of 72.7-percent SiO_2. The loop seal did not contain pure sand at zero "run time" hours since there was a short period of coal and coke breeze feed prior to the establishment of steady coal feed at hour zero. The coal and coke breeze fed prior to hour zero diluted the loop seal sand with carbon and other materials derived from coal.

The two data points shown in Table 3.4-4 seem to indicate that bed materials such as CaO, Al_2O_3, and MgO did not quickly replace the start-up sand in the loop seal, however, since the samples were taken only 24 hours apart, the bed material possibly did not have enough time to replace the sand between samples. Previous test runs have confirmed that process-derived materials do indeed replace the start-up sand, however, the lack of more loop seal solids data does not allow for more detailed analysis.

The loop seal organic carbon contents for the two dipleg samples were 15.3- and 0.7-percent carbon. Thus, the early sample contained carbon content much higher than that of the standpipe, while the latter sample possessed carbon content only slightly higher than that of the standpipe.

The sulfur level in the loop seal solids was low, with values less than 1.0- and 0.0-percent CaS, both slightly higher than those in the standpipe. The loop seal $CaCO_3$ was 1.5- and 0.3-weight percent for the two TC12 samples, indicating that only a small, variable, amount of inorganic carbon was in the loop seal solids. The calcium of the first loop seal sample was around 84-percent calcined to CaO, while the second was 98-percent calcined. The volatile compound (sulfur and carbon) compositions were 4.4- and 0.8-weight percent in the loop seal solids (as received), higher than those in the standpipe solids taken in the same time period.

3.4.5 Gasifier Products Solids Analysis

Figure 3.4-7 plots the organic carbon (total carbon minus CO_2 carbon) for the PCD solids sampled from FD0520. The organic carbon content for every PCD fines sample analyzed is also given in Table 3.4-5. Since FD0520 ran continuously during TC12, solid samples were taken often, with a goal of one sample every 4 hours. Of the TC12 PCD solids that were sampled, 33 percent were analyzed.

In situ PCD inlet particulate solids recovered were also analyzed. The in situ carbon contents are compared with the FD0520 solids in Figure 3.4-7. The in situ solids organic carbon analyses were in agreement with the FD0520 solids for 15 of the 19 in situ solid samples. The in situ samples not in agreement occurred at hours 39, 86, 242, and 721. The sample at hour 39 occurred during air-blown operations, while the others occurred in oxygen mode. The data do not indicate any apparent reason why the carbon content of these in situ samples disagreed with the FD0520 samples. The organic carbon values were typical for PRB coal.

Small amounts of coke breeze were added to the gasifier through the FD0252 feeder from hours 464 to 487 and hours 496 to 509. The coke breeze did not appear to affect the organic carbon content of the FD0520 samples.

The PCD fines organic carbon ranged from 10 to 20 percent during the first 120 hours of TC12, indicating excellent carbon conversion. Between 120 and 150 hours the PCD fines organic carbon climbed to 50 percent and then fluctuated between 20 and 50 percent from after the outage at hour 159 until the end of the test run. The higher carbon content was the result of a significant decrease in carbon conversion. The increase in organic carbon occurred within 50 hours of entering oxygen-blown mode. Section 3.5.5 gives a more detailed discussion of the carbon conversion.

Figure 3.4-8 and Table 3.4-5 give the amounts of SiO_2 and CaO in the PCD solids as sampled from FD0520. Also plotted on Figure 3.4-8 are the in situ solids concentrations for SiO_2 and CaO. All 19 in situ data showed good agreement with the FD0520 solids for both CaO and SiO_2, except for the final in-situ sample taken at hour 721. The CaO content started the test run around 10 percent, and then rose to 30 percent during a period of high limestone feed, before falling back to 10 percent just before the scheduled outage. After the outage and corresponding sand addition, the CaO content remained close to 10 percent until the end of the run, with a lone exception at hour 661 when another period of high limestone feed occurred.

The SiO_2 contents of all 19 of the in-situ solids samples compared well with the values obtained from the FD0520 samples. The SiO_2 concentrations began the test run high, at over 60 percent. As the test run progressed, the SiO_2 content dropped to around 30 percent.

Figure 3.4-9 and Table 3.4-5 give the concentrations of $CaCO_3$ and CaS in the PCD solids as sampled from FD0520. Also plotted on Figure 3.4-9 are the in-situ solids concentrations for $CaCO_3$ and CaS. All of the in-situ samples $CaCO_3$ concentrations agreed well with those of the FD0520 solids, except for the final in-situ sample taken at hour 721. The TC12 PCD fines $CaCO_3$ concentrations were over a wider range (1 to 14 percent $CaCO_3$) than that seen in previous PRB testing either with limestone (TC06 and TC07 at 2 to 10 percent $CaCO_3$) or without (TC08 at 1 to 4 percent $CaCO_3$). It was also generally higher than that of Falkirk lignite (1 to 5 percent) and the Hiawatha bituminous test without limestone (TC09 – 1.5 to 3.0 percent $CaCO_3$, during the last 250 hours of the test run). After the scheduled outage at hour 159, however, it was lower than most other test runs (2 to 4 percent, with one outlier at 8 percent), until the final two solids samples taken during the period of high sorbent feed rate that occurred at the end of the test run.

All of the in situ CaS concentrations agreed well with the FD0520 solids CaS concentrations, as they had in previous runs. The FD0520 CaS varied from 0.02 to 1.2 percent during TC12 indicating that some sulfur occasionally left the system through the PCD fines.

The PCD fines calcination is defined as:

$$\% \text{ Calcination} = \frac{\text{M\% CaO}}{\text{M\% CaO} + \text{M\% CaCO}_3} \quad (1)$$

The PCD fines calcination is plotted on Figure 3.4-10. The PCD fines calcination fluctuated between 80 percent and 90 percent for the majority of TC12. Occasionally, it dropped to between 75 and 80 percent, and once rose as high as 99 percent. The mode of operation (air or oxygen mode) did not appear to affect the calcination. All previous runs with both PRB and Hiawatha bituminous coal with and without sorbent all had calcination values of between 80 and 90 percent, as did the air-blown and enhanced-air-blown portions of the TC11 Falkirk Lignite test run.

The calcium sulfation is defined as:

$$\% \text{Sulfation} = \frac{\text{M\%CaS}}{\text{M\%CaO} + \text{M\%CaCO}_3 + \text{M\%CaS}} \quad (2)$$

The PCD fines sulfation is plotted on Figure 3.4-10 with the PCD fines calcination. The PCD fines sulfation started TC12 at about 7 percent and then decreased to nearly zero by hour 59, just before the transition to oxygen-blown mode. The calcium sulfation started at 8 percent at hour 171, just after the scheduled outage, and remained around 3 percent for several hours, before falling to 1 percent around hour 400. The sulfation then fluctuated between 1 and 6 percent, once dropping to near zero at hour 661, for the remainder of the test run. The results are consistent with past data in that all previous runs with both PRB and Hiawatha bituminous with or without sorbent all had 0- to 10-percent sulfation percentages, as did the air and enhanced-air TC11 Falkirk Lignite sulfation percentages.

Table 3.4-5 gives the PCD fines compositions for the samples collected in FD0520. Additional components in Table 3.4-5, other than those plotted on Figures 3.4-7, -8, and -9, are MgO, FeO, and Al_2O_3. The MgO concentrations were between 2 and 10 percent. The Al_2O_3 concentrations were between 5 and 14 percent, with one outlier at 20 percent. Also given in Table 3.4-5 are the HHV, LHV, and organic carbon for the PCD fines. As expected, the trend of heating values follows the carbon content of the PCD fines. Note the samples with very low heating values of the samples taken at hours 7 and 79.

3.4.6 Solids Analysis Comparison

With the addition of the loop seal solids sampling system, sampling solids at three different points in the Transport Gasifier is now possible, allowing one to compare the various species concentrations as the run progresses. The additional analyses should give clues to the operation of the Transport Gasifier for different feeds and operating conditions.

A comparison of the total organic carbon contents for the standpipe, cyclone dipleg, and spent fines samples is shown in Figure 3.4-11. The PCD solids contained the highest amounts of organic carbon, significantly higher than the solids in the standpipe. During TC10 the loop seal carbon content was significantly higher than the standpipe carbon content and often was nearly as high as the PCD fines carbon content (see Figure 3.4-13 in the TC10 report). The TC11 data, on the other hand, indicate that the loop seal solids were very similar to the standpipe solids. Further testing will be required to determine whether this difference in loop seal carbon is a result of the different coals tested or the different mode of operation. TC10 and TC12 were mostly oxygen blown, while TC11 was predominantly air blown.

Figure 3.4-12 compares the silica (SiO_2) content between the standpipe, loop seal, and PCD solids samples. Consistent with the relative carbon contents discussed above, the standpipe solids have the highest SiO_2 content, and the PCD solids contain the lowest SiO_2 content. As the test run progressed, the standpipe silica concentrations began to approach the values of the PCD fines.

Figure 3.4-13 compares the calcium concentration between the standpipe, cyclone dipleg, and PCD solids samples. Note that the calcium is distributed between CaO, $CaCO_3$, and CaS. The PCD solids typically had the highest calcium content, but the calcium content of the standpipe solids often was very close to that of the PCD solids. Over time the calcium levels increased for

both the standpipe solids and the PCD solids, since the calcium from the coal ash slowly replaced the start-up sand (silica). The major decrease in calcium content occurred after the scheduled outage at hour 159 when sand addition occurred. Another decrease in standpipe calcium content occurred around hour 359, when sand was added, and the calcium content also decreased slightly during a period of coke breeze feed around hour 489. The standpipe calcium concentrations always started lower than the PCD concentration, then they rapidly approached the PCD concentrations as the test run progressed, probably indicating that the steady-state standpipe calcium solids concentration is the PCD fines calcium concentration. The change in the gasifier solids calcium concentration with time was very similar to that seen in TC10 and TC11.

3.4.7 Feeds Particle Size

The TC11 Sauter mean diameter (SMD) and mass mean diameter (D_{50}) particle sizes of the coal sampled from FD0210 are plotted on Figure 3.4-14. The PRB coal SMD particle size began the test run at μ microns and ranged between 200 and 400 μ during the first 475 hours of the test run. After 475 hours, the SMD dropped to around 175 μ, where it remained fairly constant for the remainder of the test run. The coal D_{50} began the test run at 680 μ and increased up to 960 μ by hour 35, before dropping to 520 μ at hour 51. After hour 51, the D_{50} followed the same trend as the TC12 SMD, but ranged slightly higher at between 390 and 560 μ for the middle portion of the test run, and between 260 and 360 for the last 200 hours. After hour 51, the D_{50} varied typically from 60 to 160 μ larger than the SMD. The TC12 D_{50} data was consistent with previous tests TC06 through TC09 and TC11. TC10 had a slightly higher D_{50} particle size than TC12 and the other test runs.

In past test runs, a high percentage of fines in the coal has resulted in an increased number of coal feeder outages due to packing of coal fines in the lock vessel. A measure of the amount of fines in the coal is the percentage of the smallest size fraction. To show the level of fines in the coal feed, the percent of ground coal less than 45 μ is plotted in Figure 3.4-15. As the coal particle size decreased, the percentage of coal fines less than 45 μ increased.

During TC12 the percent coal fines decreased from 6 to about 3 percent during the first 40 hours of TC12. The fines percentage remained around 3 percent, with an occasional spike up to 10 percent until hour 493, when the fines percentage jumped to 15 percent, due to problems in the coal milling system. After this point, the fines percentage fluctuated around 15 percent with a large spike up to 30 percent at hour 685. The high coal fines contributed to the coal feeder trips that occurred during the last 200 hours of TC12.

3.4.8 Gasifier Solids Particle Size

The TC12 standpipe solids particle sizes are given in Figure 3.4-16. The particle size of the solids increased as coal ash replaced the start-up sand. Sand added during the outage at hours 159 and 367 temporarily decreased the particle size back to around 150 μ (close to the particle size of the 122 μ D_{50} sand). Other sand additions did not affect the particle size dramatically. The particle size of the gasifier solids then increased again as coal ash accumulated in the gasifier. The SMD of the gasifier solids slowly increased from 160 microns at hour 39 to 265 μ at hour 127. After the outage, the standpipe SMD decreased to 150 μ and then increased to over 300 μ before the

sand addition of hour 367. The standpipe particle size then climbed slowly from 150 μ to 250 μ over the last 300 hours of the test run. Subsequent sand additions did not have as large an effect on particle size, possibly because the standpipe particle size was lower. The TC12 D_{50} was about 20 μ less than the TC12 SMD and followed the same trend as the SMD.

The standpipe solids seemed to reach a steady-state particle size of about 250 μ (SMD) during the first part of the test run. The steady-state value after the outage was around 300 μ (SMD), where it remained until the second major sand addition. After the second sand addition, the solids never again achieved a steady-state particle size, possibly due to many small sand additions that occurred later in the test run. Both steady states occurred during oxygen-blown operation (the air-blown portion of the test run having only lasted a short time).

Only one particle size sample was available from the loop seal in TC12 due to the pluggage or the sample system. The particle size of the loop seal sample was 142 μ SMD and 127 μ D_{50}.

Figure 3.4-17 plots the SMD and D_{50} for the PCD solids sampled from FD0520 and the 19 in-situ solids recovered during the PCD inlet sampling. All of the 19 in situ solids particle sizes agreed well with the particle size of the solids collected by FD0520. The PCD fines SMD typically ranged between 6 and 12 microns during all three modes of operation in TC12. The PCD fines D_{50} was about 5 μ larger then the SMD and followed the same trend as the SMD particle sizes.

3.4.9 Particle Size Comparison

Figure 3.4-18 plots all of the solids SMD particle sizes. The Transport Gasifier received coal at an average SMD size of 265 μ, while producing an average of 217 μ SMD gasifier solids and 10 μ SMD PCD fines. Surprisingly, the SMD of the standpipe was slightly higher than that of the coal fed during the last 100 hours of TC12. Since carbon typically is much more concentrated in the PCD fines than the standpipe solids, it is assumed that the coal shatters upon heating and produces very fine particulates. The cyclone performance also determines the standpipe particle size in that the cyclone determines the amount of fines that leave the circulating solids.

The D_{50} diameters were larger than the SMD for the FD210 samples (coal), and the FD0520 samples (PCD fines), while the TC11 SMD particle sizes are larger than the D_{50} particle sizes for the standpipe solids. This trend was also seen in TC06 to TC11. The standpipe solids have a nonGaussian (bimodal) distribution which probably caused the standpipe SMD to be larger than the standpipe D_{50}.

3.4.10 Standpipe and PCD Fines Bulk Densities

The TC12 standpipe, loop seal, and PCD fines bulk densities are given in Figure 3.4-19. The bulk density of the standpipe solids decreased very slowly as ash replaced the start-up sand after both the original startup and the sand additions around hours 159, 367, 471, and 650. The standpipe solids bulk density decreased from 90 to 80 lb/ft³ in about 90 hours after the sand addition around hour 367. The decrease in bulk density immediately after startup was not as pronounced, possibly because the ash from the coke breeze and sporadic coal feed during startup had already dropped the bulk density to around 80 lb/ft³. The standpipe solids bulk density in

test runs TC06 through TC11 behaved similarly to the TC12 standpipe bulk density, starting at 90 lb/ft^3 just after sand addition and then decreasing to about 80 lb/ft^3.

Only one loop seal solids sample was available for analysis. Its bulk density was similar to the standpipe density at the time of the sample.

The bulk densities for the FD0520 PCD solids samples from both FD0520 and the in situ PCD inlet are also plotted on Figure 3.4-19. The FD0520 and in situ solid samples bulk densities agreed very well with each other. The bulk densities of the FD0520 PCD fines were nearly constant at the beginning of the test run, varying from 20 to 30 lb/ft^3. Just prior to the outage at hour 159, the density dropped to around15 lb/ft^3. The sand addition during the outage caused the density to climb to 40 lb/ft^3, but the value fell quickly back to 15 lb/ft^3, where it remained for the rest of the test run (except for brief spikes that occurred whenever sand was added).

Table 3.4-1

Coal Analyses[1]

	Powder River Basin	
	Average Value[3]	Standard Deviation
Moisture, wt%	21.65	0.66
Carbon, wt%	54.98	0.96
Hydrogen[2], wt%	3.56	0.09
Nitrogen, wt%	0.74	0.03
Oxygen, wt%	13.56	0.66
Sulfur, wt%	0.26	0.07
Ash, wt%	5.27	1.04
Volatiles, wt%	32.94	0.57
Fixed Carbon, wt%	40.04	1.30
Higher Heating Value, Btu/lb	9,253	155
Lower Heating Value, Btu/lb	8,924	153
CaO, wt %	1.04	0.34
SiO_2, wt %	2.07	0.63
Al_2O_3, wt %	0.98	0.24
MgO, wt %	0.30	0.09
Fe_2O_3, wt %	0.35	0.06
Ca/S, mole/mole	3.00	1.22

Notes:

1. All analyses are as sampled at FD0210.

2. Hydrogen in coal is reported separately from hydrogen in moisture.

3. Sample AB12881 not included in averages due to discrepencies.

Table 3.4-2

Sorbent Analyses[1]

	Ohio Bucyrus	
	Value	Standard Deviation
$CaCO_3$, wt %	76.5	1.68
$MgCO_3$, wt %	16.5	0.03
$CaSO_4$, wt%	0.4	0.09
SiO_2, wt %	2.6	0.06
Al_2O_3, wt %	0.6	0.01
Fe_2O_3, wt %	1.5	1.28
Other Inerts[2]	0.1	0.00
Moisture, wt %	0.3	0.05
Total	98.5	

Notes:

1. All sorbent analyses are as sampled at FD0220.

2. Other inerts consist of P_2O_5, Na_2O, K_2O, and TiO_2.

Table 3.4-3
Standpipe Analyses

Sample Number	Sample Date & Time	Sample Run Time Hours	SiO_2 Wt. %	Al_2O_3 Wt. %	FeO Wt. %	Other Inerts[1] Wt. %	$CaCO_3$ Wt. %	CaS Wt. %	CaO Wt. %	MgO Wt. %	Organic Carbon Wt. %	Total Wt. %
AB12838	5/19/2003 10:00	39	82.4	4.9	1.9	2.2	0.1	0.0	6.0	1.1	0.3	99.0
AB12849	5/19/2003 18:00	47	81.2	4.6	1.8	2.0	0.2	0.0	6.4	1.1	1.6	99.1
AB12850	5/20/2003 2:00	55	81.4	5.7	1.8	2.2	0.1	0.0	6.9	1.2	0.1	99.3
AB12880	5/21/2003 2:00	79	76.1	5.8	2.1	2.4	0.0	0.0	11.1	1.6	0.1	99.3
AB12896	5/22/2003 2:00	103	62.8	8.2	2.7	2.6	0.3	0.0	20.4	2.7	0.2	99.9
AB12918	5/23/2003 2:00	127	36.6	8.5	2.7	2.4	0.0	0.0	43.7	5.8	0.2	99.8
AB12934	5/24/2003 2:00	151	36.3	9.9	3.1	2.4	0.3	0.0	41.7	5.7	0.0	99.6
AB13047	6/20/2003 18:00	175	90.2	3.2	0.8	2.2	0.0	0.0	2.7	0.6	0.1	99.7
AB13050	6/21/2003 18:00	199	84.9	3.8	1.5	2.3	0.0	0.0	5.6	1.3	0.0	99.4
AB13051	6/22/2003 2:00	207	81.9	4.3	1.8	2.2	0.0	0.0	7.3	1.6	0.1	99.4
AB13095	6/23/2003 10:00	239	76.5	6.8	2.1	2.6	0.0	0.0	8.7	1.9	0.2	99.0
AB13102	6/24/2003 2:00	255	74.0	7.5	2.5	2.9	0.0	0.0	10.3	2.2	0.1	99.5
AB13128	6/25/2003 10:00	287	76.2	6.2	2.4	2.8	0.0	0.0	9.4	2.1	0.4	99.4
AB13145	6/26/2003 10:00	311	71.6	8.5	2.6	3.1	0.0	0.0	10.9	2.3	0.5	99.5
AB13149	6/27/2003 2:00	327	70.6	9.1	2.7	3.1	0.1	0.0	11.0	2.4	0.2	99.3
AB13187	6/28/2003 10:00	359	67.6	10.0	3.1	3.4	0.0	0.0	12.3	2.6	0.1	99.1
AB13192	6/30/2003 2:00	399	83.4	4.7	1.6	2.2	0.0	0.0	6.2	1.3	0.0	99.4
AB13217	7/1/2003 10:00	431	79.7	6.8	1.9	2.7	0.0	0.0	6.9	1.5	0.2	99.8
AB13228	7/2/2003 10:00	455	73.5	9.2	2.4	3.2	0.1	0.0	9.0	1.9	0.4	99.8
AB13243[2]	7/3/2003 2:00	471	71.7	10.2	2.8	3.3	0.0	0.0	8.7	1.9	0.9	99.7
AB13282[2]	7/4/2003 18:00	489	78.4	7.2	3.4	2.7	0.0	0.0	5.9	1.4	1.0	99.9
AB13286	7/6/2003 2:00	521	75.7	8.9	4.3	2.8	0.0	0.0	6.3	1.5	0.2	99.6
AB13288	7/6/2003 18:00	537	70.5	11.7	4.4	3.3	0.0	0.0	7.8	1.8	0.1	99.5
AB13311	7/7/2003 18:00	561	67.0	12.5	5.0	3.7	0.1	0.0	8.6	2.0	0.1	99.1
AB13329	7/8/2003 10:40	578	63.4	13.7	5.2	3.9	0.0	0.0	10.4	2.3	0.3	99.2
AB13352	7/9/2003 10:00	601	64.1	13.7	5.1	3.8	0.0	0.0	10.2	2.3	0.1	99.2
AB13355	7/10/2003 2:00	617	59.8	15.5	5.6	4.3	0.0	0.0	11.2	2.5	0.1	99.0
AB13383	7/11/2003 10:00	649	60.2	15.6	5.3	4.0	0.0	0.0	11.1	2.5	0.1	98.8
AB13415	7/12/2003 10:00	673	49.8	16.9	5.8	4.5	0.1	0.0	18.3	3.5	0.2	99.0
AB13418	7/13/2003 10:00	697	48.3	18.5	6.0	5.1	0.0	0.0	17.5	3.5	0.1	99.0
AB13422	7/14/2003 10:00	721	48.8	16.6	5.6	4.5	0.0	0.0	19.6	3.7	0.3	99.0

Notes:

1. Other inerts consist of P_2O_5, Na_2O, K_2O, & TiO_2

2. Samples AB13243 and AB13282 were taken during or after periods of extensive coke breeze feed.

Table 3.4-4

Loop Seal Analyses

Sample Number	Sample Date & Time	Sample Run Time Hours	SiO_2 Wt. %	Al_2O_3 Wt. %	FeO Wt. %	Other Inerts[1] Wt. %	$CaCO_3$ Wt. %	CaS Wt. %	CaO Wt. %	MgO Wt. %	Organic Carbon Wt. %	Total Wt. %
AB12823	5/18/2003 10:00	15	72.7	7.2	3.4	3.2	1.5	1.0	4.3	1.5	15.3	110.0
AB12939	5/19/2003 10:00	39	82.1	5.2	1.8	2.3	0.3	0.0	6.7	1.2	0.7	100.3

Notes:

1. Other inerts consist of P_2O_5, Na_2O, K_2O, & TiO_2

Table 3.4-5 (Page 1 of 2)

PCD Fines From FD0520 Analyses

Sample Number	Sample Date & Time	Sample Run Time Hours	SiO$_2$ Wt. %	Al$_2$O$_3$ Wt. %	FeO Wt. %	Other Inerts[1] Wt. %	CaCO$_3$ Wt. %	CaS Wt. %	CaO Wt. %	MgO Wt. %	Organic C (C-CO$_2$) Wt. %	Total Wt. %	HHV Btu/lb.	LHV Btu/lb.
AB12830	5/18/2003 2:00	7	60.4	7.6	4.4	4.0	1.2	0.6	5.8	1.9	12.6	98.4	1,179	1,159
AB12832	5/18/2003 14:00	19	46.6	11.9	3.2	3.1	2.6	0.3	10.9	2.6	20.1	101.4	2,676	2,646
AB12836	5/19/2003 6:00	35	35.3	12.1	3.3	2.4	3.7	0.9	19.1	4.3	17.6	98.6	2,674	2,648
AB12854	5/19/2003 22:00	51	27.4	9.8	3.6	1.9	6.3	1.2	23.5	5.5	20.4	99.6	3,158	3,126
AB12856	5/20/2003 6:00	59	26.7	9.7	3.6	1.9	7.0	0.3	26.7	6.0	19.6	101.3	2,710	2,680
AB12875	5/21/2003 2:00	79	29.2	9.2	3.1	1.6	7.8	0.0	29.3	6.5	13.5	100.4	1,903	1,882
AB12882	5/21/2003 10:00	87	24.9	8.2	2.8	1.5	10.3	0.0	27.3	6.9	17.4	99.2	2,629	2,602
AB12893	5/22/2003 2:00	103	21.3	6.5	2.1	1.2	12.9	0.0	30.3	8.7	16.2	99.2	2,395	2,362
AB12914	5/22/2003 22:00	123	11.9	5.2	1.8	1.3	13.4	0.0	36.9	9.9	18.2	98.7	2,774	2,748
AB12915	5/23/2003 2:00	127	11.4	5.9	1.8	1.4	12.6	0.0	32.2	8.5	24.6	98.5	3,735	3,696
AB12923	5/23/2003 10:00	135	12.2	6.0	1.9	1.5	12.7	0.0	24.8	7.0	32.4	98.6	4,951	4,902
AB12936	5/23/2003 18:00	143	18.5	10.0	2.6	2.4	4.8	0.2	16.8	3.7	38.9	98.0	5,897	5,839
AB12937	5/23/2003 22:00	147	20.1	10.7	2.7	2.5	4.7	0.2	16.3	3.6	37.0	97.7	5,682	5,627
AB12939	5/24/2003 6:00	155	18.1	10.2	2.3	2.1	4.7	0.2	11.3	2.7	46.6	98.2	7,024	6,954
AB13055	6/20/2003 14:00	171	31.0	9.1	2.6	2.9	2.7	1.1	8.3	2.4	41.8	101.9	5,790	5,750
AB13057	6/20/2003 22:00	179	33.7	10.2	2.8	2.8	3.8	0.3	11.4	3.0	33.2	101.3	4,600	4,560
AB13059	6/21/2003 6:00	187	32.0	9.9	2.7	2.8	3.6	0.4	10.8	2.8	33.9	99.1	4,943	4,900
AB13063	6/21/2003 22:00	203	34.0	8.9	2.4	2.7	3.0	0.4	9.4	2.5	35.5	98.8	5,261	5,218
AB13064	6/22/2003 2:00	207	29.2	8.3	2.2	2.3	3.5	0.5	8.5	2.4	42.0	98.9	6,129	6,080
AB13070	6/23/2003 2:00	231	26.5	7.6	2.0	2.1	3.8	0.4	6.9	2.1	46.9	98.3	6,988	6,927
AB13072	6/23/2003 10:00	239	27.4	7.6	2.1	1.9	2.3	0.4	8.0	2.1	45.8	97.6	6,882	6,829
AB13111	6/24/2003 9:00	262	30.7	8.5	2.3	2.4	3.6	0.4	8.6	2.4	39.6	98.5	5,927	5,882
AB13115	6/25/2003 2:00	279	29.1	8.3	2.1	2.3	3.6	0.3	7.3	2.2	43.1	98.3	6,467	6,414
AB13135	6/25/2003 18:00	295	28.9	8.8	2.3	2.4	3.6	0.3	7.9	2.3	42.2	98.6	6,201	6,150
AB13141	6/26/2003 10:00	311	27.0	8.9	2.4	2.2	3.2	0.4	8.6	2.3	44.8	99.8	6,501	6,451
AB13155	6/26/2003 22:00	323	27.9	9.6	2.6	2.3	4.2	0.4	8.7	2.4	41.2	99.2	6,069	6,023
AB13157	6/27/2003 6:00	331	23.9	8.7	2.3	2.0	4.3	0.4	7.2	2.1	47.8	98.7	7,143	7,088
AB13158	6/27/2003 18:00	343	23.6	8.4	2.3	2.0	3.7	0.4	7.2	2.0	48.3	98.0	7,212	7,152

Notes:

1. Other inerts consist of P2O5, Na2O, K2O, & TiO2

2. Samples AB13246, AB13248 and AB13290 were taken during or just after a period of coke breeze feed.

Table 3.4-5 (Page 2 of 2)

PCD Fines From FD0520 Analyses

Sample Number	Sample Date & Time	Sample Run Time Hours	SiO_2 Wt. %	Al_2O_3 Wt. %	FeO Wt. %	Other Inerts[1] Wt. %	$CaCO_3$ Wt. %	CaS Wt. %	CaO Wt. %	MgO Wt. %	Organic C $(C-CO_2)$ Wt. %	Total Wt. %	HHV Btu/lb.	LHV Btu/lb.
AB13159	6/27/2003 22:00	347	27.8	9.4	2.5	2.3	3.9	0.4	8.2	2.3	42.3	99.3	6,185	6,135
AB13163	6/28/2003 14:00	363	24.0	7.9	2.1	2.0	3.3	0.4	8.0	2.1	50.1	99.9	7,364	7,302
AB13172	6/30/2003 2:00	399	31.4	11.5	2.9	2.6	2.7	0.2	12.4	2.8	32.0	98.5	4,671	4,624
AB13194	6/30/2003 10:00	407	26.0	10.2	2.7	2.3	2.0	0.2	11.4	2.6	41.5	98.8	6,061	5,999
AB13214	7/1/2003 10:00	431	33.5	12.6	3.0	2.8	2.6	0.1	12.6	3.0	28.5	98.5	4,185	4,154
AB13227	7/2/2003 6:00	451	25.9	10.6	2.6	2.3	3.0	0.2	10.6	2.7	39.3	97.3	5,984	5,932
AB13245	7/2/2003 18:00	463	29.7	11.0	2.6	2.6	3.1	0.2	10.5	2.7	36.3	98.6	5,476	5,448
AB13246	7/2/2003 22:00	467	42.9	13.8	3.4	3.4	0.5	0.2	12.5	2.8	19.6	99.1	2,657	2,651
AB13248	7/3/2003 6:00	475	42.4	13.6	4.2	3.2	0.3	0.3	10.5	2.4	22.7	99.6	3,003	3,002
AB13290	7/4/2003 18:00	489	35.6	11.7	4.4	2.7	1.3	0.4	7.9	2.0	34.0	99.9	4,673	4,654
AB13296	7/6/2003 2:00	521	38.2	13.1	6.9	2.8	2.0	0.3	16.4	3.5	15.1	98.4	2,221	2,205
AB13298	7/6/2003 10:00	529	31.8	12.4	5.4	2.6	3.0	0.4	15.3	3.2	24.0	98.0	3,566	3,535
AB13302	7/7/2003 2:00	545	33.5	13.0	5.4	2.8	2.9	0.4	15.8	3.3	21.3	98.5	3,156	3,131
AB13315	7/7/2003 18:00	561	28.4	11.3	4.8	2.4	3.7	0.6	12.4	2.8	32.6	99.0	4,909	4,867
AB13328	7/8/2003 10:40	578	22.5	9.5	3.2	2.0	4.3	0.6	8.4	2.2	46.9	99.6	6,926	6,868
AB13334	7/8/2003 14:00	581	19.5	12.3	3.0	2.0	3.0	0.9	8.3	2.1	46.8	97.8	7,086	7,027
AB13337	7/9/2003 2:00	593	31.2	11.8	3.8	2.5	3.9	0.6	9.0	2.3	35.5	100.5	5,297	5,267
AB13362	7/10/2003 2:00	617	26.8	11.5	3.9	2.5	3.1	0.4	12.0	2.8	36.1	99.1	5,313	5,268
AB13363	7/10/2003 6:00	621	30.6	12.5	3.8	2.6	3.7	0.2	11.7	2.9	29.6	97.7	4,434	4,405
AB13377	7/11/2003 2:00	641	30.4	13.3	3.9	2.8	3.0	0.3	12.6	2.9	29.2	98.5	4,349	4,317
AB13380	7/11/2003 10:00	649	28.5	20.2	3.6	2.8	3.4	0.5	11.3	2.8	27.6	100.6	3,862	3,822
AB13397	7/11/2003 22:00	661	21.9	8.7	2.7	1.7	8.2	0.0	26.8	5.9	23.0	99.1	3,472	3,438
AB13400	7/12/2003 10:00	673	23.1	10.6	3.2	2.2	4.2	0.3	11.5	2.7	40.3	98.2	6,119	6,062
AB13402	7/12/2003 18:00	681	23.8	11.2	3.1	2.4	3.8	0.2	11.5	2.7	39.6	98.5	5,927	5,871
AB13407	7/13/2003 14:00	701	25.9	12.7	3.7	2.7	3.5	0.2	13.7	3.1	33.8	99.4	4,933	4,882
AB13411	7/14/2003 6:00	717	22.0	11.4	3.5	2.4	3.9	0.3	11.6	2.8	40.1	97.8	5,993	5,935
AB13412	7/14/2003 10:00	721	21.1	10.5	3.3	2.2	7.1	0.2	13.4	3.7	36.4	98.1	5,477	5,425
AB13431	7/14/2003 22:00	733	19.7	9.1	2.7	1.9	9.0	0.3	21.5	4.9	29.6	98.7	4,546	4,504

Notes:

1. Other inerts consist of P_2O_5, Na_2O, K_2O, & TiO_2

2. Samples AB13246, AB13248 and AB13290 were taken during or just after a period of coke breeze feed.
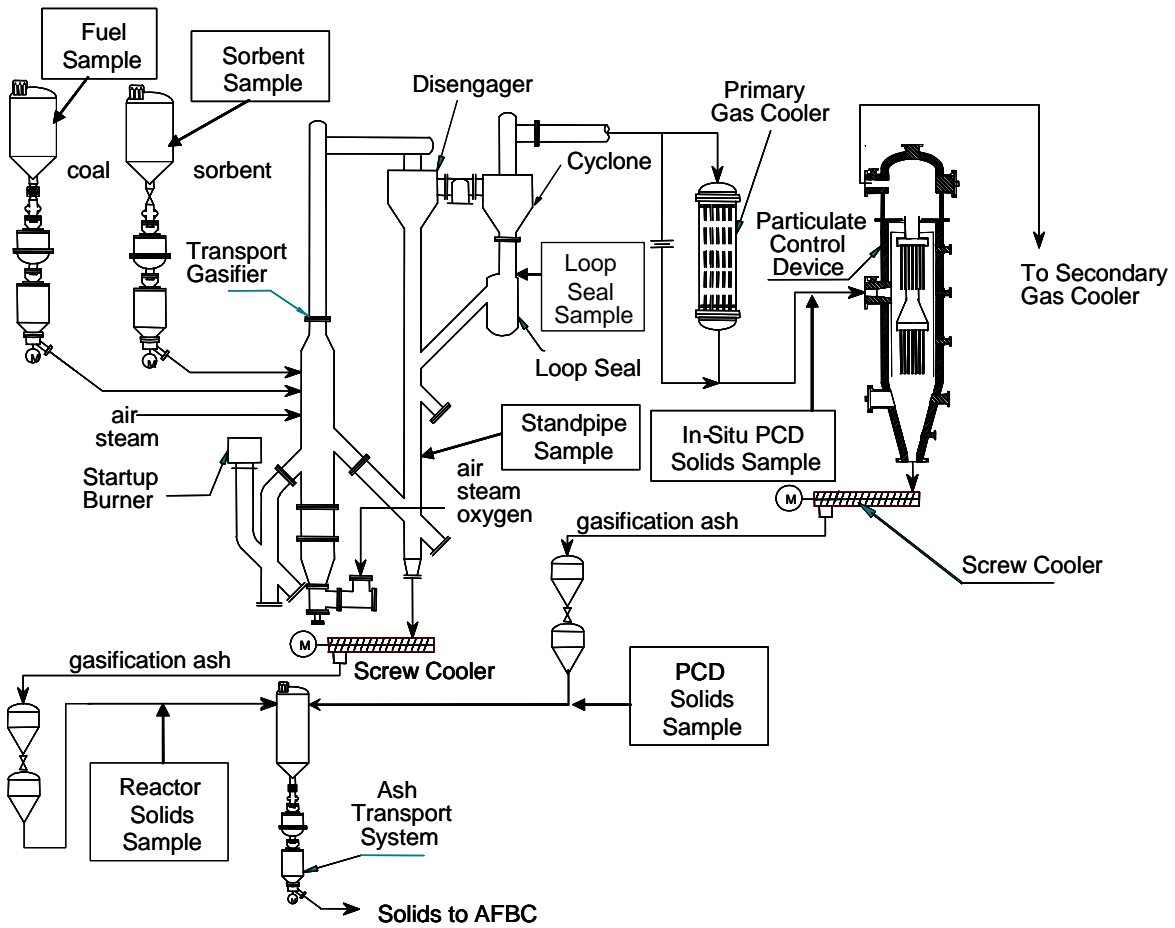
Figure 3.4-1 Solid Sample Locations
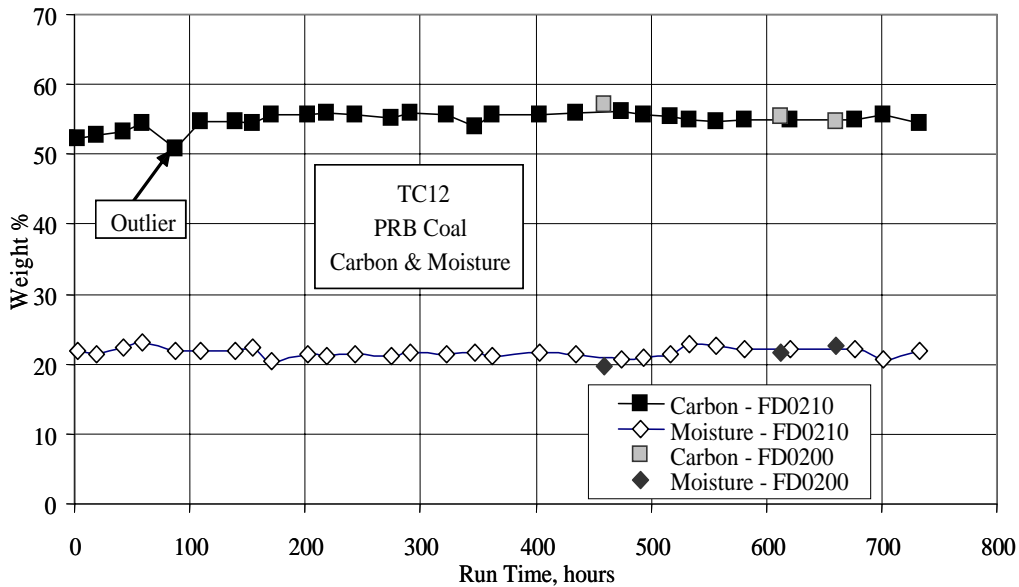
Figure 3.4-2 Coal Carbon and Moisture
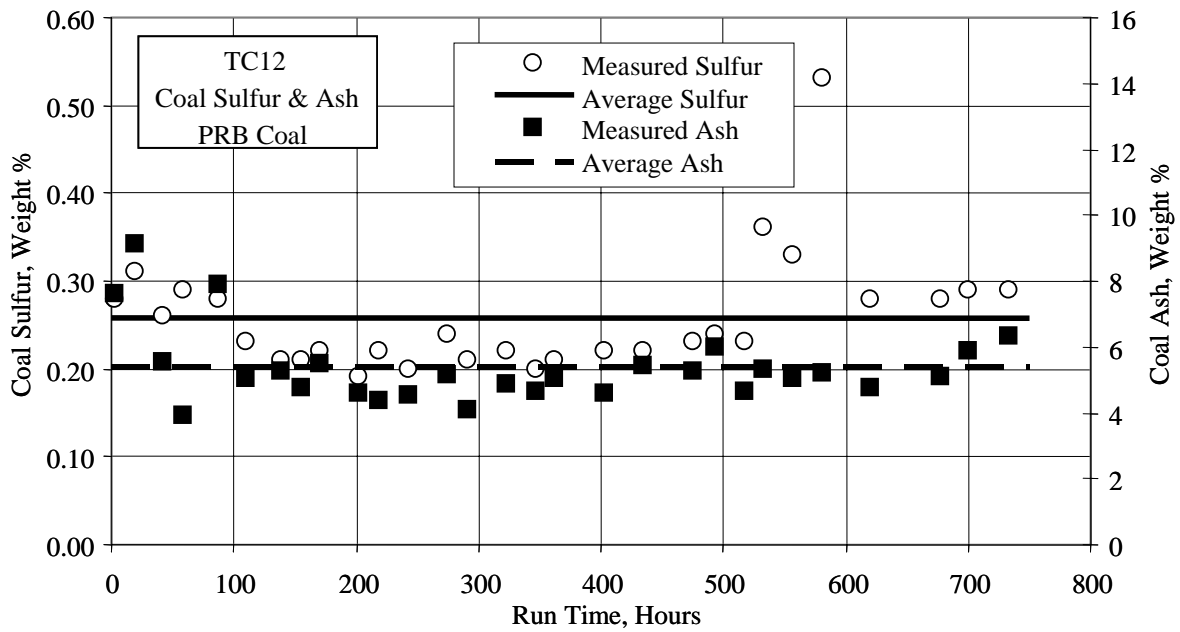
Figure 3.4-3 Coal Sulfur and Ash
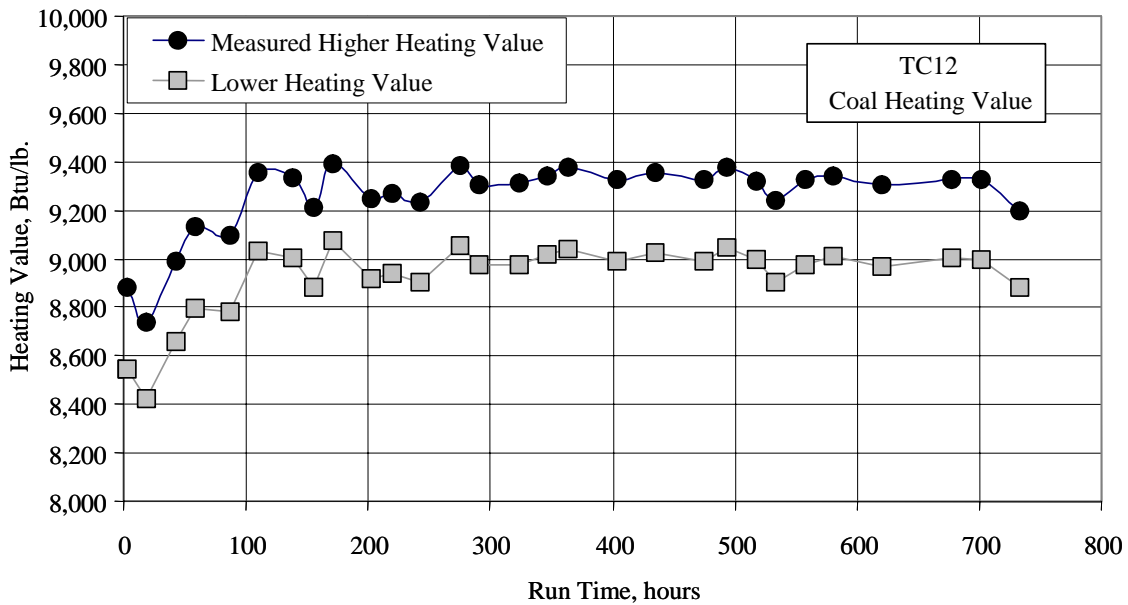
Figure 3.4-4 Coal Heating Value
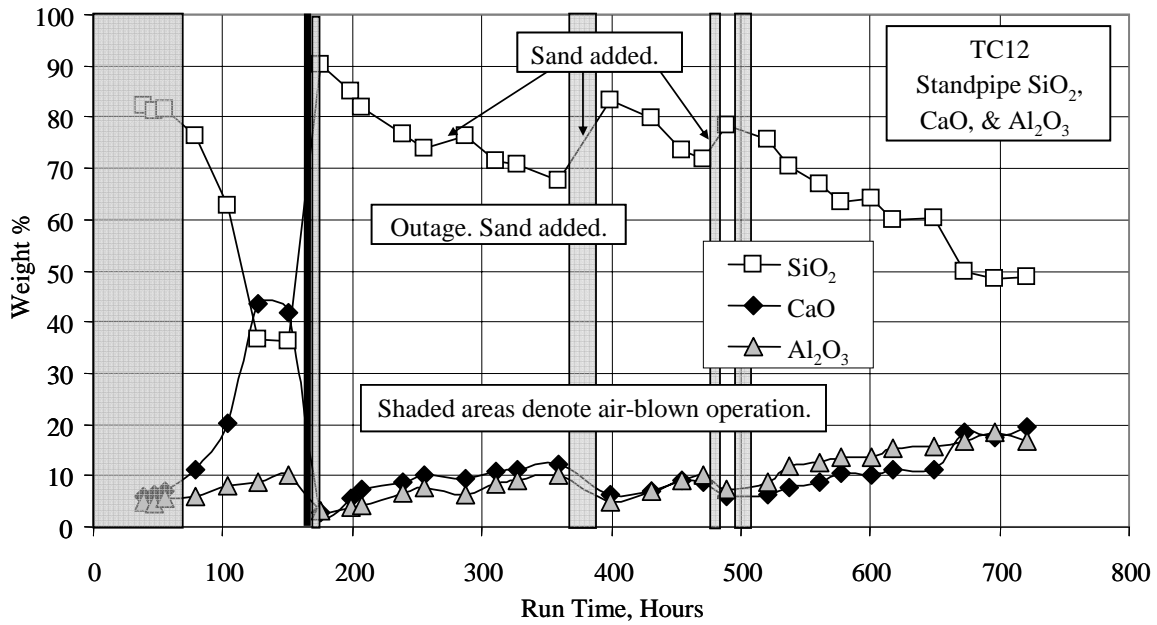
Figure 3.4-5 Standpipe SiO₂, CaO, and Al₂O₃
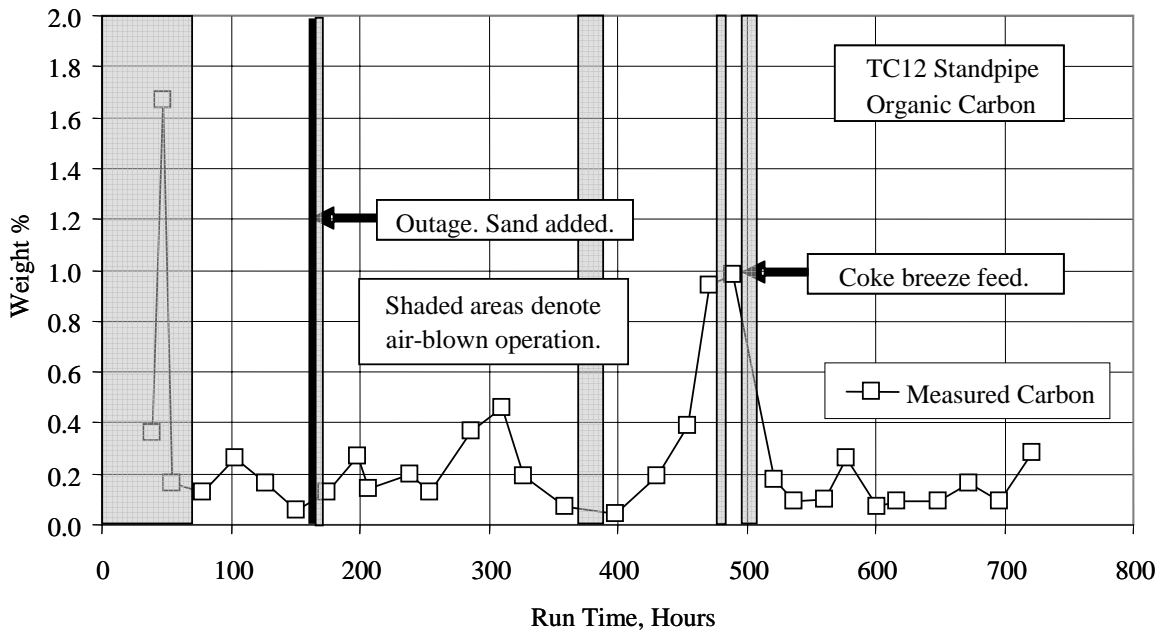
Figure 3.4-6 Standpipe Organic Carbon
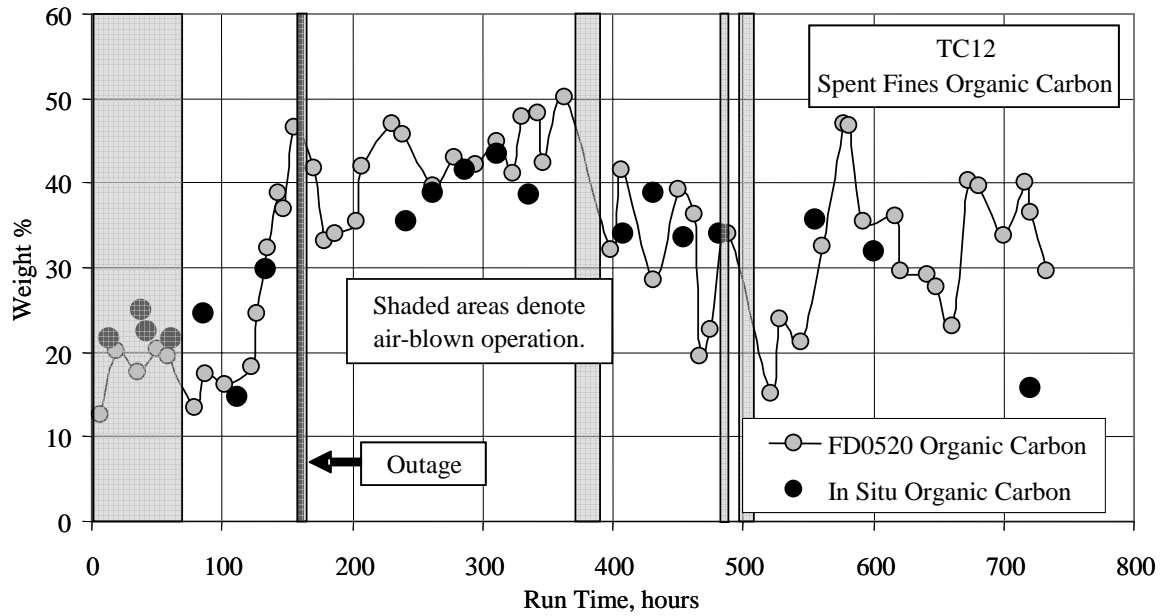
Figure 3.4-7 PCD Fines Organic Carbon
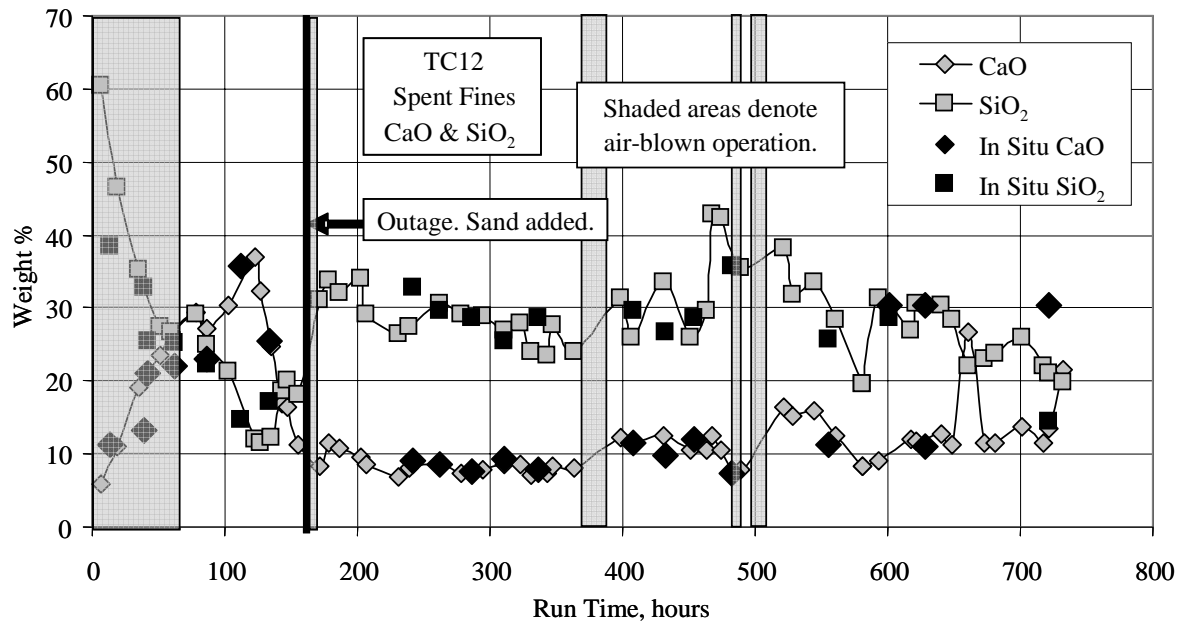
Figure 3.4-8 PCD Fines SiO2 and CaO
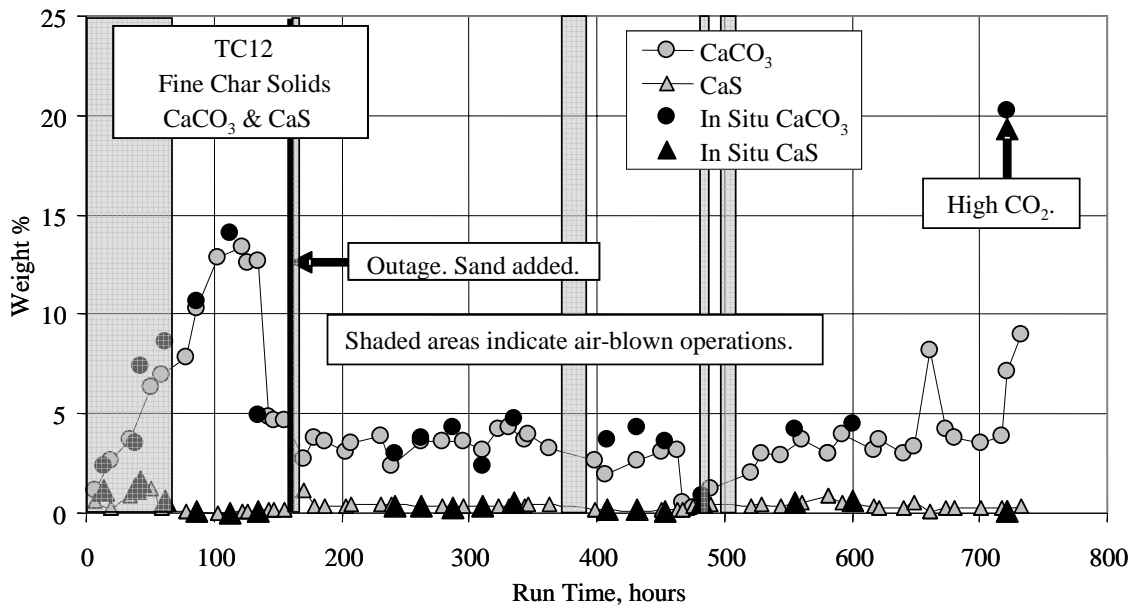
Figure 3.4-9 PCD Fines $CaCO_3$ and CaS
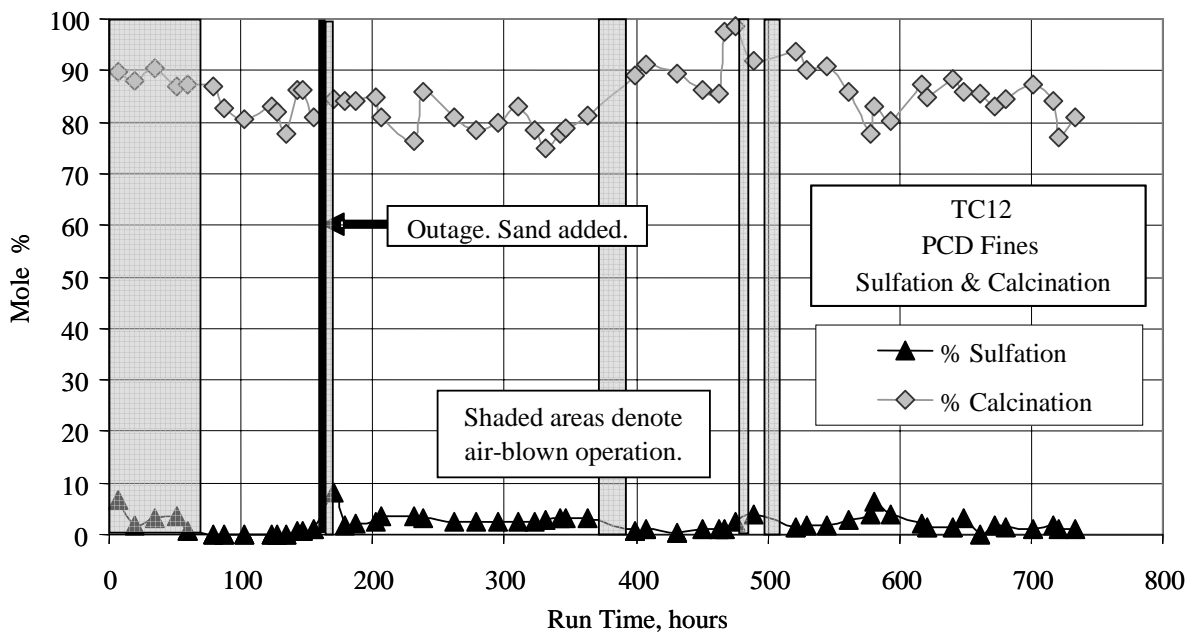
Figure 3.4-10 PCD Fines Calcination and Sulfation
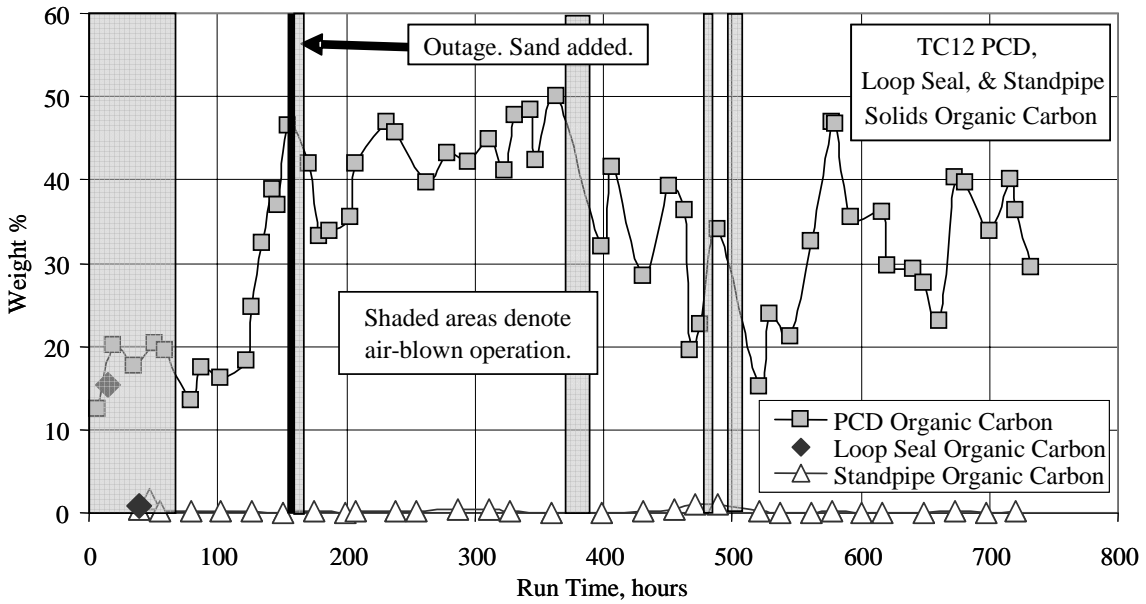
Figure 3.4-11 Gasifier Solids Organic Carbon
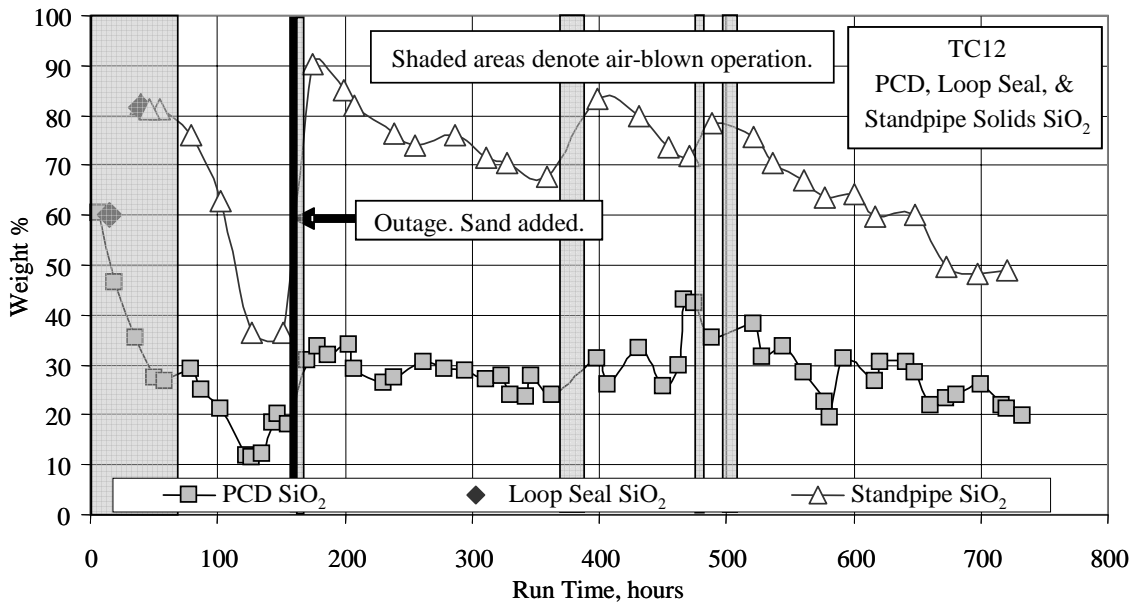
Figure 3.4-12 Gasifier Solids Silica
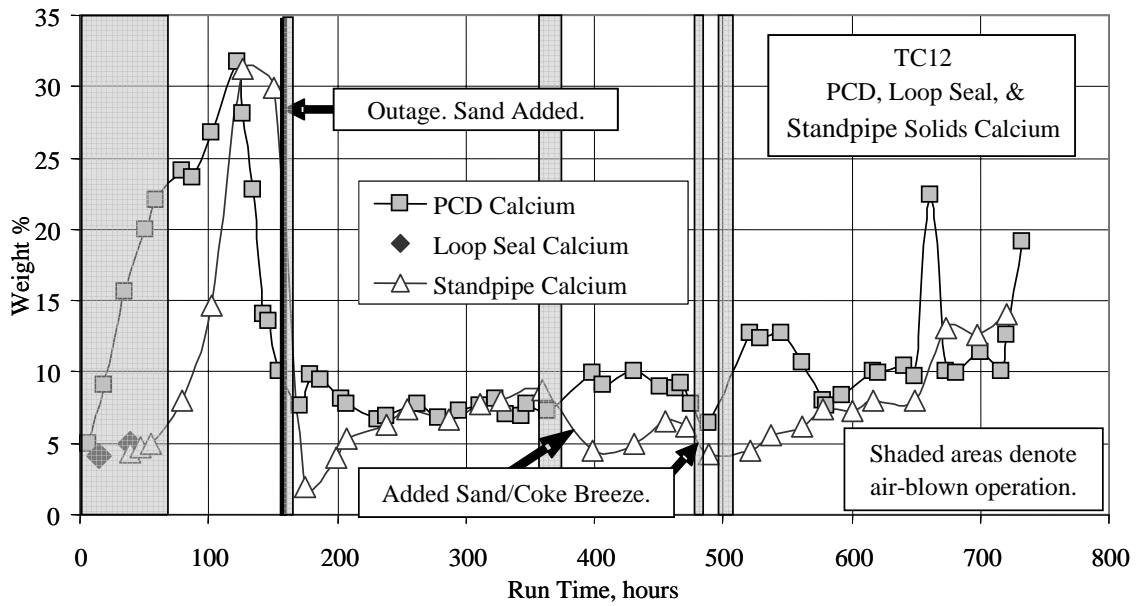
Figure 3.4-13 Gasifier Solids Calcium
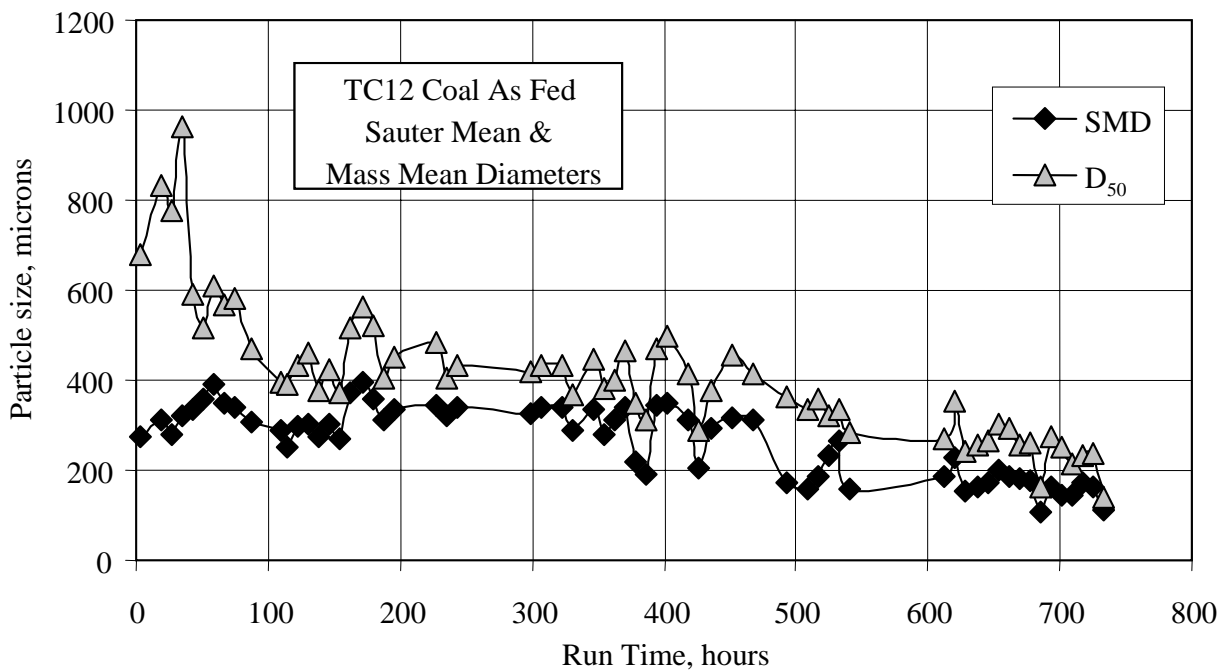
Figure 3.4-14 Coal Particle Size
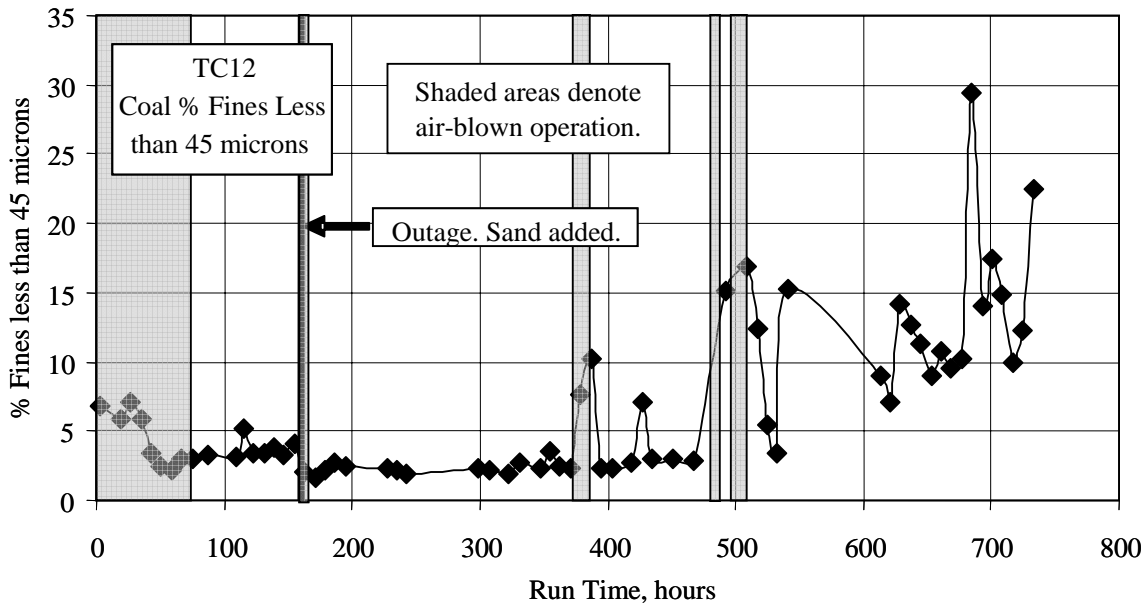
Figure 3.4-15 Percent Coal Fines
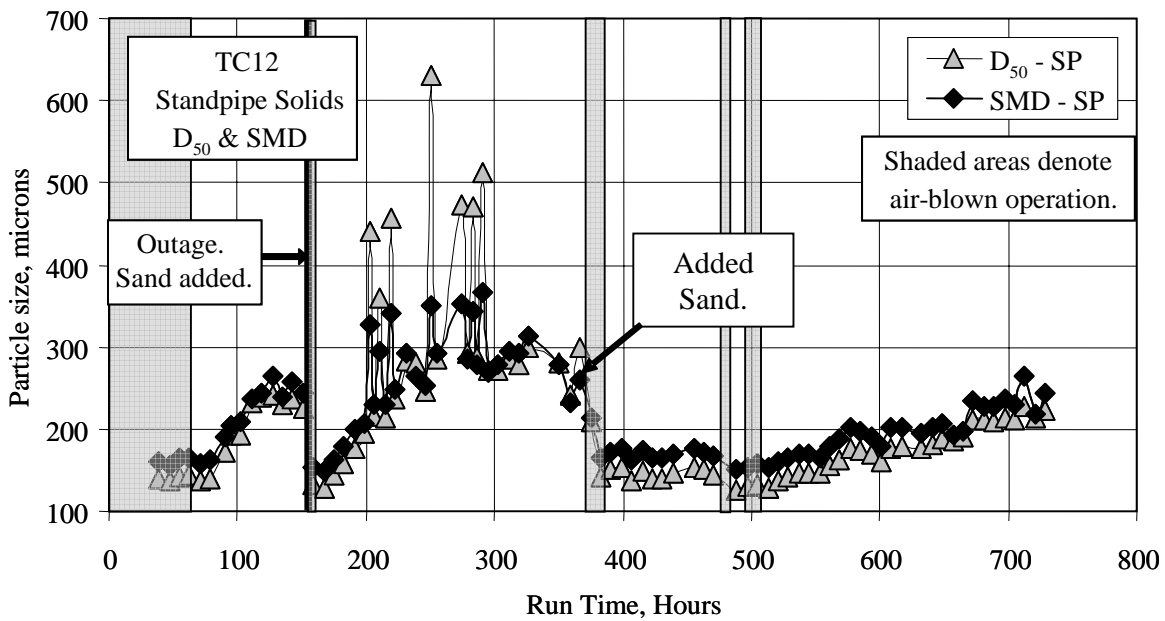
Figure 3.4-16 Standpipe Solids Particle Size
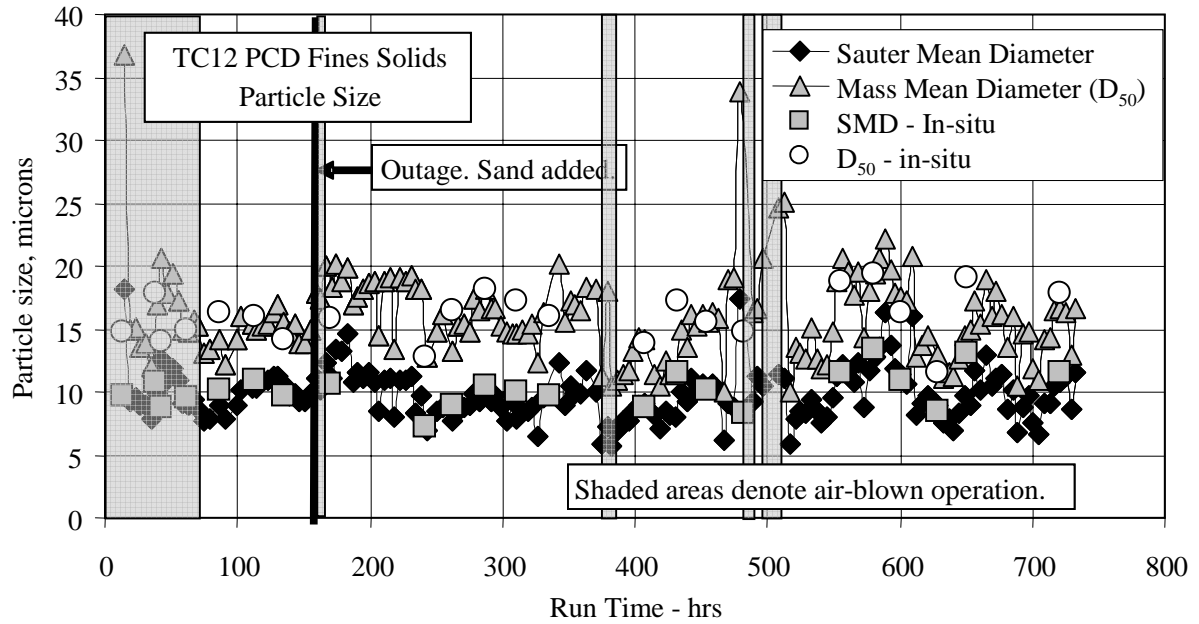
Figure 3.4-17 PCD Fines Particle Size
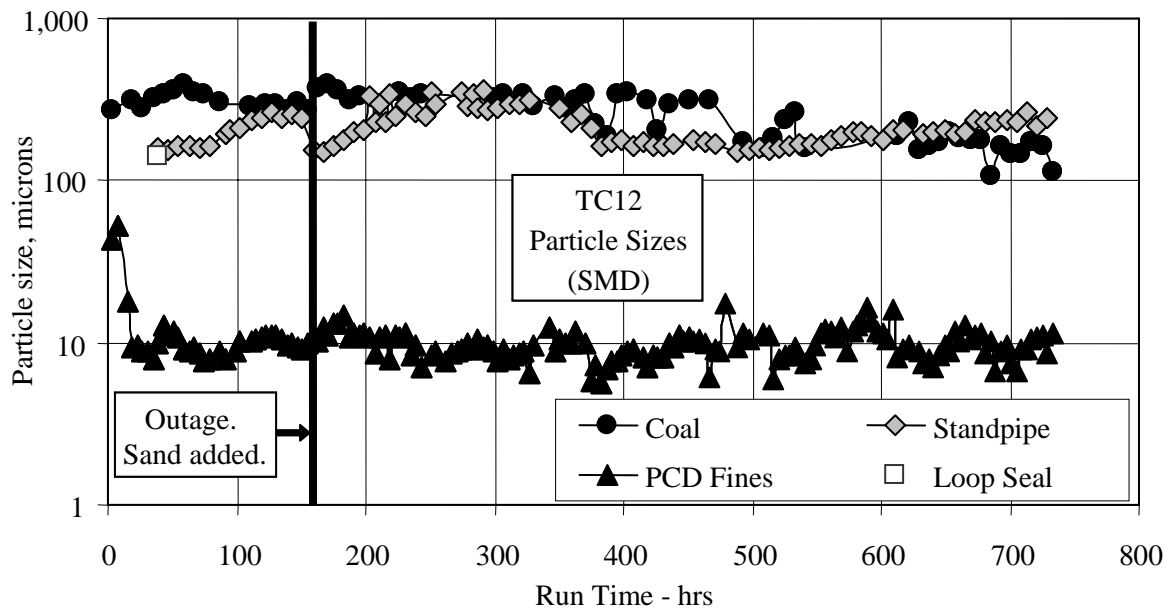
Figure 3.4-18 Particle Size Distribution
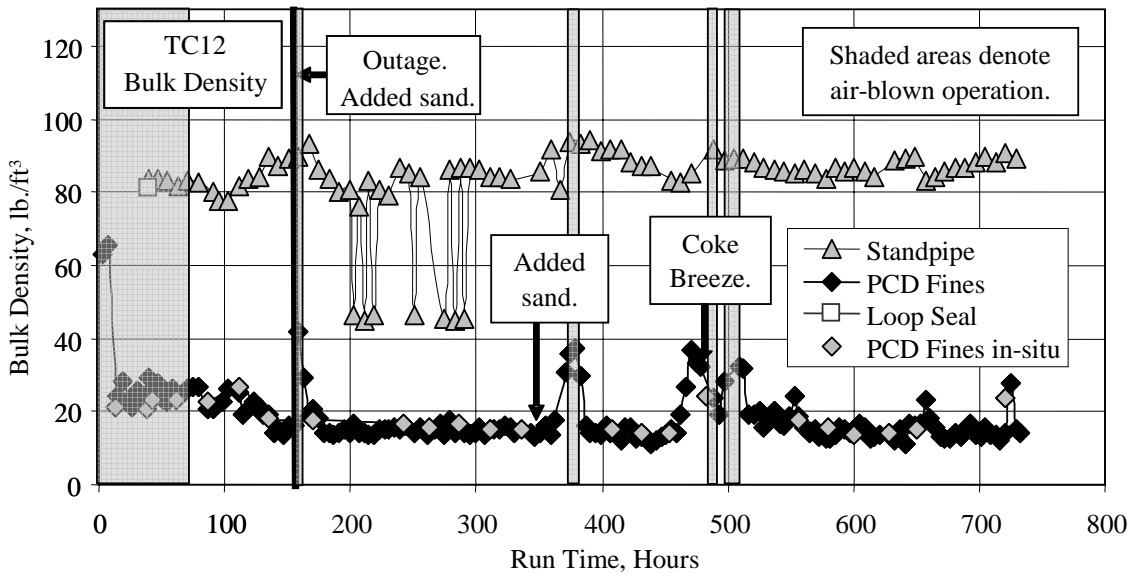
Figure 3.4-19 Gasifier Solids Bulk Density

3.5 MASS AND ENERGY BALANCES

3.5.1 Summary and Conclusions

- Carbon conversions were between 96 and 98 percent in air-blown mode, and between 92 and 98 percent in oxygen-blown mode.
- Carbon balances were good ±11 percent, with a slight bias towards the carbon fed.
- Coal rates varied from 1,260 to 5,150 lb/hr.
- Oxygen-to-coal ratio (pound-per-pound) was 0.60 to 0.84, with one outlier at 1.46.
- Overall mass balance was good at ±8 percent, most within ±5 percent.
- Nitrogen balances were good at ±10 percent (with three outliers).
- Sulfur balance was marginal with most oxygen-blown periods at ±25 percent. The air-blown periods were only within ±40 percent.
- Sulfur removal averaged 22 percent for air blown with sorbent, 10 percent for air blown without sorbent, and 5 percent for oxygen blown with or without sorbent.
- Sulfur emissions ranged from 0.25 to 0.73 lb SO_2 /MBtu coal.
- Hydrogen balances were good at ±10 percent (five outliers).
- Oxygen balances were good at ±10 percent (most within ±5 percent).
- Calcium balances were poor at ±65 percent for air-blown mode and ±76 percent in oxygen-blown mode (with one outlier).
- Silica balances were very poor, with most periods experiencing error well over ±25 percent.
- Energy balances were good with most periods within -2 to +16-percent error. Only a few periods had errors between 15 and 21 percent and these were biased towards the energy fed rather than the energy exiting.
- The raw cold gasification efficiency (by the products method) was between 53 and 55 percent in air-blown mode and from 54 to 65 percent in oxygen-blown mode, with one outlier at 27 percent (coke breeze and coal cofiring).
- The raw hot gasification efficiency was between 85 and 88 percent for air-blown mode, and between 80 and 87 percent for oxygen-blown mode, with one outlier at 74 percent (coke breeze and coal cofiring).
- The corrected cold gas efficiency was 70 to 73 percent for air-blown mode, and from 72 to 83 percent in oxygen-blown mode, with one outlier at 70 percent.

3.5.2 Introduction

The process flows into the Transport Gasifier process are:

- Coal flow through FD0210 and FD0200.
- Limestone flow through FD0220.
- Coke breeze feed through FD0252.
- Air flow measured by FI205 for air-blown mode and by FI201 for oxygen-blown mode.
- Oxygen flow measured by FI726.
- Pure nitrogen flow measured by FI609.

- Steam flow measured by the sum of FI204, FI727B, FI734, and FI733.

Sand was added through FD0220 to increase the Transport Gasifier standpipe level both during outages and coal feed.

The process flows from the Transport Gasifier process are:

- Syngas flow rate from the PCD measured by FI465.
- PCD solids flow through FD0520.
- Gasifier solids flow through FD0510.

3.5.3 Feed Rates

The coal flow through FD0210 can be determined by three different methods:

- FD0210 surge bin weigh cell.
- Transport Gasifier carbon balance.
- Syngas combustor carbon balance.

The FD0210 and FD0200 surge bin weigh cells use the time between filling cycles and the weigh differential between dumps to determine the coal-feed rate. Historically, using the coal weigh cell method to determine coal-feed rate tends to over predict the actual coal-feed rate into the Transport Gasifier. However, throughout TC12, the FD0210 and FD0200 weigh cell coal rates were consistent with the other two coal-feed rates, and the weigh cell coal-feed rate seemed to provide the most representative value. Therefore, unless specified, all coal-feed rates from the FD0200 and the FD0210 feeders are the rates determined from the weigh cells.

The Transport Gasifier carbon balance method uses the carbon content and flow of the syngas plus the carbon content and flow of the PCD fines to determine the carbon-feed rate. Using this method assumes that the Transport Gasifier carbon balance is perfect. Figure 3.5-1 compares the coal-feed rate determined by the weigh cells to the coal-feed rate necessary for a perfect carbon balance. Almost all of the operating periods showed less than 10-percent error between the two values, even though the feed rates ranged from 1,200 to 5,000 pph. This reinforces that the weigh cells were providing a reliable estimate of the coal-feed rate.

The syngas combustor carbon balance method uses the carbon content and flow of the flue gas from the syngas combustor plus the carbon content and flow of the PCD fines to determine the carbon-feed rate. The coal rates used for the further analysis are listed in Table 3.5-1 for each operating period.

The Transport Gasifier carbon balance coal rates, syngas combustor carbon balance coal rates, and FD0210/FD0200 weigh cell coal rates for the operating periods are compared on Figure 3.5-2.

Throughout TC12 the coal-feed rate obtained from the gasifier carbon balance was slightly higher than the coal-feed rate determined from the syngas combustor carbon balance, but

slightly lower than the coal-feed rate obtained from the coal weigh cells. All three coal-feed rates agreed with each other within a few percentages of error, with the rates derived from the weigh cell and gasifier carbon balance agreeing more closely with each other than with the rate determined from the syngas combustor balance.

The weigh cell coal-flow rates for the operating periods are given in Table 3.5-1. The coal rate ranged from 3,500 to 4,200 lb/hr during the air-blown testing and from 2,800 to 5,000 lb/hr during the oxygen-blown testing except for one period of low coal-feed rate supplemented with coke breeze. As shown in Table 3.5-1, coke breeze feed only took place during one steady-state period, TC12-37. During this time the FD0252 feeder fed about 200 pph of material to the gasifier. The coke breeze weigh cells were used to determine the coke breeze feed rate for this period, dividing the total amount of material fed by the length of the steady-state period.

The limestone/sand flow through the sorbent feeder FD0220 was determined in much the same way as the coke breeze feed rate, by calculating from the weigh cells the total amount of sorbent fed to the gasifier during a steady-state period, then dividing it by the length of the steady-state period. The calculation assumes a constant flow of limestone during the steady-state period.

The operating period steam, oxygen, and nitrogen flow rates are shown in Figure 3.5-3 and in Table 3.5-1. The total nitrogen included FI609 plus the small amount of nitrogen that flowed via FI6080 to the Transport Gasifier through the coke breeze feed line which kept the line clear when coke breeze was not being fed. The nitrogen rate for most of TC12 ranged between 5,800 and 6,600 pph, with the exception of TC12-37 (the coal/coke-breeze cofeed period) when the flow rate increased to 7,200 pph. FI6080 was approximately 200 pph for the first 246 hours of the test run. It was close to zero for the remainder of the test run, with the exception of TC12-37, when it increased to 900 pph to convey the coke breeze to the gasifier.

The oxygen rate was zero for air-blown operating periods (TC12-1 through TC12-8). In oxygen-blown mode, the oxygen flow rate was between 1,600 and 2,800 pph. During the coal/coke breeze cofeeding period, the oxygen flow rate was 1,600 pph.

The total steam rate to the gasifier is calculated by the sum of FI204 (total steam flow to the upper mixing zone), FI727B (steam mixed with the air fed to the lower mixing zone), FI734 (steam fed into the lower mixing zone), and FI733 (steam fed to a shroud into the lower mixing zone). The steam feed rates for each operating period are shown on Figure 3.5-3 and listed in Table 3.5-1. In TC12-6, TC12-7, and TC12-8, one of the main steam flow indicators was out of service, giving an improper reading. Thus, the steam flow rates used for these three periods are estimated from a hydrogen balance around the system. During the eight air blown operating periods, the steam flow was relatively low at about 650 to 900 lb/hr. The steam rate was then 2,500 lb/hr for the first oxygen-blown operating period (TC12-9), and ranged between 1,900 and 3,200 pph for the first few oxygen-blown tests. During the TC12-18, the steam flow rate dropped to 1,300 pph and remained between 1,300 pph and 1,800 pph for the next several tests. At this point, a deposit formed in the gasifier, and a high steam flow rate was necessary to combat further agglomeration. The steam flow rate ran as high as 4,600 pph, before being gradually reduced to 1,800 pph over the remainder of the test run. The higher steam rate in test periods TC12-33 and TC12-35 contributed to the lower LHV exhibited during those periods.

The air feed rates for each of the operating periods are shown in Figure 3.5-3 and listed in Table 3.5-1. The air flow rate during the first air-blown periods was between 11,000 and 13,000 lb/hr and tracked the coal rate. During oxygen-blown mode, a very small amount of air continued to flow to the Transport Gasifier to keep the upper mixing zone air nozzles clear and to ensure proper riser velocity. Even though the air flow rate range as high as 2,500 pph during oxygen-blown mode, the vast majority of the oxygen entering the gasifier came from pure oxygen. Thus, all oxygen-enriched periods in TC12 were basically oxygen-blown. Air was also used to control temperatures in the gasifier, which is why the flow rate varied during the oxygen-blown periods of TC12.

3.5.4 Product Rates

The operating period syngas flow rate, taken from the FI463 flow indicator, is shown in Figure 3.5-4 and listed in Table 3.5-1. As mentioned above, the oxygen, carbon, and hydrogen balance around the syngas combustor found the syngas rate to be in good agreement with the syngas combustor data for most of the operating periods (see Figures 3.3-23, -24, and -25). The syngas flow rate was from 21,000 to 24,000 lb/hr for the air-blown operating periods. During the oxygen-blown operating periods, the syngas rate was between 12,000 and 19,000 lb/hr. The syngas flow rate is a strong function of the air and oxygen flow rates and a weak function of the steam and nitrogen flow rates.

The solids flow from the PCD can be determined from two different methods by using:

- In situ particulate sampling data upstream of the PCD.
- Weigh cell data from the FD0530 ash feeder.

The best measurements of the PCD solids flow are the in situ PCD inlet particulate determinations. Using the syngas flow rate and the in situ PCD inlet particulate measurement, the solids flow to the PCD can be determined. The flow of solids to the PCD is a strong function of the solids fed into the Transport Gasifier (coal ash and limestone) and the carbon conversion.

The FD0530 weigh cell data can determine the PCD solids flow only if both the FD0530 feeder and the FD0510 feeder (standpipe solids) are turned off and only FD0520 is feeding into FD0530. This method assumes that the solids level in the PCD and the FD0502 screw cooler are constant. A good check on the PCD fines rates is the calcium and silica balances, since calcium and silica are only present in the feed coal and the PCD fines. Figure 3.5-5 compares the two PCD fines flow rate methods, plotting the 23 points determined from the in situ data along with the rates determined from the FD0530 weigh cells. The FD0530 weigh cell measurements had a large scatter and were usually lower than the in situ samples PCD fines flow rate, especially for the first 125 hours. During the remainder of the test run, however, the two methods began to agree more closely. Since the in situ PCD fines flow rate is more reliable than the FD0530 weigh cell PCD fines rate, the in situ PCD fines solids flow rate was used for further analyses. Also plotted on Figure 3.5-5 are the interpolated PCD solids flow rates (based on the in situ measurements) used for the operating periods.

The operating periods PCD fines flow rates were from just above 200 to almost 500 lb/hr and changed considerably during the first eight (air-blown) operating periods. The PCD fines rates used in mass balances are shown in Table 3.5-1. At hour 155 the PCD fines flow rate increased above 400 pph due to a high coal-feed rate. After hour 170 the PCD fines flow rate stabilized between 200 and 300 pph. Later, the PCD fines flow rate became erratic again, most noticeably during the high limestone feed period at hour 723 (TC12-52).

FD0510 was operated during several of the operating periods. As shown in Table 3.5-1, the flow rate of the material removed from FD0510 ranged from 0 to 276 pph.

Calculating the amount of solids accumulation in the standpipe yields very small values and the accuracy of the calculation is uncertain. However, for completeness, Table 3.5-1 also presents the estimated solids accumulation in the gasifier based on changes in the standpipe level. Note that the highest values are less than 50 pph and are mostly negligible from a calculation standpoint.

3.5.5 Carbon Balances and Carbon Conversion

The carbon balances are given on Figure 3.5-6 and in Table 3.5-2. All carbon balances, except for two, were within ±9-percent error, presenting some of the best agreement seen to date. The two exceptions were period TC12-16 when the FD0200 feeder ran and TC12-37, when the coke breeze/coal cofeed test occurred. In both cases the errors that resulted were only slightly above 10 percent each.

The carbon conversion is defined as the percent of the fuel carbon that is gasified to CO, CO_2, CH_4, C_2H_6, and higher hydrocarbons. For the coke breeze addition period of TC12-37, the coke breeze carbon was considered potential carbon for gasification. The rejected carbon to the gasifier or PCD fines solids is typically burned in an atmospheric combustor or sent for disposal.

Due to inaccuracies in the carbon measurements, the carbon conversion can be calculated at least three different ways:

1. The first method is based on the feed carbon (coal plus coke breeze) and the carbon in the syngas. This assumes that the feed carbon and the syngas carbon are correct. (Gas analyses method)
2. The second method is based on the feed carbon and the syngas carbon determined by a Transport Gasifier carbon balance, not the gas analyses. This assumes that the syngas carbon is incorrect. (Solids analyses)
3. The third method is based on the feed carbon determined by Transport Gasifier carbon balance and the syngas carbon. This method assumes that the coal feed is in error. (Products analyses)

The carbon conversions given by all three methods are plotted on Figure 3.5-7. The products method carbon conversions for each operating period are given in Table 3.5-2. The carbon conversions by the solids and products method are approximately the same for TC12. The carbon conversion by the gas method is larger than the carbon conversion by the products method when the carbon balance error is less than zero and is greater than the products method

when the carbon balance error is greater than zero. The carbon conversion predicted by the gas method estimates that the carbon conversion is over 100 percent for approximately 25 percent of the balance periods which is certainly unrealistic. The products method is the most reasonable since it is not based on the coal-feed rate, but on the syngas and PCD solids flow rates.

The products method carbon conversion was between 95 and 98 percent during first 145 hours of TC12, and then slowly decreased to between 92 and 96 percent for a several operating periods (hours 155 to 490). A decrease in temperature appears to have caused the decrease in carbon conversion. At the end of the test run (hours 520 to the end) the carbon conversion attained values of around 95 to 98 percent, with two outlying periods at hours 578 and 723. No apparent reason exists for the decrease in carbon conversion for these two periods. A high, and possibly incorrect, PCD fines flow rate measured at the time may have caused the calculation to yield the decrease in carbon conversion.

The carbon conversion should be a function of gasifier temperature and the carbon conversion should increase as the temperature increases. The products method carbon conversions for TC12 are plotted against the riser exit temperature, TI367, in Figure 3.5-8. The data show a slight increase in carbon conversion with temperature. The 160ºF temperature range of operation (1,650 to 1,730ºF) is sufficient to notice a small effect of temperature on carbon conversion. The effect of temperature is more pronounced in the TC12 data than the effect seen in previous test runs.

The carbon conversions of the Powder River Basin, Hiawatha bituminous, and Falkirk lignite coals are compared on Figure 3.5-9 for both air and oxygen operation. The PRB coal generally has a higher carbon conversion than Hiawatha bituminous, but lower carbon conversion than the Falkirk lignite in both air- and oxygen-blown modes.

3.5.6 Overall Material Balance

Material balances are useful in checking the accuracy and consistency of data as well as determining periods of operation where the data is suitable for model development or commercial plant design. Total material balances for each operating period are given on Figure 3.5-10 which compares the total mass in and the total mass out. The overall material balance agreement was very good, with all of the relative differences at ±8 percent, and most of the relative differences less than ±5 percent. The relative difference (relative error) is defined as the Transport Gasifier feeds in minus products out divided by the feeds ({In-Out}/In).

The details of the overall mass balance are given in Table 3.5-1 with the relative and absolute differences. The absolute difference (absolute error) is defined as the difference between the feeds and the products (In-Out).

The major factors influencing the material balance are the syngas-flow rate (12,000 to 24,000 lb/hr), the air-feed rate (600 to 13,000 lb/hr), the oxygen-feed rate (0 to 2,800 lb/hr), the steam-feed rate (700 to 4,600 lb/hr), the nitrogen-flow rate (5,600 to 7,200 lb/hr), and the coal-feed rate (1,300 to 5,600 lb/hr).

The oxygen-to-coal ratios are listed on Table 3.5-1. The oxygen-to-coal ratio varied from 0.71 to 0.80 for air-blown operation and from 0.60 to 0.84 for oxygen-blown operation, with one outlier at 1.46 during the period of coal and coke breeze cofeeding.

3.5.7 Nitrogen Balance

The nitrogen balances for the TC12 operating periods are plotted on Figure 3.5-11 by comparing the nitrogen flow rate into and out of the Transport Gasifier in Table 3.5-3. Detailed nitrogen flow rates for a typical air-blown test, TC12-5, are shown in Table 3.5-4, and the flow rates for a typical oxygen-blown test, TC12-10, are shown on Table 3.5-5. As in previous gasification tests (TC06 to TC10), the analyses for TC12 assumed that an approximately 250 pph of nitrogen in oxygen-blown mode and 1,000 pph of nitrogen in air-blown mode did not enter the gasifier since it was used in various seals and lock hoppers and vented to the atmosphere. The lower loss of nitrogen entering the gasifier in oxygen blown might be due to the lower pressure operation of oxygen-blown mode as compared to air-blown mode.

As shown on Figure 3.5-11, the air-blown nitrogen balances were excellent, with errors less than ±3 percent. The oxygen-blown nitrogen balances were good with errors less than 10 percent for all but three of the operating periods. The remaining three periods had errors of +10, -10.5, and -13.5 percent, respectively. Neither the oxygen- nor the air-blown periods appeared to exhibit a positive bias (feeds larger than the products) or a negative bias (feeds smaller than the products). Note that air-blown mode nitrogen rates were much higher than the enhanced-air and oxygen-blown nitrogen rates. The nitrogen flows shown in Tables 3.5-4 and 3.5-5 and on Figure 3.5-3 are dominated by the air, nitrogen, and syngas flows. None of the solid streams contribute significantly to the nitrogen balance. The TC12 nitrogen balances were consistent with nitrogen balances from previous test runs.

Using the ammonia analyzer data, the coal rates, and the coal nitrogen concentration, the amount of fuel nitrogen converted to NH_3 can be calculated. The amount of fuel nitrogen converted to NH_3 is shown on Figure 3.5-12. This conversion varied from 48 to 62 percent during air-blown operation, and varied between 61 and 90 percent during oxygen-blown operation, with one outlier at 36 percent--the period of coke breeze/coal cofeeding. The ammonia concentration is important in combustion turbine applications because high ammonia leads to higher NO_X emissions.

 The PCD inlet and Transport Gasifier temperatures did not seem to affect the percent fuel nitrogen-to-ammonia conversion. The only parameters found that did affect the ammonia conversion was the coal-feed rate and the overall percent O_2 in the gasses fed to the Transport Gasifier. The trend of the fuel nitrogen conversion with overall per cent O_2 in the feed gases is shown in Figure 3.5-13. The graph shows a general trend of increasing nitrogen conversion to ammonia as the percentage oxygen in the feed gas increases. The data exhibit a great deal of scatter, making it difficult to draw exact conclusions at this time.

3.5.8 Sulfur Balance and Sulfur Removal

Sulfur balances for all TC12 operating periods are given in Figure 3.5-14 and Table 3.5-6. The syngas sulfur compounds were not directly measured, but estimated from syngas combustor SO_2

analyzer data and the syngas combustor flue gas flow. The coal sulfur values were interpolated between the solids sampling times. The TC12 sulfur balances were marginal, with most of the sulfur balances having relative errors of less than ±25 percent. The air-blown periods exhibited a much greater discrepancy than did the oxygen-blown periods. The data indicated a positive bias, that is, the sulfur in was usually greater than the sulfur out with the oxygen-blown sulfur balances having a lower bias than the air-blown balances. The sulfur balances were similar to the sulfur balances for TC06 through TC10, but less accurate than the balances seen in the TC11 Falkirk lignite test run, perhaps due to the higher sulfur content in the Falkirk lignite. Low sulfur levels make accurately measuring the solid and gaseous sulfur concentrations more difficult.

The minimum equilibrium H_2S concentration in the syngas is a useful tool in checking the amount of sulfur in the gaseous stream. Previous PSDF reports have described the calculation of the minimum equilibrium syngas H_2S concentration. In summary, the minimum equilibrium H_2S concentration is a function of the partial pressures of H_2O and CO_2 as long as there is calcium sulfide present in the solids. (The equilibrium H_2S concentration is a function of system temperature, while the minimum equilibrium H_2S concentration is not a function of temperature.) As the partial pressures of H_2O and CO_2 increase, the H_2S concentration should increase. Using Aspen simulations, the minimum equilibrium H_2S concentrations determined for all of the operating periods are listed in Table 3.5-6.

Figure 3.5-15 plots the TRS and equilibrium H_2S directly against each other for TC12. All of the data are expected to fall above the 45-degree line since the minimum equilibrium H_2S concentration should be the lowest H_2S concentration in a system with calcium sulfide present. Most of the data indicate sulfur emissions slightly less than equilibrium. However, sulfur emissions less than the equilibrium H_2S concentration indicate some Transport Gasifier sulfur capture.

To assist in sulfur removal, the gasifier operated with sorbent addition during test periods TC12-4, 5, 6, 7, 8, 9, 10, 11, 12, 13, 47, and 52, but with the errors in the sulfur balances, it is difficult to determine the actual sulfur removal. Similar to the coal conversions calculations, three different methods exist to determine the Transport Gasifier sulfur removal:

1. From syngas sulfur emissions (using the syngas combustor flue gas rate and syngas combustor flue gas SO_2 measurement) and the feed sulfur rate (using the feed coal rate and coal sulfur content). (Gas analyses method)
2. From PCD solids analysis (using PCD solids flow rate and PCD solids sulfur content) and the feed sulfur rate. (Solids analyses method)
3. From the gas analysis data and the PCD solids data. (Product analyses method)

The three sulfur removals are plotted on Figure 3.5-16 and given on Table 3.5-6. The values obtained from the solids method are suspect in that the sulfur in the fuel is an inaccurate measurement due to the multiplication of a very small number (coal sulfur) by a large number (coal-feed rate). Theoretically, the gaseous sulfur flow should be accurate, although it is also the product of a small number (syngas combustor SO_2 content) and a large number (syngas combustor flue gas rate). The syngas H_2S was measured by the H_2S analyzer AI419J and seemed to be in agreement with the TRS by the syngas combustor AI476P from hours 206 to 456 and

from hours 618 to 733. The PCD fines sulfur rates have inaccuracies due to the low sulfur in the PCD solids. The gasifier likely did not accumulate sulfur-containing solids during TC12, because the standpipe and FD0510 gasifier samples contained only negligible amounts of sulfur throughout the test run.

Theory aside, the TC12 results indicate that the gas method is less accurate than the product and the solids methods. The solids and products methods usually agreed with each other and seemed to change slowly and consistently during the run. The negative sulfur removals were due to estimated sulfur flows out that were larger than the sulfur flows in. The products method is probably the best means of determining the sulfur removal.

The sulfur removal by the products method started TC12 at 10 percent and increased to as high as 31 percent during air-blown operations. During oxygen-blown operations, the sulfur removal dropped to 1 percent, where it remained for several periods before increasing to 16 percent. It remained between 1 and 10 percent for the remainder of the test run. Adding sorbent did not appear to have a major effect in oxygen-blown operations, although it may have in air blown. Due to the errors in the sulfur balance all that can be concluded from the data is that the sulfur removal was between 0 and 31 percent for TC12 and seemed to be higher during air-blown operations.

The syngas combustor SO_2 data was used for the sulfur emissions shown in Table 3.5-6. The sulfur emissions were from 0.25 to 0.73 lb SO_2/MBtu coal fed.

Figure 3.5-17 plots the measured sulfur emissions against the sulfur out of the reactor (sulfur emissions plus the PCD fines sulfur). On Figure 3.5-17, the 45-degree line is the 0-percent sulfur removal line (PCD fines sulfur equals zero) and the X-axis is the 100-percent sulfur removal line (zero sulfur emissions). This plot once again shows the products method sulfur removal calculation since it is based on the PCD fines sulfur and the syngas sulfur. Figure 3.5-17 highlights the minimal sulfur capture during TC12 as nearly all of the points are just under the 0-percent capture line. The air-blown data with limestone obtained the best removal and averaged 25-percent sulfur capture, but the data was quite scattered. The air-blown data without limestone addition was about 10-percent sulfur capture. The oxygen-blown sulfur capture averaged about 5 percent with or without limestone addition.

3.5.9 Hydrogen Balance

Operating period hydrogen balances are given in Figure 3.5-18 and in Table 3.5-3. Typical hydrogen flows for air-blown test TC12-5 are shown in Table 3.5-4 and typical hydrogen flows for oxygen-blown test TC12-10 are shown on Table 3.5-5. The hydrogen balance is very good with all but five of the operating periods within ±10 percent of perfect agreement. The worst hydrogen balance is TC12-36a at -17.6-percent error. The coal, steam, and syngas streams dominate the hydrogen balance. The TC12 hydrogen balance is one of the best hydrogen balances seen to date. During TC12, the steam flow indicator recorded all of the TC12 steam flow rates, with the exception of TC12-6, TC12-7, and TC12-8, when the steam flow indicator was out of service. The steam rate used for these periods was back-calculated using the hydrogen balance as detailed below. (Note the 0-percent error in the hydrogen balance for these three periods.)

The steam rate for each operating period was calculated using a hydrogen balance, which is the difference between the hydrogen in the coal feed and hydrogen in the syngas. The hydrogen balance steam rate is compared with the measured steam rate on Figure 3.5-19. Note the lower steam rates in air-blown mode. The vast majority of the measured steam rates are within 15 percent of the hydrogen balance steam rates with the calculated rates tending to be slightly higher than the measured rates. The three periods that occurred when the steam flow indicator was out of service are also shown on the figure.

3.5.10 Oxygen Balance

Operating period balances in oxygen-blown mode are given in Figure 3.5-20 and Table 3.5-3. Oxygen flows for a typical air-blown test (TC12-5) are shown in Table 3.5-4, and oxygen flows for a typical oxygen-blown test (TC12-10) are shown on Table 3.5-5. The oxygen balance determines if the steam, oxygen, and air rates are consistent with the syngas rate and composition.

The oxygen balances for the TC12 operating periods while in air-blown mode were very good with all operating periods having relative errors less than ±10 percent. The data did not show a bias toward the oxygen fed nor the oxygen in the product gas. Acceptable oxygen balances indicate that the measured steam rates are consistent with the other oxygen flows (air, oxygen, and syngas).

3.5.11 Calcium Balance

Operating period calcium balances are given in Figure 3.5-21 and Table 3.5-3. Typical calcium flows for an air-blown mode test (TC12-5) are shown in Table 3.5-4 and typical calcium flows for an oxygen-blown mode test (TC12-10) are shown on Table 3.5-5. Except for the periods with limestone feed (TC12-4, -5, -6, -7, -8,-9, -10, -11, -12, -13, -47, and -52), the calcium balances are essentially a comparison between the calcium concentration in the coal and the calcium concentration in the PCD fines since there was only minimal flow through FD0510, and the amount of solids accumulated in the gasifier was small.

The TC12 calcium balances were poor, since 32 of the operating periods had errors greater than 25 percent, with a no bias towards the calcium fed or the calcium removed. Accurate calcium balances are difficult to achieve since the comparison is between two solid streams that are difficult to measure. Due to the lack of sorbent feed in most of the test periods, most of the calcium flows were fairly low and small measurement errors would lead to large relative errors. These relative errors in the calcium balances for TC12 are typical of those seen in other PRB test runs.

Figure 3.5-22 plots TC12 sulfur removal (products method) as a function of calcium-to-sulfur molar ratio (Ca/S) measured in the PCD solids samples from FD0520. The graph only shows periods with a Ca/S ratio less than 120, since showing the data points with large Ca/S ratios would only distort the graph and make it difficult to read. The sulfur removals ranged from 5 to 31 percent.

The trends in PCD solids Ca/S with sulfur emissions provided on Figure 3.5-23 are opposite of what are expected if the amount of excess sorbent is limiting sulfur capture. In that case, the sulfur removal should increase with Ca/S. However, since a slow mass transfer rate probably limits the sulfur capture, the amount of excess calcium does not effect sulfur capture. When the PCD solids contain very little sulfur (high Ca/S) the sulfur removals are low, which is reasonable by sulfur balance. The calcium sulfation percent is the reciprocal (times 100) of the Ca/S ratio based on the PCD fines solids.

Figure 3.5-23 plots TC12 sulfur emissions (expressed as lb SO_2 emitted per MBtu coal fed) as a function of calcium to sulfur ratio (Ca/S) measured in the PCD solids sampled from FD0520. The sulfur emissions varied from 0.253 to 0.733 lb SO_2 emitted per MBtu coal fed and were independent of the Ca/S ratio. Since the sulfur content of PRB is than the sulfur content of Falkirk lignite or Hiawatha bituminous, the flue gas contained a lower sulfur level. PRB sulfur emissions typically range from 0.13 to 0.7 lb SO_2 per MBtu, while Hiawatha bituminous sulfur emissions ranged from 0.6 to 1.01 lb SO_2 per MBtu, and Falkirk lignite sulfur emissions range from 1.41 to 2.16 lb SO_2 per MBtu. Although sulfur emissions are higher in oxygen-blown mode (due to less nitrogen dilution), Figure 3.5-23 indicates that limestone feed cannot significantly reduce sulfur emissions.

Figure 3.5-24 plots the sulfur removal (by the products method) versus the calcium-to-sulfur ratio in the limestone and coal, respectively (the calcium in coal was neglected). Due to the extremely low sulfur content of the PRB coal, the sulfur removal percentage did not increase with increasing calcium-to-sulfur ratio.

3.5.12 Silica Balance

Operating period silica balances are given in Figure 3.5-25 and Table 3.5-3. Typical silica flows for an air-blown mode test (TC12-5) are shown in Table 3.5-4 and typical silica flows for an oxygen-blown mode test (TC12-10) are shown on Table 3.5-5. The silica balances are essentially a comparison between the coal silica and the PCD fines silica, since those two streams are the only significant streams which contain silica during the operating periods.

The TC12 silica balances were poor with only 13 of the operating periods having errors less than 25 percent. The data exhibited a strong bias towards the silica out. Silica balances are usually in error because the comparison is between two solid streams that are difficult to measure and involve multiplying a large number (coal-feed rate, PCD solids rate) by a small number (silica content). A potential problem with the silica balance is that the frequent sand additions cause the standpipe silica content to vary during operating periods.

3.5.13 Energy Balance

The TC12 Transport Gasifier energy balance is given in Figure 3.5-26 with standard conditions chosen to be one atmosphere (14.7 psia) pressure and 80°F temperature. Table 3.5-7 breaks down the individual components of the energy balance for each operating period. The "energy in" consists of the coal, air, and steam fed to the Transport Gasifier. The nitrogen, oxygen, and sorbent fed to the gasifier were considered to be at the standard conditions (80°F) and hence

have zero enthalpy. The "energy out" consisted of the syngas and PCD solids. The lower heating value of the coal and PCD solids were used in order to be consistent with the lower heating value of the syngas. The energy of the syngas was determined at the Transport Gasifier cyclone exit. To determine the syngas energy at the Transport Gasifier exit, about 1,500 pounds N_2 per hour fed to the PCD inlet and outlet particulate sampling trains has been subtracted from the syngas rate to determine the actual syngas rate from the cyclone. The sensible enthalpy of the syngas was determined by the overall gas heat capacity from the syngas compositions. The syngas and PCD solids energy consists of both latent and sensible heat. The heat loss from the Transport Gasifier was estimated to be 3.5 MBtu/hr based on the estimated heat loss in gasification and previous gasification tests.

The TC12 energy balances were all within 16-percent error. The data exhibited a bias towards the energy fed to the gasifier rather than the energy removed in the product streams for all operating periods except three (TC12-5, TC12-16, TC12-21). A heat loss of 6.3 MBtu/hr minimizes the error for the TC12 energy balances.

3.5.14 Gasification Efficiencies

Gasification efficiency is defined as the percent of the energy in (coal energy and steam energy) that is converted to potentially useful syngas energy. Two types of gasification efficiencies have been defined: cold gas efficiency and the hot gas efficiency. The cold gas efficiency is the amount of energy feed that is available to a gas turbine as syngas latent heat.

Similar to sulfur removal and carbon conversion, the cold gas efficiency can be calculated at least three different ways. The three calculation methods that were performed for cold gasification efficiency are consistent with the three methods of sulfur removal:

1. One method is based on the feed heat (coal latent heat plus steam heat) and the latent heat of the syngas. This method assumes that the feed heat and the syngas latent heat are correct. (Gas analyses)
2. Another method is based on the feed heat (coal latent heat plus steam heat) and the latent heat of the syngas determined by a Transport Gasifier energy balance, not the gas analyses. This method assumes that the syngas latent heat is incorrect. (Solids analyses)
3. The third method is based on the feed heat determined by Transport Gasifier energy balance and the syngas sensible heat. This method assumes that the coal feed or the steam rate is in error. (Products analyses)

The cold gas gasification efficiencies for the three calculation methods are plotted in Figure 3.5-27. Only the products method is listed in Table 3.5-7 because the products method is the most accurate method. The products analyses cold gas gasification efficiencies started TC12 at nearly 55 percent due to the high coal rate and low steam rate and remained at approximately 55 percent for all of the air blown testing, since the coal-feed rate and steam-flow rate were fairly constant. The cold gas efficiency then increased to around 65 percent as the gasifier transitioned to oxygen-blown mode

The coal-feed rate has a dramatic affect on the cold gas efficiency in that higher coal-feed rates—with all other variables kept constant—allow the gasifier to produce a higher quality

syngas. The steam rate effect on cold gas efficiency is not due to steam dilution but due to the increased loss in efficiency of heating steam to the Transport Gasifier temperature. An increase in steam rate decreases the syngas LHV and increases the syngas sensible heat such that the total syngas enthalpy remains about the same.

Figure 3.5-28 shows the trend in cold gas efficiency with steam-to-coal ratio showing that as the steam-to-coal ratio increases, the cold gas efficiency decreases. The oxygen-blown operating periods have higher cold gas efficiencies than the air-blown operating periods at the same steam-to-coal ratio by about 10 to 15 percent because of the inefficiency of heating the air nitrogen while operating in air-blown mode.

The hot gasification efficiency is the amount of feed energy that is available to a gas turbine plus the heat recovery steam generator. The hot gas efficiency counts both the latent and sensible heat of the syngas. Similar to the cold gasification efficiency and the sulfur removal, the hot gas efficiency can be calculated at least three different ways. The three calculation methods for hot gasification are identical to the three methods of cold gasification efficiency calculation with the exception of including the syngas sensible heat.

Since the hot gasification efficiency includes the sensible heat of the syngas as well as the latent heat, it is always higher than the cold gasification efficiency. The three hot gasification calculation methods are plotted in Figure 3.5-29 with the results from products method shown in Table 3.5-7.

As with the cold gasification efficiencies, the products method hot gasification efficiencies started TC12 high, at 88 percent due to low steam and high coal rates and generally trended the coal-feed rate. Higher steam flow rates reduced the hot gas efficiency slightly, but not as severely as in the case of the cold gas efficiency. The air-blown hot gas efficiencies were between 85 and 88 percent. The oxygen-blown hot gasification efficiencies were between 80 and 87 percent.

Figure 3.5-30 plots the hot gas efficiency against the steam-to-coal ratio. The air-blown data seem to indicate the same trend of decreasing gasification efficiency with increasing steam to coal ratio, but not as clearly as the cold gasification trend. The oxygen-blown hot gasification efficiencies do not seem to be a function of steam-to-coal ratio.

The two main sources of efficiency losses are the gasifier heat loss and the latent heat of the PCD solids. The gasifier heat loss of 3.5 MBtu/hr was about 10 percent of the feed energy, while the total energy of the PCD solids was about 3 to 6 percent of the feed energy. The heat loss percentage will be smaller in larger gasifiers. While the Transport Gasifier does not recover the latent heat of the PCD solids, this latent heat could be recovered in a combustor. The total enthalpy of the PCD solids can be decreased by decreasing both the PCD solids carbon content (heating value) and the PCD solids rate.

Gasification efficiencies can be calculated from the adiabatic nitrogen-corrected gas heating values and corrected flow rates that were determined in Section 3.3. The products adiabatic nitrogen-corrected cold gasification efficiencies are plotted on Figure 3.5-31 against the corrected steam-to-coal ratio and are listed in Table 3.5-7 for all of the operating periods. Only

the cold gasification efficiencies based on the products calculation method are given in Figure 3.5-31 and in Table 3.5-7 because they tend to be the most representative of the actual gasification efficiencies. Since the nitrogen and adiabatic syngas LHV corrections reduce the coal rate and the steam rate (for oxygen blown only), the corrected coal rates and the corrected steam rates were used in Figure 3.5-31. The corrected efficiencies are calculated assuming an adiabatic gasifier, since zero heat loss was one of the assumptions in determining the corrected LHV in Section 3.3. The corrected cold gas efficiencies were from 70 to 73 percent for air-blown mode and between 72 and 83 percent for oxygen-blown mode, with a decreasing trend of efficiency with increasing steam to coal ratio.

The adiabatic nitrogen correction does not increase the hot gasification efficiency because the deleted nitrogen lowers the syngas sensible heat and increases the syngas latent heat. Both changes essentially cancel each other.

Table 3.5-1 (Page 1 of 2)

Feed Rates, Product Rates, and Mass Balance

Operating Period	Average Relative Hours	Coal[3] FD0252 lb/hr	Coke Br. FD0252 lb/hr	Limestone/Sand FD0220[6] lb/hr	Air[5] lb/hr	Oxygen[2] FI726 lb/hr	Nitrogen FI609[1] lb/hr	Steam[4] lb/hr	Total lb/hr	Syngas FI465 lb/hr	PCD Solids FD0520 lb/hr	SP Solids FD0510[7] lb/hr	Total lb/hr	SP Solids Total lb/hr	In - Out - Acc lb/hr	(In- Out - Acc)/In %	Oxygen/ Coal Ratio
TC12-1	8	4,157	0	0	12,944	0	6,642	875	24,619	24,141	294	0	24,435	42	142	0.6	0.73
TC12-2	10	4,242	0	0	12,973	0	6,615	876	24,705	24,124	294	0	24,418	36	252	1.0	0.71
TC12-3	17	4,097	0	0	13,055	0	6,333	910	24,395	23,968	296	0	24,263	4	128	0.5	0.74
TC12-4	32	3,727	0	136	12,272	0	6,433	898	23,467	22,525	303	0	22,829	1	501	2.1	0.77
TC12-5	40	3,604	0	182	12,339	0	6,153	884	23,162	23,092	383	198	23,673	-10	-683	-3.0	0.80
TC12-6	46	3,895	0	153	12,428	0	6,341	713	23,531	22,998	415	108	23,521	9	-152	-0.7	0.74
TC12-7	51	4,272	0	191	13,062	0	6,423	653	24,602	23,931	408	26	24,364	-8	54	0.2	0.71
TC12-8	59	3,530	0	153	11,845	0	5,670	815	22,013	21,490	397	0	21,887	-10	-17	-0.1	0.78
TC12-9	79	4,034	0	257	751	2,495	6,355	2,547	16,438	15,324	447	90	15,860	-5	326	2.0	0.66
TC12-10	86	3,813	0	281	1,806	2,359	5,952	2,366	16,577	15,762	467	0	16,229	14	54	0.3	0.73
TC12-11	104	3,620	0	554	933	2,423	6,308	1,967	15,805	15,090	434	38	15,562	9	-319	-2.1	0.73
TC12-12	124	4,056	0	226	993	2,548	6,247	1,914	15,984	15,494	418	122	16,034	-1	-275	-1.7	0.69
TC12-13	128	4,054	0	493	834	2,461	6,311	2,003	16,156	15,292	418	195	15,905	11	-253	-1.6	0.65
TC12-14	135	3,849	0	0	1,378	2,398	5,873	2,416	15,914	15,804	224	244	16,272	-28	-330	-2.1	0.71
TC12-15	142	3,892	0	0	789	2,516	5,935	1,910	15,042	14,014	224	83	14,321	21	700	4.7	0.69
TC12-16	146	3,410	0	0	1,544	2,387	5,927	2,380	15,647	16,419	238	0	16,657	-7	-1,003	-6.4	0.81
TC12-17	155	5,156	0	0	1,205	2,824	6,090	3,294	18,568	19,314	432	0	19,746	9	-1,186	-6.4	0.60
TC12-18	172	2,850	0	0	2,468	1,589	6,342	1,278	14,527	13,885	202	0	14,087	19	422	2.9	0.76
TC12-19	184	2,992	0	0	623	2,013	6,349	1,326	13,304	12,495	211	0	12,705	15	584	4.4	0.72
TC12-20	197	3,133	0	235	1,026	2,064	6,490	1,241	14,189	12,892	220	0	13,113	46	795	5.7	0.73
TC12-21	206	3,136	0	0	662	1,967	5,992	1,249	13,006	12,248	227	26	12,500	-5	512	3.9	0.68
TC12-22	218	3,273	0	0	839	2,121	6,151	1,250	13,633	12,667	235	0	12,902	16	715	5.2	0.71
TC12-23	231	3,252	0	0	796	1,957	6,259	1,249	13,512	13,197	245	0	13,441	5	67	0.5	0.66
TC12-24	246	3,042	0	50	1,344	1,917	6,079	1,321	13,753	12,903	255	69	13,227	-4	480	3.5	0.73
TC12-25	260	3,188	0	169	917	1,917	5,950	1,595	13,736	12,571	269	0	12,840	13	714	5.3	0.67
TC12-26	267	3,436	0	49	1,557	2,009	6,092	1,329	14,473	13,253	273	247	13,773	-24	675	4.7	0.69
TC12-27	285	3,359	0	126	1,229	2,060	6,536	1,512	14,822	14,096	280	84	14,460	-11	247	1.7	0.70

Notes:

1. FI6080 added to FI609 to get true total, then nitrogen feed rate reduced by 1000 pounds in air-blown mode and 250 pounds per hour in oxygen-blown mode to account for losses in feed systems and seals.

2. TC12-1 through TC12-8 were air-blown; all others were oxygen-blown.

3. Coal rate by weigh cells.

4. Steam determined by sum of steam flow readings, except for TC12-6,7,8, when the H_2 balance was used.

5. Air flow rate is by FI205 during air blow mode and by FI201 during oxygen blown mode.

6. The feed from FD0220 was limestone for TC12-4 through TC12-13, TC12-47, and TC12-52. It was sand for all others.

7. The standpipe removal rate was estimated from the change in LI339 while the standpipe screw cooler was running.

Table 3.5-1 (Page 2 of 2)

Feed Rates, Product Rates, and Mass Balance

Operating Period	Average Relative Hours	Coal[3] lb/hr	Coke Br. FD0252 lb/hr	Limestone/Sand FD0220[6] lb/hr	Air[5] lb/hr	Oxygen[2] FI726 lb/hr	Nitrogen FI609[1] lb/hr	Steam[4] lb/hr	Total lb/hr	Syngas FI465 lb/hr	PCD Solids FD0520 lb/hr	SP Solids FD0510[7] lb/hr	Total lb/hr	SP Solids Total lb/hr	In - Out - Acc lb/hr	(In- Out - Acc)/In %	Oxygen/ Coal Ratio
TC12-28a	299	3,395	0	0	1,416	2,102	6,311	1,619	14,842	14,404	278	176	14,858	-4	-12	-0.1	0.72
TC12-28b	312	3,454	0	66	1,360	2,108	6,219	1,680	14,886	14,467	275	276	15,018	-2	-196	-1.3	0.70
TC12-28c	325	3,452	0	17	1,458	2,095	6,323	1,770	15,116	14,775	275	116	15,166	-4	-63	-0.4	0.71
TC12-29	337	3,138	0	0	1,468	1,889	5,961	1,448	13,905	13,588	276	44	13,908	11	-14	-0.1	0.71
TC12-30	341	3,367	0	0	1,472	1,919	6,336	1,470	14,564	14,284	276	69	14,629	-7	-58	-0.4	0.67
TC12-31	345	3,292	0	0	1,402	1,995	6,287	1,548	14,524	14,270	276	0	14,546	1	-23	-0.2	0.71
TC12-32	354	3,551	0	148	1,339	2,072	6,444	1,621	15,174	14,560	276	0	14,836	21	169	1.1	0.67
TC12-33	403	3,479	0	40	794	2,570	6,400	4,569	17,851	18,398	272	0	18,671	-4	-855	-4.8	0.79
TC12-34	413	3,910	0	34	677	2,691	6,322	4,605	18,239	18,974	313	176	19,463	4	-1,262	-6.9	0.73
TC12-35	427	4,176	0	54	648	2,839	6,321	4,064	18,102	18,774	341	178	19,293	13	-1,258	-7.0	0.72
TC12-36a	444	3,749	0	0	667	2,645	6,264	3,090	16,415	16,993	309	36	17,338	-2	-922	-5.6	0.75
TC12-36b	456	3,783	0	46	885	2,519	5,848	3,057	16,138	16,418	265	121	16,803	8	-719	-4.5	0.72
TC12-37	471	1,260	200	0	1,649	1,457	7,244	3,350	15,161	15,743	209	81	16,033	-24	-849	-5.6	1.46
TC12-38	490	2,999	0	0	1,377	2,098	5,885	2,776	15,134	15,153	235	140	15,528	29	-423	-2.8	0.81
TC12-39	520	3,061	0	0	1,242	2,132	5,821	2,917	15,174	15,277	235	179	15,691	0	-518	-3.4	0.79
TC12-40	532	3,170	0	0	936	2,230	5,641	2,931	14,908	14,669	235	21	14,925	2	-18	-0.1	0.77
TC12-41	547	2,984	0	0	864	2,145	5,783	2,910	14,686	14,582	235	0	14,817	-5	-126	-0.9	0.79
TC12-42	561	3,226	0	0	1,366	2,051	5,786	2,521	14,949	14,023	274	0	14,298	13	638	4.3	0.73
TC12-43	578	4,366	0	92	1,440	2,556	5,935	2,658	17,047	16,111	391	0	16,502	-9	463	2.7	0.66
TC12-44	598	3,260	0	0	1,730	2,040	6,035	2,361	15,426	14,911	211	0	15,122	-2	306	2.0	0.75
TC12-45	618	3,785	0	54	1,030	2,542	5,970	2,820	16,201	15,824	261	207	16,292	0	-145	-0.9	0.74
TC12-46	643	3,492	0	51	786	2,450	6,299	2,708	15,786	15,162	304	0	15,466	3	267	1.7	0.75
TC12-47	650	3,462	0	122	835	2,470	5,939	2,694	15,522	14,640	282	123	15,045	31	324	2.1	0.77
TC12-48	662	4,056	0	0	897	2,603	6,356	2,705	16,617	15,924	280	70	16,273	-20	364	2.2	0.69
TC12-49	675	3,550	0	0	942	2,542	6,000	2,702	15,737	15,408	280	224	15,912	-5	-170	-1.1	0.78
TC12-50	699	3,489	0	34	998	2,354	5,940	2,838	15,653	14,727	280	0	15,007	-7	619	4.0	0.74
TC12-51	716	3,696	0	0	1,536	2,205	6,204	2,678	16,318	16,011	280	0	16,291	6	21	0.1	0.69
TC12-52	723	3,555	0	812	1,675	2,587	5,932	2,665	17,225	16,288	499	0	16,787	-1	-372	-2.3	0.84
TC12-53	733	4,099	0	0	1,305	2,457	6,022	1,769	15,652	14,402	280	0	14,682	15	955	6.1	0.67

Notes:

1. FI6080 added to FI609 to get true total, then nitrogen feed rate reduced by 1000 pounds in air-blown mode and 250 pounds per hour in oxygen-blown mode to account for losses in feed systems and seals.

2. TC12-1 through TC12-8 were air-blown; all others were oxygen-blown.

3. Coal rate by weigh cells.

4. Steam determined by sum of steam flow readings, except for TC12-6,7,8, when the H_2 balance was used.

5. Air flow rate is by FI205 during air blow mode and by FI201 during oxygen blown mode.

6. The feed from FD0220 was limestone for TC12-4 through TC12-13, TC12-47, and TC12-52. It was sand for all others.

7. The standpipe removal rate was estimated from the change in LI339 while the standpipe screw cooler was running.

Table 3.5-2
Carbon Balance

Operating Period[3]	Average Relative Hours	Carbon In (Feed)				Carbon Out (Products)				(In-Out-Acc) In-Out-Acc	(In-Out-Acc) In	Carbon Conversion[5]
		Coal[1] lb/hr	Sorbent lb/hr	Coke B. lb/hr	Total lb/hr	Syngas lb/hr	Standpipe[2] lb/hr	PCD Solids lb/hr	Total lb/hr	lb/hr[4]	%	%
TC12-1	8	2,182	0	0	2,182	2,043	0.0	38	2,081	100	5	98.2
TC12-2	10	2,228	0	0	2,228	2,065	0.0	42	2,107	121	5	98.0
TC12-3	17	2,160	0	0	2,160	2,058	0.0	55	2,114	46	2	97.4
TC12-4	32	1,976	16	0	1,992	1,871	0.0	56	1,927	65	3	97.1
TC12-5	40	1,917	21	0	1,938	1,971	1.3	73	2,045	-107	-6	96.4
TC12-6	46	2,082	18	0	2,100	2,033	1.5	83	2,117	-18	-1	96.0
TC12-7	51	2,302	22	0	2,324	2,121	0.2	86	2,207	117	5	96.1
TC12-8	59	1,921	18	0	1,939	1,862	0.0	81	1,943	-3	0	95.8
TC12-9	79	2,086	30	0	2,116	2,170	0.1	66	2,236	-120	-6	97.1
TC12-10	86	1,939	33	0	1,972	2,003	0.0	85	2,088	-116	-6	95.9
TC12-11	104	1,944	65	0	2,008	1,903	0.1	78	1,981	27	1	96.0
TC12-12	124	2,220	26	0	2,247	2,099	0.2	92	2,192	55	2	95.8
TC12-13	128	2,219	58	0	2,277	2,010	0.3	113	2,124	153	7	94.7
TC12-14	135	2,106	0	0	2,106	1,986	0.3	76	2,062	44	2	96.3
TC12-15	142	2,128	0	0	2,128	1,897	0.1	87	1,984	144	7	95.6
TC12-16	146	1,862	0	0	1,862	1,980	0.0	91	2,071	-208	-11	95.6
TC12-17	155	2,810	0	0	2,810	2,590	0.0	202	2,792	18	1	92.8
TC12-18	172	1,590	0	0	1,590	1,439	0.0	83	1,521	68	4	94.6
TC12-19	184	1,667	0	0	1,667	1,534	0.0	72	1,605	61	4	95.5
TC12-20	197	1,743	0	0	1,743	1,590	0.0	78	1,668	76	4	95.3
TC12-21	206	1,747	0	0	1,747	1,606	0.0	92	1,698	49	3	94.6
TC12-22	218	1,832	0	0	1,832	1,648	0.0	105	1,753	79	4	94.0
TC12-23	231	1,816	0	0	1,816	1,622	0.0	115	1,737	79	4	93.4
TC12-24	246	1,693	0	0	1,693	1,524	0.1	114	1,638	54	3	93.0
TC12-25	260	1,765	0	0	1,765	1,532	0.0	109	1,641	124	7	93.3
TC12-26	267	1,902	0	0	1,902	1,671	0.5	112	1,784	118	6	93.7
TC12-27	285	1,869	0	0	1,869	1,639	0.3	121	1,761	109	6	93.1
TC12-28a	299	1,897	0	0	1,897	1,677	0.7	120	1,798	99	5	93.3
TC12-28b	312	1,923	0	0	1,923	1,666	1.2	122	1,789	135	7	93.1
TC12-28c	325	1,912	0	0	1,912	1,692	0.3	122	1,814	98	5	93.3
TC12-29	337	1,716	0	0	1,716	1,497	0.1	134	1,631	85	5	91.8
TC12-30	341	1,831	0	0	1,831	1,613	0.1	134	1,747	84	5	92.3
TC12-31	345	1,782	0	0	1,782	1,634	0.0	124	1,758	23	1	92.9
TC12-32	354	1,943	0	0	1,943	1,685	0.0	127	1,812	131	7	93.0
TC12-33	403	1,939	0	0	1,939	1,796	0.0	101	1,897	42	2	94.7
TC12-34	413	2,180	0	0	2,180	1,899	0.2	120	2,019	161	7	94.1
TC12-35	427	2,330	0	0	2,330	2,070	0.3	108	2,179	152	7	95.0
TC12-36a	444	2,097	0	0	2,097	1,935	0.1	112	2,047	50	2	94.5
TC12-36b	456	2,120	0	0	2,120	1,868	0.6	101	1,970	150	7	94.8
TC12-37	471	708	0	140	848	894	0.7	46	941	-93	-11	95.0
TC12-38	490	1,667	0	0	1,667	1,603	1.3	78	1,683	-16	-1	95.3
TC12-39	520	1,695	0	0	1,695	1,593	0.4	39	1,633	62	4	97.6
TC12-40	532	1,740	0	0	1,740	1,631	0.0	54	1,685	55	3	96.8
TC12-41	547	1,631	0	0	1,631	1,611	0.0	55	1,666	-34	-2	96.7
TC12-42	561	1,763	0	0	1,763	1,600	0.0	91	1,691	72	4	94.6
TC12-43	578	2,399	0	0	2,399	2,154	0.0	180	2,334	65	3	92.3
TC12-44	598	1,791	0	0	1,791	1,645	0.0	76	1,722	69	4	95.6
TC12-45	618	2,076	0	0	2,076	1,963	0.2	88	2,051	25	1	95.7
TC12-46	643	1,917	0	0	1,917	1,782	0.0	89	1,870	47	2	95.3
TC12-47	650	1,901	14	0	1,916	1,783	0.1	78	1,861	54	3	95.8
TC12-48	662	2,229	0	0	2,229	1,982	0.1	73	2,055	174	8	96.4
TC12-49	675	1,954	0	0	1,954	1,907	0.3	107	2,015	-61	-3	94.7
TC12-50	699	1,939	0	0	1,939	1,681	0.0	98	1,778	161	8	94.5
TC12-51	716	2,037	0	0	2,037	1,825	0.0	112	1,937	101	5	94.2
TC12-52	723	1,952	95	0	2,047	2,041	0.0	182	2,223	-176	-9	91.8
TC12-53	733	2,237	0	0	2,237	1,976	0.0	86	2,062	175	8	95.8

Notes:
1. Coal carbon determined by coal feeder weigh cells.
2. Standpipe carbon flow intermittent. Rate shown is average FD0510 rate during operating period.
3. TC12-1 through TC12-8 were air-blown; all others were oxygen-blown.
4. Carbon accumulation in gasifier negligible for all operating periods.
5. Carbon conversion based on products method.

Table 3.5-3 Nitrogen, Hydrogen, Oxygen, Calcium, and Silica Mass Balances

Operating Period[2]	Average Relative Hours	Nitrogen[1] (In-Out) In %	In - Out lb/hr	Hydrogen (In-Out) In %	In - Out lb/hr	Oxygen (In-Out) In %	In - Out lb/hr	Calcium[4] (In-Out) In %	In - Out lb/hr	Silicon (In-Out) In %	In - Out lb/hr
TC12-1	8	0.5	78	3.7	13	-3.2	-166	65	28	-132.6	-100
TC12-2	10	0.9	153	3.9	14	-3.3	-170	61	27	-119.2	-92
TC12-3	17	0.6	95	1.7	6	-3.5	-180	42	18	-94.8	-71
TC12-4	32	2.6	404	5.8	19	-0.6	-31	46	37	-59.3	-42
TC12-5	40	-2.8	-430	8.9	28	1.1	52	20	19	-314.8	-221
TC12-6	46	1.8	288	0.0[3]	0	-5.7	-280	6	5	-188.2	-141
TC12-7	51	1.8	291	0.0[3]	0	-6.0	-307	19	20	-62.4	-52
TC12-8	59	1.9	285	0.0[3]	0	-5.0	-235	-4	-3	-56.1	-38
TC12-9	79	10.0	698	2.4	12	-1.2	-77	5	5	-156.0	-125
TC12-10	86	4.3	319	-2.0	-10	-0.5	-31	12	15	-54.0	-41
TC12-11	104	0.6	41	-1.0	-4	0.1	8	40	83	-51.4	-41
TC12-12	124	0.9	66	-2.1	-10	-2.3	-134	-46	-51	-91.8	-73
TC12-13	128	1.1	80	-1.0	-5	-0.1	-5	9	17	-145.6	-126
TC12-14	135	-0.2	-14	-3.4	-17	-4.1	-252	-214	-86	-231.5	-162
TC12-15	142	6.4	419	-0.9	-4	2.2	127	-46	-19	-54.2	-38
TC12-16	146	-7.4	-530	-9.4	-44	-5.2	-309	9	3	24.4	15
TC12-17	155	-13.6	-958	-1.0	-6	-4.5	-345	18	10	16.1	15
TC12-18	172	1.4	115	1.0	3	5.1	215	45	13	-22.4	-12
TC12-19	184	4.1	282	0.1	0	5.4	234	35	11	-26.8	-15
TC12-20	197	6.7	489	-1.8	-6	5.7	254	42	14	73.6	204
TC12-21	206	4.6	300	-1.2	-4	3.6	155	41	14	-59.1	-34
TC12-22	218	5.4	367	-1.1	-4	5.7	255	50	17	-10.3	-6
TC12-23	231	-1.1	-77	-1.5	-5	0.8	36	51	17	-10.2	-6
TC12-24	246	3.7	261	-0.9	-3	4.7	206	28	9	-27.3	-28
TC12-25	260	2.1	139	9.6	35	8.8	406	38	12	62.4	135
TC12-26	267	6.8	495	-0.3	-1	5.1	239	-6	-2	-165.7	-181
TC12-27	285	1.3	98	-2.6	-9	2.0	96	27	10	15.5	28
TC12-28a	299	-0.4	-27	-4.7	-18	1.6	79	6	2	-267.2	-165
TC12-28b	312	-2.4	-177	-3.8	-15	1.8	90	-18	-7	-145.4	-181
TC12-28c	325	-1.6	-121	-4.8	-19	0.8	41	15	6	-114.2	-91
TC12-29	337	-3.2	-228	-1.2	-4	2.7	124	30	10	-80.1	-46
TC12-30	341	-2.3	-175	-2.0	-7	0.3	15	29	10	-100.8	-62
TC12-31	345	-1.9	-142	-3.1	-12	0.6	29	40	14	-20.6	-12
TC12-32	354	-1.9	-141	-0.8	-3	2.5	125	44	16	64.6	132
TC12-33	403	-4.9	-345	-11.1	-80	-6.2	-490	29	10	22.5	23
TC12-34	413	-9.0	-619	-11.0	-82	-6.8	-562	8	3	-127.8	-132
TC12-35	427	-7.8	-532	-13.4	-94	-7.4	-588	3	1	-102.3	-130
TC12-36a	444	-5.9	-398	-17.6	-100	-6.4	-435	21	8	-72.7	-50
TC12-36b	456	-5.2	-338	-15.4	-87	-5.2	-345	21	8	-55.8	-62
TC12-37	471	-10.5	-895	7.0	32	3.7	191	-73	-10	-579.1	-133
TC12-38	490	-1.2	-84	-7.7	-37	-2.2	-131	31	10	-269.0	-147
TC12-39	520	-5.5	-373	-3.5	-18	0.0	-1	-17	-5	-329.3	-183
TC12-40	532	-2.7	-174	-3.1	-16	2.0	121	8	3	-63.1	-36
TC12-41	547	-2.0	-131	-5.2	-26	0.8	46	6	2	-41.3	-22
TC12-42	561	-0.3	-20	6.8	32	9.5	538	13	4	-31.9	-19
TC12-43	578	2.4	170	-2.1	-12	2.6	171	30	13	48.1	80
TC12-44	598	0.2	17	-3.6	-17	3.0	167	46	16	-7.6	-4
TC12-45	618	-0.9	-63	-5.8	-31	0.9	61	-7	-3	-108.0	-129
TC12-46	643	2.1	147	-5.4	-27	1.6	100	15	5	18.5	21
TC12-47	650	3.0	199	-0.7	-3	4.5	281	44	32	-175.5	-116
TC12-48	662	1.1	75	-2.0	-11	1.8	116	-56	-24	-62.7	-46
TC12-49	675	1.1	77	-7.4	-38	0.2	16	-65	-24	-291.8	-189
TC12-50	699	1.5	98	2.1	11	5.3	329	14	5	24.5	23
TC12-51	716	-2.2	-160	-1.7	-9	0.6	38	26	10	8.0	5
TC12-52	723	1.6	116	-4.0	-20	3.5	243	76	217	-22.9	-19
TC12-53	733	6.2	439	1.3	6	4.6	260	-63	-21	26.0	19

Notes:

1. Nitrogen feed rate reduced by 1000 pph (O_2-blown) or 250 pph (air-blown) to account for losses in feed systems and seals.

2. TC12-1 through TC12-8 were air-blown. All others were oxygen-blown.

3. Steam flow indicator out of service. Used hydrogen balance to determine steam flow rate.

4. Limestone feed during TC12-4,5,6,7,8,9,10,11,12,13,47, and 52 only.

Table 3.5-4

Typical Air-Blown Component Mass Balances

	Nitrogen[1]	Hydrogen	Oxygen	Calcium	Silica
Operating Period	TC12-5	TC12-5	TC12-5	TC12-5	TC12-5
Date Start	5/19/2003	5/19/2003	5/19/2003	5/19/2003	5/19/2003
Time Start	8:30	8:30	8:30	8:30	8:30
Time End	14:15	14:15	14:15	14:15	14:15
Fuel	PRB	PRB	PRB	PRB	PRB
Riser Temperature, $^\circ$F	1,751	1,751	1,751	1,751	1,751
Pressure, psig	210	210	210	210	210
In, pounds/hr					
Fuel	26	215	1,185	37	75
Sorbent	0	0	85	55	5
Coke Breeze	0	0	0	0	0
Air	9,412	0	2,859	0	0
Nitrogen	6,153	0	0	0	0
Steam	0	98	786	0	0
Total	15,591	313	4,914	93	79
Out, pounds/hr					
Synthesis Gas	16,020	283	4,817	0	0
PCD Solids	1	2	38	66	125
Standpipe Solids	0	0	7	9	167
Total	16,021	285	4,863	74	291
Accumulation, pounds/hr	0	0	0	0	-9
(In-Out-Acc)/In, %	-2.8%	8.9%	1.1%	20.5%	-256.1%
(In-Out-Acc), pounds per hour	-430	28	52	19	-212

Note: 1. Feed nitrogen decreased by 1000 pounds per hour.

Table 3.5-5

Typical Oxygen-Blown Component Mass Balances

	Nitrogen[1]	Hydrogen	Oxygen	Calcium	Silica
Operating Period	TC12-10	TC12-10	TC12-10	TC12-10	TC12-10
Date Start	05/21/03	5/21/03	5/21/03	5/21/03	5/21/03
Time Start	7:15	7:15	7:15	7:15	7:15
Time End	11:30	11:30	11:30	11:30	11:30
Fuel	PRB	PRB	PRB	PRB	PRB
Riser Temperature, °F	1,759	1,759	1,759	1,759	1,759
Pressure, psig	150	150	150	150	150
In, pounds/hr					
Fuel	28	227	1,253	40	79
Sorbent	0	0	131	86	7
Coke Breeze	0	0	0	0	0
Oxygen	0	0	2,359	0	0
Air[2]	1,378	0	419	0	0
Nitrogen	5,952	0	0	0	0
Steam	0	263	2,103	0	0
Total	7,358	490	6,265	125	86
Out, pounds/hr					
Synthesis Gas	7,038	498	6,224	0	0
PCD Solids	1	2	72	111	118
Standpipe Solids	0	0	0	0	0
Total	7,039	500	6,296	111	118
Accumulation, pounds/hr	0	0	1	1	11
(In-Out)/In, %	4.3%	-2.0%	-0.5%	10.6%	-50.0%
(In-Out), pounds per hour	319	-10	-31	15	-32

Notes:

1. Feed nitrogen decreased by 250 pounds per hour.

Table 3.5-6 (Page 1 of 2)

Sulfur Balance

| Operating Period[2,5] | Average Relative Hours | Feeds (In) Coal lb/hr | Products (Out) | | | | Accumulation Standpipe lb/hr | In-Out-Acc lb/hr | (In-Out-Acc)/In % | Sulfur Removal[3] | | | Sulfur Emissions[1] lb SO$_2$/MMBtu | Equilibrium H$_2$S ppm[4] | Measured TRS ppm |
			Syngas lb/hr	PCD Solids lb/hr	SP Solids lb/hr	Total lb/hr				Gas %	Products %	Solids %			
TC12-1	8	12.0	6.4	0.7	0.0	7.1	0.0	4.8	40.4	47	10	6	0.35	234	222
TC12-2	10	12.4	6.5	0.7	0.0	7.2	0.0	5.2	41.9	47	9	6	0.35	234	226
TC12-3	17	12.5	7.1	0.5	0.0	7.6	0.0	4.8	38.7	43	6	4	0.40	239	249
TC12-4	32	10.5	5.5	1.0	0.0	6.5	0.0	4.0	37.9	48	16	10	0.33	235	206
TC12-5	40	9.6	5.3	1.7	0.0	7.0	0.0	2.6	26.8	45	24	18	0.33	188	193
TC12-6	46	10.3	4.5	2.0	0.0	6.5	0.0	3.8	37.0	57	31	20	0.25	223	163
TC12-7	51	11.7	5.2	2.0	0.0	7.3	0.0	4.5	37.9	55	28	17	0.27	228	184
TC12-8	59	10.2	5.2	0.6	0.0	5.9	0.0	4.3	42.4	49	11	6	0.33	246	204
TC12-9	79	11.4	8.1	0.1	0.0	8.2	0.0	3.2	28.5	29	1	1	0.44	563	404
TC12-10	86	10.7	7.3	0.1	0.0	7.4	0.0	3.3	30.6	32	1	1	0.42	546	358
TC12-11	104	8.8	6.4	0.1	0.0	6.5	0.0	2.3	26.2	27	1	1	0.38	534	335
TC12-12	124	8.9	8.0	0.1	0.0	8.1	0.0	0.8	9.1	10	1	1	0.42	505	401
TC12-13	128	8.8	6.4	0.1	0.0	6.5	0.0	2.3	26.3	27	1	1	0.34	531	323
TC12-14	135	8.2	5.7	0.0	0.0	5.8	0.0	2.4	29.5	30	1	1	0.32	565	277
TC12-15	142	8.2	6.8	0.1	0.0	6.9	0.0	1.2	15.2	17	2	2	0.37	502	370
TC12-16	146	7.2	7.2	0.2	0.0	7.4	0.0	-0.2	-2.8	-1	2	2	0.46	512	338
TC12-17	155	10.8	12.3	0.4	0.0	12.7	0.0	-1.9	-17.5	-14	3	4	0.52	575	486
TC12-18	172	6.2	4.9	0.9	0.0	5.8	0.0	0.4	6.4	21	16	15	0.37	328	283
TC12-19	184	6.2	4.5	0.3	0.0	4.8	0.0	1.4	22.2	27	7	5	0.32	355	282
TC12-20	197	6.1	4.2	0.4	0.0	4.6	0.0	1.5	24.7	31	8	6	0.29	345	256
TC12-21	206	6.1	3.7	0.4	0.0	4.1	0.0	2.0	32.9	40	11	7	0.25	345	232
TC12-22	218	7.1	4.9	0.5	0.0	5.4	0.0	1.7	24.2	31	9	7	0.33	334	302
TC12-23	231	6.8	4.1	0.5	0.0	4.6	0.0	2.2	32.8	40	10	7	0.27	330	243
TC12-24	246	6.2	4.5	0.4	0.0	4.9	0.0	1.3	20.2	27	9	7	0.32	347	272
TC12-25	260	7.1	4.3	0.4	0.0	4.7	0.0	2.4	33.5	40	9	6	0.29	357	264
TC12-26	267	7.9	5.4	0.4	0.0	5.8	0.0	2.1	26.6	32	7	5	0.33	345	314
TC12-27	285	7.4	4.8	0.4	0.0	5.2	0.0	2.2	30.2	36	8	5	0.31	378	265

Notes:

1. Synthesis gas sulfur emissions determined from synthesis gas combustor SO$_2$ analyzer.

2. Sorbent feed to the Transport Gasifier occurred during TC12-4,5,6,7,8,9,10,11,12,13,47,52.

3. Negative sulfur removals are assumed to actually be 0% sulfur removal.

4. Minimum equilibrium H$_2$S determined by equilibrium calculations and the carbon dioxide and water partial pressures.

5. TC12-1 through TC12-8 were air blown. The remainder were oxygen blown.

Table 3.5-6 (Page 2 of 2)

Sulfur Balance

Operating Period[2,5]	Average Relative Hours	Feeds (In) Coal lb/hr	Products (Out) Syngas lb/hr	PCD Solids lb/hr	SP Solids lb/hr	Total lb/hr	Accumulation Standpipe lb/hr	In-Out-Acc lb/hr	(In-Out-Acc)/In %	Sulfur Removal[3] Gas %	Products %	Solids %	Sulfur Emissions[1] lb SO$_2$/MMBtu	Equilibrium H$_2$S ppm[4]	Measured TRS ppm
TC12-28a	299	7.2	5.4	0.4	0.0	5.8	0.0	1.4	19.7	26	7	6	0.34	397	289
TC12-28b	312	7.5	6.2	0.4	0.0	6.7	0.0	0.8	10.8	17	7	6	0.39	409	332
TC12-28c	325	7.5	6.2	0.5	0.0	6.7	0.0	0.8	11.2	18	7	6	0.39	417	324
TC12-29	337	6.5	5.9	0.5	0.0	6.3	0.0	0.2	3.1	10	7	7	0.40	380	338
TC12-30	341	6.9	6.5	0.5	0.0	7.0	0.0	-0.1	-1.7	5	7	7	0.42	372	359
TC12-31	345	6.6	6.7	0.5	0.0	7.2	0.0	-0.6	-8.5	-1	7	8	0.43	383	365
TC12-32	354	7.3	6.5	0.5	0.0	7.1	0.0	0.2	2.8	10	8	7	0.39	384	348
TC12-33	403	7.6	7.3	0.2	0.0	7.5	0.0	0.1	1.7	4	3	3	0.45	808	290
TC12-34	413	8.6	7.7	0.2	0.0	7.9	0.0	0.7	8.2	11	3	3	0.42	807	294
TC12-35	427	9.2	7.8	0.2	0.0	8.0	0.0	1.2	12.7	15	2	2	0.40	745	304
TC12-36a	444	8.3	7.1	0.2	0.0	7.3	0.0	1.0	11.9	14	3	2	0.41	644	309
TC12-36b	456	8.5	7.3	0.2	0.0	7.6	0.0	1.0	11.4	14	3	2	0.42	658	329
TC12-37	471	2.9	3.0	0.3	0.0	3.2	0.0	-0.4	-12.4	-3	8	9	0.51	592	152
TC12-38	490	7.2	7.8	0.4	0.0	8.3	0.0	-1.1	-15.1	-9	5	6	0.56	608	392
TC12-39	520	7.7	10.4	0.3	0.0	10.7	0.0	-3.1	-40.3	-36	3	4	0.73	598	514
TC12-40	532	10.7	10.5	0.4	0.0	10.9	0.0	-0.1	-1.2	3	4	4	0.71	617	536
TC12-41	547	10.2	10.2	0.4	0.0	10.6	0.0	-0.4	-3.6	1	4	4	0.73	608	524
TC12-42	561	11.7	9.3	0.7	0.0	10.0	0.0	1.8	14.9	21	7	6	0.62	488	510
TC12-43	578	21.8	12.2	1.1	0.0	13.4	0.0	8.4	38.7	44	8	5	0.60	515	568
TC12-44	598	13.8	10.1	0.5	0.0	10.6	0.0	3.2	23.1	27	5	4	0.67	504	518
TC12-45	618	11.6	9.5	0.4	0.0	9.9	0.0	1.7	14.7	18	4	3	0.54	569	449
TC12-46	643	9.8	9.7	0.5	0.0	10.1	0.0	-0.4	-3.7	1	5	5	0.59	573	476
TC12-47	650	9.7	9.6	0.6	0.0	10.2	0.0	-0.5	-5.3	1	6	6	0.59	580	494
TC12-48	662	11.4	9.7	0.1	0.0	9.8	0.0	1.6	13.8	15	1	1	0.51	554	458
TC12-49	675	10.0	9.4	0.3	0.0	9.7	0.0	0.2	2.5	6	3	3	0.57	575	457
TC12-50	699	10.1	7.6	0.3	0.0	7.9	0.0	2.2	22.0	25	4	3	0.47	594	389
TC12-51	716	10.7	8.7	0.4	0.0	9.1	0.0	1.6	15.4	19	4	3	0.51	540	414
TC12-52	723	10.3	11.6	0.6	0.0	12.2	0.0	-1.9	-18.0	-13	5	5	0.71	574	548
TC12-53	733	11.9	8.8	0.4	0.0	9.2	0.0	2.7	22.6	26	4	3	0.47	424	466

Notes:

1. Synthesis gas sulfur emissions determined from synthesis gas combustor SO$_2$ analyzer.

2. Sorbent feed to the Transport Gasifier occurred during TC12-4,5,6,7,8,9,10,11,12,13,47,52.

3. Negative sulfur removals are assumed to actually be 0% sulfur removal.

4. Minimum equilibrium H$_2$S determined by equilibrium calculations and the carbon dioxide and water partial pressures.

5. TC12-1 through TC12-8 were air blown. The remainder were oxygen blown.

Table 3.5-7 (Page 1 of 2)

Energy Balance[3]

Operating Period[4]	Average Relative Hours	Feeds (In)[1]					Products (Out)					In - Out	(In- Out)/In	Efficiency[5]		Corrected[2]
														Raw		
		Coal	Coke Breeze	Air	Steam	Total	Syngas	PCD Solids	Gasifier Solids	Heat Loss	Total			Cold	Hot	Cold
		10^6 Btu/hr	10^6 Btu/hr	10^6 Btu/hr	10^6 Btu/hr	10^6 Btu/hr	10^6 Btu/hr	10^6 Btu/hr	10^6 Btu/hr	10^6 Btu/hr	10^6 Btu/hr	10^6 Btu/hr	%	%	%	%
TC12-1	8	35.4	0.0	0.8	1.2	37.4	29.9	0.5	0.0	3.5	33.9	3.4	9.1	55.2	88.1	72.8
TC12-2	10	36.0	0.0	0.8	1.2	38.0	30.4	0.6	0.0	3.5	34.5	3.5	9.1	55.4	88.1	72.6
TC12-3	17	34.6	0.0	0.8	1.2	36.6	30.5	0.8	0.0	3.5	34.8	1.8	5.0	55.0	87.6	71.9
TC12-4	32	31.9	0.0	0.7	1.2	33.8	27.2	0.9	0.0	3.5	31.6	2.2	6.6	52.8	86.0	70.6
TC12-5	40	31.1	0.0	0.8	1.2	33.1	29.0	1.2	0.1	3.5	33.7	-0.7	-2.1	54.1	85.9	72.0
TC12-6	46	33.8	0.0	0.8	0.9	35.5	29.5	1.3	0.1	3.5	34.4	1.2	3.3	55.0	85.8	71.4
TC12-7	51	37.3	0.0	0.8	0.9	38.9	30.7	1.3	0.0	3.5	35.6	3.4	8.7	55.2	86.4	71.1
TC12-8	59	31.0	0.0	0.7	1.1	32.8	26.7	1.2	0.0	3.5	31.5	1.3	4.1	53.2	85.0	70.1
TC12-9	79	35.4	0.0	0.0	3.4	38.8	30.5	1.1	0.0	3.5	35.2	3.6	9.4	64.5	86.8	80.6
TC12-10	86	33.5	0.0	0.1	3.1	36.7	28.6	1.6	0.0	3.5	33.6	3.1	8.4	60.4	84.9	77.3
TC12-11	104	32.5	0.0	0.0	2.6	35.1	26.3	1.4	0.0	3.5	31.2	3.9	11.1	59.6	84.1	78.1
TC12-12	124	36.6	0.0	0.1	2.5	39.2	30.0	1.7	0.1	3.5	35.2	4.0	10.1	62.5	85.1	78.9
TC12-13	128	36.5	0.0	0.0	2.6	39.2	28.7	2.1	0.1	3.5	34.4	4.8	12.3	60.8	83.5	77.4
TC12-14	135	34.7	0.0	0.1	3.2	37.9	28.6	1.2	0.1	3.5	33.4	4.5	11.9	60.3	85.5	77.9
TC12-15	142	35.0	0.0	0.0	2.5	37.5	27.6	1.3	0.0	3.5	32.5	5.0	13.4	62.9	85.0	79.8
TC12-16	146	30.5	0.0	0.1	3.1	33.7	28.9	1.4	0.0	3.5	33.7	0.0	0.0	60.2	85.5	78.2
TC12-17	155	45.8	0.0	0.1	4.4	50.2	37.9	3.0	0.0	3.5	44.4	5.9	11.7	62.4	85.4	76.3
TC12-18	172	25.8	0.0	0.1	1.7	27.7	21.8	1.1	0.0	3.5	26.4	1.3	4.8	57.3	82.6	81.0
TC12-19	184	27.0	0.0	0.0	1.8	28.7	23.3	1.1	0.0	3.5	27.9	0.8	2.9	62.0	83.6	82.9
TC12-20	197	28.0	0.0	0.0	1.6	29.7	24.1	1.2	0.0	3.5	28.8	0.9	3.0	62.1	83.7	82.3
TC12-21	206	28.0	0.0	0.0	1.6	29.6	24.5	1.3	0.0	3.5	29.3	0.3	1.1	63.4	83.5	82.6
TC12-22	218	29.2	0.0	0.0	1.6	30.9	24.9	1.5	0.0	3.5	29.9	1.0	3.3	62.9	83.3	81.7
TC12-23	231	29.0	0.0	0.0	1.6	30.7	24.5	1.7	0.0	3.5	29.6	1.1	3.5	61.2	82.6	81.0
TC12-24	246	27.1	0.0	0.1	1.7	28.9	23.0	1.6	0.0	3.5	28.2	0.8	2.6	59.2	81.8	79.8
TC12-25	260	28.6	0.0	0.0	2.1	30.8	22.8	1.6	0.0	3.5	27.9	2.8	9.2	60.3	81.8	80.8
TC12-26	267	30.9	0.0	0.1	1.7	32.7	25.2	1.6	0.1	3.5	30.4	2.3	7.0	61.8	82.8	80.1
TC12-27	285	30.2	0.0	0.1	2.0	32.3	24.5	1.8	0.0	3.5	29.9	2.4	7.5	59.6	82.1	78.9

Notes:

1. Nitrogen and sorbent assumed to enter the system at ambient temperature and therefore have zero enthalpy.

2. Correction is to assume that the only nitrogen in the synthesis gas is from air and that the gasifier is adiabatic.

3. Reference conditions are 80°F and 14.7 psia.

4. TC12-1 through TC12-8 were air-blown. All others were oxygen-blown.

5. All efficiencies are based on the products method.

Table 3.5-7 (Page 2 of 2)
Energy Balance[3]

Operating Period[4]	Average Relative Hours	Feeds (In)[1]					Products (Out)					In - Out 10^6 Btu/hr	(In- Out)/In %	Efficiency[5]		Corrected[2]
		Coal 10^6 Btu/hr	Coke Breeze 10^6 Btu/hr	Air 10^6 Btu/hr	Steam 10^6 Btu/hr	Total 10^6 Btu/hr	Syngas 10^6 Btu/hr	PCD Solids 10^6 Btu/hr	Gasifier Solids 10^6 Btu/hr	Heat Loss 10^6 Btu/hr	Total 10^6 Btu/hr			Raw Cold %	Hot %	Cold %
TC12-28a	299	30.5	0.0	0.1	2.1	32.6	25.3	1.7	0.1	3.5	30.5	2.1	6.5	59.8	82.7	78.7
TC12-28b	312	31.0	0.0	0.1	2.2	33.3	25.1	1.7	0.1	3.5	30.5	2.8	8.3	59.3	82.5	78.4
TC12-28c	325	31.0	0.0	0.1	2.3	33.4	25.6	1.7	0.1	3.5	30.8	2.6	7.7	59.5	82.9	78.4
TC12-29	337	28.3	0.0	0.1	1.9	30.2	22.3	1.9	0.0	3.5	27.8	2.5	8.1	56.6	80.3	77.3
TC12-30	341	30.3	0.0	0.1	1.9	32.3	23.9	1.9	0.0	3.5	29.4	3.0	9.2	58.5	81.3	78.1
TC12-31	345	29.7	0.0	0.1	2.0	31.8	24.3	1.7	0.0	3.5	29.6	2.2	7.0	59.1	82.3	78.7
TC12-32	354	32.1	0.0	0.1	2.1	34.3	25.3	1.8	0.0	3.5	30.6	3.7	10.7	59.9	82.8	79.1
TC12-33	403	31.3	0.0	0.0	6.0	37.4	27.5	1.5	0.0	3.5	32.5	4.9	13.1	53.9	84.7	72.4
TC12-34	413	35.2	0.0	0.0	6.1	41.3	29.3	1.7	0.1	3.5	34.6	6.7	16.3	54.3	84.7	72.0
TC12-35	427	37.6	0.0	0.0	5.4	43.1	32.3	1.8	0.1	3.5	37.6	5.5	12.7	57.6	85.8	73.8
TC12-36a	444	33.8	0.0	0.0	4.1	37.9	30.6	1.7	0.0	3.5	35.8	2.1	5.5	59.8	85.5	76.5
TC12-36b	456	34.1	0.0	0.0	4.0	38.1	29.6	1.6	0.1	3.5	34.7	3.4	9.0	59.4	85.3	76.3
TC12-37	471	11.3	2.6	0.1	4.4	18.4	12.1	0.7	0.0	3.5	16.4	2.1	11.1	27.2	74.0	68.3
TC12-38	490	27.1	0.0	0.1	3.6	30.8	24.0	1.1	0.1	3.5	28.6	2.2	7.2	56.3	83.7	76.6
TC12-39	520	27.5	0.0	0.1	3.8	31.4	24.1	0.5	0.1	3.5	28.2	3.2	10.2	56.9	85.5	78.5
TC12-40	532	28.3	0.0	0.1	3.8	32.2	24.6	0.8	0.0	3.5	28.9	3.2	10.0	59.0	85.2	79.1
TC12-41	547	26.7	0.0	0.0	3.9	30.6	24.6	0.9	0.0	3.5	29.0	1.6	5.2	59.1	84.9	79.4
TC12-42	561	29.0	0.0	0.1	3.4	32.4	24.2	1.5	0.0	3.5	29.2	3.2	9.9	59.3	83.0	79.1
TC12-43	578	39.3	0.0	0.1	3.5	42.9	33.2	2.8	0.0	3.5	39.5	3.4	7.9	62.3	84.0	76.6
TC12-44	598	29.3	0.0	0.1	3.1	32.5	25.3	1.1	0.0	3.5	29.9	2.7	8.3	59.7	84.7	79.4
TC12-45	618	34.0	0.0	0.1	3.8	37.8	30.2	1.3	0.1	3.5	35.1	2.7	7.2	62.2	86.0	78.8
TC12-46	643	31.4	0.0	0.0	3.6	35.0	27.5	1.3	0.0	3.5	32.3	2.7	7.6	60.2	85.1	78.3
TC12-47	650	31.1	0.0	0.0	3.6	34.7	26.6	1.0	0.1	3.5	31.1	3.6	10.4	60.4	85.3	78.9
TC12-48	662	36.5	0.0	0.0	3.6	40.1	30.0	1.1	0.0	3.5	34.7	5.4	13.6	62.3	86.5	79.4
TC12-49	675	32.0	0.0	0.0	3.6	35.6	28.9	1.6	0.1	3.5	34.1	1.5	4.2	61.2	84.8	77.8
TC12-50	699	31.4	0.0	0.0	3.7	35.2	25.1	1.4	0.0	3.5	30.0	5.2	14.9	58.3	83.7	77.3
TC12-51	716	33.0	0.0	0.1	3.5	36.7	27.5	1.6	0.0	3.5	32.6	4.0	11.0	59.5	84.4	77.8
TC12-52	723	31.7	0.0	0.1	3.5	35.3	28.7	2.3	0.0	3.5	34.5	0.8	2.3	58.4	83.2	74.7
TC12-53	733	36.4	0.0	0.1	2.3	38.8	29.6	1.3	0.0	3.5	34.4	4.4	11.3	64.9	86.1	81.2

Notes:

1. Nitrogen and sorbent assumed to enter the system at ambient temperature and therefore have zero enthalpy.

2. Correction is to assume that the only nitrogen in the synthesis gas is from air and that the gasifier is adiabatic.

3. Reference conditions are 80°F and 14.7 psia.

4. TC12-1 through TC12-8 were air-blown. All others were oxygen-blown.

5. All efficiencies are based on the products method.
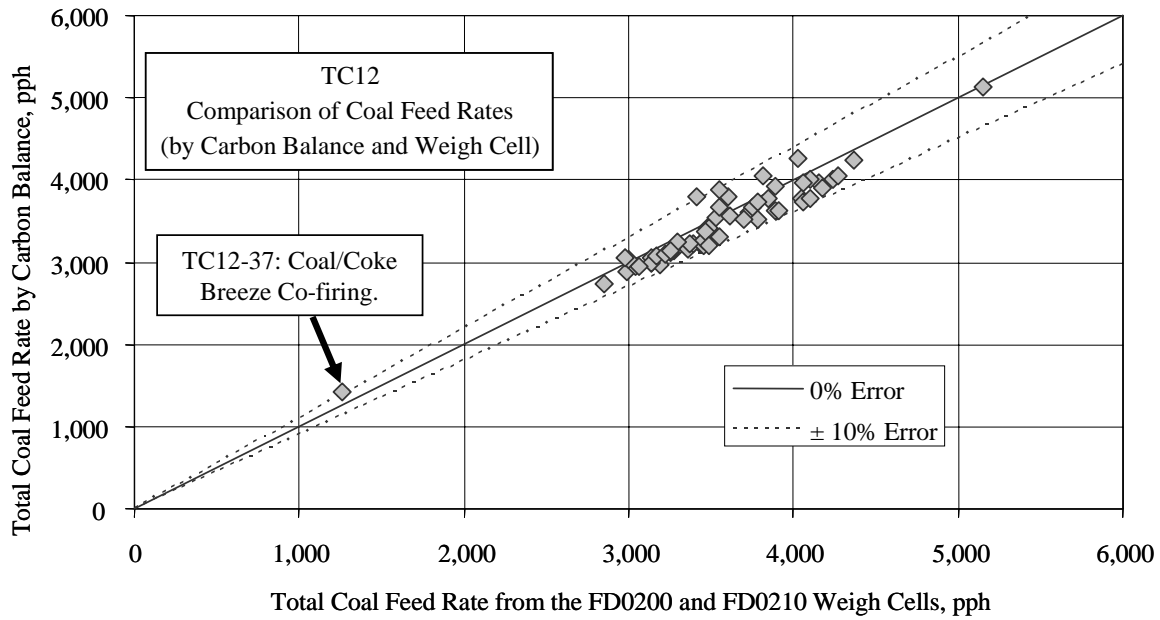
Figure 3.5-1 Comparison of Coal Rates by Two Methods
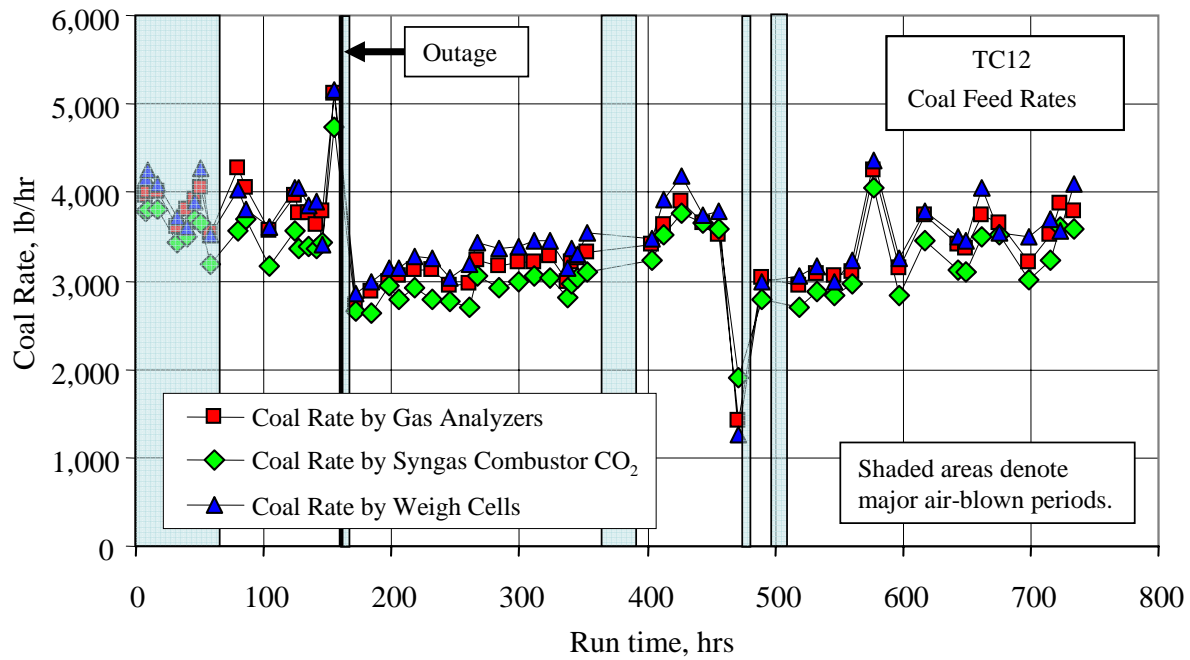
Figure 3.5-2 Coal Rates
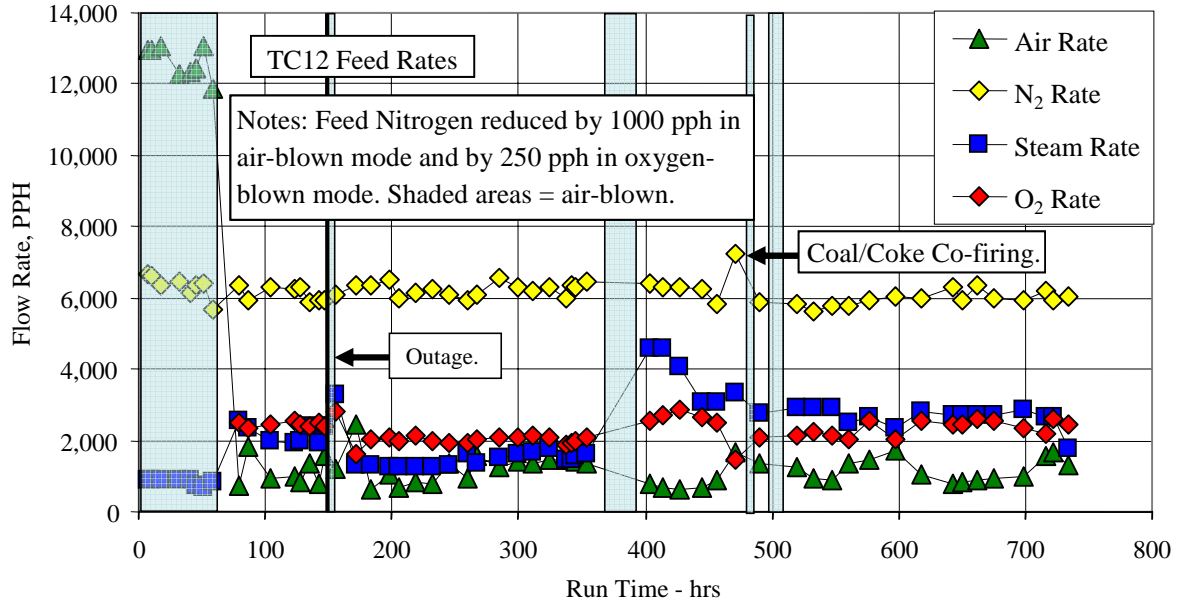
Figure 3.5-3 Air, Nitrogen, Oxygen, and Steam Rates
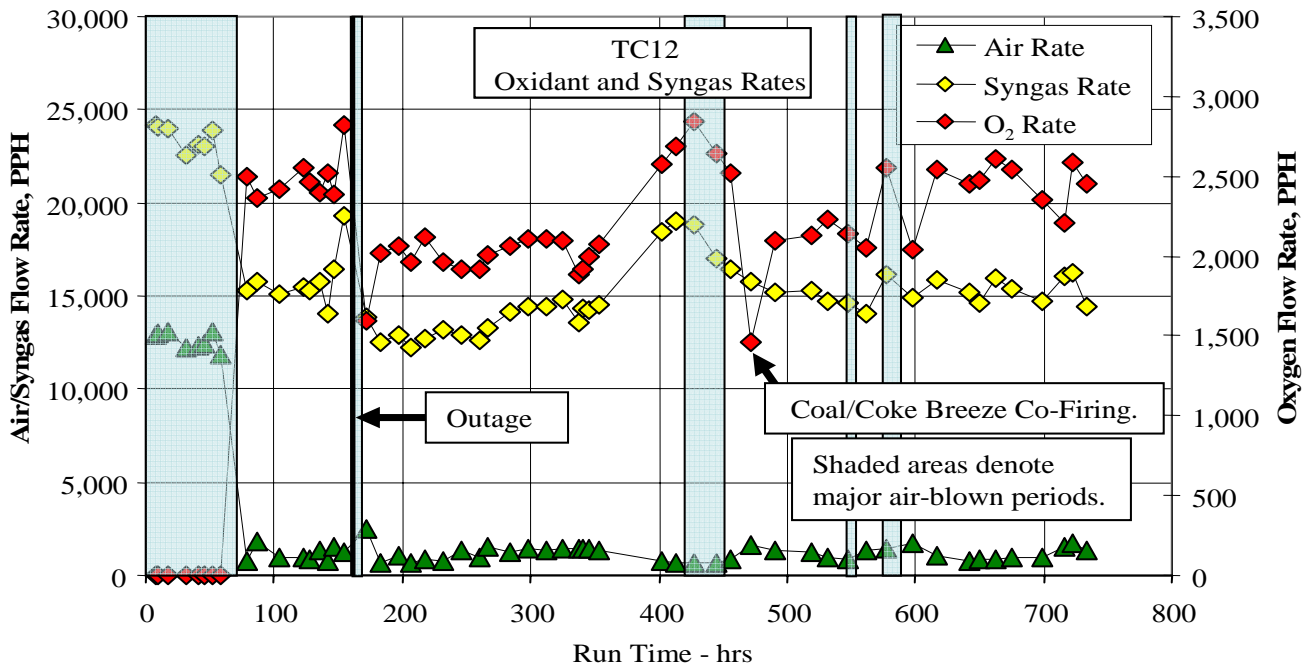
Figure 3.5-4 Syngas and Oxidant Flow Rates
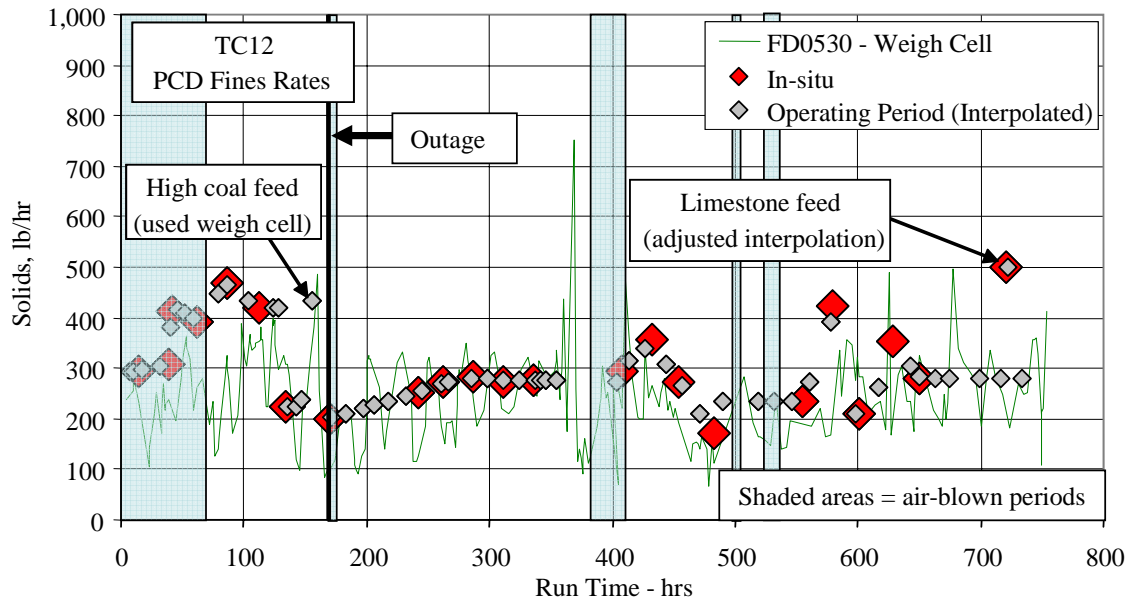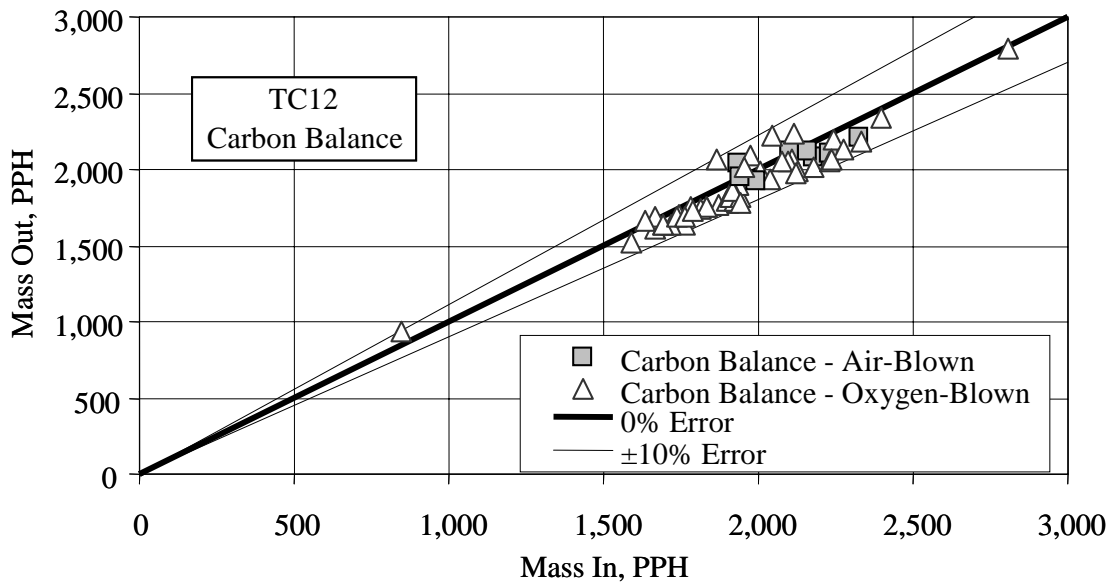
Figure 3.5-5 PCD Fines Rates
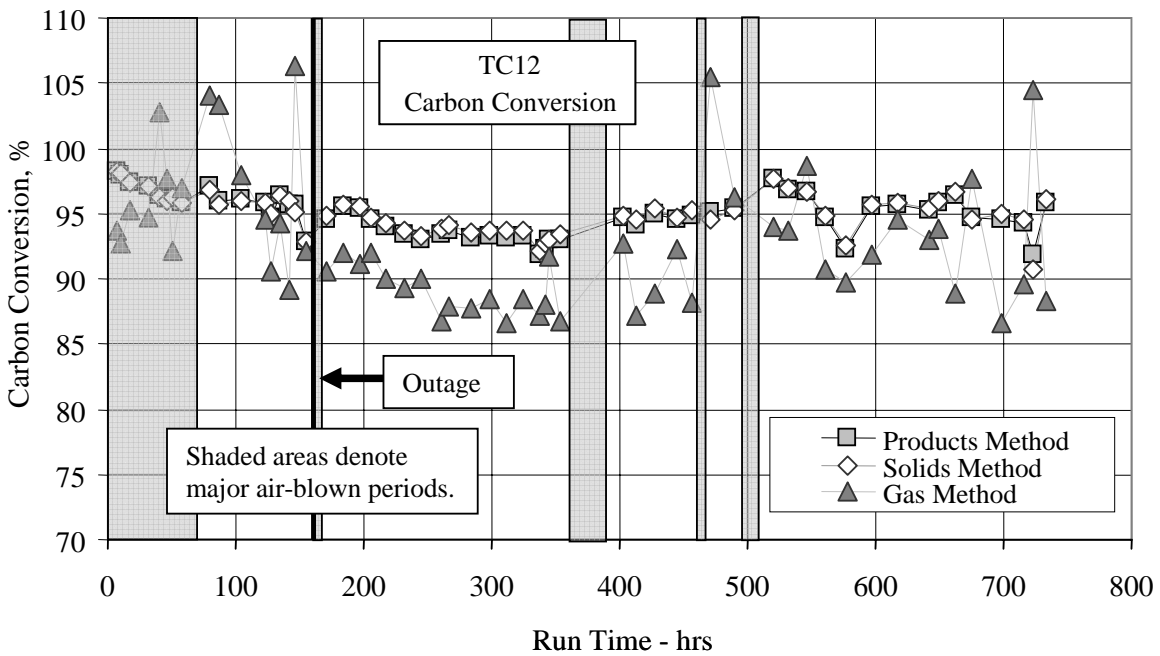

Figure 3.5-6 Carbon Balance
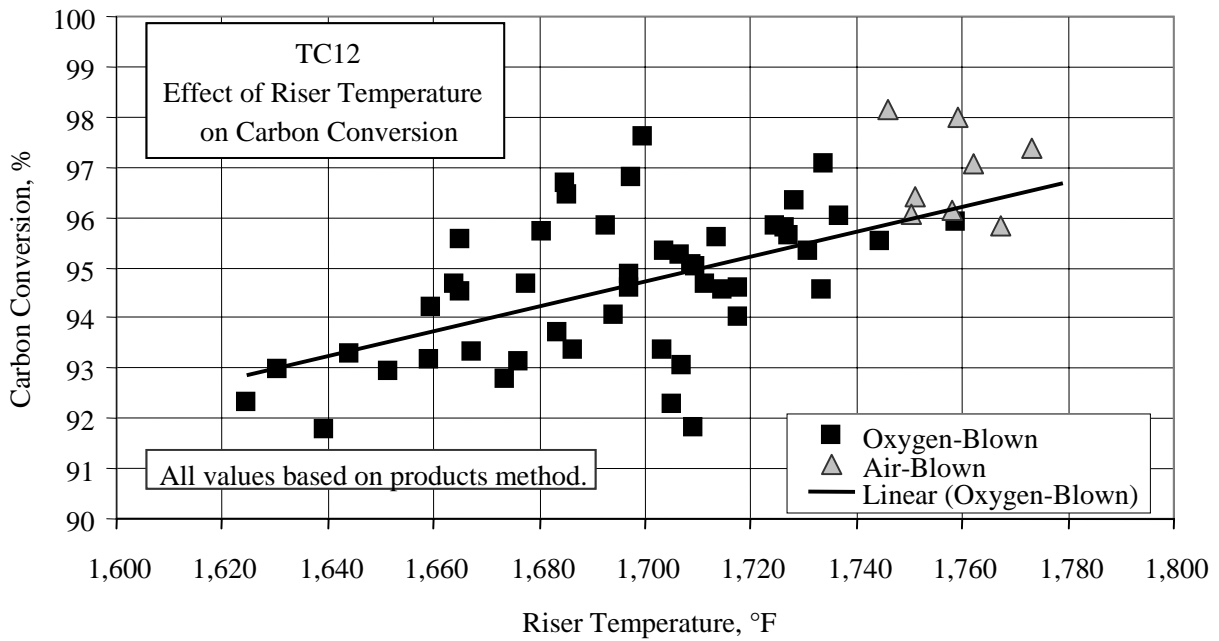
Figure 3.5-7 Carbon Conversion

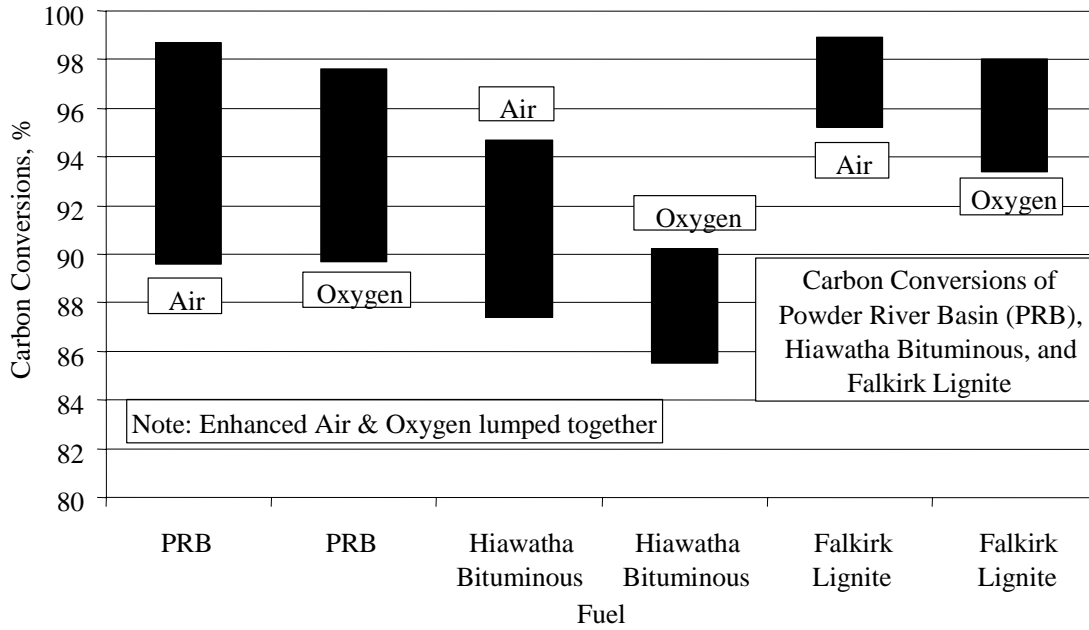Figure 3.5-8 Carbon Conversion and Riser Temperature

Figure 3.5-9 Carbon Conversion of Three Coals

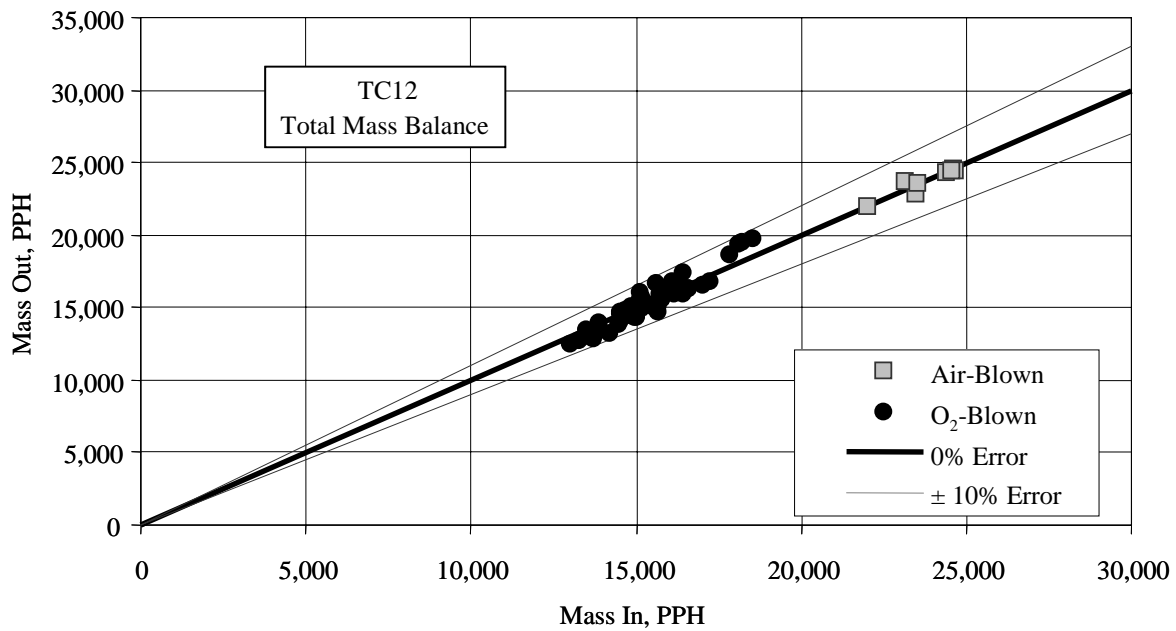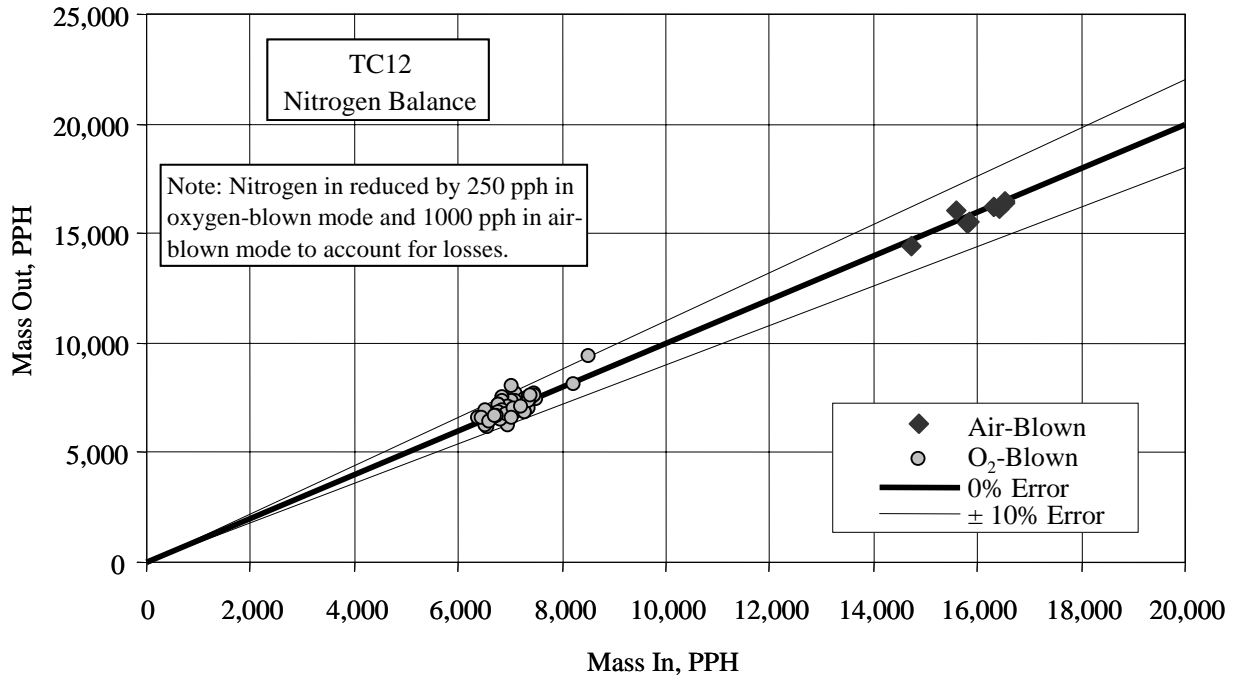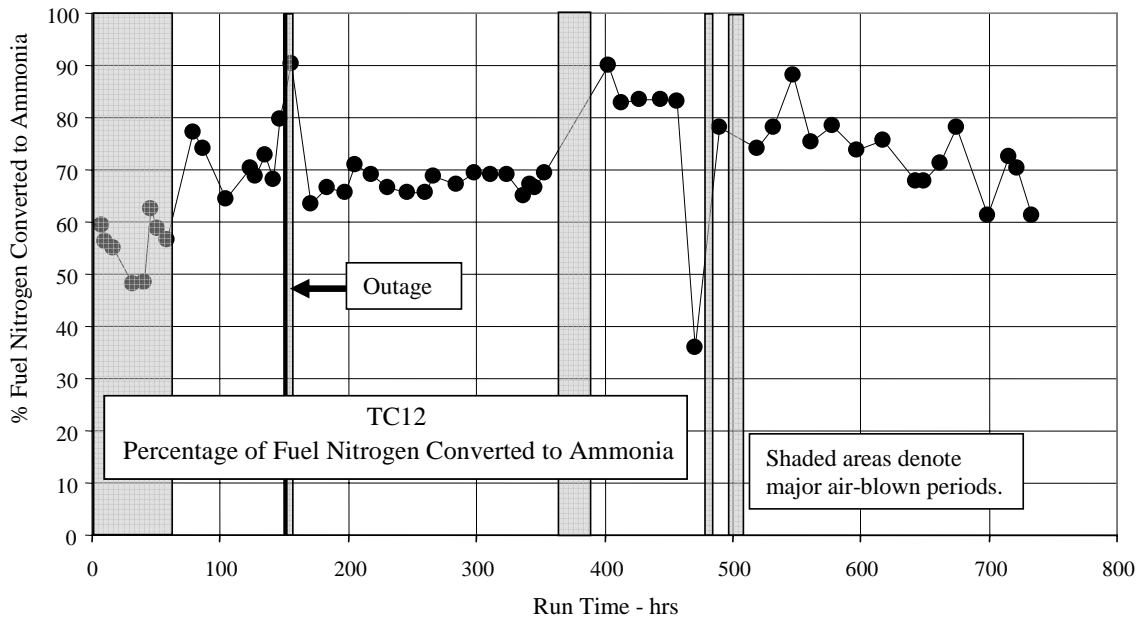Figure 3.5-10 Overall Material Balance

Figure 3.5-11 Nitrogen Balance

Figure 3.5-12 Fuel Nitrogen Conversion to Ammonia
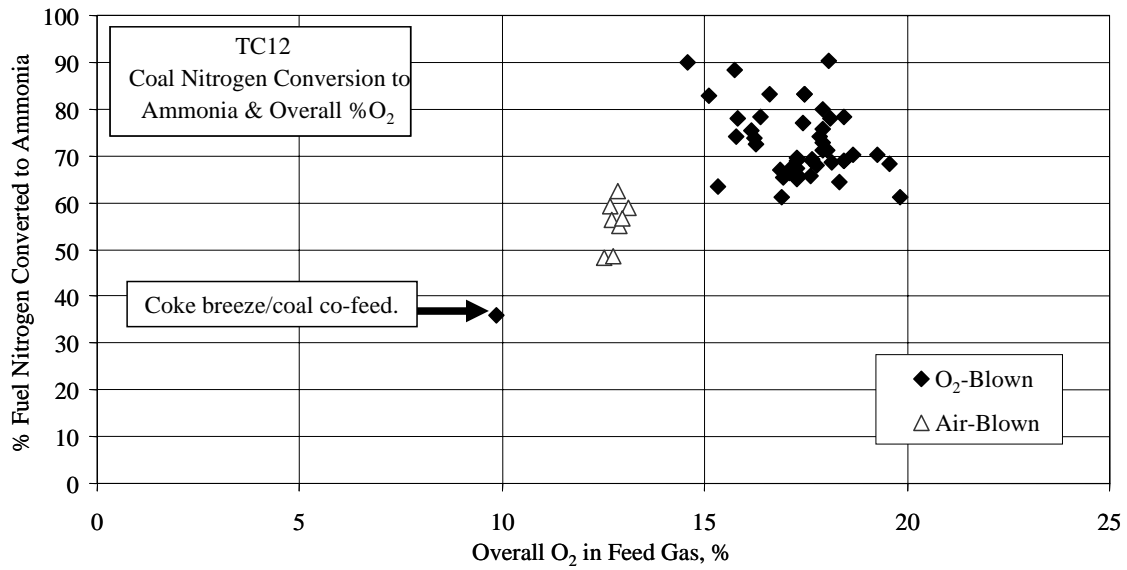
Figure 3.5-13 The Effect of Overall Oxygen Percentage on Coal Nitrogen to Ammonia Conversion
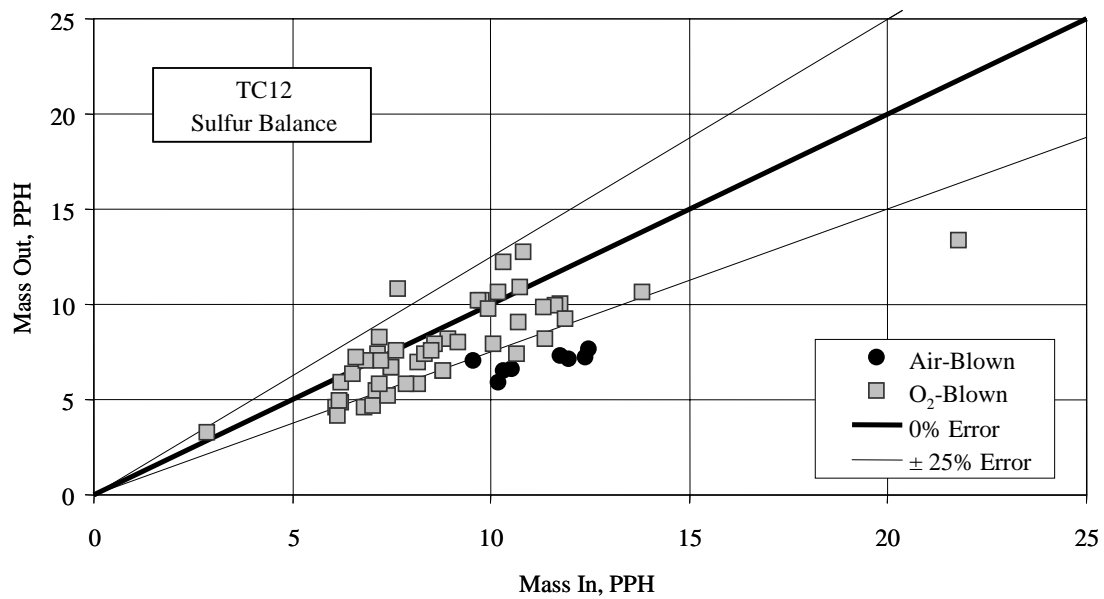
Figure 3.5-14 Sulfur Balance
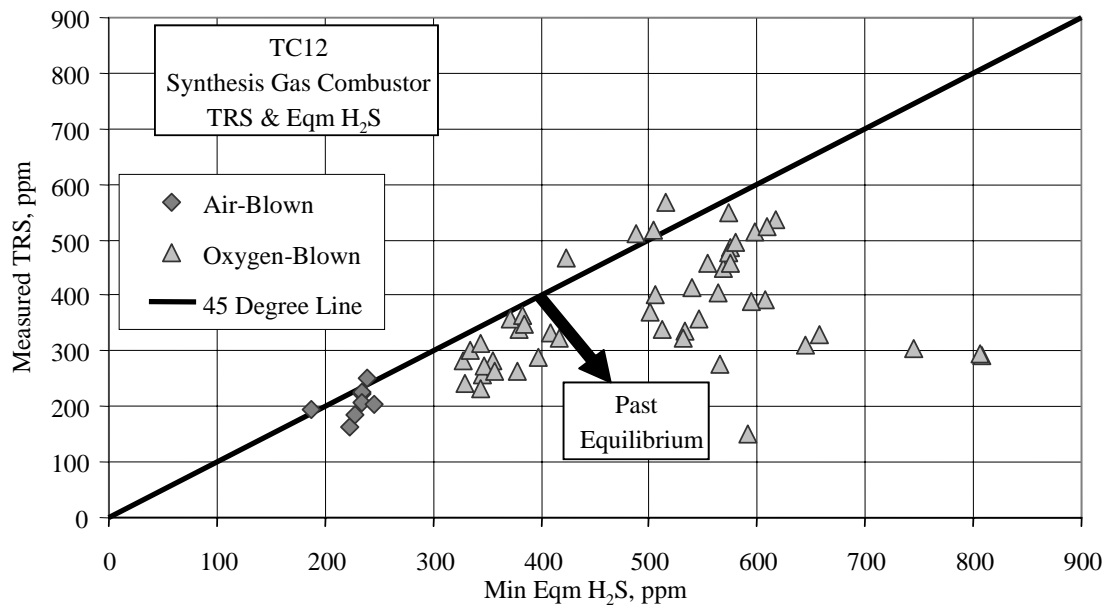
Figure 3.5-15 Minimum Equilibrium H₂S and Total Reduced Sulfur
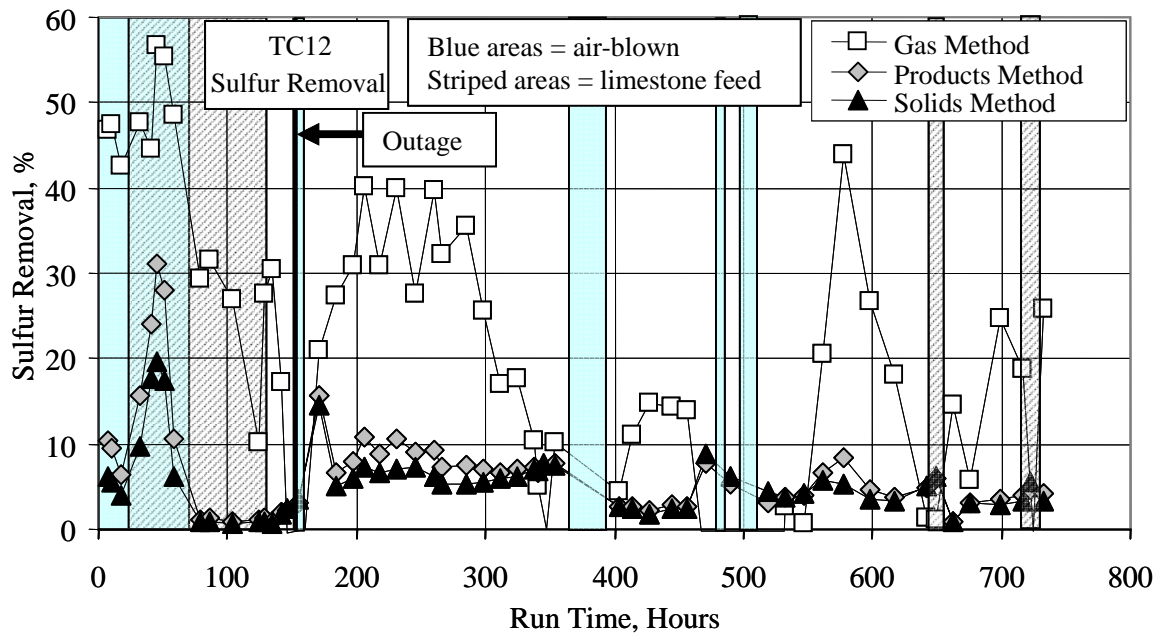
Figure 3.5-16 Coal Sulfur Removal
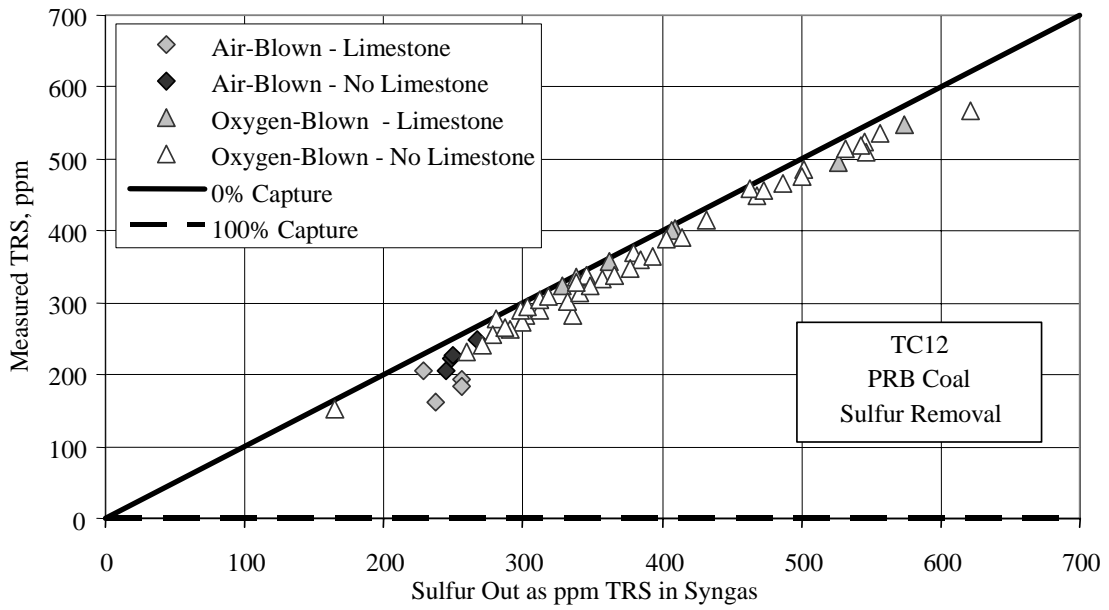
Figure 3.5-17 Sulfur Emissions
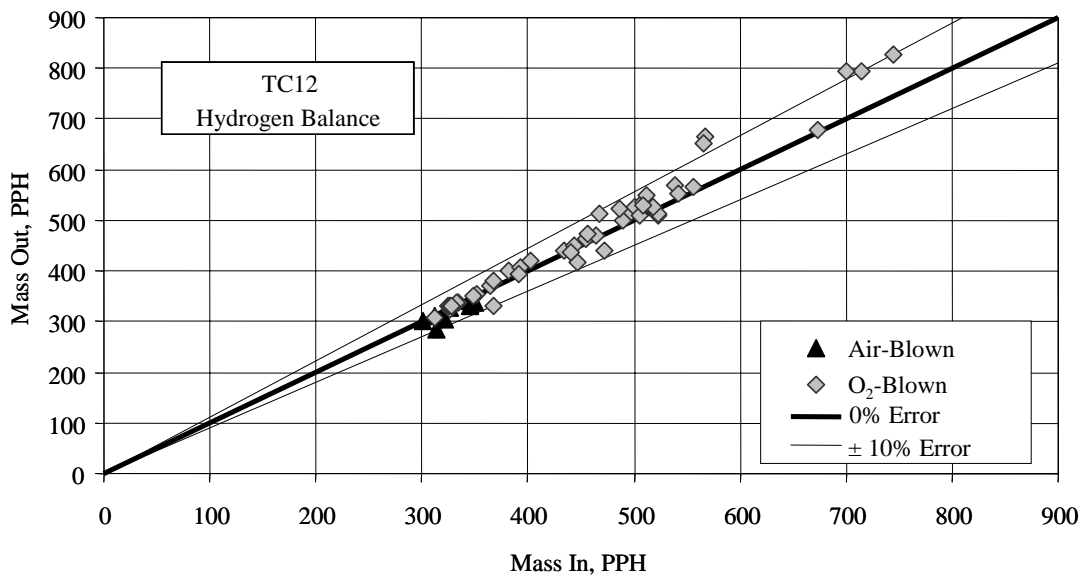
Figure 3.5-18 Hydrogen Balance
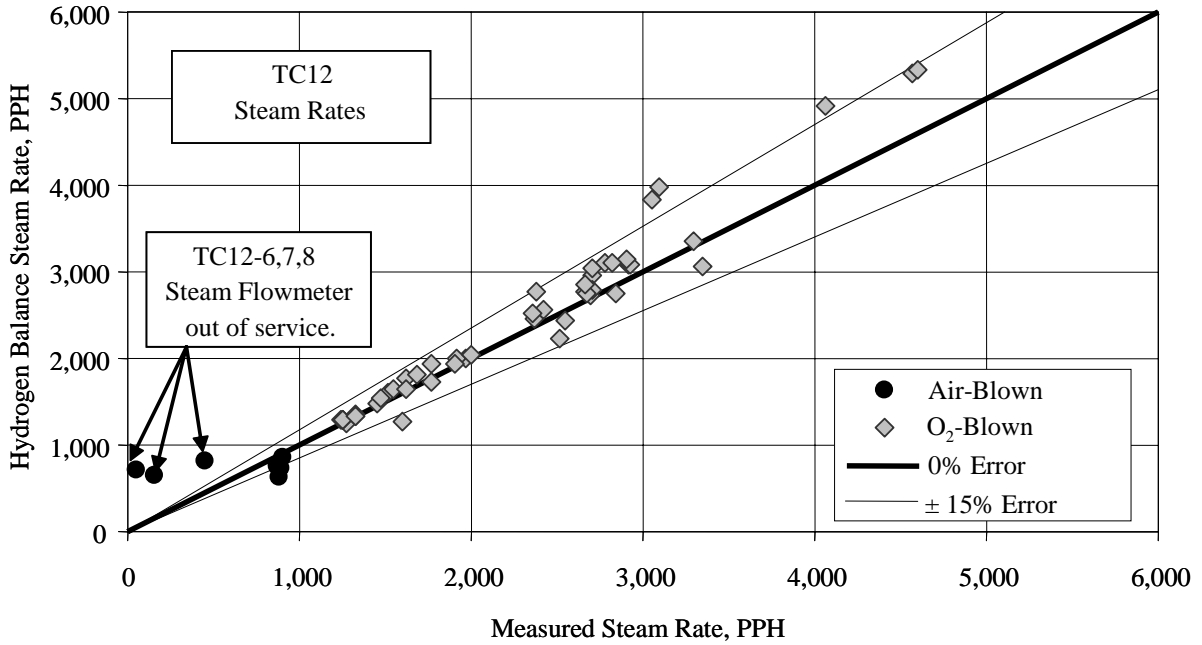
Figure 3.5-19 Steam Rates
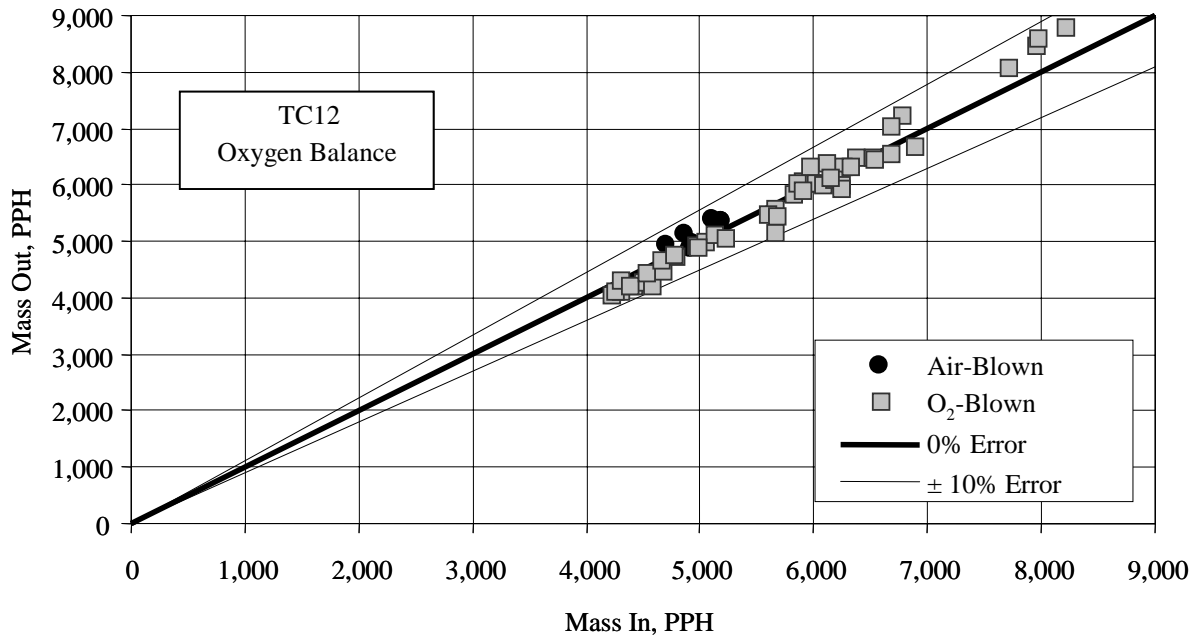
Figure 3.5-20 Oxygen Balance
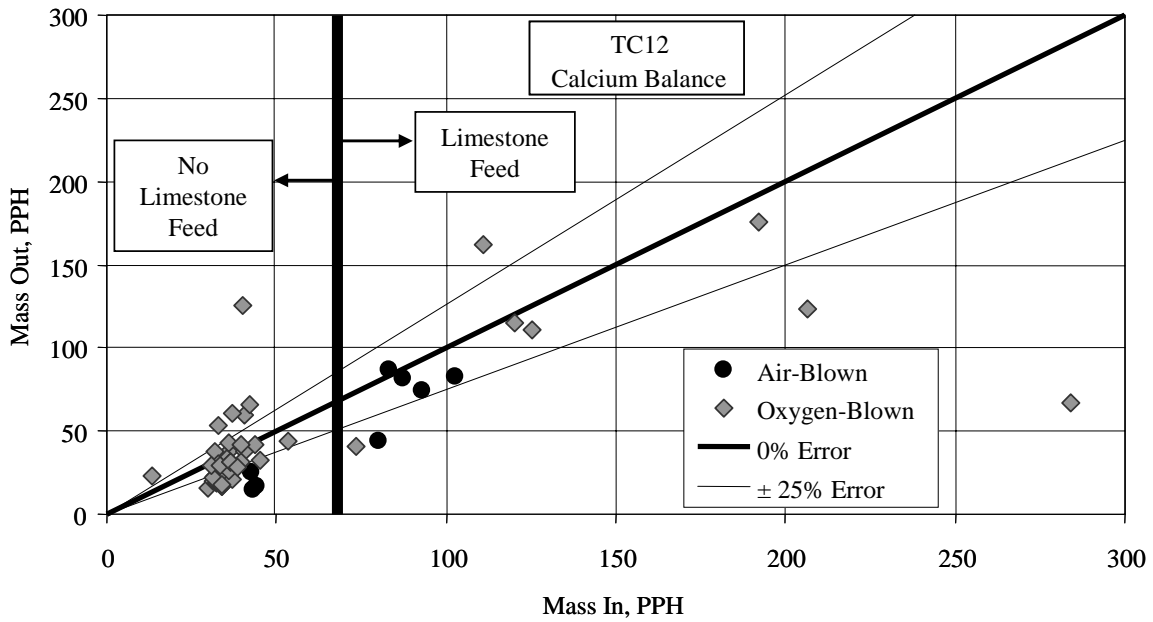
Figure 3.5-21 Calcium Balance
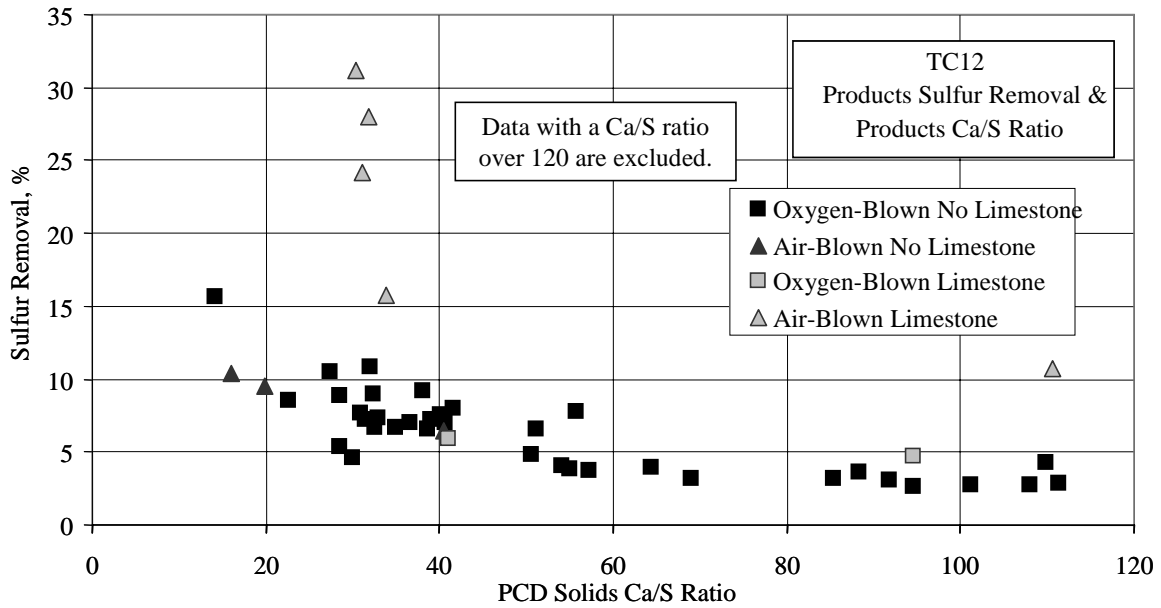
Figure 3.5-22 Sulfur Removal and PCD Solids Ca/S Ratio
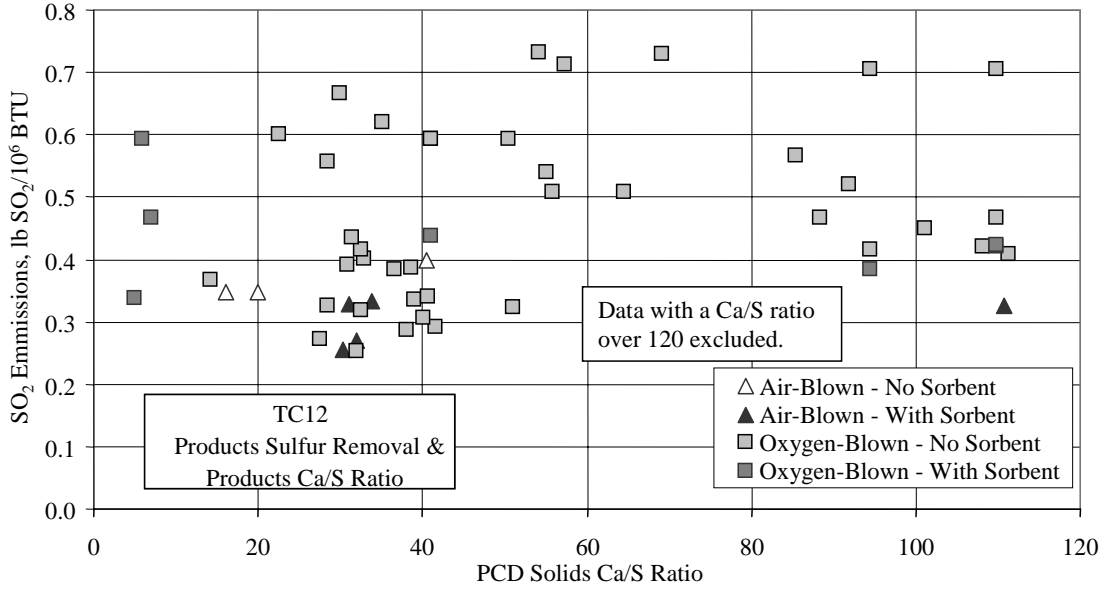
Figure 3.5-23 Sulfur Emissions and PCD Solids Ca/S Ratio
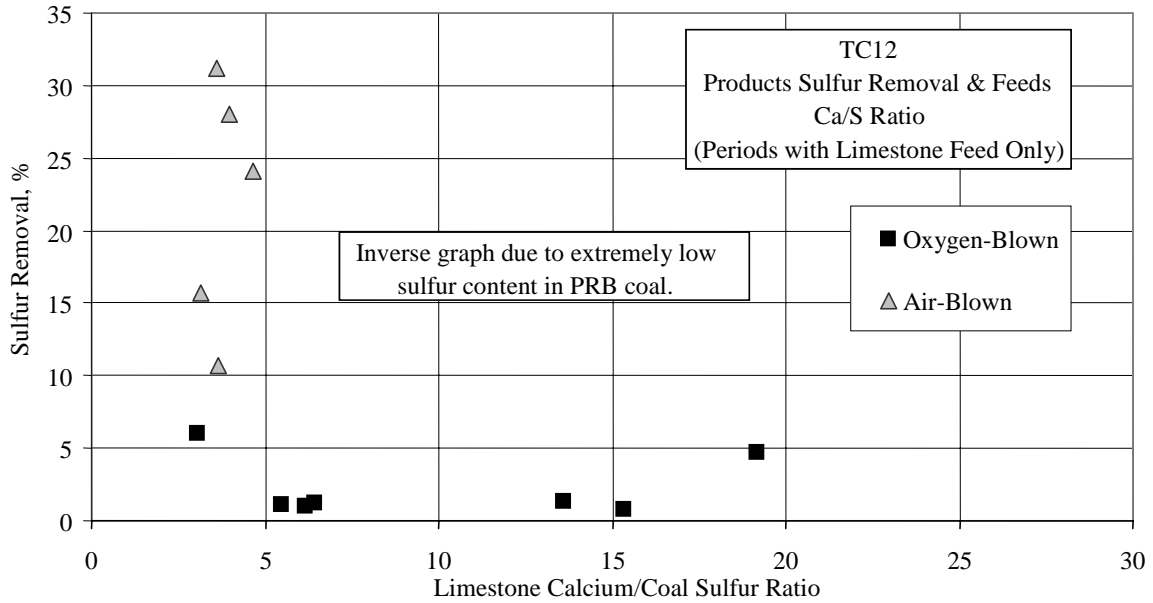
Figure 3.5-24 Sulfur Emissions and Feed Solids Ca/S Ratio
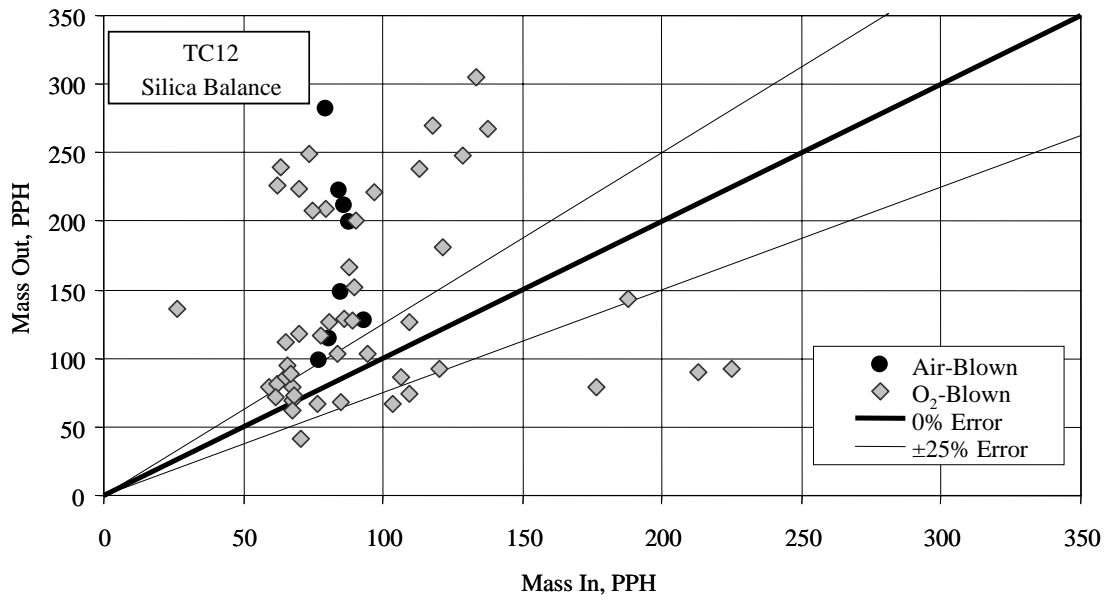
Figure 3.5-25 Silica Balance
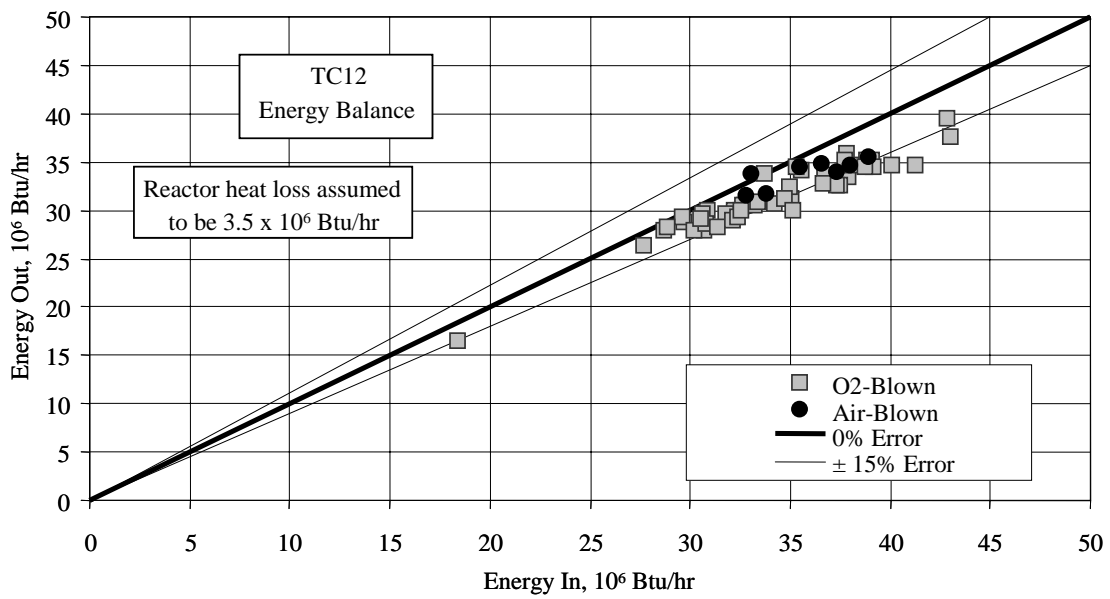
Figure 3.5-26 Energy Balance
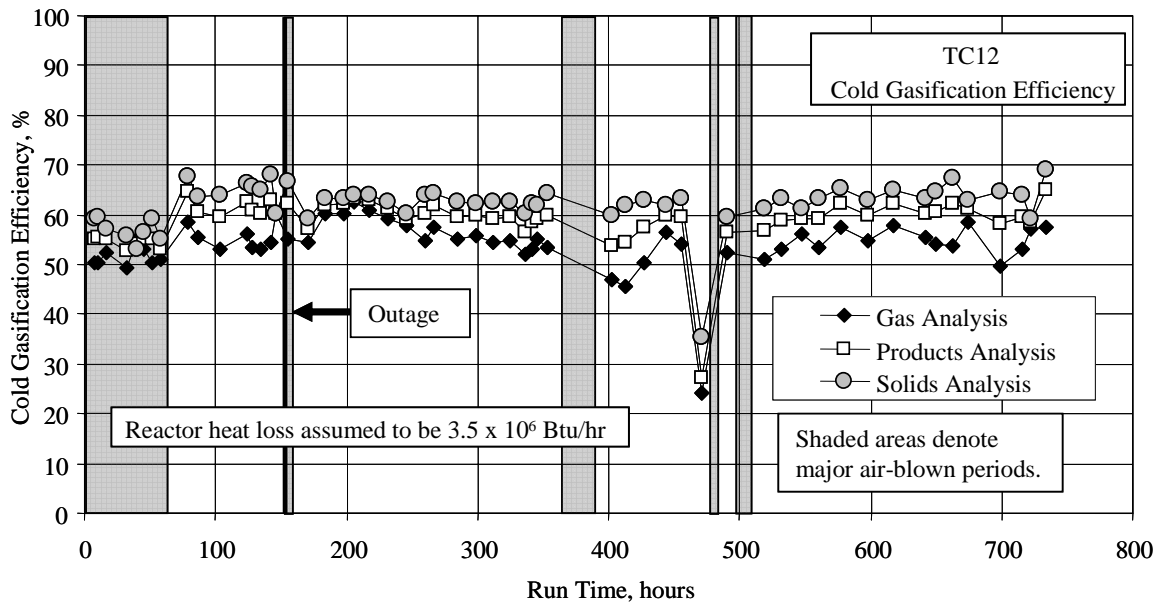
Figure 3.5-27 Cold Gasification Efficiency
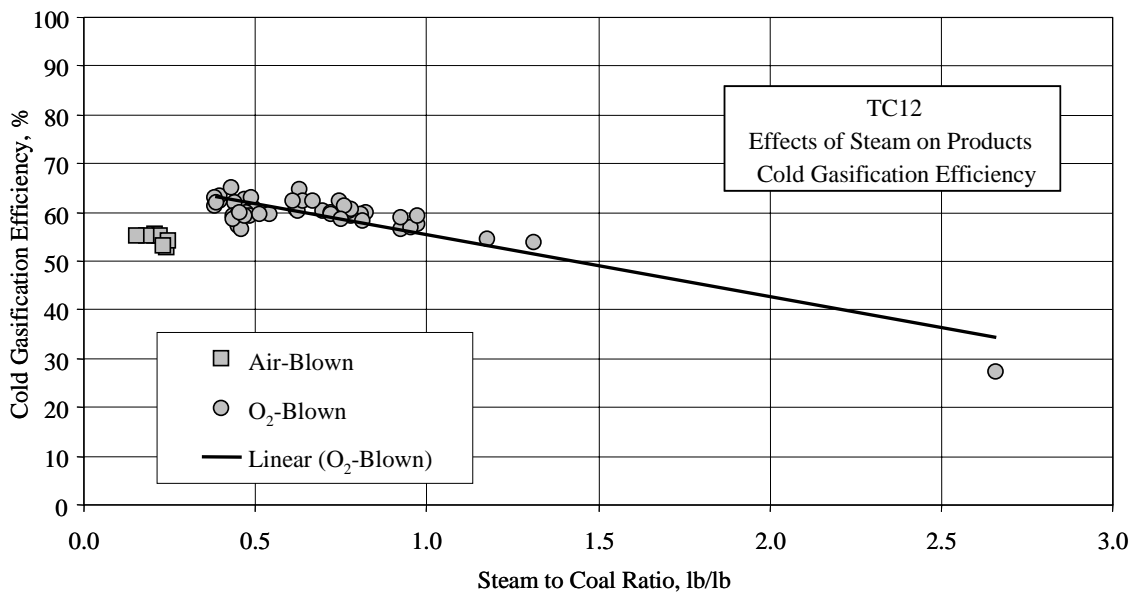
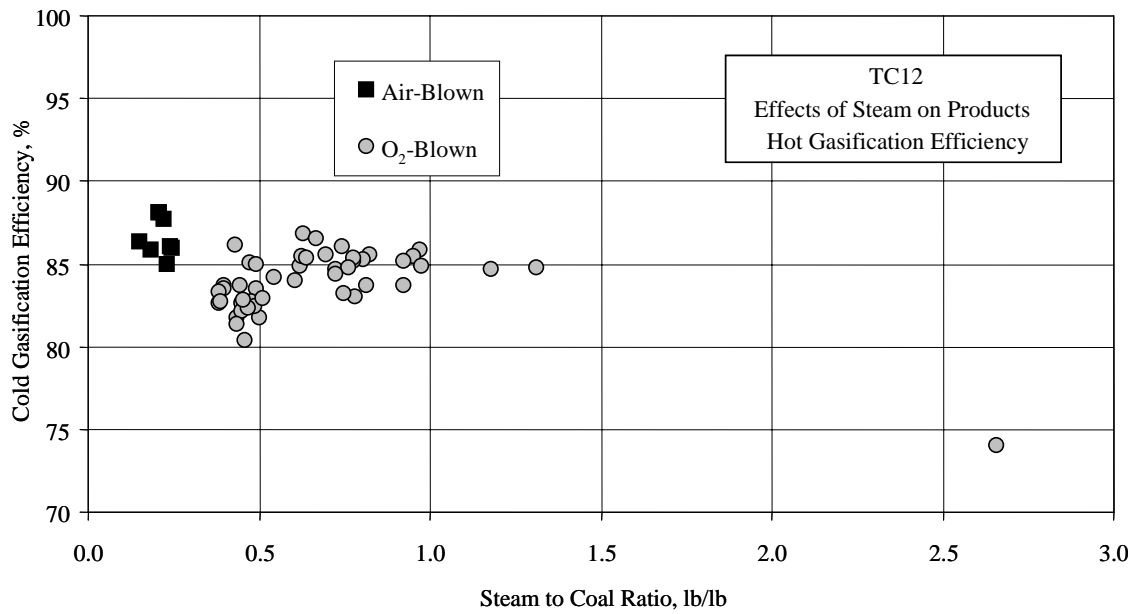Figure 3.5-28 Cold Gasification Efficiency and Steam-to-Coal Ratio
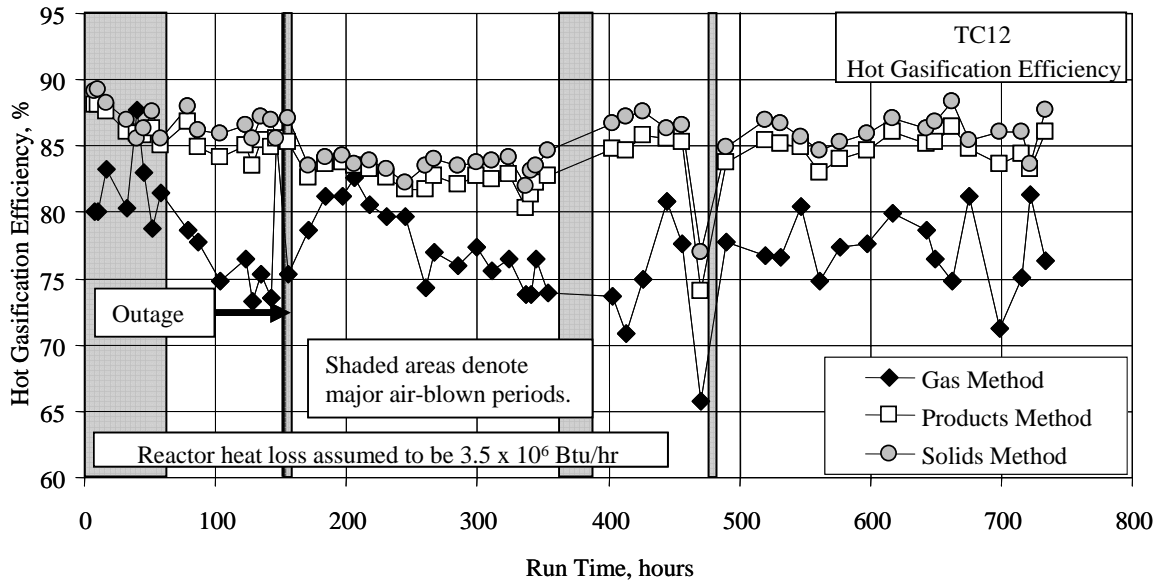
Figure 3.5-29 Hot Gasification Efficiency

Figure 3.5-30 Hot Gasification Efficiency and Steam-to-Coal Ratio
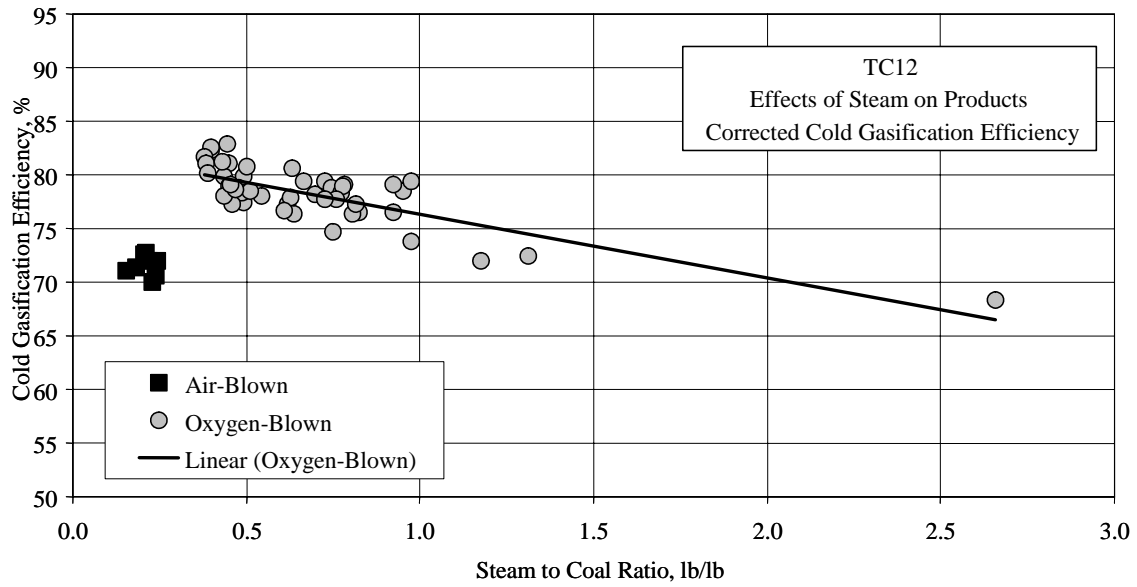
Figure 3.5-31 Nitrogen-Corrected Cold Gasification Efficiency

3.6 PROCESS GAS COOLERS

Heat transfer calculations were done on the Primary Gas Cooler (HX0202) and the Secondary Gas Cooler (HX0402) to determine if their performance had deteriorated during TC12 due to tar or other compounds depositing on the tubes.

The Primary Gas Cooler, HX0202, is between the cyclone (CY0201) and the Siemens Westinghouse PCD (FL0301). During TC12, HX0202 was not bypassed, and took the full gas flow from the Transport Gasifier. The Primary Gas Cooler is a single pass heat exchanger with hot gas from the gasifier flowing through the tubes and the shell side generating steam for the plant steam system. The pertinent equations are:

$$Q = UA\Delta T_{LM} \tag{1}$$

$$Q = c_p M(T_1 - T_2) \tag{2}$$

$$\Delta T_{LM} = \frac{(T_1 - t_2) - (T_2 - t_1)}{\ln \frac{(T_1 - t_2)}{(T_2 - t_1)}} \tag{3}$$

Q = Heat transferred, Btu/hour
U = Heat transfer coefficient, $Btu/hr/ft^2/°F$
A = Heat exchanger area, ft^2
ΔT_{LM} = Log mean temperature difference, °F
c_p = Gas heat capacity, Btu/lb/°F
M = Mass flow of gas through heat exchanger, lb/hr
T_1 = Gas inlet temperature, °F
T_2 = Gas outlet temperature, °F
$t_1 = t_2$ = Steam temperature, °F

Using equations (1) through (3) and the process data, the product of the heat transfer coefficient and the heat exchanger area (UA) can be calculated. The TC12 HX0202 UA is shown on Figure 3.6-1 as 4-hour averages, along with the design UA of 5,200 Btu/hr/°F and the pressure drop across HX0202. If HX0202 is plugging, the UA should decrease and the pressure drop should increase. The UA deterioration is a better indication of heat exchanger plugging because the pressure drop is affected by changes in flow, pressure, and temperature.

The UA was very near the design UA of 5,200 Btu/hr/°F for most of TC12. During the first few days of operation, while the gasifier was in air-blown operation, the UA was approximately 7,600 Btu/hr/°F. After transitioning to oxygen-blown operation the UA dropped to 5,300 Btu/hr/°F. For the rest of the test run, the UA varied between 4,200 and

6,200 Btu/hr/°F with an average of 5,100 Btu/hr/°F. The pressure drop across HX0202 was fairly steady during TC12. During the first part of the testing in May, the pressure drop was around 1.8 psi. After the gasifier was restarted in June, the pressure drop stayed between 0.5 and 1.2 psi for the rest of TC12.

The Secondary Gas Cooler, HX0402, is a single-pass heat exchanger with hot gas from the PCD flowing through the tubes and the shell side generating steam for the plant steam system. Some heat transfer and pressure drop calculations were done around HX0402 to determine if there was any plugging or heat exchanger performance deterioration during TC12.

Using equations (1) through (3) and the process data, the product of the heat transfer coefficient and the heat exchanger area (UA) can be calculated. The UA for TC12 testing is shown on Figure 3.6-2 as 2-hour averages, along with the design UA of 13,100 Btu/hr/°f. If HX0402 is plugging, the UA should decrease and the pressure drop should increase. Pressure drop data for HX0402 is unavailable for TC12 because of a problem with a pressure gauge.

During the air blown-operation early in TC12, the UA for HX0402 was very close to the design of 13,100 Btu/hr/°F varying from 13,000 to 14,000 Btu/hr/°F. Once the gasifier was transitioned to oxygen-blown operation, decreasing the gas flow through the gas cooler, the UA dropped below design. The UA was very steady for the remainder of the test run, varying from 9,400 to 11,700 Btu/hr/°F.
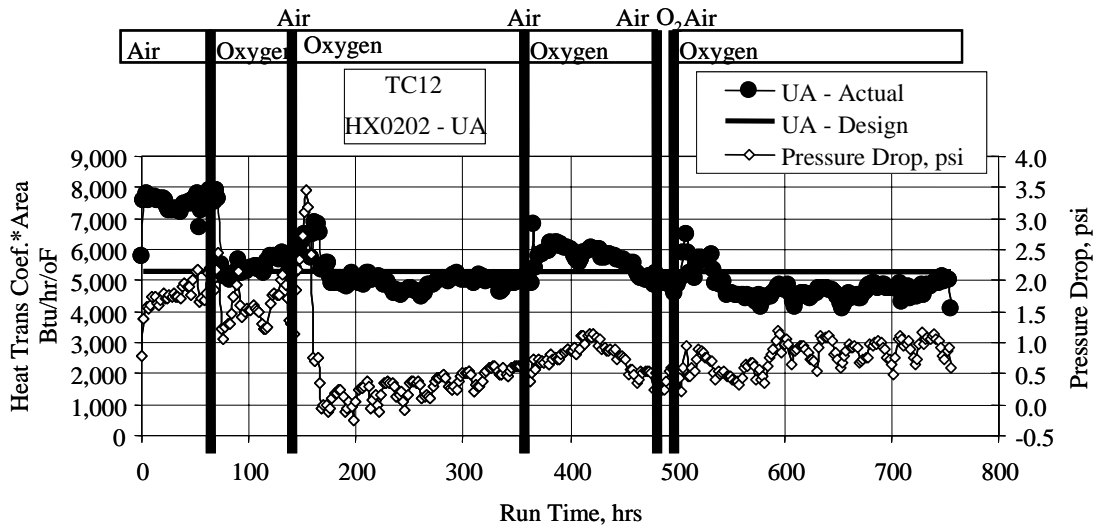
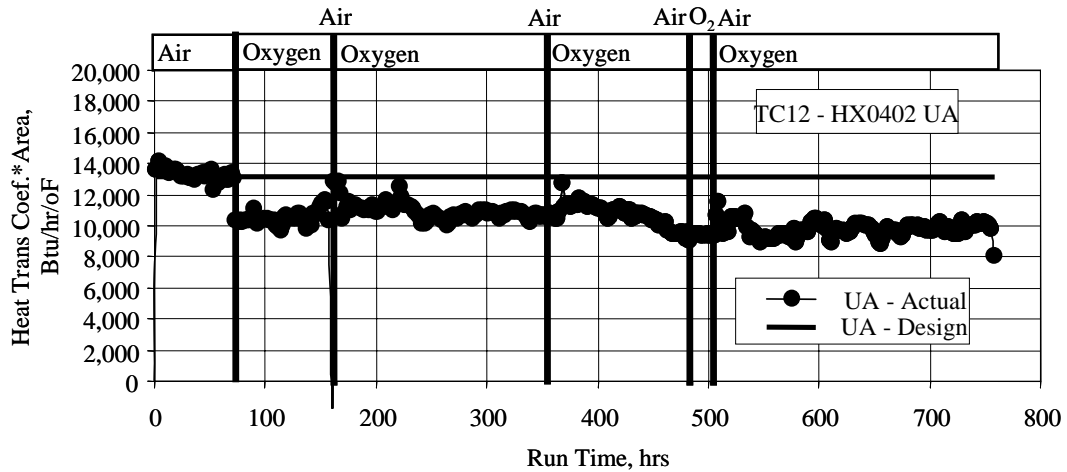Figure 3.6-1 HX0202 Heat Transfer Coefficient and Pressure Drop

Figure 3.6-2 HX0402 Heat Transfer Coefficient

4.0 PARTICLE FILTER SYSTEM

4.1 TC12 RUN OVERVIEW

TC12, a test using PRB coal with both oxygen- and air-blown gasifier operation, was characterized by stable PCD operation. Although the normalized dustcake drag was the highest observed since TC06, PCD pressure drop was well controlled, and no problems such as bridging occurred. Outlet loading samples showed excellent sealing of the filter vessel, and no filter element failures occurred. Despite occasional disturbances in system conditions, the PCD proved to be robust and reliable.

This test run consisted of two periods of operation, 159 hours on coal in May 2003 and 574 hours of on-coal operation in June and July 2003. The two portions of the run were separated by a short outage which allowed the installation of a fuel cell test skid and related equipment. During this outage, a manway inspection of the PCD revealed clean filter elements and no noticeable problems. Following the final portion of the run, a thorough inspection of the PCD internals was completed. No problems with any part of the internals were found, with the exception of ash buildup found in one of the Westinghouse inverted filter element assemblies.

Outlet loading samples were taken throughout the run. All the measurements showed outlet concentrations below the current sampling system lower limit of detection of 0.1 ppmw (except for the samples taken during solids injection tests for failsafe evaluation and outlet monitor calibration). Samples taken during failsafe testing showed good sealing with the Pall fuse in both the short- and long-term tests, while the PSDF-designed failsafe allowed a small amount of particle penetration in the short term, but sealed well in the long term.

This report contains the following sections:

- PCD Operation Report, Section 4.2—This section describes the main events and operating parameters affecting PCD operation. Operation of the fines removal system is also included in this section.

- Inspection Report, Section 4.3—The complete inspection performed following TC12 is discussed in this section including details of the post-run conditions of various PCD components and of the fines removal system.

- Gasification Ash Characteristics and PCD Performance, Section 4.4—This section includes a detailed discussion of physical and chemical properties for gasification ash (g-ash), as well as the effects of these characteristics on PCD performance. The results of PCD inlet and outlet solids concentration sampling are presented in this section.

- Failsafe Testing, Section 4.5—Results of failsafe testing completed to date are included in this section. Failsafe testing completed in TC12 included solids injection and gas exposure.

4.2 TC12 PCD OPERATION REPORT

4.2.1 Introduction

PCD operation was successful during TC12. There were no filter element failures and no g-ash bridging. In addition, outlet loading samples showed that the PCD was leak-tight. Several tests were completed during the run such as failsafe testing with solids injection and back-pulse parameter optimization testing.

Typically, the baseline pressure drop ranged from approximately 40 to 90 inH$_2$O, and the face velocity was 3.2 to 5.0 ft/min. At times these parameters were unstable due to the occasional unsteadiness of the coal-feed rate as both the FD0210 coal feeder and the newly developed FD0200 feeder were used. Because of the fairly low pressure drop, it was possible to test longer back-pulse frequencies of up to 20 minutes. Also, lower back-pulse pressures than those used in recent runs were used at different times.

The fines removal system operation was stable for the majority of the run. On one occasion, the FD0520 lock hopper system dispense vessel spheri valve seal ruptured and had to be replaced. While FD0520 was out of commission, the FD0520 bypass system was successfully used to remove solids from the PCD cone. Evaluation of newly developed resistance probes used as level indicators in the FD0520 lock vessel was begun, and the probes showed consistent readings.

Run statistics for TC12 are shown in Table 4.2-1. Layout 28, the filter element layout implemented for the run, is shown in Figure 4.2-1.

4.2.2 Test Objectives

The primary objectives for the filter system for TC12 were the following:

Failsafe Device Testing – On-line tests of the PSDF-designed failsafe and the Pall fuse were conducted, which included hot char injection into the clean side of two filters. These tests were conducted to confirm the testing completed on these failsafe devices in TC11. The effectiveness of each device was evaluated by monitoring pressure differential measurements across the filters and failsafes tested, and by SRI outlet sampling during the injections. In addition, several Ceramem ceramic failsafe devices were reinstalled for gas exposure.

Filter Element Testing – During TC12, iron aluminide filters were tested. In addition, seven of the Westinghouse inverted filter assemblies were retested.

Back-pulse Parameter Optimization – To assess the effects of back-pulse pressure on PCD and system performance, both the top plenum and bottom plenum back-pulse pressures were varied during the run, and tube sheet pressure drop as well as pressure measurements were taken at different points along the reactor train.

Inlet Particulate Sampling and Characterization – As in previous tests, in situ particulate samples were collected at the PCD inlet under various process conditions. In addition to

quantifying the inlet particulate loading, these samples were used to identify any variations in the physical properties and chemistry of the g-ash associated with various changes in operating conditions. The measured inlet particulate loadings were used in combination with PCD pressure drop data to determine the drag of the transient dustcake under various conditions. The transient dustcake drag values were compared to drag values measured in the laboratory to determine whether the pressure drop has been influenced by any outside factors other than the dustcake. Since a large effect of carbon content (carbon conversion) was observed in TC11, the properties and flow resistance of the TC12 gasification ash were examined as a function of carbon content.

Outlet Particulate Sampling and Monitoring – In situ particulate sampling and monitoring was performed throughout TC12 to document the outlet particulate loadings and the particulate collection efficiency of the PCD.

Semidirty Shutdown and Dustcake Sampling – The PCD was shut down "semidirty" to preserve the "transient" dustcake on the top plenum and the "residual" dustcake on the bottom plenum. The top plenum back-pulsing was stopped just before coal feed stopped, and the bottom plenum was back-pulsed twice after coal feed stopped. Measurements were made of the dustcake thickness and areal loading, and samples were taken of both dustcakes.

4.2.3 Observations/Events – May 15, 2003, Through July 14, 2003

Refer to Figures 4.2-2 through -11 for operating trends corresponding to the following list of events.

A.   <u>System Startup</u>. At 13:40 on May 16, 2003, back-pulsing began. The main air compressor and the start-up burner were started on May 16, 2003 at 21:30.

B.   <u>Back-Pulse Measurements</u>. During heat-up, high-speed pressure differential measurements were taken at various back-pulse pressures. These measurements are discussed further in Section 4.2.4.

C.   <u>Coal Feed Started</u>. At 16:30 on May 17, 2003, prior to coal feed, the back-pulse pressure was set at 320 psid (i.e., 320 psi above system pressure) on the top plenum and 600 psid on the bottom plenum. The back-pulse timer was set at 5 minutes and was kept at this setting for the entire first portion of TC12. Coke breeze feed was then started, and coal feed began at 18:24 on May 17, 2003.

D.   <u>Back-pulse Pressure Lowered</u>. At 16:00 on May 18, 2003, back-pulse pressure was lowered to test the effect of back-pulse pressure on baseline pressure drop. The top plenum pressure was lowered to 220 psid, and the bottom plenum pressure was lowered to 400 psid.

E.   <u>Gasifier Trip</u>. At 00:52 on May 20, 2003, an electrical problem caused a brief gasifier trip.

F.   <u>Tested FD0520 Bypass Line</u>. At 14:30 on May 20, 2003, the FD0502 screw cooler was stopped to allow solids to build up in the PCD cone so that the FD0520 bypass line could be tested. This test was repeated three other times in the run, on May 20 at 21:00,

on May 21 at 12:00, and on May 23 at 10:00. Each time, the bypass was unsuccessful due to an inadequate valve open time.

G.   Transition to Oxygen-Blown Operation. At 18:30 on May 20 system pressure was lowered so that oxygen-blown gasifier operation could begin.

H.   Coal Feeder Trip. Due to a logic conflict, the coal feeder tripped at 11:30 on May 21, but was quickly put back on line.

I.   Increased Face Velocity. The PCD pressure drop increased due to an increase in face velocity.

J.   System Shutdown. At 09:40 on May 24 the system was shutdown. This concluded the first portion of TC12.

K.   System Start-Up. TC12 was resumed in June. At 03:40 on June 19, 2003, back-pulsing was started and the system heat up progressed.

L.   Coal Feed Started. At 17:30 on June 19, 2003, prior to coal feed, the back-pulse pressure was set at 220 psid on the top plenum and 400 psid on the bottom plenum. This setting was used throughout the second portion of TC12. A 5 minute timer was used at this time, although the timer was adjusted during the run. Coke breeze feed was then started and coal feed began at 02:00 on June 20.

M.   Coal Feeder Trip. At 03:25 on June 22, the coal feeder tripped but was quickly back on line.

N.   Increased Back-Pulse Timer. The back-pulse cycle frequency was decreased to 10 minutes on June 27 at 06:00, so the peak pressure drop across the tube sheet increased. The back-pulse frequency was also varied several other times during the run to test the effect on baseline pressure drop and bridging tendency.

O.   Coal Feeder Trip and Reactor Upset. At 15:05 on June 28 the coal feeder tripped. Shortly thereafter, a reactor upset caused a heavy carryover of solids to the PCD and thermal excursions on the filter element surfaces.

P.   Increased Coal-Feed Rate. At 07:30 on June 29 the coal-feed and gas-flow rates were increased, resulting in an increased face velocity and pressure drop.

Q.   Coal Feeder Trips. A coal feeder trip occurred on July 3 at 09:00, although it was quickly back on line. Several coal feeder trips occurred during the duration of the run, but these did not result in major thermal excursions.

R.   Increased Back-Pulse Timer. The back-pulse timer was increased to 20 minutes, which caused the peak pressure drop to increase.

S.   System Shutdown. Coal feed was terminated at 23:25 on July 14 and the PCD was shutdown leaving the top plenum dustcake intact and back-pulsing the bottom plenum twice.

4.2.4 Run Summary and Analysis

Coal feed for the first portion of TC12 began on May 17, 2003, and ended on May 24, 2003. The second portion of the run began on June 19, 2003, and lasted until July 14, 2003. During both portions of the run, coal was fed from both the FD0210 and the FD0200 feeders. FD0210 was used as the primary coal feeder, and the FD0200 system was operated for short periods of time during the run. There were a few coal feeder trips, although these did not cause significant problems for PCD operation. The baseline pressure drop increased with increasing coal-feed rate, and generally showed a slight upward trend during both portions of the run. The pressure drop was fairly low and controllable throughout the run.

High-speed pressure differential measurements were taken at various back-pulse pressures during system heatup. The data were taken at 100 Hz using a local data acquisition device so that the full and rapid response to back-pulsing could be recorded and compared to the measurements taken during TC11. The pressure taps used for these recordings were located at the PCD outlet; the PCD inlet; the primary gas cooler inlet; and the crossover, riser, loop seal, and the lower mixing zone (LMZ) sections of the gasifier. Measurements were taken during a top plenum back-pulse and during a bottom plenum back-pulse. Data was first recorded during system heat-up with coke breeze feed on, and was later recorded while on coal feed. The pressure measurements taken during bottom plenum back-pulsing in both TC11 and TC12 are shown in Figure 4.2-12. From this figure, it can be seen that the location with the highest measurements relative to the other locations was at the gasifier standpipe. (This higher measurement likely resulted in part from plugging of the particular pressure tap that was used for measurement.) Other locations showed expected response, with pressure spikes from back-pulsing decreasing with distance from the PCD.

In addition to testing the pressure responses to back-pulsing, the effects of back-pulse pressure and back-pulse frequency on pressure drop were tested. In most recent runs, the back-pulse pressure had been consistently kept at 400/600 psid (400 psid on the top plenum and 600 psid on the bottom plenum), and the back-pulse timer had been kept at 5 minutes to achieve adequate cleaning and to prevent bridging. However, in an effort to optimize back-pulse parameters, the back-pulse pressures were lowered during the first portion of the run to 220/400 psid, and the resulting pressure drop across the tube sheet was monitored. During the second portion of the run, back-pulse pressure was maintained at 220/400 psid, and back-pulse cycle times of 5, 10, 15, and 20 minutes were used. Both the pressure and cycle frequency testing showed no significant increase in pressure drop and no evidence of inadequate cleaning or bridging. Therefore, lower back-pulse pressures and longer cycle times will be tested further in upcoming runs.

Table 4.2-1

TC12 Run Statistics and Steady-State Operating Parameters,
May 16, 2003, Through July 14, 2003

Start Time:	5/16/03 13:40 (for back-pulse system)
End Time:	7/14/03 23:45
Coal Type:	Powder River Basin
Hours on Coal:	Approx. 733 hrs
Number of Filter Elements:	85
Filter Element Layout No.:	28 (Figure 4.2-1)
Filtration Area:	241.4 ft2 (22.4 m2)
Pulse Valve Open Time:	0.2 sec
Pulse Time Trigger:	5 to 20 min
Pulse Pressure, Top Plenum	220-320 psi above System Pressure
Pulse Pressure, Bottom Plenum:	400-600 psi above System Pressure
Pulse dP Trigger:	275 inH$_2$O
Inlet Gas Temperature:	Approx. 600 to 800°F (315 to 425°C)
Face Velocity:	Approx. 3.2 to 5 ft/min (1.6 to 2.5 cm/sec)
Inlet Loading Concentration:	Approx. 11,600 to 30,800 ppmw
Outlet Loading Concentration:	Below detection limit of 0.1 ppmw
Baseline Pressure Drop:	Approx. 40 to 90 inH$_2$O (100 to 225 mbar)

Layout 28 (TC12)
(1.5m Filters, A=241.4 ft^2)

- Pall FEAL/Fuse (36)
- Pall FEAL (49)
- Inverted Filter Cans
- Blank (6)

— Support at Level a
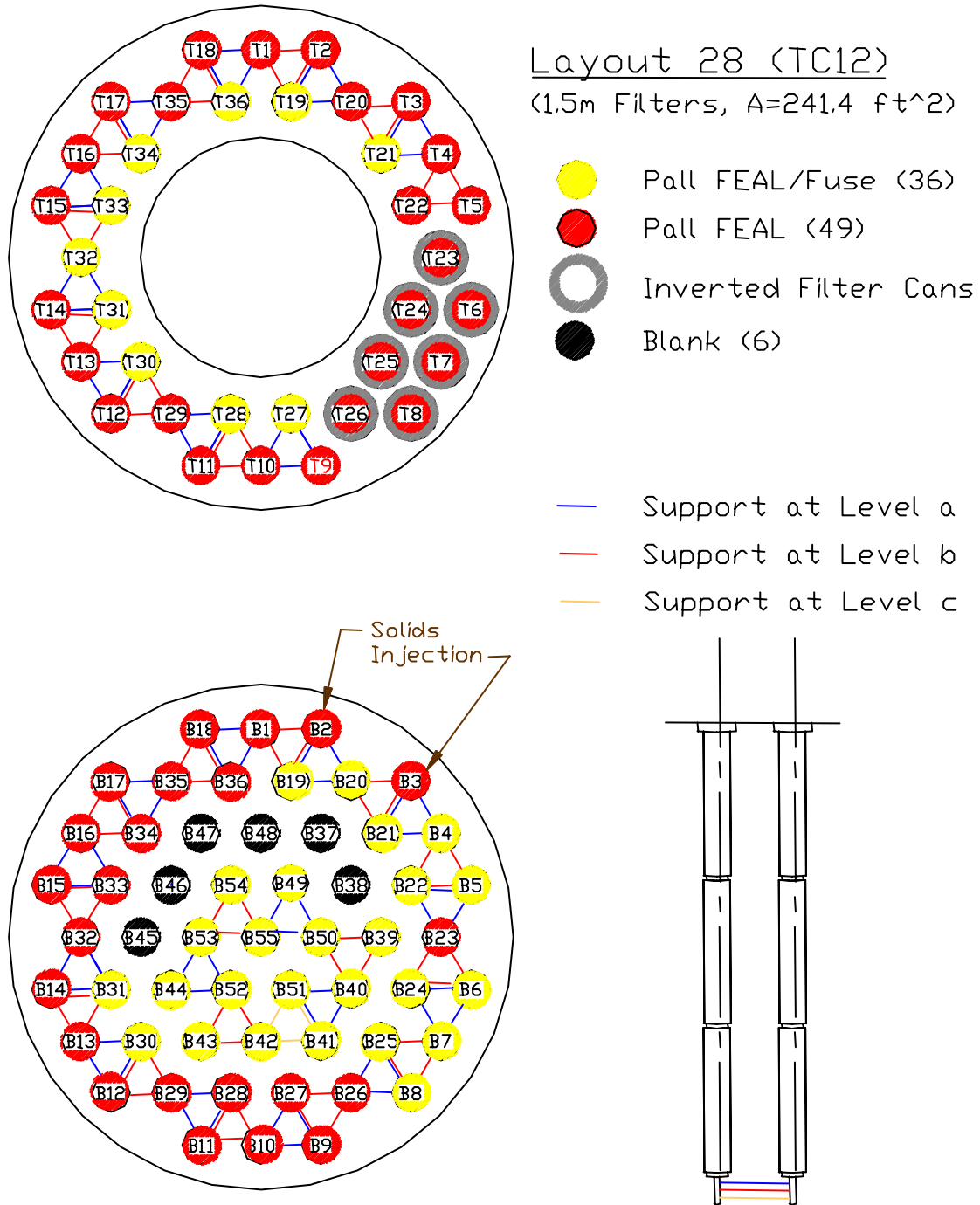— Support at Level b
— Support at Level c

Solids Injection

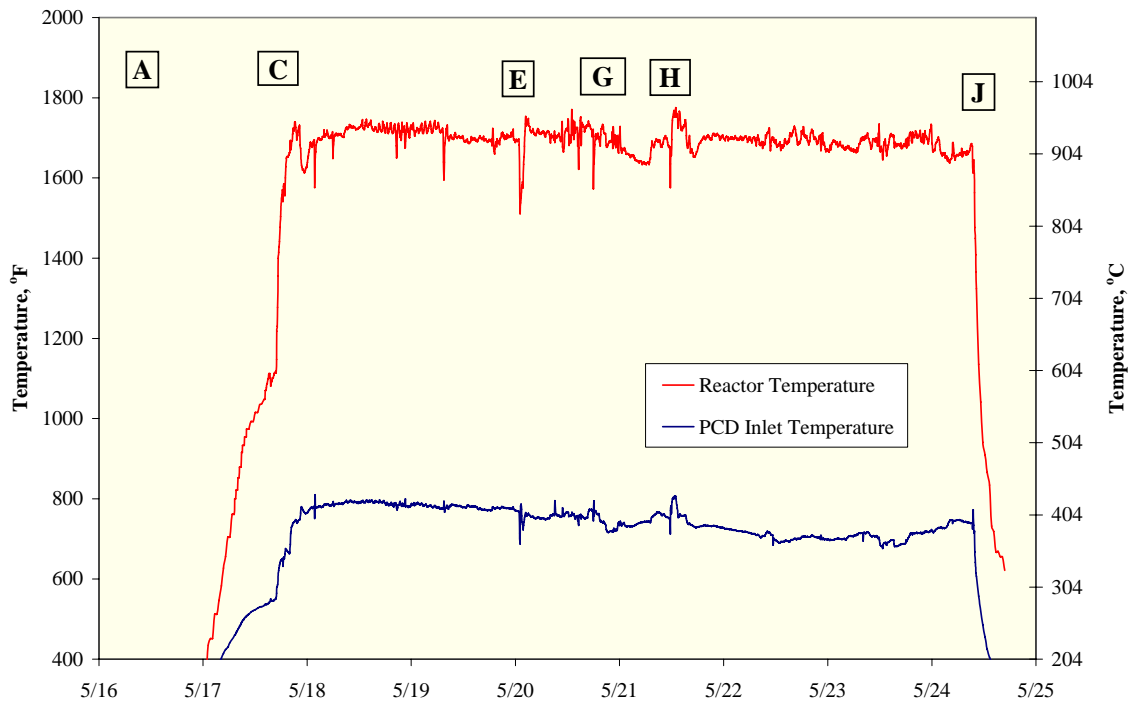Figure 4.2-1 Filter Element Layout 28

Figure 4.2-2 Reactor and PCD Temperatures, May 16, 2003, Through May 25, 2003
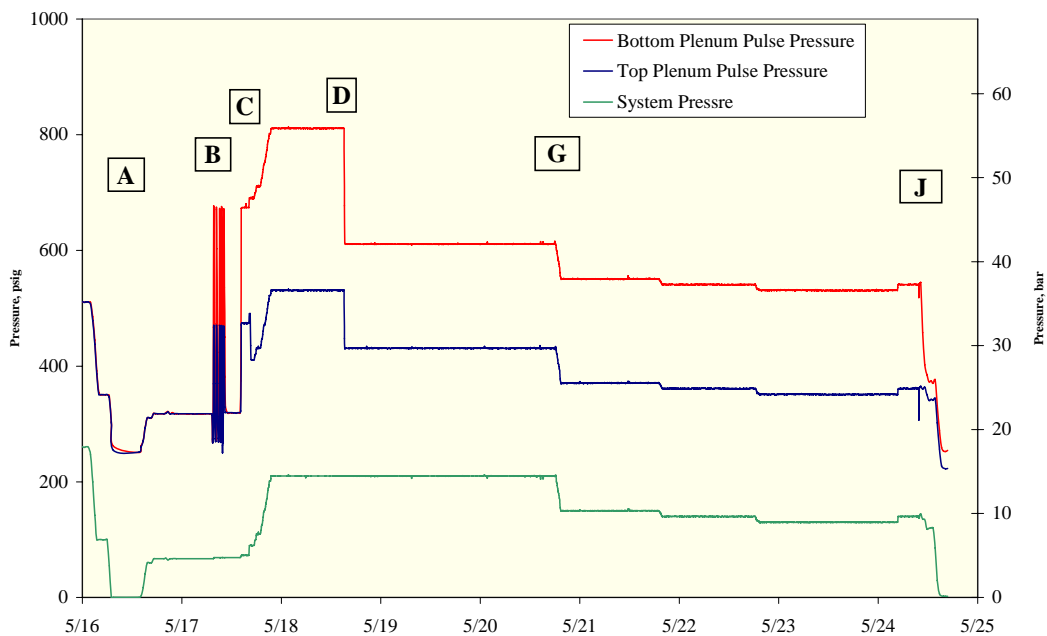

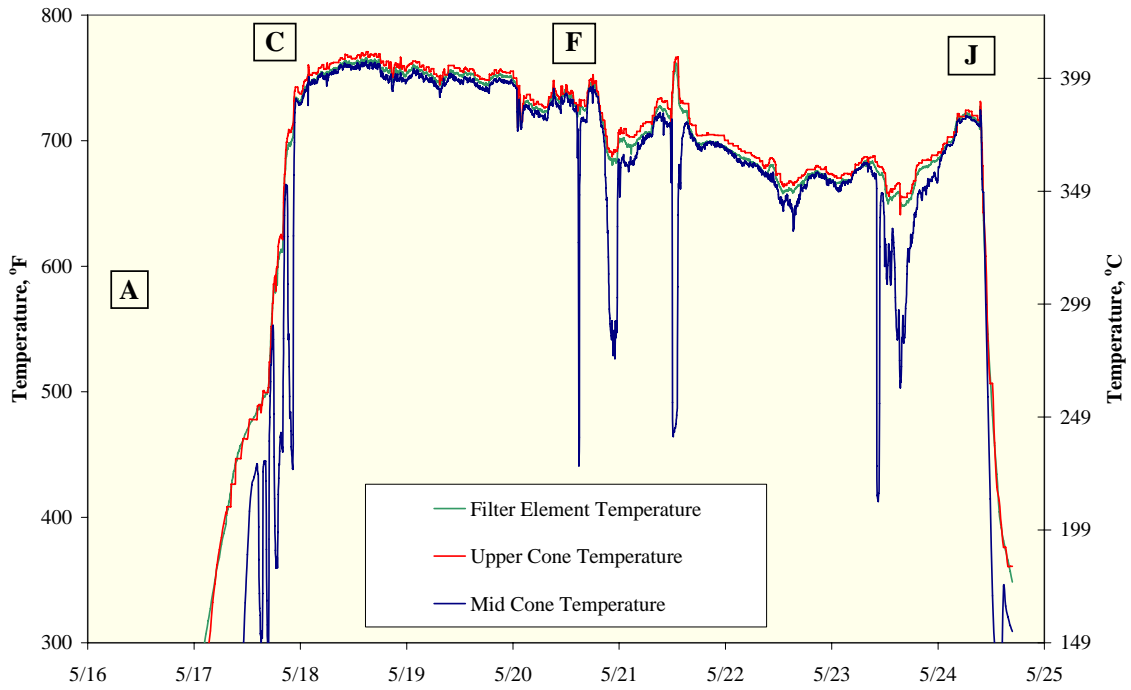Figure 4.2-3 System and Pulse Pressures, May 16, 2003, Through May 25, 2003

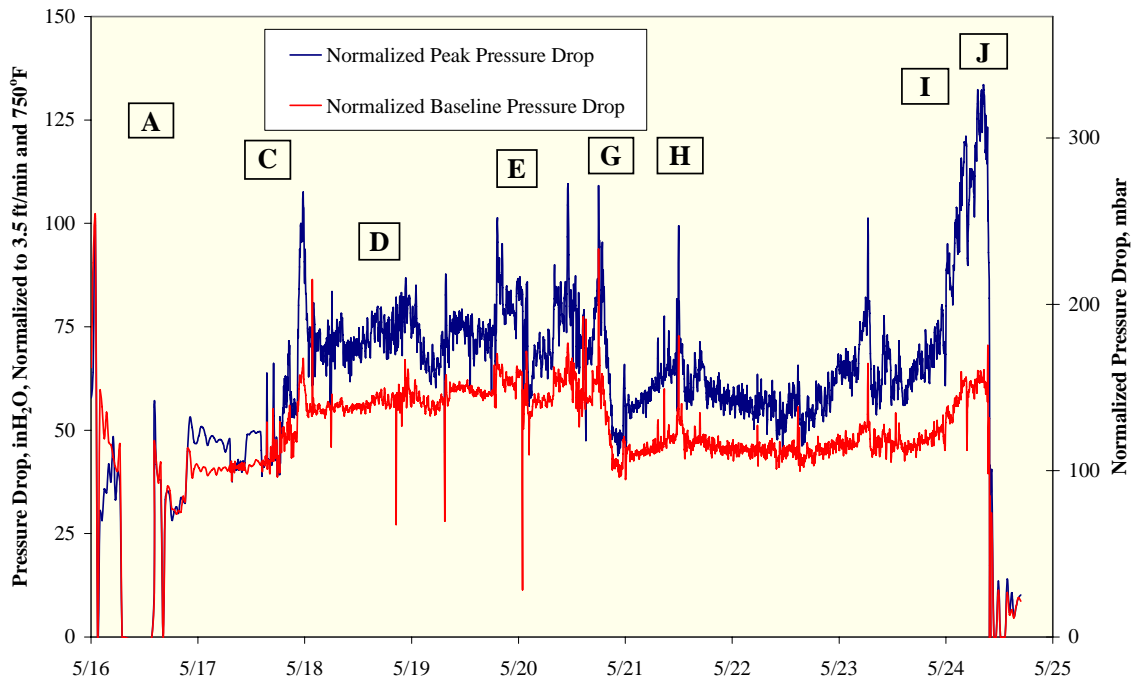Figure 4.2-4 Filter Element and Cone Temperatures, May 16, 2003, Through May 25, 2003

Figure 4.2-5 Normalized PCD Pressure Drop, May 16, 2003, Through May 25, 2003
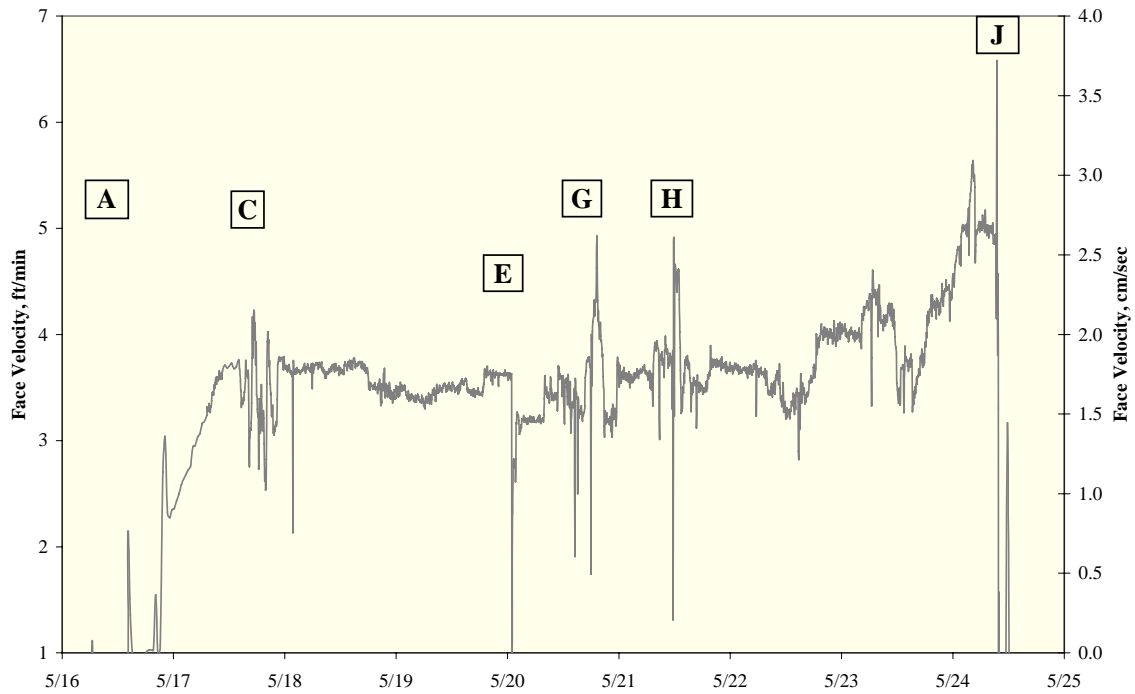
Figure 4.2-6 PCD Face Velocity, May 16, 2003, Through May 25, 2003

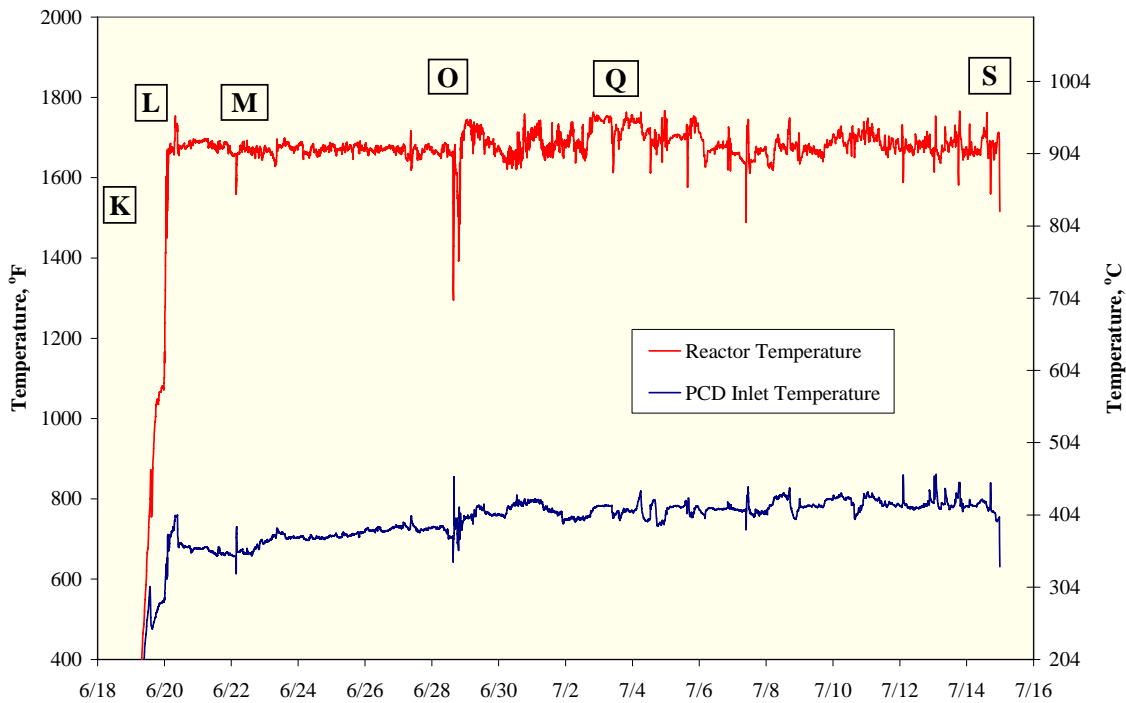Figure 4.2-7 Reactor and PCD Temperatures, June 18, 2003, Through July 16, 2003

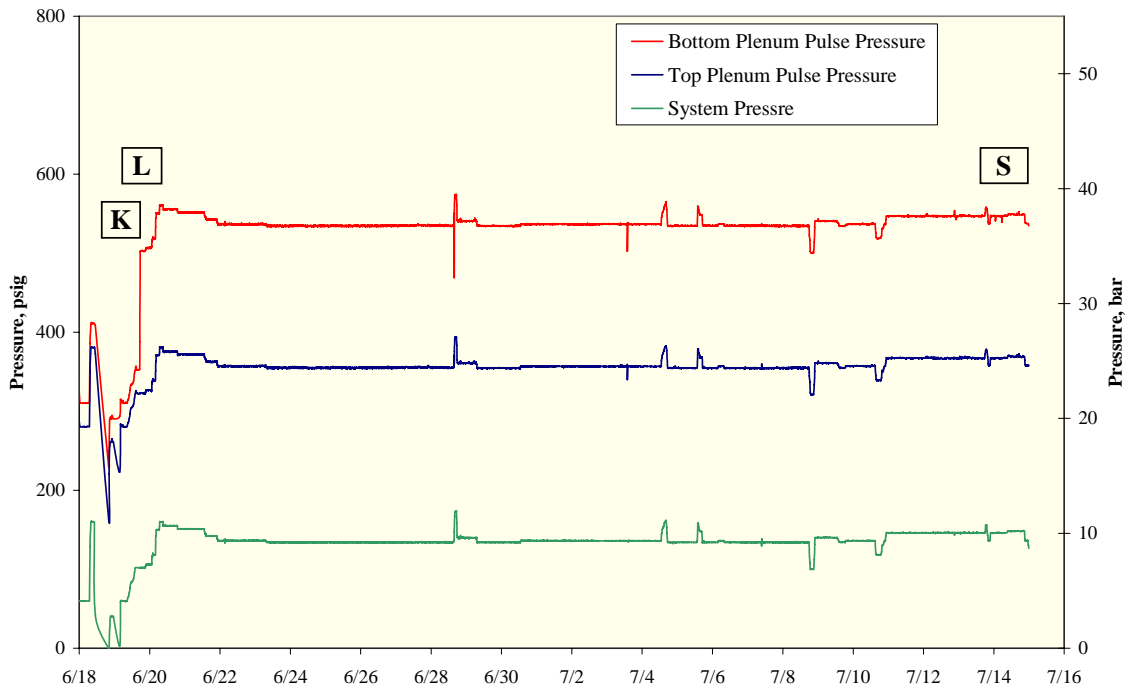Figure 4.2-8 System and Pulse Pressures, June 18, 2003, Through July 16, 2003
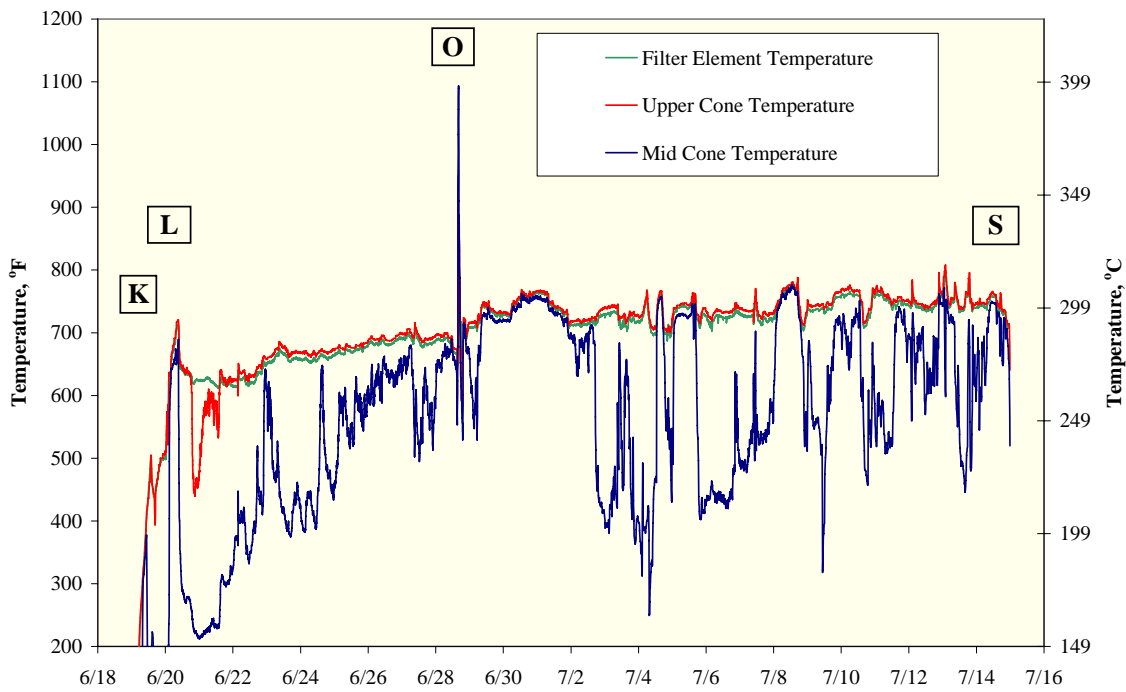

Figure 4.2-9 Filter Element and Cone Temperatures, June 18, 2003, Through July 16, 2003
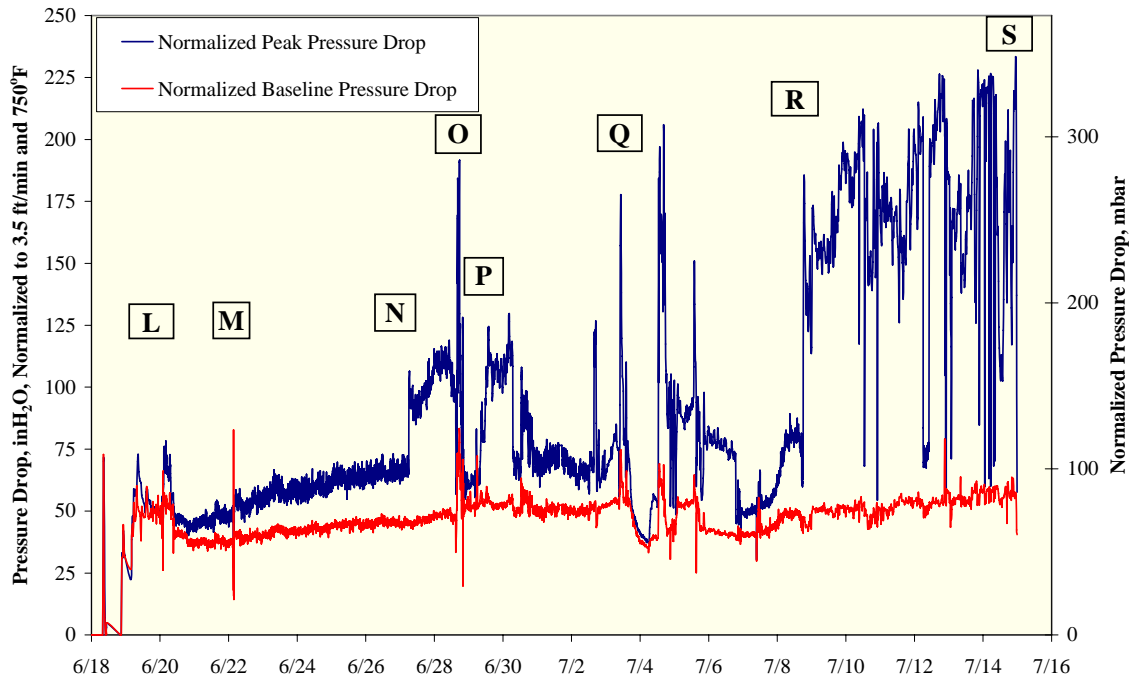
Figure 4.2-10 Normalized PCD Pressure Drop, June 18, 2003, Through July 16, 2003
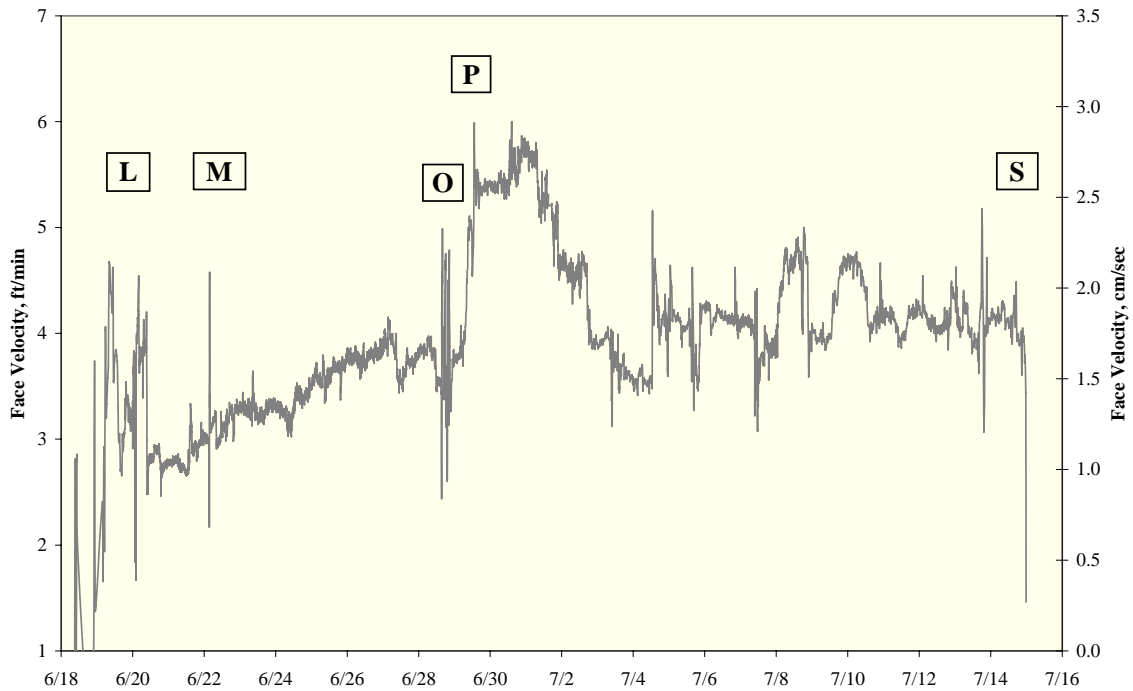

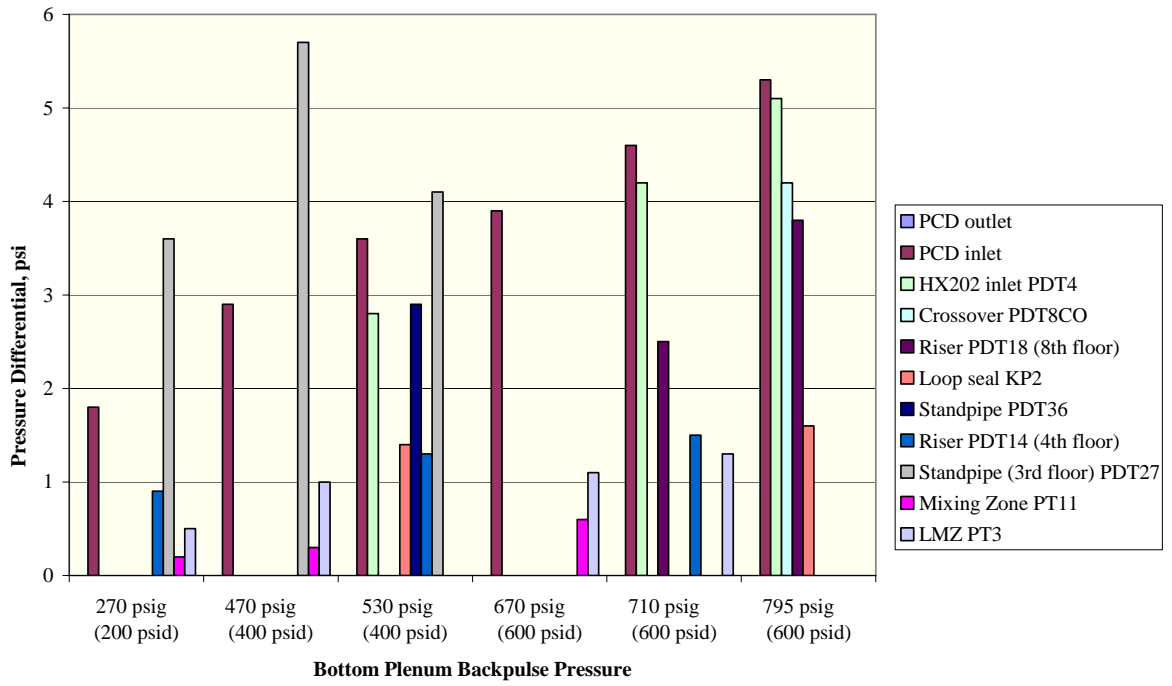Figure 4.2-11 PCD Face Velocity, June 18, 2003, Through July 16, 2003

Figure 4.2-12 Pressure Drop Response to Bottom Plenum Back-Pulse During TC11 and TC12

4.3   TC12 INSPECTION REPORT

4.3.1 Introduction

During the TC12 outage, the PCD internals were removed from the vessel and inspected. The outage inspection included examinations of the filter elements, their fixtures to the plenums, solids deposition, and auxiliary equipment. The subsequent sections will detail the findings of the inspections.

4.3.2 Filter Elements

For TC12, the following filter elements were installed (see Figure 4.2-1): 36 Pall 1.5-meter FEAL filter elements with fuses and 49 Pall 1.5-meter FEAL filter elements without fuses. During the outage between TC10 and TC11, it was discovered that the Pall Hastelloy X and HR160 filter elements leaked during back-pulsing. Until these issues with solids penetration through the filter media are resolved, only Pall FEAL filter elements will be tested in the PCD.

A total of 12 Pall FEAL filter elements were removed. Each filter element was closely inspected and no damage was noted. The welds were examined and no separation from the filter media or cracks was noticed. The Pall FEAL filter elements have accumulated many gasification hours. The following table outlines the exposure hours of the Pall FEAL filter elements that were installed before TC12.

Exposure Hours After TC12	Number of FEAL Filters Exposed
3,822	5
3,352	2
2,409	23
1,341	9
925	45
733	1

Ten of the twelve filter elements removed after TC12 were flow tested. The filter elements tested were all from the bottom plenum. Hours on these elements ranged from 925 to 3,352. Six of the elements had a fuse and four did not. All flow tests were conducted using air at ambient temperature. Loose g-ash was blown off the outside surfaces with compressed air before testing, but the filter elements were not water-washed or chemically cleaned. The results are shown in Figure 4.3-1 as a plot of pressure drops versus face velocities. At a face velocity of 3 ft/min, the pressure drop measured on elements with no fuse ranged from 7.8 to 9.1 inH_2O, and the pressure drop measured on elements with a fuse ranged from 18.9 to 24.5 inH_2O. These values are similar to those measured after previous gasification runs. All elements tested with no fuse had 925 hours. The elements tested with a fuse had from 925 to 3,352 hours, and there was no correlation between hours and pressure drop.

4.3.3 G-Ash Deposition

The plenum was pulled out of the PCD vessel on July 18, 2003. Figures 4.3-2 and -3 show the upper and lower plenum after TC12. Both figures show that there was no g-ash bridging present. The shutdown was "semidirty," which means that the top plenum was not back-pulsed after shutdown, while the bottom plenum was back-pulsed. The average residual dustcake thickness was ~ 0.01 in. The residual dustcake thickness was consistent with other measurements made after other gasification runs. The transient dustcake thickness on the top plenum varied between 0.06 to 0.09 in. The inspection revealed that the g-ash buildup on the filter element holders, upper and lower ash shed, and filter element support brackets was not very significant. The thin residual and transient dustcake on the filter elements and the small buildup on the different PCD internals indicate that tar condensation was not a problem during TC12.

4.3.4   Failsafes

During TC12, the following failsafe devices were tested (See Figure 4.3-4):

- Forty-seven PSDF-designed failsafes.
- Thirty-five Pall fuses.
- Three SWPC ceramic failsafes.

In addition to these failsafe devices, six metal fiber failsafe devices designed by SWPC were installed above blanks. These were installed solely for gas exposure of the metal alloys, as the design itself has proven to be inadequate for stopping solids penetration in the event of filter failure. These failsafe devices were not removed during this outage. During TC12 two failsafe devices, PSDF-design and Pall fuse, were tested using online g-ash injection to measure the collection efficiency. The results of this test are reported in Section 4.5.

After TC12, three PSDF-designed failsafes were removed for inspection. The failsafe devices appeared to be in good condition with no damage. One of the test objectives for the PSDF-designed failsafe is to determine whether or not the porous material blinds over time. Each failsafe device removed was flow tested. Figures 4.3-5 through -7 show the results of the flow tests for each failsafe tested. The table below outlines the total exposure hours for each failsafe device that was tested and its corresponding ratio-of-flow coefficients. The ratio-of-flow coefficients in the table below are determined by taking the flow coefficient after TC12 and dividing it by the flow coefficient before TC12.

Failsafe ID	Total Exposure Hours	Ratio-of-Flow Coefficients
PSDF #12	1,649	1.11
PSDF #10	1,649	1.05
PSDF #39	733	0.90

The table shows that there was not any significant change in flow coefficients that would indicate pore blinding due to corrosion. PSDF-designed failsafe #39 lost some of its original flow coefficient, while PSDF-designed failsafe #12 and #10 regained some of their flow coefficient. This trend has been reported in past run reports (See TC10 and TC11 run reports) where failsafe devices initially lose some of their original flow coefficient while failsafe devices with longer exposure time maintain or regain some of their flow coefficient. It is believed that the recovery of flow coefficient is due to some of the solids being dislodged during back-pulsing.

During the outage, all three second-generation CeraMem ceramic failsafe devices were removed. Each failsafe device was visually inspected and flow tested. No damage was noted on any of the failsafes during the inspection. The post-TC12 flow coefficients for the three failsafe devices were between 97.8 and 99.3 percent of the values measured when the failsafe devices were new. The ceramic failsafe devices were installed for about 930 hours of gasification operation during TC11 and TC12.

4.3.5   Auxiliary Equipment

During TC12, seven prototype inverted filter element assemblies supplied by SWPC were installed in the PCD and tested. Figure 4.2-1 shows their position on the top plenum. These inverted filter assemblies have been tested since TC08. During the post-test inspection after each run, no indication of dust leakage or bridging was noted. Since these initial test results were positive, it was decided to continue testing the inverted design for TC12. Figure 4.3-8 shows the inverted filter element assemblies after TC12. The inspection during TC12 revealed a small amount of g-ash buildup about 3 inches down from the top on one of the inverted filter elements. The other six filters did not have any excess material or damage to the assemblies. Therefore, further testing will continue during TC13.

Twelve resistance probes (these probes were described in TC08 Run Report) were tested during TC12. All 12 resistance probes failed (shorted internally) during the test. One of the resistance probes (II0305G) was removed for inspection. When the ceramic insulator was removed, one of the thermocouple wires was found to be corroded. Figure 4.3-9 shows a side view of the thermocouple wire where it emerges from the sheath. Figure 4.3-10 shows an end view of the thermocouple wire. Figure 4.3-10 clearly shows that a corrosion product has permeated the MgO insulation out to about twice the original diameter of the wire and is almost touching the sheath. Undoubtedly the corrosion product was touching the sheath before the thermocouple was filed off. Corrosion of the thermocouple wire is the same failure mode that caused the failure of the resistance probes during TC11. The failure of the resistance probes appears to be related to the exposure time. The following table outlines the approximate syngas exposure time before failure.

Exposure Hours	Number of Probes to Fail
0 – 400	0
400 – 500	9
500 – 600	7
600 – 700	1
700 – 800	1

The table includes probes that failed during TC11 and TC12. Initially, it was thought that the failures during TC11 were due to something in the syngas produced by lignite gasification. However, it appears that the probe failures were due to gas exposure time. As a result of these findings, 500 ft of special mineral-insulated cable has been ordered to make new probes to replace the current failed probes.

The back-pulse pipes were removed and inspected during this outage. There was no significant damage noted on the pulse pipes. The inner liner appeared to be in good condition with no damage noted (See Figure 4.3-11). In the past some pitting has been noted on the back-pulse pipe near the flange. The pitting did not appear any worse than after the last outage. Figure 4.3-12 shows a thin layer of condensed tar on the pipe, which has been a concern from a corrosion perspective. The back-pulse pipe is inserted through a flange on top of the PCD vessel. The pipe has to go through a layer of insulation, which results in a temperature profile along the length of the pipe. As expected, tars condensed along the length of the back-pulse pipe as the temperature decreased. However, it does not appear that these tars are detrimental to the back-pulse pipes. These pipes have been exposed to over 3,000 hours of on-coal gasification operation without any significant signs of corrosion.

4.3.6   Fine Solid Removal System

The screw cooler (FD0502) performed well during TC12. This is based on the fact that during 733 hours of on-coal operation it did not fail. Other than minor packing adjustments, FD0502 did not require any attention from maintenance during operation. Before TC07 several modifications were made to the drive-end stuffing box to increase reliability. These modifications were documented in the TC07 run report. Since the modifications improved the performance during TC07, it was decided to implement the same changes to the nondrive end before TC08. The screw cooler has performed well ever since the modifications were applied. The current modifications have accumulated 2,012 hours on the nondrive end, while the drive end has accumulated 2,307 hours without failure.

One of the methods that have been used to determine the success of the new stuffing box modifications is tracking the packing follower gap. The packing follower is used to compress the shaft seal rings to prevent process gas from leaking. Once there is no more room to compress the follower, it is time to replace the seals. The packing follower gaps for both the drive and nondrive end are recorded in the table below:

Run	Drive-End Gap, Inches	Nondrive-End Gap, Inches
Before TC12	9/16	1 7/16
After TC12	9/16	1 5/16

The table above shows that there was only minor packing adjustment required during TC12. The difference in the drive-end packing follower gap was not significant. Also, the table shows that there is still plenty of room for compression. Therefore, it was decided not to disassemble FD0502 during this outage in order to accumulate operating experience with the new modifications.

The fine solids depressurization system (FD0520) performed well during TC12 with one exception, the lower spheri valve seal failed. Around the same time the seal in FD0520 failed, the coal feeder failed; therefore, it was decided to feed coke breeze to the reactor while FD0210 and FD0520 were being repaired.

During this time, the new solids bypass line was tested. The solids bypass line is a pipe that runs between FD0502 and FD0530, while bypassing FD0520. The purpose of this line is to remove solids from the cone of the PCD in the case of emergency (i.e., FD0520 online repair). The bypass line uses the process head pressure to force solids out the PCD to FD0530. The bypass line utilizes two Everlasting valves and one ball valve for isolation between the process and FD0530.

Since the bypass line was operated many times during TC12, it was thoroughly inspected for pipe and valve erosion. All the sealing surfaces on the Everlasting valves were in good condition. There were no significant signs of damage on the isolation ball valve. Finally, the conveying pipe was in good condition.

Before TC12, an Everlasting Rotating Disc valve was installed above the current spheri valve on the lock vessel. The spheri valve seal has been the source of failure that has resulted in many process shutdowns despite all efforts to increase its performance. Therefore, the decision was made to find a more reliable and robust valve for this high-temperature, high-pressure environment.

The Everlasting Rotating Disc valve was chosen because of its robust design. The Everlasting valve has a self-lapping metal-to-metal seat design that promotes repeated tight shutoff. According to the vendor, this unique sealing design should improve with use. Figure 4.3-13 shows the internals of the Everlasting Rotating Disc valve. The sealing surface of the disc is always in contact with the valve seat. The valve disc stays in contact with the sealing surface through a force exerted by coiled springs. The spring compensates for thermal expansion by allowing the disc to move vertically. Also, the force exerted by the spring prevents solids from lodging between the sealing surfaces. The rotation of the metal disc on the metal seat polishes the metal seat with each cycle; thereby, promoting a tighter seal with each cycle.

The Everlasting valve was installed as the primary valve for TC12, while the spheri valve was left in service only as a backup. The Everlasting valve cycled a total of 10,299 times during TC12 without failure. One of the objectives in testing the Everlasting valve was to determine whether or not solids would accumulate and pack in the valve body (See Figures 4.3-13 and -14). The Everlasting valve was inspected by using a borescope, and there was no sign of solids packing within the valve body. The initial results on the Everlasting valve look promising. Future testing with the Everlasting valve will continue in order to accumulate long-term experience.

During the outage, both vent valves (XV8539A and XV8539B) on the lock-vessel were inspected. Both ball valves appeared to be in good condition. Figures 4.3-15 and -16 show the ball surface of each valve after TC12. The figures show both valves were in good condition. Therefore, each valve was reinstalled for use in TC13.
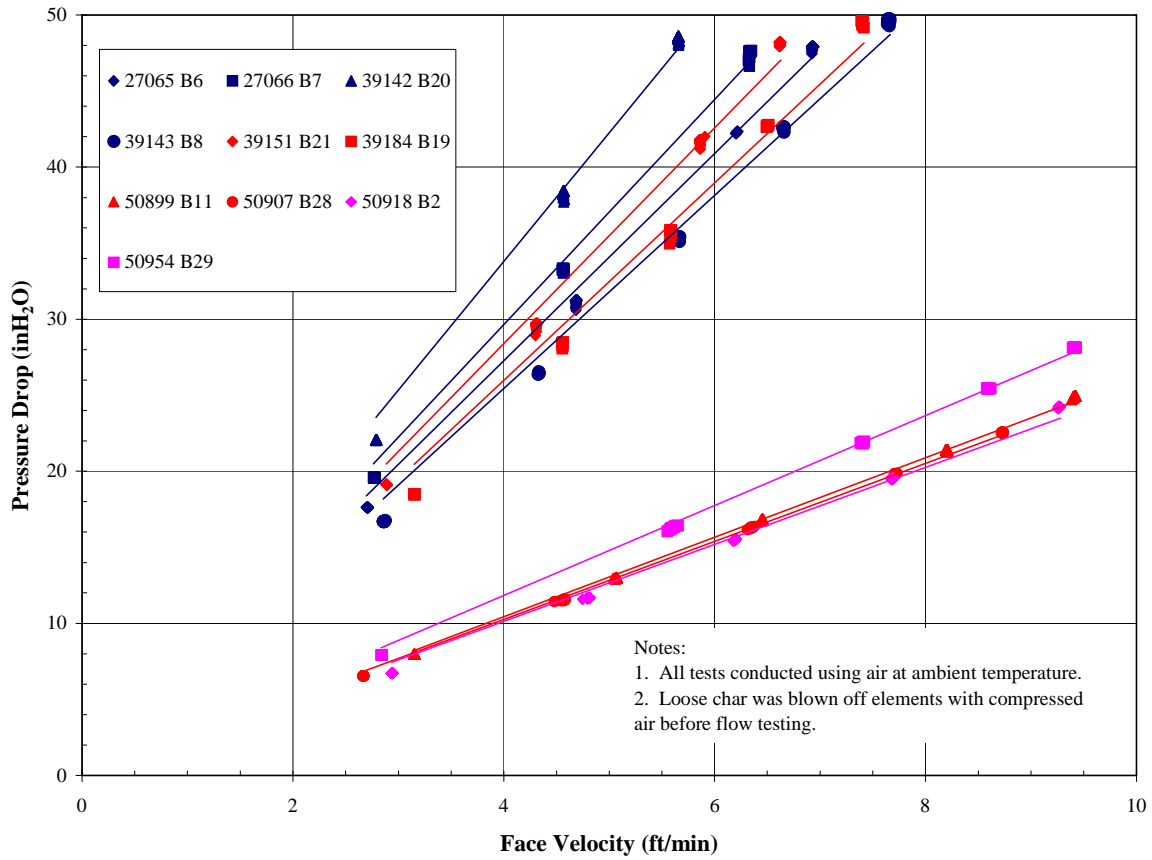
Figure 4.3-1 Pressure Drop Versus Face Velocity for Pall FEAL Elements After TC12

Figure 4.3-2 Top Plenum After TC12

Figure 4.3-3 Bottom Plenum After TC12
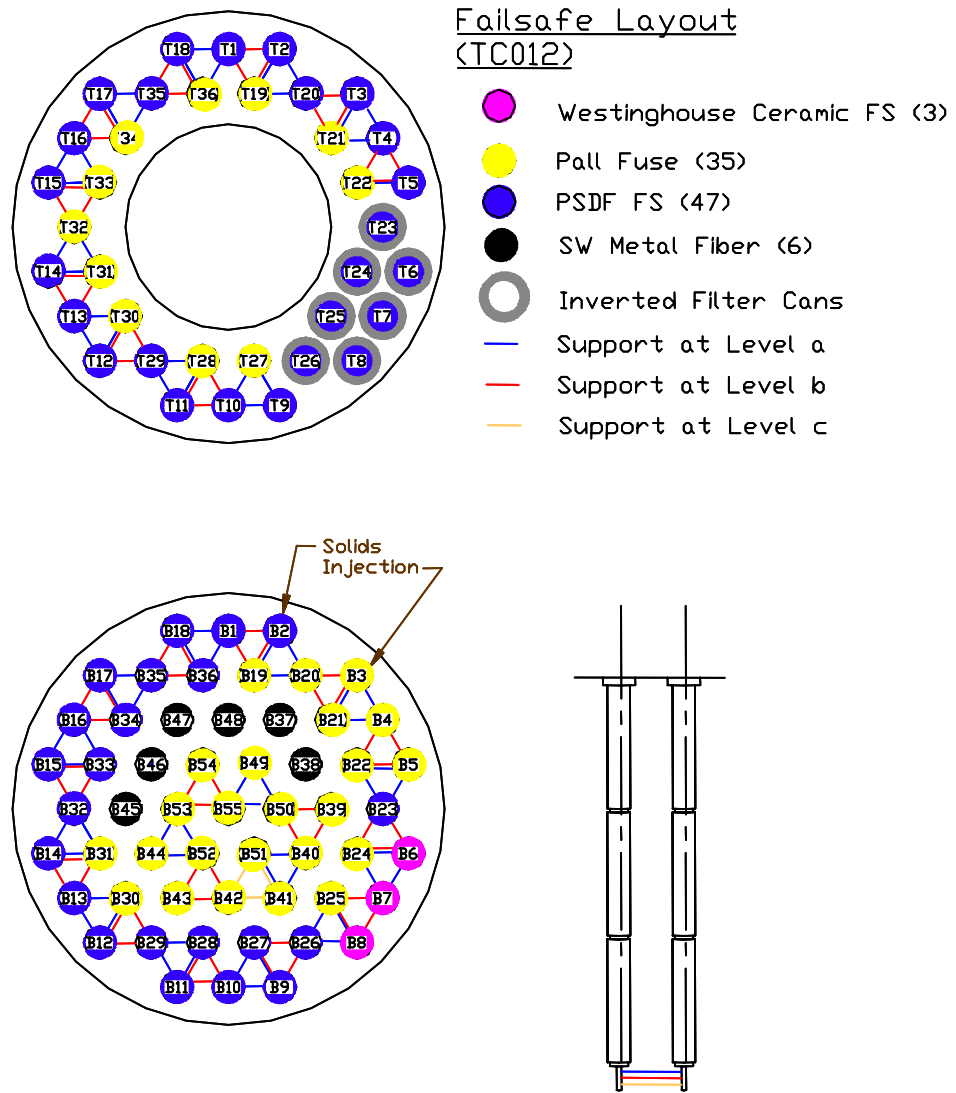
Figure 4.3-4 Failsafe Layout for TC12
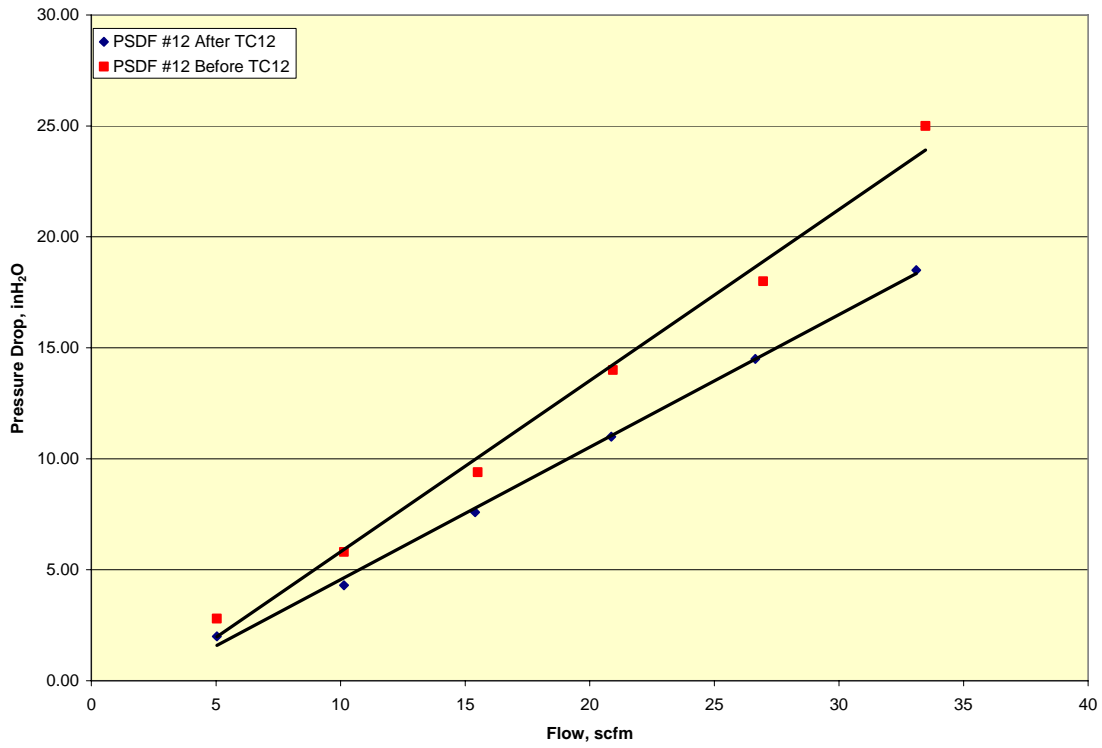
Figure 4.3-5 Flow Curve for PSDF-Designed Failsafe #12 Before and After TC12
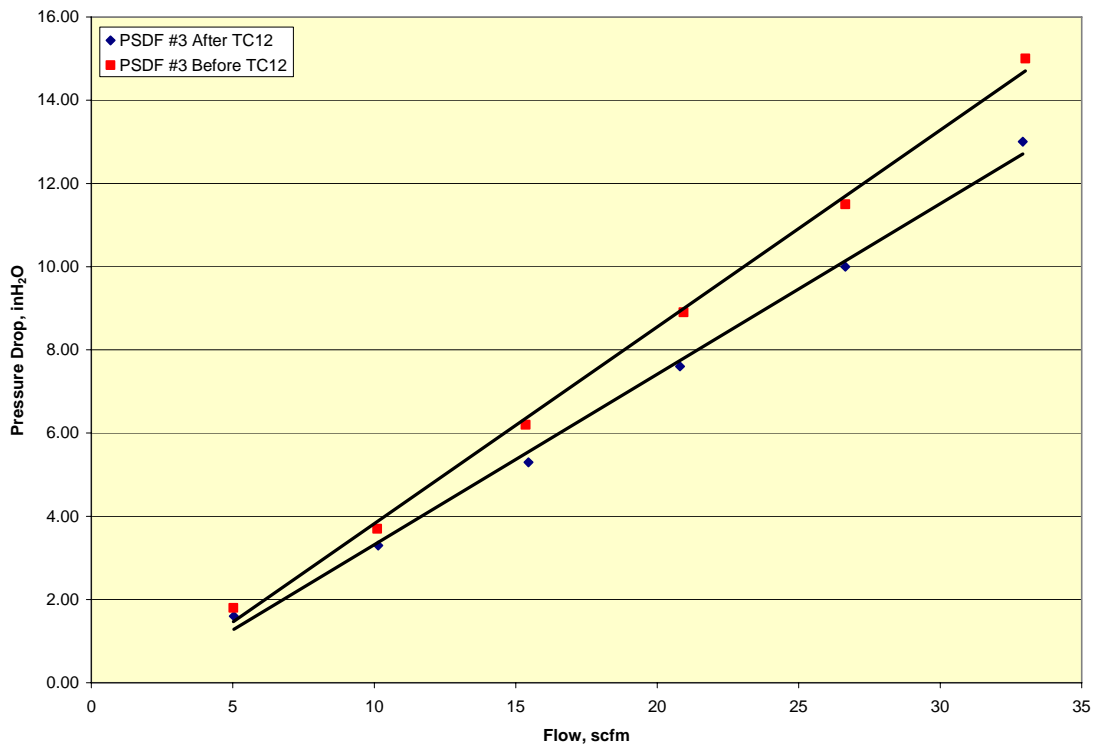
Figure 4.3-6 Flow Curve for PSDF-Designed Failsafe #3 Before and After TC12
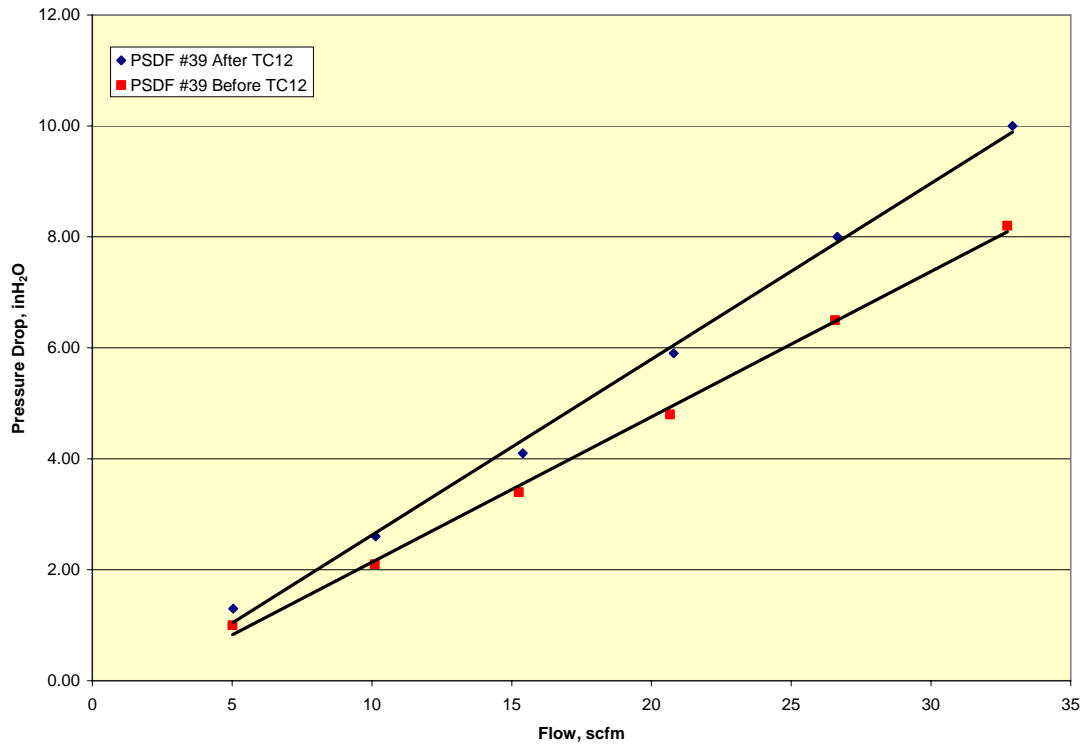
Figure 4.3-7 Flow Curve for PSDF-Designed Failsafe #39 Before and After TC12
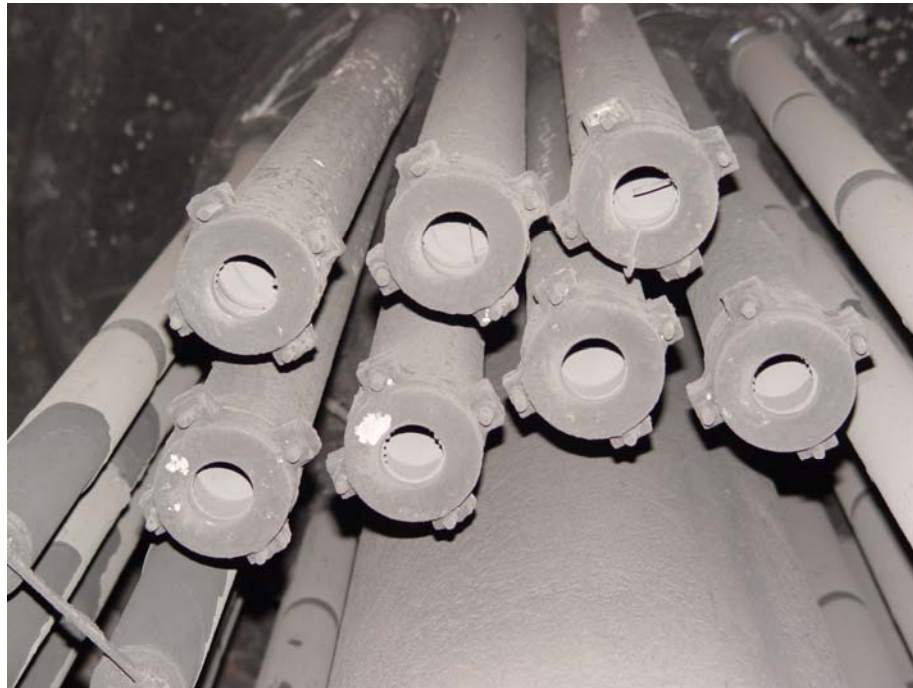
Figure 4.3-8 Inverted Candle Assemblies After TC12

Figure 4.3-9 Corroded Resistance Probe After TC12
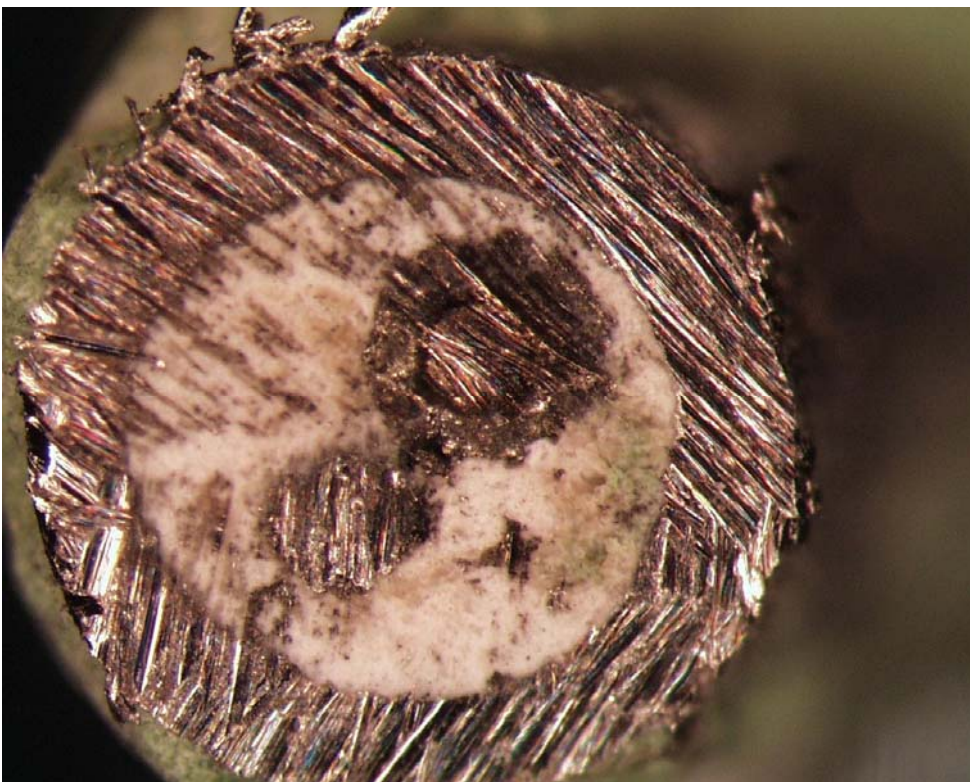
Figure 4.3-10 End View of Resistance Probe After TC12

Figure 4.3-11 Back-Pulse Pipe Inner Liner After TC12

Figure 4.3-12 Back-Pulse Pipe After TC12

Figure 4.3-13 Everlasting Valve Rotating Disc Valve
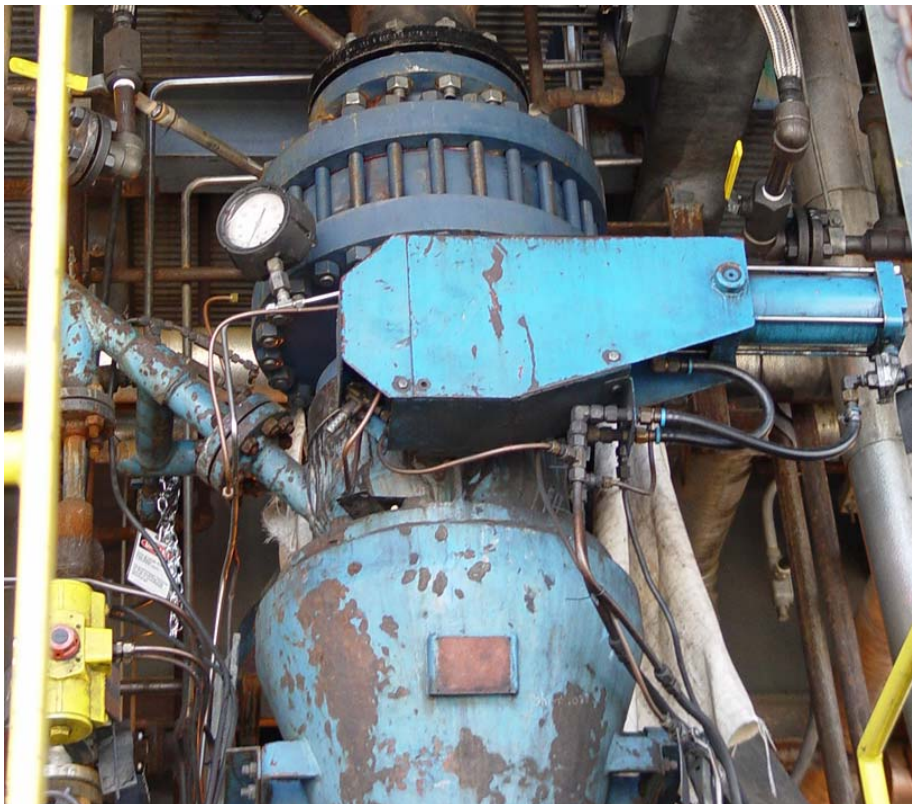
Figure 4.3-14 Everlasting Valve Above FD0520 Lock Vessel Before TC12
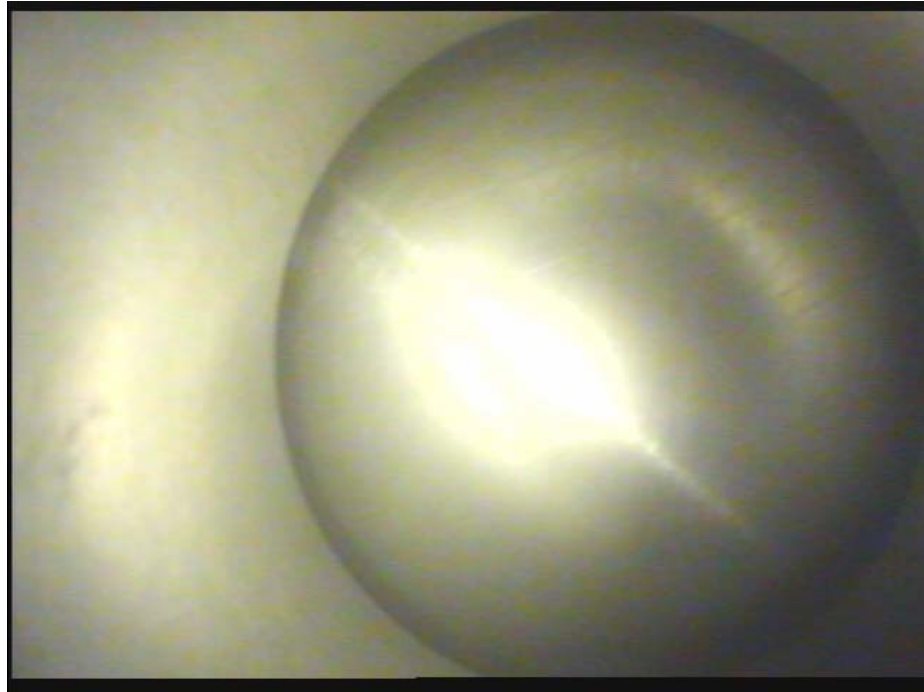
Figure 4.3-15   XV8539A After TC12
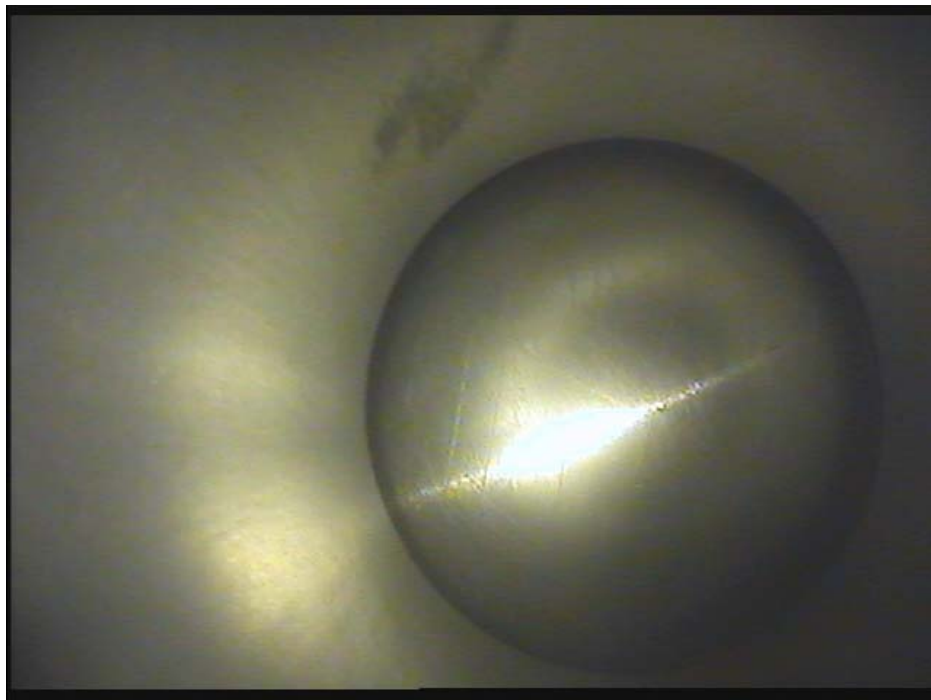
Figure 4.3-16 XV8539B After TC12

4.4 TC12 GASIFICATION ASH CHARACTERISTICS AND PCD PERFORMANCE

This section addresses the characteristics of the gasification ash (g-ash) produced in TC12 and relates the g-ash characteristics to the performance of the PCD. Of particular interest in TC12 were the potential changes in g-ash characteristics and PCD performance associated with changes in coal-feed rate, addition of limestone for supplemental sulfur capture, and addition of a nickel oxide (NiO) catalyst for ammonia decomposition. The latter effect had not been examined previously, since TC12 was the first run where the NiO catalyst was tested.

Prior to TC12, an effect of carbon conversion on particulate properties and drag had been observed with the Falkirk lignite in TC11. The TC11 drag measurements showed that the drag increased with increasing carbon content. Since the effect of carbon content on drag had not been noted in previous runs with PRB coal, it was suspected that the effect might be limited to the Falkirk lignite or, perhaps, to lignites in general. To determine whether the effect also occurred with PRB coal, the PCD transient drag values determined for each TC12 in situ sampling run were plotted as a function of the carbon content of the in situ sample. As discussed below, this investigation showed that the transient drag increased as the carbon content of the g-ash increased. Laboratory drag measurements showed the same trend in samples collected from the PCD hopper. As in TC11, it was also noted that the specific-surface area of the g-ash increased with increasing carbon content. This trend was true for both the in situ samples and the PCD hopper samples used for the laboratory drag measurements.

In addition to the effect of carbon conversion, the drag measurements showed that drag was reduced by the addition of limestone. This effect was seen in both the calculated values of PCD transient drag and in the laboratory drag measurements. The remainder of this section examines how the solids carried over to the PCD are influenced by limestone addition, coal-feed rate, carbon conversion, and injection of the NiO catalyst. In addition to the effect on the rate of solids carryover, we examine the effects on the particle-size distribution, physical properties, and chemical composition of the solids. To the extent possible, the physical characteristics and chemical composition of the TC12 g-ash are related to the PCD transient drag to allow a better understanding of the effects on PCD performance. The properties and drag of the TC12 g-ash are also compared to those of other g-ash from previous runs to provide insight into how the effects vary with different types of coal.

4.4.1 In situ Sampling

During the air-blown portion of TC12, SRI performed four in situ particulate sampling runs at the PCD inlet and three runs at the PCD outlet. Two of the four inlet runs were performed with limestone addition to the gasifier, and two runs were done without limestone addition. During the oxygen-blown portion, 19 inlet runs and 19 outlet runs were conducted. Three of the oxygen-blown runs were done with limestone addition, and the other 16 runs were done without any addition of limestone to the gasifier. Two of the oxygen-blown runs were performed during the injection of a proprietary nickel oxide- (NiO) based catalyst that was being tested to crack ammonia. The results of the inlet and outlet sampling are discussed in the next two sections (Sections 4.4.1.1 and 4.4.1.2 respectively).

4.4.1.1 PCD Inlet Particle Mass Concentrations

Particle mass concentrations and mass rates measured at the PCD inlet are given in Table 4.4-1, and the particulate mass rate is plotted as a function of coal-feed rate in Figure 4.4-1. The plot of particulate mass rate versus coal-feed rate shows that, in the absence of other effects, there is no difference between concentrations produced during the air and oxygen operation. However, it is clear from the figure that the addition of limestone increased the inlet particle concentration, as did, to a lesser extent, nickel oxide (NiO) injection. During air-blown operation without limestone addition, the particulate mass concentration varied from 12,500 to 13,400 ppmw, corresponding to mass rates of 293 to 307 lb/hr. When limestone was added the concentration increased to 17,400 to 18,100 ppmw or 393 to 415 lb/hr.

As expected, the particle concentrations measured at the PCD inlet were higher during oxygen-blown operation because of the reduced gas mass-flow rate produced for the same coal-feed rate. Also, as expected, the particle mass rates were approximately the same for the two conditions. In the absence of limestone addition or NiO injection, the particle concentrations varied from 14,300 to 21,800 ppmw corresponding to mass rates of 169 to 354 lb/hr. With limestone addition, the particle concentrations varied from 29,500 to 30,800 ppmw corresponding to mass rates of 421 to 499 lb/hr. The wider range of values with oxygen operation was caused by a wider range of operating conditions than were encountered during the short air operating period. As expected, the addition of limestone and NiO increased the inlet loadings and mass rates. The NiO powder was mixed in ratios of 1:3 to 1:5 with fine sand, so only a fraction of the increase in inlet loading was attributable to actual NiO material. The contribution of the NiO material to the solids carryover is discussed in more detail in Section 4.4.5.1.

4.4.1.2 PCD Outlet Particle Mass Concentrations

Particle concentrations measured at the PCD outlet are included in Table 4.4-1 and compared to other test programs in Figure 4.4-2. The data show that, except for periods when dust was injected for failsafe leakage tests or for PCME particle monitor testing, the particle concentration never exceeded the lower resolution limit of the measurement system (0.1 ppmw). No significant levels of particle penetration through the filters, contamination of samples with large foreign particles, or tar contamination occurred for the entire test program. In this regard, this was one of the most successful tests since the start of gasification.

4.4.1.3 Failsafe Leakage Tests

Failsafe leakage tests were performed on both a Pall FEAL fuse and the PSDF-designed failsafe utilizing a Pall HR-160 Dynalloy filter. The results of these tests are shown in Table 4.4-1. However, these results will not be discussed further here because a detailed discussion of these tests can be found in Section 4.5.

4.4.1.4 Syngas Moisture Content

Also included in Table 4.4-1 are the syngas moisture measurements made in conjunction with the particulate sampling runs at the PCD outlet. The measurements yielded moisture values in

the range of 8.9 to 10.4 percent by volume during air-blown operation and 14.2 to 38.8 percent by volume during oxygen-blown operation. The syngas moisture content is normally higher during oxygen-blown operation because higher rates of steam addition are required to cool the lower mixing zone.

4.4.1.5   Real-Time Particle Monitoring

The PCME DustAlert-90 particulate monitor was operational and apparently functioning throughout TC12. As expected, the PCME did not respond during the failsafe injection tests as the concentrations at the PCD outlet were below the instrument's lower resolution limit. The PCME did exhibit a few episodes of elevated readings that did not correspond to a known particle emission, but these were short in duration. In general, the instrument performed well during TC12.

To evaluate the response of the PCME, one test was conducted with g-ash injection directly into the outlet duct. The PCME did detect these particles and returned an average value of 2.8 percent during the 1-hour test. The in situ sampling system measured an average particle concentration of 8.2 ppmw (Outlet Run No. 20) over the same period. The result of this test is compared to previous results in Figure 4.4-3. The solid line on the graph is a linear regression to PCME output vs particle concentration results from TC06 and TC07, both of which appeared to fit to the same line. The dashed lines are the 95-percent prediction interval to the regression (there is a 95 percent probability that any new data points that fit the regression will fall inside these lines.) The data point for TC12 falls outside the 95-percent interval and lies about a factor of 3 on the x-axis from the regression line. That is, we would have expected about a 3 times higher output from the PCME for the measured dust concentration. Subsequent inspection and evaluation did not reveal any obvious problem with the PCME. This type of test will be repeated in subsequent test programs to determine if the TC12 point is simply an outlier or if the calibration curve has indeed shifted.

4.4.2 Particle-Size Analysis of In situ Particulate Samples and PCD Hopper Samples

As in previous tests, a Microtrac X-100 particle-size analyzer was used to measure the particle-size distributions of the in-situ particulate samples collected at the PCD inlet and the PCD hopper samples used for the laboratory drag measurements. The results for these two types of samples are discussed separately in the next two sections (Sections 4.4.2.1 and 4.4.2.2).

4.4.2.1   In situ Particulate Samples

Figure 4.4-4 shows differential mass particle-size distributions measured on the PCD inlet in situ samples. Five data sets are compared on the graph, air-blown both with and without limestone addition, likewise oxygen-blown with and without limestone, and oxygen-blown operation with NiO addition. From this graph it appears that the distributions have a similar shape, but some of the samples contain more mass than others. As expected, oxygen-blown operation produced higher mass concentration across the distribution than did air-blown gasification. Addition of limestone increased the particles in all size ranges for both operating conditions as did injection of NiO.

To examine the differences in particle-size distribution without the influence of any differences in the total particulate loading, the size distributions must be compared on the basis of percentage mass rather than mass concentration. Figure 4.4-5 shows a comparison of the average particle-size distributions on the basis of percentage mass for the five groups identified. This presentation indicates that there are only minor differences in the relative size distributions of the particles exiting the Transport Gasifier. This is not surprising since the particle-size distribution exiting the Transport Gasifier is largely controlled by the cyclones in the recycle loop.

4.4.2.2   PCD Hopper Samples

Figure 4.4-6 compares one of the in situ size distributions from the previous graph with the three hopper composite samples used for the RAPTOR drag measurements. Although there are some minor differences in the very largest portion of the distributions, these particles generally do not end up in the RAPTOR sample and thus do not affect the results. Therefore, from these data it appears that the hopper samples chosen are representative of the TC12 dust.

4.4.3 Measurement and Sampling of PCD Dustcakes

TC12 was concluded with a semidirty shutdown of the PCD. After the coal feed was terminated, the top plenum was not subsequently pulsed, and the bottom plenum was pulsed twice. Experience from previous runs suggests that this procedure usually does a good job of preserving the entire (transient-plus-residual) cake on the top plenum, while leaving only the residual cake on the bottom plenum. The post-run PCD inspection confirmed that the semidirty shutdown performed at the end of TC12 was fairly successful. The transient cake appeared to be preserved on about 90 to 95 percent of the top plenum surface area. On the bottom plenum, only the residual cake appeared to be present on much of the filtering surface area. However, some transient cake remained on some of the bottom plenum filters, suggesting that the pulse cleaning was not completely effective in removing all of the transient cake.

The transient dustcake on the outer row of the top plenum filters contained an elevated ridge running along the length of the candle. The elevated ridge appeared to be the result of particle impaction associated with the impingement of high-velocity tangential gas flow between the shroud and the outer row of filters. This phenomenon was noted previously in combustion-mode testing, but this was the first time it was observed in a gasification test. To avoid any potential bias from this effect, the ridge area was avoided in making measurements of dustcake thickness and areal loading and in the collection of dustcake samples.

Table 4.4-2 summarizes the dustcake thicknesses and areal loadings measured on selected filters in the top plenum and in the bottom plenum. The table also includes the approximate percentage of the filter surface area that was covered with transient cake. On the selected top plenum filters, the thickness and areal loading measurements were restricted to areas that contained the entire dustcake. On the selected bottom plenum filters, the thickness measurements were made in areas that contained the entire dustcake and in other areas that contained only the residual cake. In the selected areas that contained the entire cake, measurements were also made of the dustcake areal loading. The residual cake was too thin to make accurate areal loading measurements of the residual dustcake alone.

The transient cake was not as thick as expected based on the solids discharge rate from the PCD. This may indicate that the areas chosen for the measurements were not representative, or it could be that the transient cake on the top plenum was thinner than the transient cake on the bottom plenum. Despite the lower-than-expected measurements of thickness and areal loading, the porosity values calculated from these parameters appear to be consistent with previous measurements. This probably indicates that the dustcake samples and measurements are reasonably representative in terms of physical characteristics.

Since all of the filter elements installed in TC12 were Pall FEAL, the data in Table 4.4-2 are organized by the type of failsafe installed above the filter element, since it is plausible that the cake thickness and areal loading may be influenced by the flow resistance of the failsafe. On the bottom plenum, both the residual and transient cake seem to be thicker on the filters with the Pall fuse. This may indicate that the high flow resistance of the Pall fuse somewhat restricts back-pulse flow to the filter installed below it. Flow tests of the dirty failsafes confirmed that the Pall failsafes had the highest flow resistance, much higher than that of the SWPC ceramic failsafe and the PSDF-designed failsafe.

Table 4.4-3 compares the average residual cake thickness measured after TC12 with the average cake thicknesses measured after earlier runs. These values suggest that the average cake thickness from all of the runs since TC06 has consistently been about 0.01 in. The consistency of the residual cake thickness suggests that it is relatively insensitive to coal type and to the characteristics of the g-ash.

Although the residual cake thickness seems to be relatively independent of coal type and g-ash characteristics, previous results have suggested that the residual cake thickness may be related to the type of filter element on which the cake is collected. After TC10, for example, it was noted that the residual cake seemed to be thicker on HR-160 and Hastelloy-X elements than it was on FEAL elements (see TC10 Run Report, Section 4.4-2). In the TC10 Run Report, we pointed out that dirty HR-160 and Hastelloy-X elements have higher flow resistance than dirty FEAL elements. Because of this difference in flow resistance, the HR-160 and Hastelloy-X elements may not be cleaned as effectively as the FEAL elements, resulting in a thicker cake on the HR-160 and Hastelloy-X elements. Since only FEAL filter elements were installed, these differences could not be investigated in TC12.

In addition to the effect of filter element type, it seems reasonable that back-pulse intensity may also have an effect on the residual cake thickness. Hopefully, it will be possible to assess this effect in the future by the use of lower back-pulse pressures.

4.4.4 Physical Properties of In situ Samples, Hopper Samples, and Residual Dustcake

This section describes the physical properties of the in situ samples collected during TC12, the PCD hopper samples used for the laboratory drag measurements, and the dustcake samples collected after TC12.

4.4.4.1　In situ Particulate Samples

Table 4.4-4 summarizes the physical properties of the TC12 in situ samples collected at the PCD inlet and the PCD hopper samples that were used for the laboratory drag measurements. As indicated in the table, the first four in situ samples were collected under air-blown conditions, and the remaining 19 in situ samples were collected under oxygen-blown conditions. Two of the four air-blown samples were collected with limestone addition, and the other two runs were done without limestone. Only 3 out of the 19 oxygen-blown runs were done during limestone addition as indicated in the table. Two of the oxygen-blown in situ samples were collected during injection of the NiO-based catalyst as part of an ammonia-cracking experiment. The following table summarizes the ranges of physical properties obtained with the two types of oxidant, with and without limestone addition, and with and without nickel oxide injection. (Run number 17 data were considered to be an outlier and therefore were excluded from the following ranges/averages.)

Oxidant	Air		Oxygen		
Limestone	No	Yes	Yes	No	No
Nickel Oxide	No	No	No	No	Yes
Bulk density, g/cc	0.33-0.34	0.37	0.36-0.43	0.22-0.29	0.23-0.25
Skeletal Particle Density, g/cc	2.42-2.53	2.49-2.50	2.48-2.72	2.14-2.52	2.34-2.43
Uncompacted Bulk Porosity, %	86.0-87.0	85.1-85.2	84.2-85.5	87.9-90.8	89.7-90.2
Specific-Surface Area, m^2/g	121-138	101-131	81-120	128-198	160-202
Mass-Median Diameter, μm	14.8-17.9	14.0-15.0	16.1-17.9	12.8-19.1	11.6-19.3
Non-Carbonate Carbon, wt %	21.7-25.0	21.7-22.5	14.8-24.5	28.2-43.5	27.5-37.6

Comparing the properties of the g-ash produced under air- and oxygen-blown conditions (without any addition of limestone or nickel oxide), it is apparent that the material from the oxygen-blown tests has lower bulk density, higher bulk porosity, and higher surface area. This difference is probably attributable to the difference in carbon content (22 to 25 wt percent for air-blown and 28 to 44 wt percent for oxygen-blown). An increase in carbon content should produce a decrease in bulk density and an increase in bulk porosity and surface area. In previous tests, we concluded that the choice of oxidant did not affect the particulate properties, but those tests did not show such a large difference in carbon content between the air- and oxygen-blown tests.

Comparing the g-ash produced with and without limestone addition, the effect of the limestone can be seen in terms of a higher bulk density and lower bulk porosity. This effect is not surprising, since calcined limestone or lime has a true particle density of 3.3 g/cc, which is considerably higher than the particle density of carbon (~ 1.8 to 2.1 g/cc) or ash (~ 2.5 g/cc). The effect of the limestone addition on surface area is unclear. There is no apparent effect in the air-blown case. Under oxygen-blown conditions, the surface area appears to be lower when limestone was added, but this difference may be attributable to the lower carbon content.

The following table compares the average properties of the TC12 in situ samples with those from other PSDF gasification tests using PRB coal.

	TC12	TC10	TC08	TC07-D	TC06
Bulk Density, g/cc	0.29	0.27	0.25	0.32	0.29
Skeletal Particle Density, g/cc	2.40	2.25	2.37	2.47	2.45
Uncompacted Bulk Porosity, %	87.8	88.0	89.5	87.0	88.2
Specific-Surface Area, m^2/g	149	146	222	170	222
Mass-Median Diameter, μm	16.1	12.3	18.7	16.9	15.3
Non-Carbonate Carbon, wt %	30.8	37.3	43.3	28.4	36.0

As shown above, the average physical properties of the TC12 g-ash fall within the range of average properties from previous gasification runs with PRB coal. TC08 and TC10 have the lowest average bulk densities, and these runs also have the highest average carbon content. As mentioned previously, bulk density should decrease with increasing carbon content. The higher (noncarbonate) carbon content in TC08 and TC10 is in part because there was no limestone added during those runs.

4.4.4.2. PCD Hopper Samples Used for Drag Measurements

Three PCD hopper samples were selected for laboratory drag measurements. All of the selected hopper samples were taken from the oxygen-blown portion of the run, because the oxygen-blown portion represented most of the run. Previous drag measurements have not shown any difference between g-ash produced from the same coal under air- and oxygen-blown conditions.

The three selected hopper samples included two samples taken with limestone addition and one sample collected without limestone addition. As with the in situ samples, the effects of the limestone addition can be seen in the higher bulk densities, lower bulk porosities, and lower surface areas of the two samples collected during limestone. The effects of the limestone addition on drag are discussed in Section 4.4.6.

4.4.4.3. Residual Dustcake Samples

As mentioned previously, TC12 was concluded with a semidirty shutdown of the PCD. Under ideal conditions, the semidirty shutdown would preserve both the transient and residual dustcakes on the top plenum and only the residual cake on the bottom plenum. However, after TC12 there were some areas of the top plenum where only residual cake was present and some areas of the bottom plenum where both transient and residual cakes were present. The transient cake on the top plenum contained an elevated ridge running along the length of the filter element. The ridge was apparently formed by the inertial impaction of particles from the tangential gas flow between the shroud and the outer row of filter elements. Separate samples were removed from the ridge and from the trailing edge (approximately 180 degrees from the

ridge) at the same elevation to quantify any differences in particle size that might confirm that the ridge was indeed formed by inertial impaction.

From the bottom plenum, samples were taken of both the thick (transient + residual) cake and the thin (presumably residual) cake. In both cases these were bulk samples that were taken from a number of different elements to get enough material for physical and chemical analysis. From the top plenum, only the thick (transient + residual) cake was sampled, with separate samples being collected of the ridge and trailing edge. The physical properties of these samples are summarized in Table 4.4-5, and they show interesting differences between the top and bottom plenums. Compared to either the thick or thin cakes from the bottom plenum, the thick cake from the top plenum has a lower bulk density, lower true (skeletal particle) density, higher bulk porosity, higher surface area, and smaller mean particle size. As discussed in Section 4.4.5.3, the cause of these differences appears to be much higher carbon content in the thick cake from the top plenum. As mentioned earlier, higher carbon content would result in lower bulk density, higher porosity, and higher surface area.

Comparison of the thick and thin cakes from the bottom plenum suggests that the residual cake has a finer particle-size distribution than does the transient cake. This difference in particle size has been seen after other runs and may partly explain the other differences between the thick and thin cakes. As seen in comparing the thick cakes from the top and bottom plenums, the differences between the residual and transient cakes may also be related to differences in chemical composition. Unfortunately, it was not possible to investigate this possibility, because the amount of residual cake collected was not adequate for chemical analysis.

As seen in previous runs, the TC12 dustcake characteristics suggest that the residual cake is enriched in fine particles. In previous reports we have proposed a mechanism for the fine-particle enrichment. In this mechanism, fine particles are liberated from the dustcake during back-pulsing and are then preferentially reentrained and recollected back into the residual cake. The larger particles are too massive to be reentrained and recollected, so they drop into the PCD hopper. Over time, this mechanism would produce a gradual enrichment of fine particles in the residual cake.

The table below compares the TC12 dustcake properties to the average properties of the TC12 in situ samples with and without limestone addition.

	Bottom Residual	Bottom Transient	Top Transient	In Situ No LS	In Situ with LS
Bulk Density, g/cc	0.29	0.37	0.21	0.26	0.38
Skeletal Particle Density, g/cc	2.27	2.35	2.03	2.34	2.56
Uncompacted Bulk Porosity, %	87.2	84.3	89.7	88.9	85.1
Specific-Surface Area, m^2/g	82	68	183	168	107
Mass-median Diameter, μm	9.6	12.4	8.8	16.2	15.9
Noncarbonate Carbon, wt %	N.M.	17.6	36.0	33.9	19.8

It is interesting that the transient cake on the top plenum appears to be similar to the g-ash generated without limestone addition, while the bottom plenum transient cake seems to more closely resemble the g-ash produced with limestone addition. This result may indicate that the sorbent particles were preferentially collected on the bottom plenum, at least during the time period that preceded the semidirty shutdown. The chemical analysis of the dustcakes, which is discussed in Section 4.4.5.3, supports this hypothesis. In the bottom plenum cake, the calcium-related compounds ($CaCO_3$, CaS, and CaO) make up about 27 percent of the solids. In the top plenum cake, the calcium-related compounds account for only 19 percent of the material. These figures include the CaO that came from the coal as well as the CaO that came from the limestone. However, most of the difference in calcium content between the top and bottom plenums is probably attributable to partitioning of the sorbent particles, since the calcium that was in the coal would become an inseparable part of the g-ash.

It may also be noteworthy that the transient cake on the top plenum has a much finer particle-size distribution than does the transient cake on the bottom plenum. This may suggest that larger particles are preferentially separated and collected in the bottom plenum. This difference may be related to the apparent preferential collection of sorbent particles in the bottom plenum. If the sorbent particles were somewhat larger and perhaps denser than the particles of carbonaceous g-ash, then the difference in particle size and density could explain the preferential collection of larger particles and calcium-related compounds in the bottom plenum.

The table below compares the average properties of the residual dustcake from TC12 with those from previous test campaigns using PRB coal. The dustcakes from TC08 and TC07 are not included because the physical properties of the TC08 cake were altered by partial oxidation, and the properties of the TC07 cake were biased by coke feed at the end of the run.

	TC12	TC10	TC06
Bulk Density, g/cc	0.29	0.23	0.25
Skeletal Particle Density, g/cc	2.27	2.07	2.28
Uncompacted Bulk Porosity, %	87.2	88.9	89.0
Specific-Surface Area, m^2/g	82	91	257
Mass-Median Diameter, μm	9.6	4.6	9.3
Non-Carbonate Carbon, wt %	N.M.	49.6	40.2

Compared to the previous residual cakes, the TC12 residual cake has a somewhat higher bulk density and lower bulk porosity. This could be related to the addition of limestone. Although limestone was not added during most of TC12, limestone was used at the beginning and at the end of the oxygen-blown portion of the run. The surface area of the TC12 residual cake is similar to that of the TC10 residual cake, but the TC06 cake has much more surface area. It is the latter value that seems to be anomalous, because the surface area is actually higher than the surface area of any of the TC06 in situ samples. In every other test, the residual cake has always had substantially less surface area than the incoming g-ash, and this was true again in TC12.

4.4.5 Chemical Composition of In situ Samples, Hopper Samples, and Residual Dustcake

This section discusses the chemical composition of the in situ samples collected during TC12, the PCD hopper samples used for the laboratory drag measurements, and the dustcake samples collected after TC12.

4.4.5.1 In situ Particulate Samples

The chemical compositions of the TC12 in situ samples are detailed in Table 4.4-6. These compositions were calculated from the elemental analyses using the same procedures that have been described in previous reports. As expected, the samples collected during limestone addition contained significantly higher levels of $CaCO_3$ and CaO. The results also suggest that the limestone addition rate used in the oxygen-blown portion may have been slightly higher than that used in the air-blown portion. The following table summarizes the ranges of compositions obtained under both air- and oxygen-blown conditions, with and without limestone addition, and with the injection of nickel oxide for ammonia cracking.

Oxidant	Air		Oxygen		
Limestone	No	Yes	Yes	No	No
Nickel Oxide	No	No	No	No	Yes
$CaCO_3$, wt %	2.4-3.5	7.4-8.6	10.7-20.3	0.8-4.9	3.7-4.7
CaS, wt %	1.1-1.2	0.6-1.6	0.02-0.04	0.1-0.6	0.8-1.4
CaO, wt %	11.3-13.3	21.0-22.0	22.9-35.8	7.3-12.1	6.7-9.5
Noncarbonate Carbon, wt %	21.7-25.0	21.7-22.5	14.8-24.5	28.2-43.5	27.5-37.6
Inerts (Ash/Sand), wt %	56.9-63.5	47.2-47.5	33.6-41.8	39.6-57.4	49.6-58.6
NiO, wt %	N.M.	N.M.	N.M.	0.01-0.09	1.5-2.4

As noted above, the compositions show the expected effect of the limestone addition in terms of $CaCO_3$ and CaO. All of the compositions make sense, except for the CaS content of the samples collected in oxygen-blown mode with limestone addition. In these three particular samples, the calculated CaS concentrations were much lower than expected due to very low reported levels of sulfur in the solids. We suspect that there was some sort of analytical problem with these particular samples.

Except for the limited problem with the CaS in a few samples, the analytical results on the TC12 in situ samples seem to be reasonable. In the absence of limestone addition, the results indicate that the g-ash produced under oxygen-blown conditions contained more carbon and less inerts than the g-ash produced under air-blown conditions. However, this difference may not be particularly significant given that there were only two samples collected under air-blown conditions without sorbent addition.

Based on the NiO concentrations reported, it appears that the injection of the NiO-based catalyst produced an incremental increase of 1.4 to 2.3-wt percent NiO in the PCD inlet solids. In a total solids rate of 400 lb/hr, this would correspond to a NiO addition rate of about 6 to 9 lb/hr. According to the catalyst supplier, Johnson-Matthey, the NiO content of the catalyst was less than 26-wt percent. Therefore, the catalyst addition rate was at least 23 to 35 lb/hr. To aid in feeding the catalyst, it was blended with fine sand in a ratio of 1:3, so the total addition rate of solids (catalyst + sand) was in the range of 69 to 105 lb/hr. The actual increase in the solids carryover that was observed (see Figure 4.4-1) was about 90 lb/hr, which is in good agreement with the rate determine from the NiO concentrations in the solids.

The following table compares the average composition of the TC12 in situ samples with those from other PSDF gasification tests using PRB coal. The compositions given in this table are the average values for all of the in situ samples.

	TC12	TC10	TC08	TC07-D	TC06
CaCO$_3$, wt %	5.6	3.7	4.2	9.1	8.7
CaS, wt %	0.5	0.4	0.7	0.1	1.3
CaO, wt %	14.1	7.3	8.1	20.3	19.0
Noncarbonate Carbon, wt %	30.8	39.4	43.7	24.2	33.0
Inerts (Ash/Sand), wt %	48.9	49.2	43.3	46.3	38.0

This comparison of the average compositions reflects the trends in limestone addition. No limestone was added in TC10 or TC08, and that is evident in the relatively low concentrations of calcium compounds. The high levels of calcium compounds in the TC07D and TC06 g-ash are the result of extensive limestone addition in those runs. In TC12, limestone was added in 4 of the 23 in situ samples, resulting in an average composition that indicates much less limestone usage than in TC07D and TC06, but more limestone usage than in TC10 and TC08.

4.4.5.2 PCD Hopper Samples Used for Drag Measurements

Table 4.4-6 includes the chemical compositions of the PCD hopper samples used for the laboratory drag measurements. As indicated in the table, two of the hopper samples were taken during limestone addition, and the compositions of these samples roughly cover the range of compositions seen in the in situ samples taken during limestone addition. Together with the hopper sample that was collected in the absence of limestone addition, the three selected hopper samples cover about the same range of compositions seen in the in situ samples. Comparing Tables 4.4-6 and -4, it is interesting to note that as the carbon content of the samples increased from 12.7 to 42.7 percent, the bulk density decreased from 0.39 to 0.21 g/cc, and the surface area increased from 74 to 185 m^2/g. Similar trends were noted in the hopper samples from TC11 (see TC11 Run Report).

4.4.5.3 Dustcake Samples

Since it was not possible to recover enough residual cake for chemical analysis, composition information was obtained only on the thick (transient + residual) cakes. Table 4.4-7 gives the calculated compositions for the thick cakes on the top and bottom plenums. The compositions confirm what was suspected from the physical properties, that more of the sorbent was collected in the bottom plenum. In addition to this difference in the sorbent-related components, there is a substantial difference in noncarbonate carbon content (about 36 percent on the top plenum and 18 percent on the bottom plenum). In fact, the difference in carbon is larger than the difference in the sorbent-related components. There appears to be some mechanism by which carbon has become more concentrated in the top plenum and sorbent-related components and inerts (ash/sand) have become more concentrated in the bottom plenum.

Since carbon and ash are bound together in the partially gasified particles that come from the coal, it is difficult to imagine that they could be separated. However, an effective enrichment of either carbon or ash could take place if the concentration of either component varies with particle size, and there is particle-size segregation between the top and bottom plenums. As discussed previously in Section 4.4.4.3, the transient cake on the top plenum (MMD = 8.8 µm) was finer than the transient cake on the bottom plenum (MMD = 12.4 µm). The top plenum cake also contained much more noncarbonate carbon than does the bottom cake (36 vs 18 wt percent). If the carbon were enriched in the finer particles, the size segregation between the top and bottom plenums could explain the difference in carbon content. A similar effect could also explain the apparent enrichment of sorbent in the bottom plenum if the sorbent particles were somewhat larger than the carbon/ash particles. Differences in density between the sorbent and the carbon/ash particles could also play a role in the segregation.

The table below compares the TC12 transient dustcake composition to the composition of the TC12 in-situ samples.

	Top Plenum Transient Cake	Bottom Plenum Transient Cake	In situ (w/o LS)	In situ (with LS)
CaCO₃, Wt %	5.3	5.1	0.8-4.7	7.4-20.3
CaS, Wt %	0.8	0.1	0.1-1.4	0.02-1.6
Free Lime (CaO), Wt %	13.2	21.5	6.7-13.3	21.0-35.8
Noncarbonate Carbon, Wt %	36.0	17.6	21.7-43.5	14.8-24.5
Inerts (Ash/Sand), Wt %	44.7	55.8	39.6-63.5	33.6-47.5

This comparison is interesting, because it suggests that the top plenum cake more closely resembles the g-ash produced without limestone addition, while the bottom plenum cake more closely resembles the g-ash produced with limestone addition. Previously, we suggested that sorbent-containing particles were preferentially collected in the bottom plenum, while carbon-enriched particles were preferentially collected in the top plenum. An alternative explanation could be that the g-ash produced during the limestone addition was preferentially collected in the bottom plenum. The concentrations of free lime and carbon are consistent with the latter

hypothesis, but that is not true of the inerts. Therefore, it seems more likely that the differences in composition are attributable to the segregation of the carbon and sorbent as previously suggested.

Prior to TC12, there was only one previous test campaign where a valid transient cake sample was obtained after a run with PRB coal. After TC10, the PCD was shut down clean, so there was no transient cake available. As mentioned previously, the cake from TC08 was damaged by partial oxidation, and the cake from TC07D was biased by coke feed at the end of the run. Therefore, TC06 was the only previous PRB run where a good transient cake sample was obtained. The compositions of the TC12 and TC06 transient dustcakes are compared in the table below.

	TC12 Top Plenum Cake	TC12 Bottom Plenum Cake	TC06 Transient Cake
$CaCO_3$, Wt %	5.3	5.1	12.7
CaS, Wt %	0.8	0.1	1.8
Free Lime (CaO), Wt %	13.2	21.5	12.2
Noncarbonate Carbon, Wt %	36.0	17.6	41.7
Inerts (Ash/Sand), Wt %	44.7	55.8	31.5

This comparison shows that the TC12 top plenum cake seems to be similar to the TC06 transient cake, while the TC12 bottom plenum cake contains much less carbon and more inerts than the TC06 cake. Previously, we suggested that the TC12 bottom plenum cake more closely resembled the TC12 g-ash produced with limestone addition. However, limestone addition was used throughout TC06, and the TC06 cake seems to be more similar to the TC12 top plenum cake, which we said resembles the TC12 g-ash produced without limestone addition. These differences suggest that the bottom plenum received a disproportionately large amount of sorbent in TC12. If the particle-size distribution of the sorbent is somewhat coarser than the particle-size distribution of the ash/carbon, then the preferential collection of the sorbent in the bottom plenum should cause the bottom plenum cake to have a larger mean particle size than does the top plenum cake. As shown previously in Table 4.4-5, the bottom plenum transient cake does indeed have a larger mean particle size (12.4 μm versus 8.8 μm for the top plenum cake).

4.4.6 Laboratory Measurements of G-Ash Drag

The RAPTOR apparatus described in previous reports was used to measure the normalized drag of the g-ash as a function of particle size. The three hopper samples used for these measurements have been described in previous sections. They were originally selected because they represented periods of stable operation both with and without limestone addition. All of the samples were from the oxygen-blown operating condition since most of the test program was conducted in that mode. It has been demonstrated repeatedly that the source of oxidant does not affect dustcake drag. After the chemical analysis of these samples was completed, we realized that the three hopper samples represented a wide range of carbon contents: 13 wt percent for the July 14, 2003, sample with limestone, 24 wt percent for the May 5, 2003, sample

with limestone, and 43 wt percent for the June 26, 2003, sample without limestone. We also noted that the surface areas of the samples increased with increasing carbon content: 74 m^2/g for the July 14, 2003, sample with limestone, 126 m^2/g for the May 22, 2003, sample with limestone, and 185 m^2/g for the June 26, 2003 sample without limestone.

The TC12 drag data are shown in Figure 4.4-7 along with average trends from previous PRB tests. The TC12 samples show that drag increases with increasing carbon content. There may also be some reduction in drag caused by the limestone addition. The effect of the limestone addition on drag may be related to the concomitant reduction in carbon content. At the finest particle sizes, the TC12 laboratory drag measurements are almost as high as those of the TC06 g-ash, before the new lower mixing zone was installed. At the largest particle sizes, the lab measurements are almost as low as those of the TC07D g-ash, after the new lower mixing zone was installed. These changes in drag between TC06, TC07, and TC12 are examined in more detail in the next section (Section 4.4.7).

4.4.7 Analysis of PCD Pressure Drop

As in previous tests, the buildup of transient pressure drop across the PCD was analyzed by calculating a corresponding value of transient drag and comparing it to the drag measured by RAPTOR. The calculation procedure, which has been described in previous reports, was applied to all of the in situ sampling runs, and the results are summarized in Table 4.4-8. The calculated transient drag at PCD conditions is listed under the column heading "PCD." The corresponding normalized value of transient drag at room temperature is listed under the heading "PCD@RT." This value can be compared directly with the RAPTOR drag values. The corresponding RAPTOR drag value for a given in situ run was determined by applying the appropriate regression fit of the laboratory data at the mean particle size of the in situ sample.

Previous laboratory drag measurements suggested that there was a reduction in drag associated with the installation of the new lower mixing zone between TC06 and TC07D. Some of the laboratory drag measurements made on the TC12 g-ash, however, were almost as high as the TC06 drag, before the new lower mixing zone was installed. The measurements made for the largest particle sizes were almost as low as the drag values from TC07D, after the new lower mixing zone was installed. To examine these differences in more detail, we compared the PCD transient drag values for TC06, TC07D, and TC12.

It was noted that in TC11 the drag varied with the noncarbonate carbon content of the g-ash (see TC11 Run Report). Therefore, the transient drag values for TC06, TC07D, and TC12 were plotted as a function of carbon content. The resulting plot (Figure 4.4-8) shows that the TC12 transient drag data span the entire range of the TC06 and TC07D. At some times during TC12, the PCD drag was as high as it was in TC06, and at other times during TC12, the PCD drag was as low as it was in TC07D. In other words, the variation in PCD drag that was seen during TC12 without any change in system hardware was just as great as the change in drag between TC06 and TC07D. This observation suggests that it is possible to have this much change in drag without any changes in the system hardware.

Based on the above discussion of PCD drag, serious doubt must be cast on the previous conclusion that the installation of the new lower mixing zone was responsible for a reduction in drag. Since the changes in drag seen in TC12 were of comparable magnitude to the differences

in drag between TC06 and TC07D, it seems most likely that the drag variations between TC06 and TC07D and the variations during TC12 were caused by some nonhardware-related changes (e.g., changes in process conditions, coal blend, or coal-feed rate). To date, we have not been able to isolate any effects associated with changes in specific process conditions (e.g., gasifier exit temperature, air-to-coal ratio, steam addition rate, etc.), although we have seen that drag is affected by changes in carbon content (or carbon conversion) and by limestone addition.

After TC12, an effort was made to correlate PCD drag with various coal parameters to investigate whether the large variations in drag could be related to variations in the coal blend. Since the PRB coal that we have been using at the PSDF is really a blend from several different mines, we suspected that the variation in drag might be related to variations in the coals or in the blending of the coals. Although we still cannot rule out possible differences in the coals or the blending, we were not able to find any correlations between the drag and the characteristics of coal samples taken from the FD0210 coal feeder. The specific coal parameters that were investigated included coal sulfur content, ash content, fixed carbon, and heating value.

Figure 4.4-9 compares the normalized PCD transient drag at room temperature (PCD@RT) to the corresponding individual values of RAPTOR drag. The two data points with NiO injection are not included on this graph because there were no laboratory data collected with those samples. Also, marked on the graph are three data points that were measured with very low coal feed and one that had very low specific-surface area. These points are some of the most scattered in the set, probably because they do not match the laboratory samples well. If these points are ignored, the remaining TC12 drag results fit the perfect agreement line quite well, indicating that the lab measurements did a good job of predicting the actual PCD results.

4.4.8 Conclusions

PCD drag varied widely in TC12, covering the entire range of drag values seen with PRB coal before and after the installation of the new lower mixing zone. At least part of this variation was attributable to changes in the carbon content of the g-ash. At the lowest carbon content (about 15 wt percent), the PCD drag was in the range of 16 to 36 $inWc/(ft/min)/(lb/ft^2)$. At the highest carbon content (about 44 wt percent), PCD drag ranged from about 60 to 90 $inWc/(ft/min)/(lb/ft^2)$. Even at a given carbon content, the PCD drag varied by about a factor of two or more. Therefore, it is clear that there are factors other than just carbon content that are causing substantial variations in the drag. Various coal properties were examined to determine whether some of the variation could be attributed to changes in the coals or in the blending of the coals, but we were not able to identify any correlations between these parameters and the PCD drag. Additional research is needed to isolate the process conditions or other factors that are causing the variations in drag.

The TC12 laboratory drag measurements were in reasonably good agreement with the PCD drag values. At the mean particle size of the incoming g-ash, the PCD hopper sample with 13-wt percent carbon had a lab-measured drag of about 40 $inWc/(ft/min)/(lb/ft^2)$. This value is fairly close to the upper limit of the PCD drag values observed when the in situ carbon content was 15 wt percent. Similarly, the PCD hopper sample with 43-wt percent carbon had a lab-measured drag of about 60 $inWc/(ft/min)/(lb/ft^2)$. The corresponding value of PCD drag ranged from 60 to 90 $inWc/(ft/min)/(lb/ft^2)$ when the in situ carbon content was 44 wt percent.

At the finest particle sizes, the laboratory drag measurements were as high as the drag values obtained before the installation of the new lower mixing zone, and, at the largest particle sizes, the laboratory measurements were almost as low as the drag values obtained after the installation of the new lower mixing zone. In other words, the variability in drag seen during TC12 was comparable to the change in drag that was apparently produced when the new lower mixing zone was placed into service. This observation casts serious doubt on the previous conclusion that the drag was permanently reduced when the new lower mixing zone was placed in service. It now seems more likely that this change in drag was simply the result of changes in carbon conversion and other process variations.

In addition to the effect on drag, the carbon content was also found to have an influence on the specific-surface area of the g-ash as seen in TC11. As the carbon content of the in situ samples increased from 15 to 44 wt percent, the specific-surface area increased from about 81 to 200 m^2/g. There also appears to be a difference between the air- and oxygen-blown samples. The air-blown samples had carbon contents in the range of 22 to 25 wt percent and surface areas in the range of about 100 to 140 m^2/g. The oxygen-blown samples without limestone addition had carbon contents in the range of 27 to 44 wt percent and surface areas in the range of about 160 to 200 m^2/g. The samples collected with limestone addition had somewhat lower carbon contents (15 to 24 wt percent) and lower surface areas (81 to 120 m^2/g). These results suggest that the sorbent addition reduced the surface area, possibly because the calcined limestone has less surface area than does the carbonaceous portion of the g-ash.

As seen in previous tests, the TC12 particulate sampling at the PCD inlet showed that the solids carryover to the PCD increased with increasing coal-feed rate as expected. The effect of limestone addition could also be seen in the measured rate of solids carryover. In air-blown operation, the carryover was increased from about 300 lb/hr without limestone addition to about 400 lb/hr with limestone addition. In oxygen-blown mode the limestone addition produced a similar increase in carryover, although there was more variability due to changes in coal feed and carbon carryover.

The injection of a NiO-based catalyst for ammonia decomposition increased the solids carryover by about 90 lb/hr and produced an incremental NiO concentration of 1.4 to 2.3 wt percent in the g-ash. Based on a total solids carryover rate of 400 lb/hr, this range of NiO concentrations would correspond to about 6 to 9 lb/hr of NiO. According to the catalyst supplier, Johnson-Matthey, the catalyst contains less than 26-wt percent NiO. Therefore, the corresponding rates of catalyst addition would be at least 23 to 35 lb/hr. For the injection tests, the catalyst was blended with sand in a ratio of 1 to 3. Therefore, the total rate of solids injection, including both catalyst and sand, was between 69 and 105 lb/hr. Considering that some of the sand (and possibly some of the catalyst) may have been captured in the cyclone ahead of the PCD, the calculated rate of catalyst-plus-sand addition seems to be reasonably consistent with the measured increase in the solids carryover to the PCD.

During the PCD inspection after TC12, it was noted that the transient dustcake on the outer candles in the top plenum contained an elevated ridge running along the length of the filter element. The ridge appeared to be formed by the impaction of particles from the high-velocity tangential gas flow between the shroud and the outer row of candles. Differences in particle size appear to confirm that the ridge was probably the result of impaction. This type of ridge formation was seen previously after some combustion runs, but this is the first time that it was

noted after a gasification test. Apparently there was some change in the distribution of the gas flow or in the particulate characteristics that produced this leading-edge impaction phenomenon in TC12. These effects may be related to the particle-size-dependent segregation of material between the top and bottom plenums.

The analysis of the transient dustcakes retained after TC12 suggests that there was some particle-size-dependent segregation of material between the top and bottom plenums. The top plenum cake is finer than the bottom plenum cake (MMD of 8.8 μm vs 12.4 μm), and the top plenum cake has a much higher surface area (183 m^2/g vs 68 m^2/g), a much higher carbon content (36 to 18 wt percent), and a lower concentration of sorbent components (CaO of 13 to 21 wt percent). These results suggest that carbon-rich particles were preferentially collected in the top plenum, while sorbent particles were preferentially collected in the bottom plenum. This segregation of the two materials may be related to differences in particle-size distribution and/or density.

As in previous gasification test campaigns, the residual dustcake had an average thickness of about 0.01 in. The residual cake thickness has been about 0.01 in. after every gasification test campaign, regardless of the coal type, the method of PCD shutdown (clean or semidirty), or the amount of backpulsing after shutdown. In some cases where the PCD was back-pulsed hundreds of times after shutdown, the residual cake thickness was still about 0.01 in. The thickness of 0.01 in. appears to represent a stable cake thickness that cannot be reduced with the existing back-pulse cleaning system.

Table 4.4-1

PCD Inlet and Outlet Particulate Measurements for TC12

| Test Date | Run No. | PCD Inlet | | | | Run No. | PCD Outlet | | | |
		Start Time	End Time	Particle Loading, ppmw	Particle Loading, lb/hr		Start Time	End Time	H_2O Vapor, vol %	Particle Loading, ppmw
				Air-Blown						
5/18/03	1	8:45	9:00	12500	293	1	8:30	12:30	9.8	< 0.10
5/19/03	2	9:35	9:55	13400	307	2	9:15	13:15	8.9	< 0.10
5/19/03	3	13:15	13:25	18100[1]	415[1]	--	--	--	--	--
5/20/03	4	8:45	9:00	17400[1]	393[1]	3	8:35	12:35	10.4	< 0.10
				Oxygen-Blown						
5/21/03	5	9:15	9:30	30300[1]	469[1]	4	9:00	11:42	24.0	< 0.10
5/22/03	6	11:10	11:25	29500[1]	421[1]	5	9:00	14:20	19.2[2]	< 0.10
5/23/03	7	9:15	9:30	14500	225	6	8:45	12:45	24.6	< 0.10
6/20/03	8	12:25	12:40	14300	196	7	10:15	14:15	14.2	< 0.10
6/23/03	9	12:44	13:00	19900	251	8	10:15	14:15	15.4	< 0.10
6/24/03	10	9:10	9:25	21800	272	9	8:00	11:00	15.3	< 0.10
6/25/03	11	9:40	9:55	21200	283	10	9:30	10:22	------[3]	-------[3]
6/26/03	12	9:45	10:00	19500	272	11	9:00	13:00	17.0	< 0.10
6/27/03	13	10:45	11:00	20700	277	12	9:45	13:45	16.6	< 0.10
6/30/03	14	10:45	11:00	16200	290	13	10:00	14:00	38.8	< 0.10
7/1/03	15	10:50	11:05	20000	354	14	10:19	11:19	33.8	-------[4]
7/2/03	16	9:10	9:25	17100	272	15	9:00	13:00	28.4	0.18[5]
7/3/03	17	13:15	13:30	11600	169	16	8:30	13:55	34.3	< 0.10[6]
7/7/03	18	12:30	12:45	17700	232	17	12:09	13:09	25.7	-------[4]
7/8/03	19	12:37	12:52	26300[8]	421[8]	18	9:00	13:00	23.1	< 0.10[7]
7/9/03	20	9:45	10:00	14700	210	19	9:30	13:30	21.9	< 0.10[7]
7/10/03	21	13:00	13:10	24200[8]	354[8]	20	13:26	14:26	32.7	8.2[9]
7/11/03	22	10:55	11:10	19300	280	21	10:05	14:05	26.2	0.10[5]
7/14/03	23	10:15	10:30	30800[1]	499[1]	22	10:00	14:00	24.1	< 0.10

Notes:
1. Limestone added to Transport Gasifier.
2. Water sample collected from 11:00 to 14:20.
3. Test aborted due to condenser pluggage.
4. Initial failsafe injection tests (#14 = PSDF, #17 = Pall). Filters contaminated with tar.
5. Long-term PSDF failsafe injection tests (#15 = 24 hours, #21 = 48+ hours).
6. Outlet run 16 paused from 9:06 till 11:20 for coal feeder trip.
7. Long-term Pall failsafe injection (#18 = 24 hours, #19 = 48 hours).
8. Nickel oxide injection.
9. PCD outlet char injection for PCME calibration.

Table 4.4-2

TC12 Dustcake Thicknesses and Areal Loadings

Failsafe Type	Element No.	Transient Coverage, %	Dustcake Thickness, in.	Areal Loading, lb/ft^2	Calculated Porosity, %
Bottom Plenum -- Thick ("Transient + Residual") Cake					
SWPC Ceramic	B-6	75-80	0.0650	0.144	80.7
PSDF	B-9	< 10	0.0614	0.143	79.6
Pall Fuse	B-5	15-20	0.0895	0.174	83.0
Average		---	0.0720	0.153	81.1
Bottom Plenum -- Thin ("Residual") Cake					
SWPC Ceramic	B-6	---	0.0098	---	---
PSDF	B-9	---	0.0085	---	---
Pall Fuse	B-5	---	0.0163	---	---
Average		---	0.0115	---	---
Top Plenum -- Thick ("Transient + Residual") Cake					
PSDF	T-14	90	0.0876	---	---
PSDF	T-15	90	---	0.132	---
Pall Fuse	T-32	95	0.0814	0.136	85.4
Average		---	0.0845	0.134	85.4

Table 4.4-3

Comparison of Average Residual Dustcake Thicknesses

Run No.	TC12	TC11	TC10	TC09	TC08	TC07	TC06
Thickness, in.	0.011	0.013	0.010	0.008	0.010	---	0.010

Table 4.4-4
Physical Properties of TC12 In situ Samples and Hopper Samples Used for RAPTOR

Sample ID	Run Number TC12-IMT-	Sample Date	Bulk Density g/cc	True Density g/cc	Uncompacted Bulk Porosity %	Specific Surface Area m^2/g	Mass-Median Diameter μm
Air-Blown In-Situ Samples							
AB12941	1	05/18/03	0.34	2.42	86.0	121	14.8
AB12942	2	05/19/03	0.33	2.53	87.0	138	17.9
AB12943	3	05/19/03	0.37	2.50	85.2[1]	101	14.0
AB12944	4	05/20/03	0.37	2.49	85.1[1]	131	15.0
Air-Blown Average			*0.35*	*2.49*	*85.9*	*123*	*15.4*
Oxygen-Blown In-Situ Samples							
AB12945	5	05/21/03	0.36	2.48	85.5[1]	120	16.3
AB12946	6	05/22/03	0.43	2.72	84.2[1]	81	16.1
AB12947	7	05/30/03	0.29	2.52	88.5	168	14.1
AB13441	8	06/20/03	0.28	2.45	88.6	148	15.9
AB13442	9	06/23/03	0.27	2.27	88.1	164	12.8
AB13443	10	06/24/03	0.25	2.14	88.3	168	16.5
AB13444	11	06/25/03	0.27	2.25	88.0	176	18.1
AB13445	12	06/26/03	0.24	2.21	89.1	198	17.3
AB13446	13	06/27/03	0.24	2.33	89.7	193	16.0
AB13447	14	06/30/03	0.24	2.26	89.4	156	13.8
AB13448	15	07/01/03	0.23	2.19	89.5	195	17.2
AB13449	16	07/02/03	0.23	2.37	90.3	181	15.5
AB13450	17	07/03/03	0.39	2.48	84.3	26	14.8
AB13451	18	07/07/03	0.28	2.32	87.9	128	18.8
AB13452	19	07/08/03	0.25	2.43	89.7[2]	202	19.3
AB13453	20	07/09/03	0.22	2.38	90.8	178	16.3
AB13454	21	07/10/03	0.23	2.34	90.2[2]	160	11.6
AB13455	22	07/11/03	0.24	2.39	90.0	179	19.1
AB13456	23	07/14/03	0.38	2.60	85.4[1]	100	17.9
Oxygen-Blown Average			*0.28*	*2.38*	*88.2*	*154*	*16.2*
Hopper Samples Used for RAPTOR (All Oxygen-Blown)							
AB12948	---	05/22/03	0.33	2.64	87.5[1]	126	15.7
AB13457	---	06/26/03	0.21	2.22	90.5	185	16.0
AB13458	---	07/14/03	0.39	2.67	85.4[1]	74	15.7
1. Limestone added to Transport Gasifier. 2. Nickel oxide injected.							

Table 4.4-5

Physical Properties of TC12 Dustcake Samples

Sample Type	Bulk Density g/cc	True Density g/cc	Uncompacted Bulk Porosity %	Specific Surface Area m^2/g	Mass-Median Diameter μm
Bottom Plenum					
Thick Cake ("Transient + Residual")	0.37	2.35	84.3	68	12.4
Thin Cake ("Residual")	0.29	2.27	87.2	82	9.6
Top Plenum					
Thick Cake ("Transient + Residual")	0.21	2.03	89.7	183	8.8
Ridge Along Leading Edge	---	---	---	---	11.5
Trailing Edge	---	---	---	---	8.6

Table 4.4-6

Chemical Composition of TC12 In situ Samples and Hopper Samples Used for RAPTOR

Sample ID	Run No.	Sample Date	CaCO$_3$ Wt %	CaS Wt %	CaO Wt %	Non-Carbonate Carbon Wt %	Inerts (Ash/Sand) Wt %	Loss on Ignition Wt %	NiO Wt %
Air-Blown In-Situ Samples									
AB12941	1	05/18/03	2.41	1.14	11.25	21.68	63.52	24.11	N.M.[3]
AB12942	2	05/19/03	3.55	1.25	13.25	25.04	56.90	25.76	N.M.
AB12943	3	05/19/03	7.43[1]	1.57	21.02	22.48	47.50	24.84	N.M.
AB12944	4	05/20/03	8.61[1]	0.58	21.98	21.67	47.16	25.09	N.M.
Air-Blown Average			5.50	1.14	16.88	22.72	53.77	24.95	---
Oxygen-Blown In-Situ Samples									
AB12945	5	05/21/03	10.68[1]	0.04	22.94	24.50	41.84	29.41	N.M.
AB12946	6	05/22/03	14.05[1]	0.02	35.75	14.75	35.42	21.26	N.M.
AB12947	7	05/30/03	4.93	0.04	25.52	29.88	39.63	33.40	N.M.
AB13441	8	06/20/03	4.00	0.31	10.46	28.24	56.99	32.18	N.M.
AB13442	9	06/23/03	2.98	0.31	9.16	35.38	52.17	38.44	N.M.
AB13443	10	06/24/03	3.80	0.36	8.51	38.91	48.43	42.22	N.M.
AB13444	11	06/25/03	4.34	0.27	7.68	41.58	46.13	44.79	N.M.
AB13445	12	06/26/03	2.39	0.38	9.39	43.46	44.38	46.51	N.M.
AB13446	13	06/27/03	4.75	0.51	7.95	38.58	48.21	41.77	N.M.
AB13447	14	06/30/03	3.70	0.16	11.55	34.09	50.51	36.57	N.M.
AB13448	15	07/01/03	4.30	0.18	9.89	38.76	46.87	41.77	N.M.
AB13449	16	07/02/03	3.64	0.09	12.06	33.52	50.69	36.44	N.M.
AB13450	17	07/03/03	0.84	0.52	7.26	34.03	57.36	34.38	N.M.
AB13451	18	07/07/03	4.18	0.51	11.29	35.72	48.29	38.11	0.01
AB13452	19	07/08/03	4.70	1.43	6.70	37.61	49.56	39.74	2.39[2]
AB13453	20	07/09/03	4.45	0.60	11.09	31.86	52.00	34.24	0.09
AB13454	21	07/10/03	3.68	0.80	9.50	27.45	58.56	29.25	1.52[2]
AB13455	22	07/11/03	4.50	0.40	11.07	34.67	49.36	37.40	0.46
AB13456	23	07/14/03	20.27[1]	0.04	30.32	15.74	33.62	24.30	N.M.
Oxygen-Blown Average			5.59	0.37	13.58	32.56	47.90	35.90	---
Hopper Samples Used for RAPTOR Measurements (All Oxygen-Blown)									
AB12948	---	05/22/03	12.86[1]	0.02	28.03	24.33	34.76	30.19	N.M.
AB13457	---	06/26/03	4.07	0.38	8.65	42.68	44.22	46.05	N.M.
AB13458	---	07/14/03	13.30[1]	0.02	38.30	12.65	35.73	17.96	N.M.

1. Limestone added to Transport Gasifier.
2. Nickel oxide injected.
3. N.M. = Not measured.

Table 4.4-7

Chemical Composition of TC12 Dustcake Samples

Sample Type	CaCO$_3$ Wt %	CaS Wt %	CaO Wt %	Non-Carbonate Carbon Wt %	Inerts (Ash/Sand) Wt %	Loss on Ignition Wt %
Bottom Plenum						
Thick Cake ("Transient + Residual")	5.07	0.13	21.46	17.57	55.76	19.55
Thin Cake ("Residual")	(1)	---	---	---	---	---
Top Plenum						
Thick Cake ("Transient + Residual")	5.32	0.79	13.20	35.95	44.73	39.91
Ridge Along Leading Edge	(1)	---	---	---	---	---
Trailing Edge	(1)	---	---	---	---	---

(1) Not enough sample for chemical analysis.

Table 4.4-8 TC12 Transient Drag Determined From PCD ∆P and From RAPTOR

Run No.	$\Delta P/\Delta t$, inwc/min	$\Delta(AL)/\Delta t$, lb/ft^2/min	FV, ft/min	MMD, μm	Drag, inwc/(lb/ft^2)/(ft/min)		
					PCD	PCD@RT	RAPTOR
Air-Blown							
1	1.64	0.019	3.29	14.8	85	50	68
2	1.83	0.020	3.19	17.9	91	54	56
3	1.67	0.028[1]	3.18	14.0	61	36	61
4	2.14	0.026[1]	3.09	15.0	83	50	56
Oxygen-Blown							
5	2.15	0.031[1]	2.90	16.3	70	43	52
6	0.68	0.028[1]	2.69	16.1	25	16	53
7	1.62	0.015	3.20	14.1	110	70	71
8	0.80	0.013	2.28	15.9	62	40	63
9	1.71	0.016	2.48	12.8	104	75	78
10	1.82	0.018	2.43	16.5	102	64	61
11	1.79	0.018	2.61	18.1	97	61	56
12	2.21	0.018	2.78	17.3	125	78	58
13	1.99	0.018	2.69	16.0	110	68	63
14	2.51	0.019	3.81	13.8	133	81	73
15	2.39	0.023	3.67	17.2	103	64	58
16	2.06	0.018	3.21	15.5	116	72	65
17	0.68	0.011	2.96	14.8	62	37	68
18	1.43	0.015	2.69	18.8	94	58	54
19	3.82	0.028[2]	3.46	19.3	139	84	52
20	2.03	0.014	2.92	16.3	147	89	62
21	2.37	0.023[2]	3.09	11.6	103	62	86
22	2.32	0.018	2.87	19.1	127	77	53
23	1.97	0.033[1]	3.19	17.9	60	36	47

1. Limestone added to Transport Gasifier.
2. Nickel oxide injected.

Nomenclature:
$\Delta P/\Delta t$ = rate of pressure drop rise during particulate sampling run, inwc/min
$\Delta(AL)/\Delta t$ = rate of increase in areal loading during sampling run, lb/min/ft^2
FV = average PCD face velocity during particulate sampling run, ft/min
MMD = mass-median diameter of in-situ particulate sample, μm
RT = room temperature, 77°F (25°C)
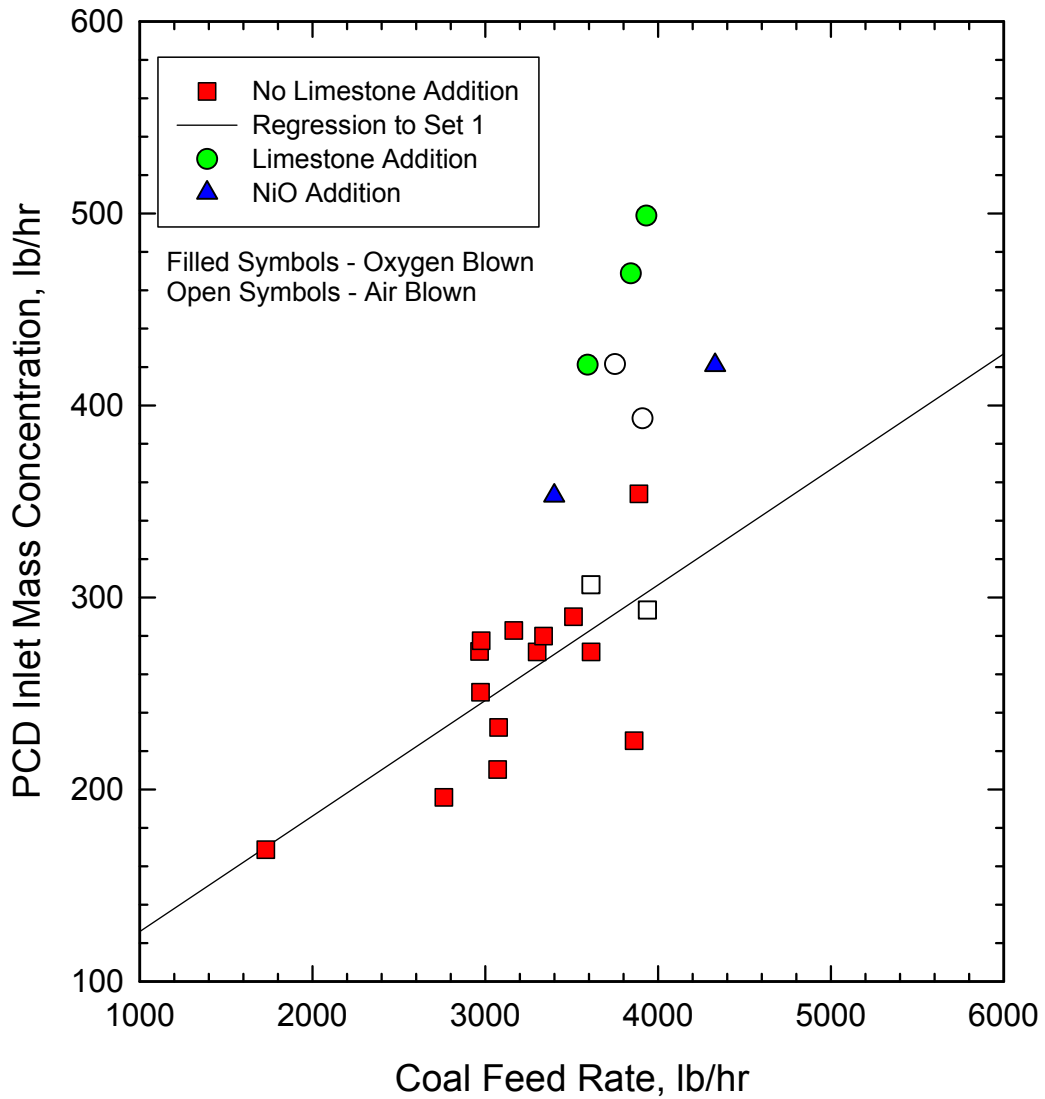RAPTOR = resuspended ash permeability tester

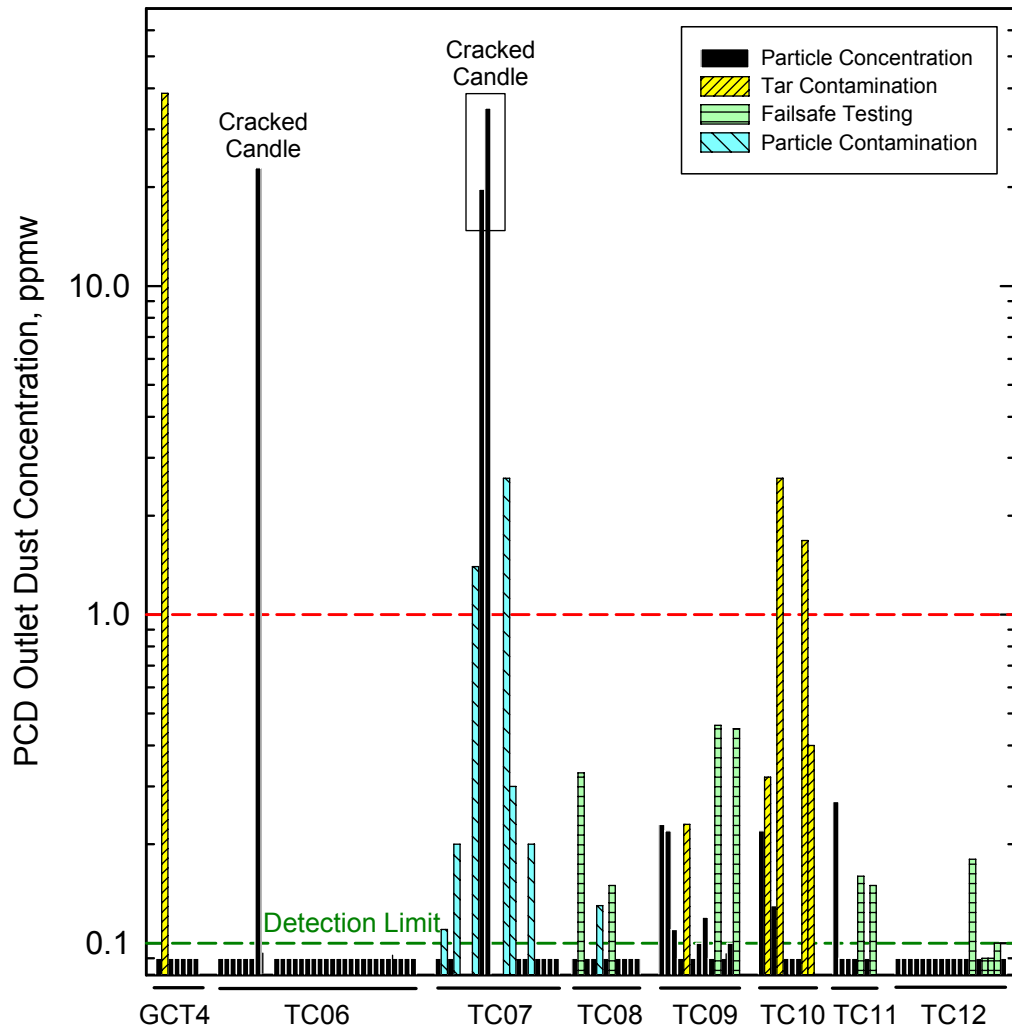Figure 4.4-1 PCD Inlet Particle Concentration as a Function of Coal-Feed Rate

Figure 4.4-2 PCD Outlet Emissions for Recent Gasification Runs
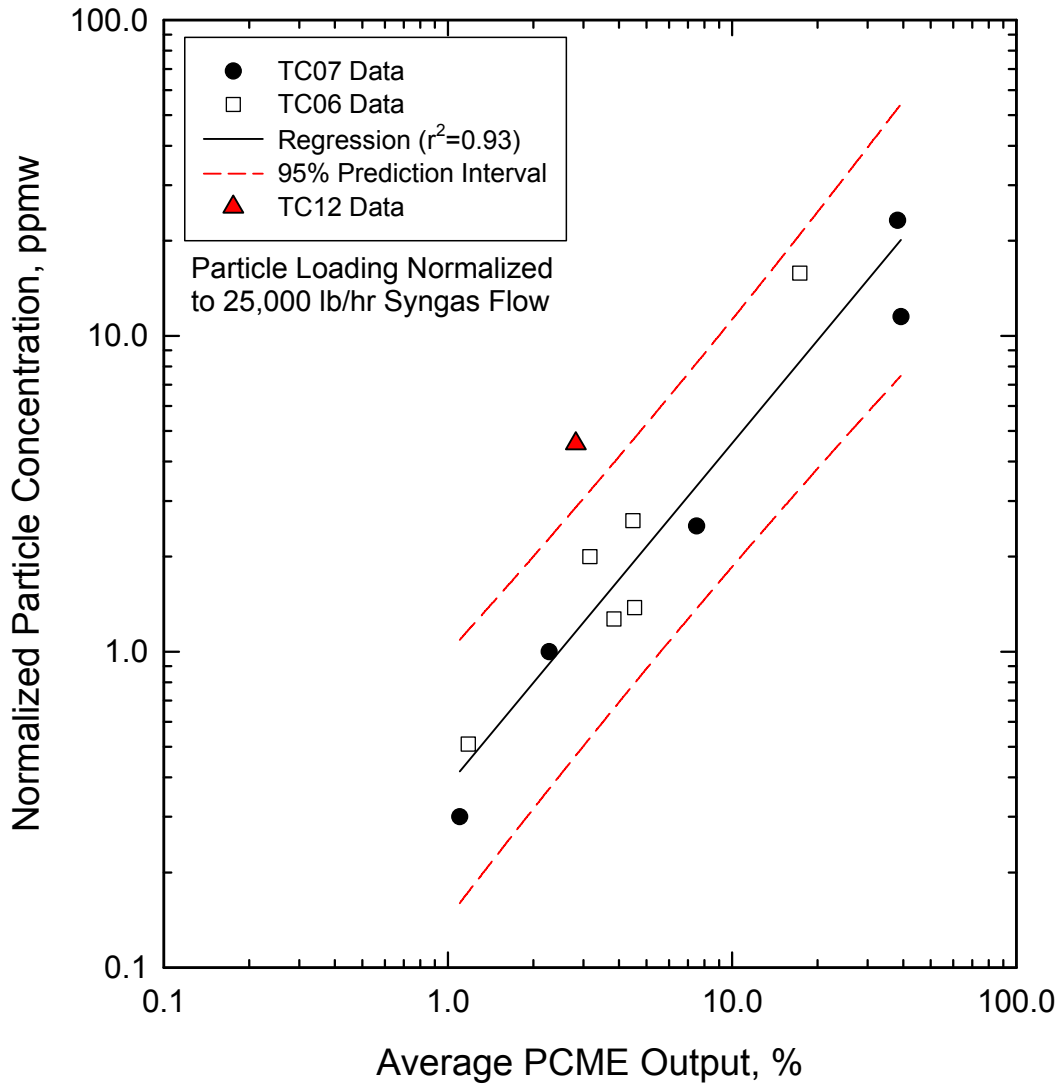
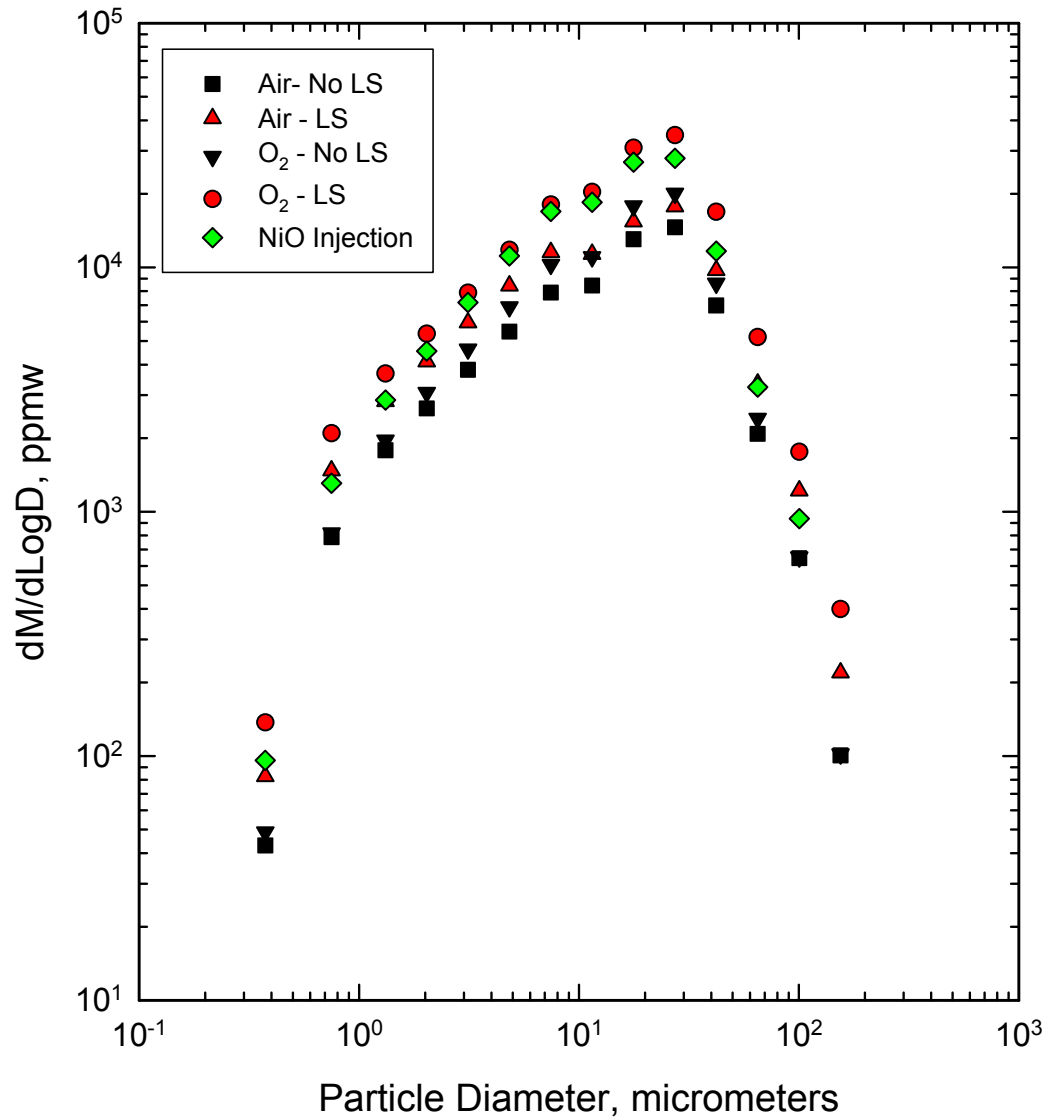Figure 4.4-3 Relationship Between PCME Output and Actual Particle Concentration

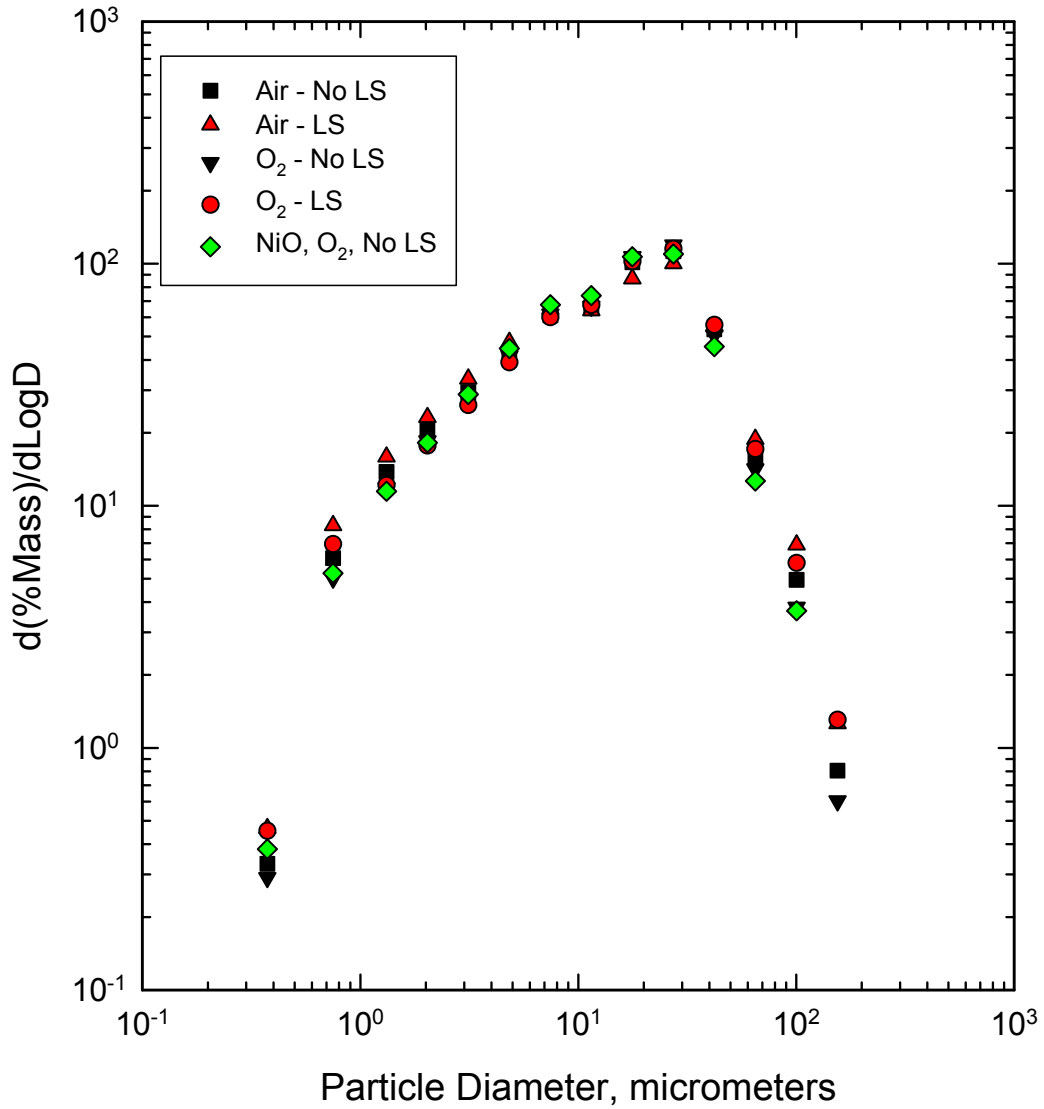Figure 4.4-4 Comparison of Average PCD Inlet Particle-Size Distributions

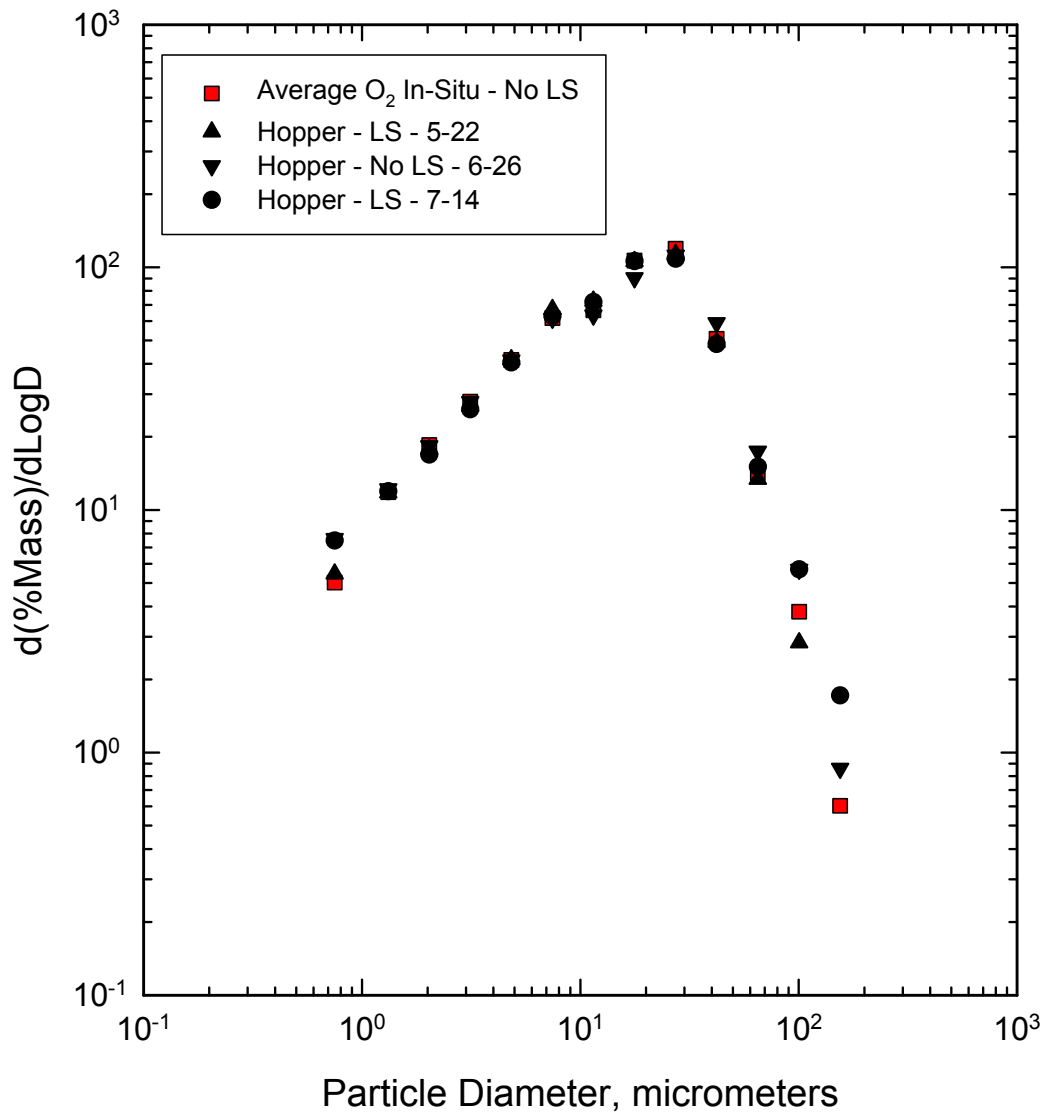Figure 4.4-5 Comparison of Average PCD Inlet Particle-Size Distributions

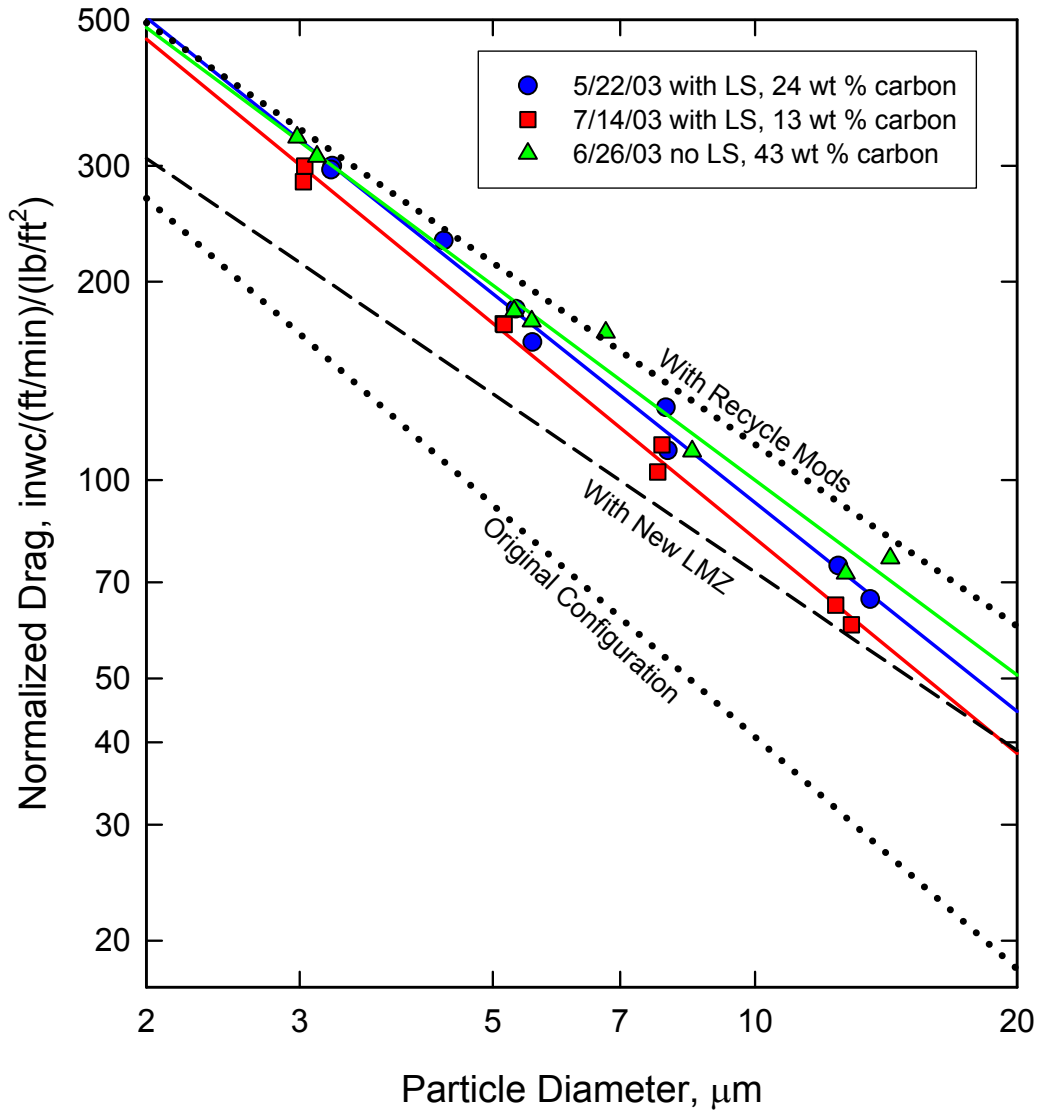Figure 4.4-6 Comparison of In situ and Hopper Particle-Size Distributions

Figure 4.4-7 Laboratory Measurements of Dustcake Drag Versus Particle Size
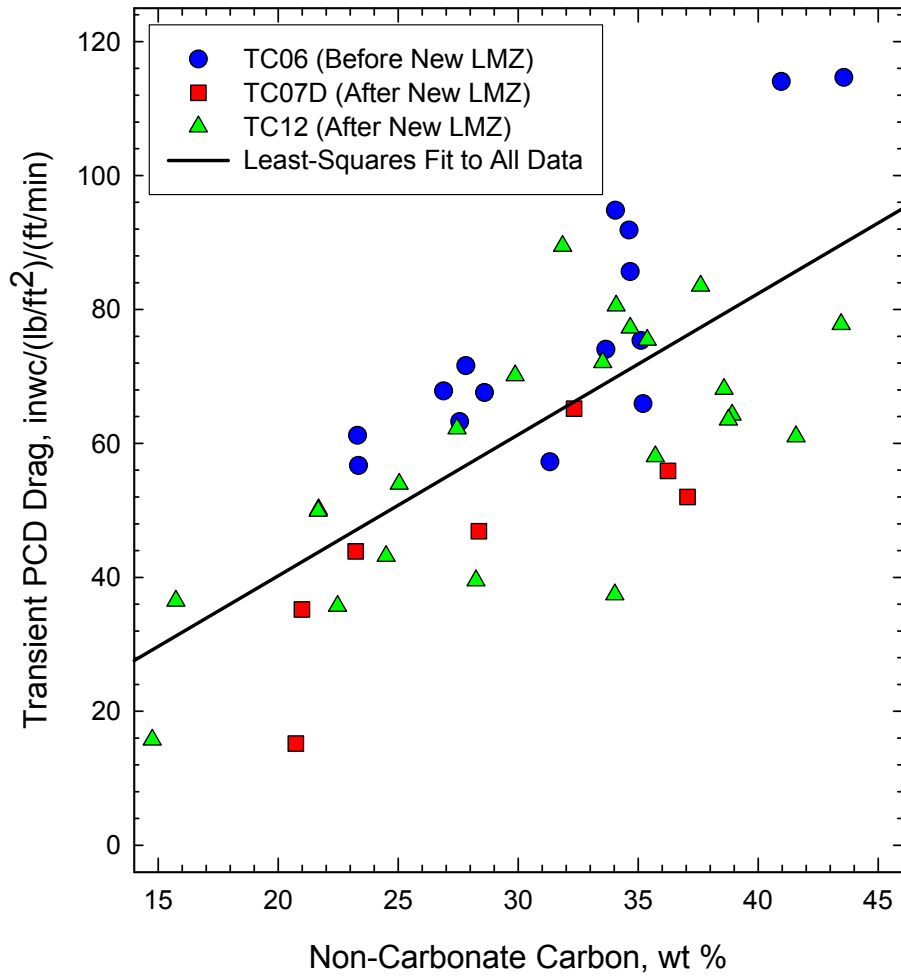(All Data With PRB Coal)

Figure 4.4-8 PCD Transient Drag Versus Carbon Content of Gasification Ash
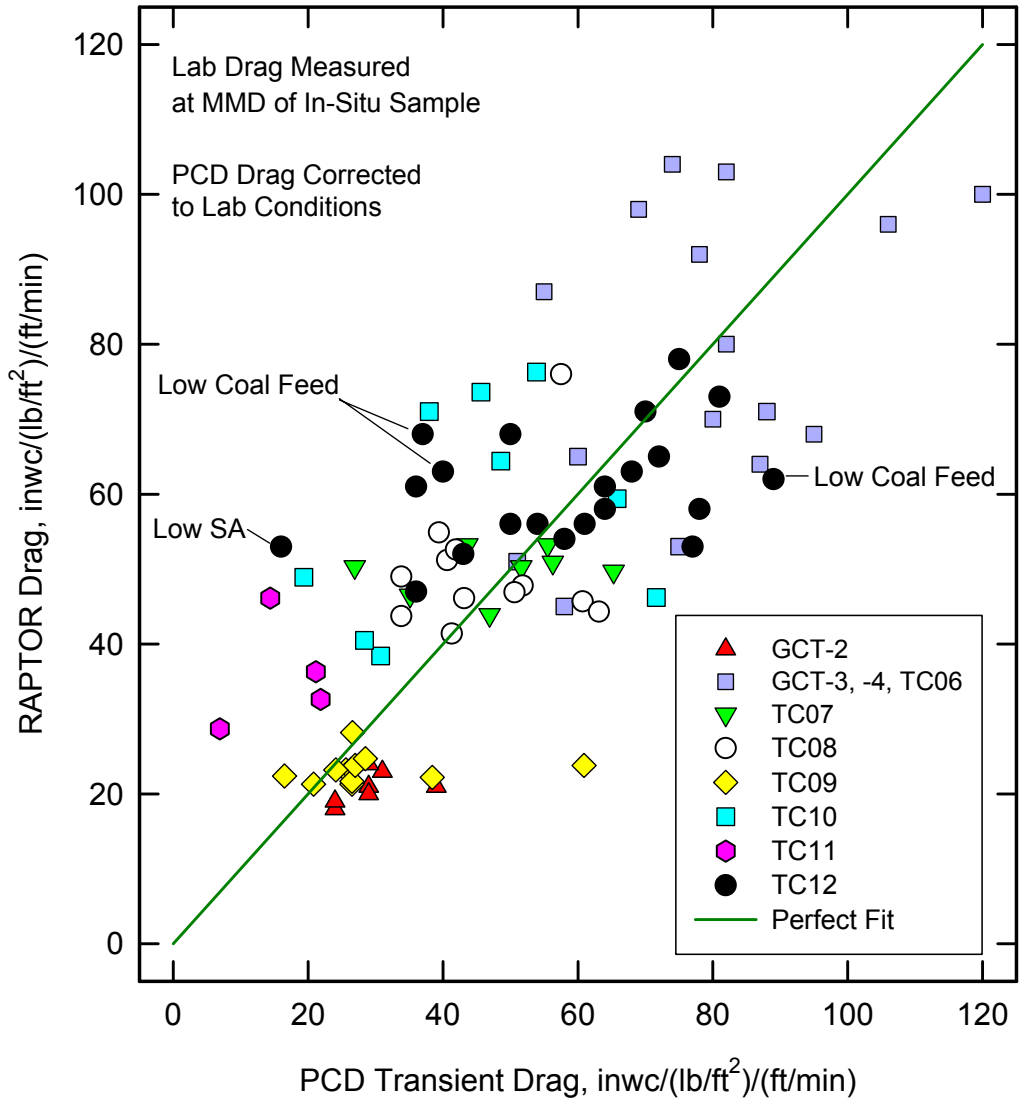(All Data With PRB Coal)

Figure 4.4-9 Comparison of PCD Transient Drag With Laboratory Measurements

4.5   TC12 FAILSAFE TESTING

4.5.1 Introduction

One of the main objectives of the PSDF is to improve the commercial readiness of high temperature, high pressure (HTHP) gas filtration technology. HTHP gas filtration systems have established that they can achieve high collection efficiencies during stable operations; however, process upsets can cause filter element failure resulting in an outlet loading that exceeds turbine requirements. In order to reduce the risk of an unscheduled shutdown due to filter failure, a reliable failsafe device is required. The failsafe device acts as a safeguard by mechanically closing or plugging in the event of a filter element failure. Currently, a successful failsafe has not been identified; therefore, the PSDF has established a failsafe testing program to identify failsafe devices that will protect the downstream turbine while screening out poor performing failsafes. This program was developed to allow testing and performance comparison of different failsafe devices under comparable testing conditions (Refer to TC08 Run Report Section 3.5 for PSDF Failsafe Test Criteria, Plan, and Setup).

4.5.2 TC12 Solids Injection Test Setup

During TC12, g-ash injection tests were performed on a PSDF-designed failsafe and a Pall FEAL fuse to determine their collection efficiency. Injection tests were previously performed on these two types of failsafe devices during TC08 and TC11. For the TC11 and TC12 tests, a solids injection system was designed that routes dirty gas out of the PCD, through an external valve and flow meter, then back into the PCD and to the inside of a filter element at location B2 or B3 (See Figure 4.2-1 for filter locations). The setup for the injection tests is shown schematically in Figure 4.5-1. Two modified Pall FEAL filter elements were installed at locations B2 and B3. Each filter element has 2½-inch tubes installed through the bottom plate. One tube is used to inject char, while the other tube is used for pressure measurements. Pressure drop measurements are made across the filter element wall and across the failsafe device. The dust leakage rate is determined by SRI's in situ outlet loading measurement. Based on the gas flow versus pressure drop characteristics, the test plumbing is equivalent to a hole in the filter element approximately 0.25 inches in diameter.

4.5.3 TC12 PSDF-Designed Failsafe Test

The PSDF-designed failsafe injection test started on July 1, 2003. The initial outlet loading measurement was started at 10:19 and the g-ash injection was started at 10:20. The outlet loading test continued for 1 hour and concluded at 11:19. Unfortunately the loading measurement was ruined by tar contamination; therefore, a valid outlet loading measurement was not obtained. The pressure drop measurements for the injection test are plotted in Figure 4.5-2. The initial plugging event was extremely rapid with the failsafe device being plugged, at least in terms of gas flow, within 3 seconds of the time when the injection test started. Also plotted in Figure 4.5-2 is the ratio of the flow meter pressure drop to the filter element pressure drop. During the initial period, the ratio was constant at around 0.15. The flow meter pressure drop is expected to be a constant fraction of the filter element pressure drop, since the filter pressure drop is the total differential across the injection system plumbing and the flow meter

pressure drop should be a fixed fraction of the pressure drop across the system. Using the relationship ΔP Filter Element ~6.5 x ΔP Flow Meter, the known characteristics of the flow meter (throat diameter = 0.300 inches, C_D=0.995) and assuming that the equivalent hole in the filter element acts as a sharp-edged orifice (C_D = 0.620), an equivalent hole diameter of 0.239 inches was calculated.

Figure 4.5-3 shows a comparison of the pressure drop measurements recorded at the start of the July 1, 2003, test with data collected during the corresponding period at the start of the PSDF-designed failsafe test during TC11 on April 16, 2003. The time scale of the initial plugging event on July 1 was shorter than the April 16 event by a factor of 3. The filter element pressure drop was higher by a factor of about 2.5 on July 1 than on April 16, which probably explains the difference.

After the initial outlet loading was concluded, solids injection was continued overnight and a second 4-hour outlet loading test was performed from 09:00 to 13:00 on July 2, 2003, corresponding to 22.67 to 26.67 hours after the solids injection test was initially started. The measured outlet loading was 0.18 ppmw. The outlet loading measurements during TC12 before the solids injection test were less than 0.10 ppmw (below the detection limit). The solids injection test was stopped at 13:20 on July 2. The pressure drop measurements recorded during the July 1 through July 2 segment of the PSDF-designed failsafe test are plotted on Figure 4.5-4. During the 27-hour injection period, the flow meter pressure drop ranged from 0.15 to 0.30 inH$_2$O, with the average declining from around 0.29 inH$_2$O at 11:00 on July 1 to about 0.18 inH$_2$O at 13:00 on July 2. During this same period, the filter pressure drop ranged from 0 to 4 inH$_2$O. Some of the variation in the filter element pressure drop measurement may have been caused by zero shift in the pressure transducer due to changing ambient temperature. The filter element pressure drop transducer is optimized for fast transient response, and is thus more subject to zero drift than the standard transducers.

Solids injection into the PSDF-designed failsafe resumed at 15:00 on July, 7, 2003. Immediately before the solids injection resumed, the filter element pressure drop was ~8 inH$_2$O, while the failsafe pressure drop ranged from about 60 to 180 inH$_2$O, which was slightly less than the tube sheet pressure drop. Therefore, the failsafe appeared to be plugged, in terms of gas flow, after a period of ~170 hours without solids injection. After the solids injection resumed, the filter element pressure drop rapidly decreased to about 2 inH$_2$O. Next, a 4-hour outlet loading test was conducted from 10:05 to 14:05 on July 11, 2003. This corresponded to 43 to 47 hours of continuous solids injection. The measured outlet loading was 0.10 ppmw. This was at but not below the detection limit; therefore, there was some measurable solids leakage through the failsafe. However, this value was well below the set target of 1 ppmw. It should be noted that this finding was not surprising, since previous test have shown that the sintered fiber filter elements are more prone to leak than the sintered metal powder filter elements.

4.5.4 TC12 Pall Fuse Test

The Pall fuse injection test was started on July 7, 2003, and continued through July 9. The initial outlet loading measurement was started at 12:09 on July 7 while the solids injection was started at 12:10. The outlet loading test continued for 1 hour and concluded at 13:09. As was the case for the initial loading test during the PSDF-designed failsafe test, the loading measurement was

ruined by tar contamination on the sample filter; therefore, the initial loading value was invalid. Out of the 22 outlet loading tests performed during TC12, only the 2 tests performed at the start of the failsafe injection tests were contaminated by tar. Therefore, it appears that the tar contamination was somehow caused by the injection test. A possible explanation is that the tar vapor is normally removed from the gas stream by absorption onto the filter cake. When the solids injection test is initially started some of the tar vapor may bypass the filter cake until the failsafe plugs. The tar vapor may then be condensed in the form of ultra-fine droplets before it reaches the outlet sampling filter. The collection of these ultra-fine tar droplets results in an artificial weight gain that is not related to any penetration of particles.

Pressure drop measurements recorded at the start of the Pall fuse test are plotted in Figure 4.5-5. There was a rapid initial plugging event, but the filter element pressure drop did not decrease as rapidly as the PSDF-designed failsafe. Figure 4.5-6 shows a comparison of the pressure drop measurements recorded at the start of the July 7 test with data collected during the corresponding period at the start of the Pall fuse injection test during TC11 on April 18, 2003. The initial plugging event during the July 7 test was faster than the April 18 test. Otherwise the data for both tests were very similar.

Solids injection into the Pall fuse continued for 50 hours. A second 4-hour outlet loading test was conducted from 09:00 to 13:00 on July 8, 2003. A third 4-hour loading test was conducted from 09:30 to 13:30 on July 9. The loading was below the detection limit (< 0.10 ppmw) for both tests. The pressure measurements recorded during the 24-hour period following the start of the Pall fuse injection test on July 3 are plotted in Figure 4.5-7. The gas flow rate through the plugged Pall fuse continued to be higher than the gas flow rate through the plugged PSDF-designed failsafe after similar periods of injection. After 24 hours of injection the pressure drop across the flow meter was about 0.5 inH$_2$O during the Pall fuse test, while after a similar period of solids injection to the PSDF-designed failsafe the flow meter pressure drop was about 0.2 inH$_2$O.

4.5.5 Post-Test Inspection/Interpretation of Test Results/Future Test Plans

After TC12, two failsafe devices were tested in the PCD to determine their collection efficiency. The initial outlet loadings for both failsafe devices were contaminated by tar condensation. However, the outlet loading for each failsafe device was determined after 24 hours of continuous solids injection. The outlet loading for the PSDF-designed failsafe was higher than that of the Pall fuse. The PSDF-designed failsafe was 0.10 ppmw after 24 hours, while the outlet loading for the Pall fuse was below the detection limit (<0.10 ppmw). During the test, it was noticed that the plugged Pall fuse flowed more gas compared to the plugged PSDF-designed failsafe. Even though the gas flow rate through the Pall fuse was slightly higher than the PSDF-designed failsafe, it does not appear that it adversely affected the collection efficiency.

During TC12, both the Pall fuse and PSDF-designed failsafe were removed and inspected. Both the Pall fuse and the filter element under the Pall fuse were found to be packed with g-ash. But the filter element under the PSDF-designed failsafe contained much less g-ash compared to the filter element under the Pall fuse. A possible explanation for these observations is that the plugged PSDF-designed failsafe is very efficient in stopping the gas flow, but emits a puff of solids during each back-pulse. This phenomenon has been noticed during testing in the cold-

flow PCD model. If the Pall fuse does not leak during each back-pulse its average solids leakage rate will be lower than the PSDF-designed failsafe. Tests of the Pall fuse are planned for the cold flow PCD model in order to verify whether or not the Pall fuse leaks during a back-pulse event. If the Pall fuse is found not to leak during a back-pulse event in the cold-flow PCD model, then the results would provide additional evidence to support the above theory.

Long-term injection tests on the PSDF-designed failsafe and Pall fuse are planned to be repeated. In order to avoid the problems associated with tar contamination, the initial outlet loading tests will be delayed until after the solids injection has started.
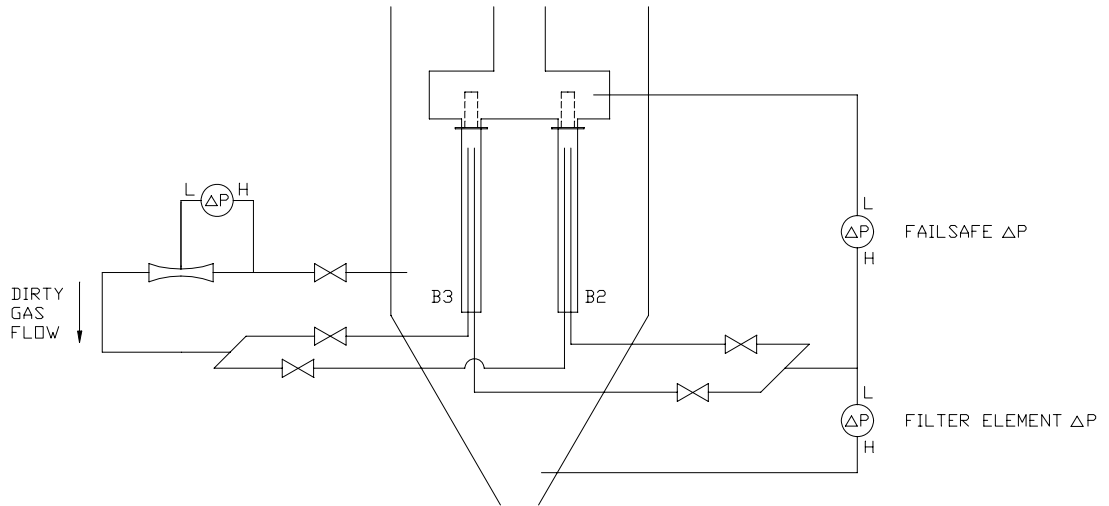
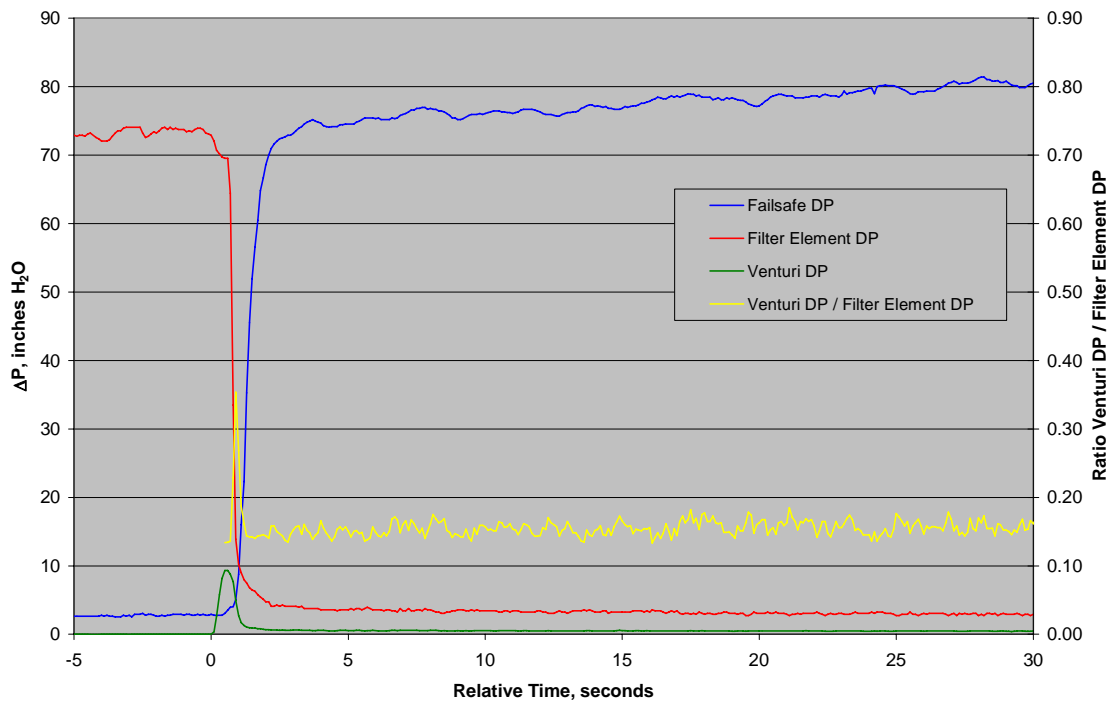Figure 4.5-1 Setup for Failsafe Injection Test

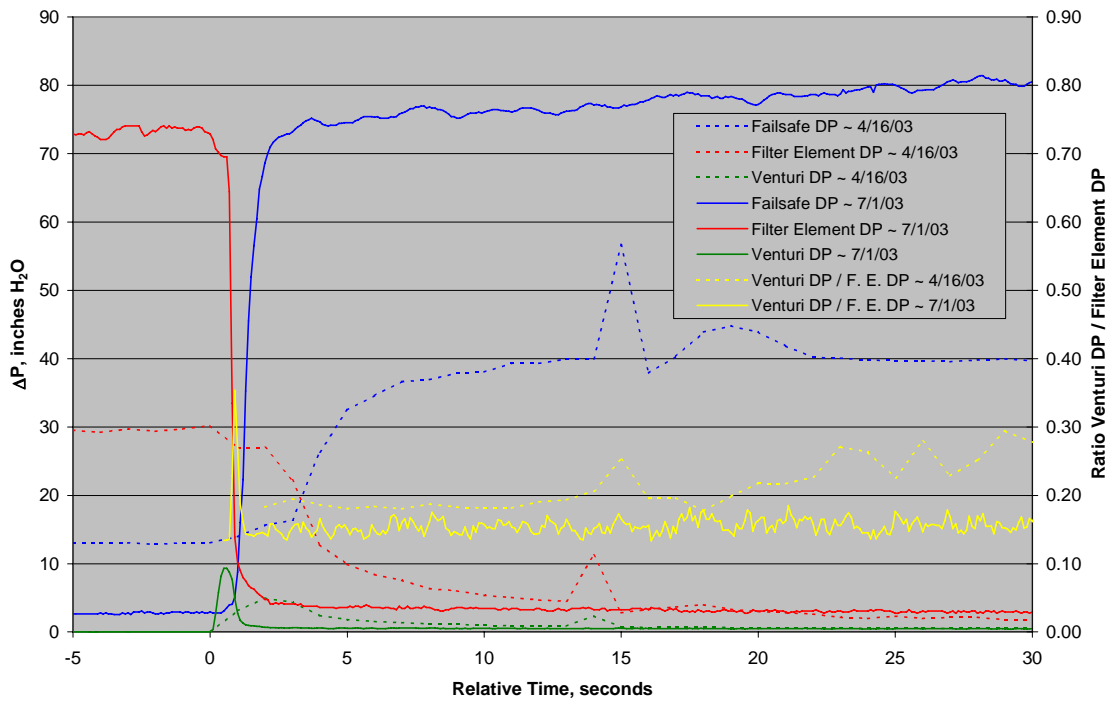Figure 4.5-2 Start of PSDF-Designed Failsafe Injection Test on July 1, 2003

Figure 4.5-3 Start of PSDF-Designed Failsafe Injection Tests on April 16, 2003, and July 7, 2003
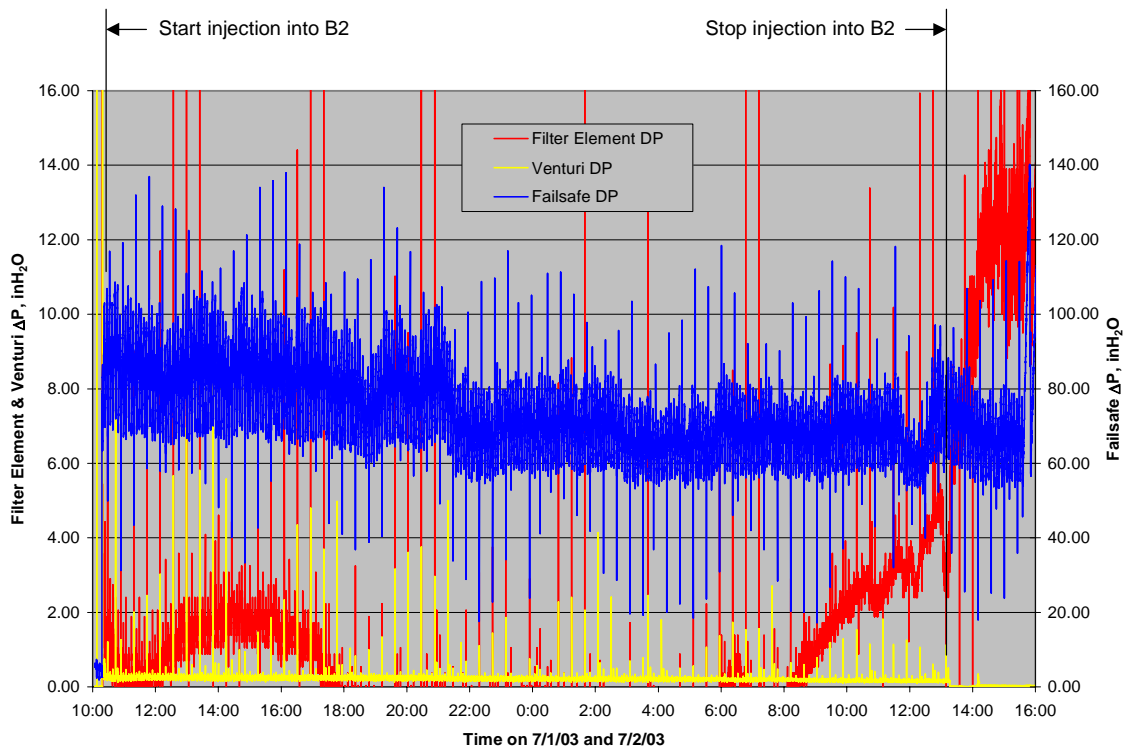

Figure 4.5-4 Pressure Drop Data for First Segment of PSDF-Designed Failsafe Injection Test on July 1, 2003, and July 2, 2003
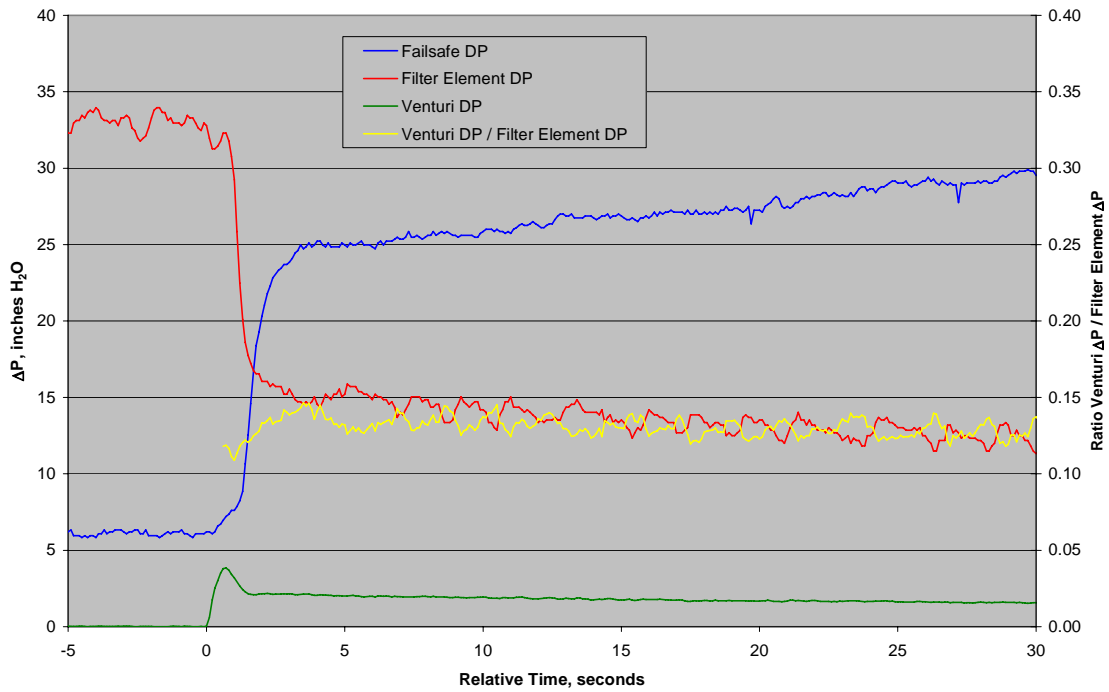
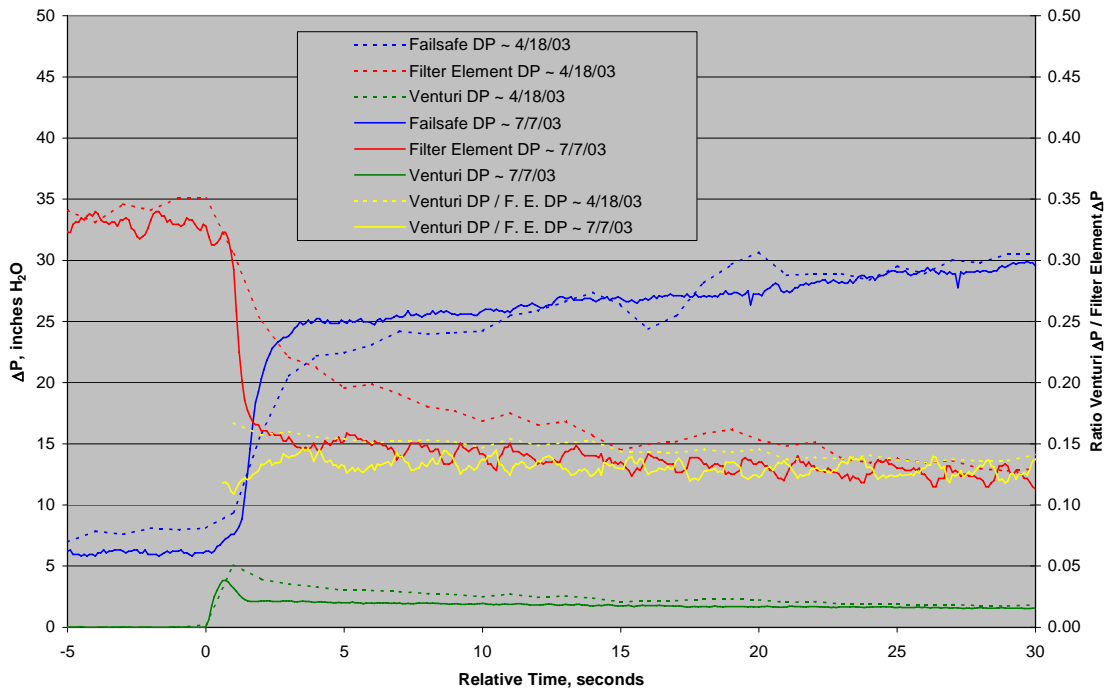Figure 4.5-5 Start of Pall Fuse Injection Test on July 7, 2003

Figure 4.5-6   Start of Pall Fuse Injection Tests on April 18, 2003, and July 7, 2003
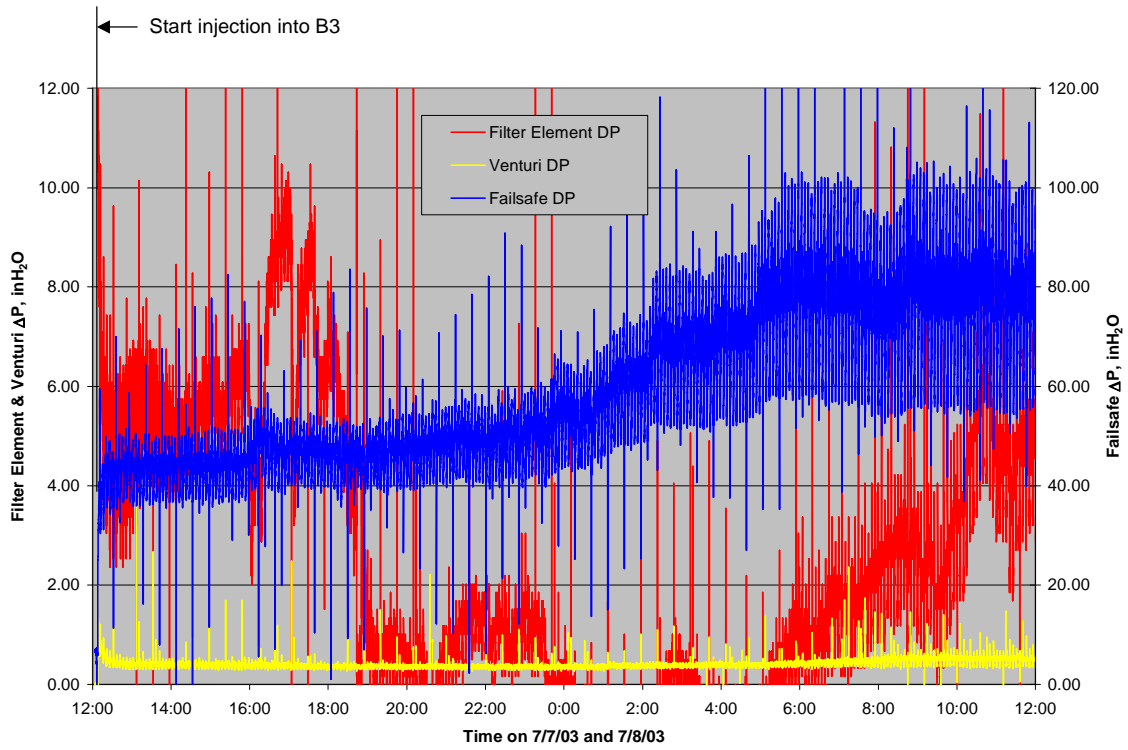
Figure 4.5-7 ΔP Data for 24-Hour Period Following Start of Pall Fuse Injection Test

TERMS

Listing of Abbreviations

AAS	Automated Analytical Solutions
ADEM	Alabama Department of Environmental Management
AFBC	Atmospheric Fluidized-Bed Combustor
APC	Alabama Power Company
APFBC	Advance Pressurized Fluidized-Bed Combustion
ASME	American Society of Mechanical Engineers
AW	Application Workstation
BET	Brunauer-Emmett-Teller (nitrogen-adsorption specific surface technique)
BFI	Browning-Ferris Industries
BFW	Boiler Feed Water
BMS	Burner Management System
BOC	BOC Gases
BOP	Balance-of-Plant
BPIR	Ball Pass Inner Race, Frequencies
BPOR	Ball Pass Outer Race, Frequencies
BSF	Ball Spin Frequency
CAD	Computer-Aided Design
CAPTOR	Compressed Ash Permeability Tester
CEM	Continuous Emissions Monitor
CFB	Circulating Fluidized Bed
CFR	Code of Federal Regulations
CHE	Combustor Heat Exchanger
COV	Coefficient of Variation (Standard Deviation/Average)
CPC	Combustion Power Company
CPR	Cardiopulmonary Resuscitation
CTE	Coefficient of Thermal Expansion
DC	Direct Current
DCS	Distributed Control System
DHL	DHL Analytical Laboratory, Inc.
DOE	U.S. Department of Energy
DSRP	Direct Sulfur Recovery Process
E&I	Electrical and Instrumentation
EDS or EDX	Energy-Dispersive X-Ray Spectroscopy
EERC	Energy and Environmental Research Center
EPRI	Electric Power Research Institute
ESCA	Electron Spectroscopy for Chemical Analysis
FCC	Fluidized Catalytic Cracker
FCP	Flow-Compacted Porosity
FFG	Flame Front Generator
FI	Flow Indicator
FIC	Flow Indicator Controller
FOAK	First-of-a-Kind
FTF	Fundamental Train Frequency

FW	Foster Wheeler
GBF	Granular Bed Filter
GC	Gas Chromatograph
GEESI	General Electric Environmental Services, Inc.
HHV	Higher Heating Valve
HP	High Pressure
HRSG	Heat Recovery Steam Generator
HTF	Heat Transfer Fluid
HTHP	High-Temperature, High-Pressure
I/O	Inputs/Outputs
ID	Inside Diameter
IF&P	Industrial Filter and Pump
IGV	Inlet Guide Vanes
IR	Infrared
KBR	Kellogg Brown & Root, Inc.
LAN	Local Area Network
LHV	Lower Heating Valve
LIMS	Laboratory Information Management System
LMZ	Lower Mixing Zone
LOC	Limiting Oxygen Concentration
LOI	Loss on Ignition
LPG	Liquefied Propane Gas
LSLL	Level Switch, Low Level
MAC	Main Air Compressor
MCC	Motor Control Center
MMD	Mass Median Diameter
MS	Microsoft Corporation
NDIR	Nondestructive Infrared
NETL	National Energy Technology Laboratory
NFPA	National Fire Protection Association
NO_x	Nitrogen Oxides
NPDES	National Pollutant Discharge Elimination System
NPS	Nominal Pipe Size
OD	Outside Diameter
ORNL	Oak Ridge National Laboratory
OSHA	Occupational Safety and Health Administration
OSI	OSI Software, Inc.
P&IDs	Piping and Instrumentation Diagrams
PC	Pulverized Coal
PCD	Particulate Control Device
PCME	Pollution Control and Measurement (Europe)
PDI	Pressure Differential Indicator
PDT	Pressure Differential Transmitter
PFBC	Pressurized Fluidized-Bed Combustion
PI	Plant Information
PLC	Programmable Logic Controller
PPE	Personal Protection Equipment

PRB	Powder River Basin
PSD	Particle-Size Distribution
PSDF	Power Systems Development Facility
ΔP or DP or dP	Pressure Drop or Differential Pressure
PT	Pressure Transmitter
RAPTOR	Resuspended Ash Permeability Tester
RFQ	Request for Quotation
RO	Restriction Orifice
RPM	Revolutions Per Minute
RSSE	Reactor Solid Separation Efficiency
RT	Room Temperature
RTI	Research Triangle Institute
SCS	Southern Company Services, Inc.
SEM	Scanning Electron Microscopy
SGC	Synthesis Gas Combustor
SGD	Safe Guard Device
SMD	Sauter Mean Diameter
SRI	Southern Research Institute
SUB	Start-Up Burner
TCLP	Toxicity Characteristic Leaching Procedure
TR	Transport Reactor
TRDU	Transport Reactor Demonstration Unit
TRS	Total Reduced Sulfur
TSS	Total Suspended Solids
UBP	Uncompacted Bulk Porosity
UMZ	Upper Mixing Zone
UND	University of North Dakota
UPS	Uninterruptible Power Supply
UV	Ultraviolet
VFD	Variable Frequency Drive
VOCs	Volatile Organic Compounds
WGS	Water-Gas Shift
WPC	William's Patent Crusher
XRD	X-Ray Diffraction
XXS	Extra, Extra Strong

Listing of Units

acfm	actual cubic feet per minute
Btu	British thermal units
°C	degrees Celsius or centigrade
°F	degrees Fahrenheit
ft	feet
FPS	feet per second
gpm	gallons per minute
g/cm^3 or g/cc	grams per cubic centimeter
g	grams
GPa	gigapascals
hp	horsepower
hr	hour
in.	inches
inWg (or inWc)	inches, water gauge (inches, water column)
in.-lb	inch pounds
°K	degrees Kelvin
kg	kilograms
kJ	kilojoules
kPa	kilopascals
ksi	thousand pounds per square inch
m	meters
MB	megabytes
min	minute
mm	millimeters
MPa	megapascals
msi	million pounds per square inch
MW	megawatts
m/s	meters per second
MBtu	Million British thermal units
m^2/g	square meters per gram
μ or μm	microns or micrometers
dp_{50}	particle-size distribution at 50 percentile
ppm	parts per million
ppm (v)	parts per million (volume)
ppm (w)	parts per million (weight)
lb	pounds
pph	pounds per hour
psi	pounds per square inch
psia	pounds per square inch absolute
psid	pounds per square inch differential
psig	pounds per square inch gauge
ΔP	pressure drop
rpm	revolutions per minute
s or sec	seconds
scf	standard cubic feet

scfh	standard cubic feet per hour
scfm	standard cubic feet per minute
V	volts
W	watts